# REPURPOSING A NON-RIBOSOMAL PEPTIDE SYNTHETASE (TYROCIDINE SYNTHETASE A) FOR AMINOACYL COA BIOSYNTHESIS

By

Ruth Njeri Muchiri

# A DISSERTATION

Submitted to
Michigan State University
in partial fulfillment of the requirements
for the degree of

Chemistry – Doctor of Philosophy

2015

#### **ABSTRACT**

# REPURPOSING A NON-RIBOSOMAL PEPTIDE SYNTHETASE (TYROCIDINE SYNTHETASE A) FOR AMINOACYL COA BIOSYNTHESIS

By

# Ruth Njeri Muchiri

In Taxus plants, the biosynthesis of the pharmaceutical paclitaxel includes the transfer of  $\beta$ -amino- $\beta$ -phenylpropanoyls from coenzyme A to the diterpenoid baccatin III by an acyl CoAdependent acyltransferase. The CoA ligase that biosynthesizes key  $\beta$ -amino- $\beta$ -phenylpropanoyl CoAs in Taxus plants has not yet been isolated or characterized. In a screen for an alternative catalyst, a multienzyme, nonribosomal peptidyl synthetase on the pathway that produces tyrocidines was identified as a surrogate CoA ligase. The tridomain starter module (Phe–ATE) of the tyrocidine synthetase A normally activates (S)- $\alpha$ -phenylalanine to an adenylate phosphate anhydride in the adenylation domain. The activated phenylalanine intermediate is then thioesterified by the pendent (i.e. covalent) pantetheine attached to the adjacent thiolation domain. In the current project, the adenylation and thiolation domains were found to function as a CoA ligase, making  $\alpha$ -,  $\beta$ -phenylalanyl, and, more importantly, phenylisoserinyl CoA. The latter two are known substrates of a phenylpropanoyltransferase (BAPT) on the biosynthetic pathway of the antimitotic paclitaxel.

Tyc(Phe–AT) was used in additional specificity studies with a focus on arylisoserines, since the corresponding CoA thioesters are important for biosynthesizing precursors of the paclitaxel analogs (such as the prostate cancer drug carbazitaxel). The stereospecificity of Tyc(Phe–AT) for the various stereoisomers of phenylisoserine was explored, showing reduced turnover for the (2R,3R) isomer, and no turnover with (2S,3R)-phenylisoserine relative to the benchmark (2R,3S)-isomer. The latter (2R,3S)-diastereoisomer of phenylisoserine matches the

stereochemistry of the natural side chain of paclitaxel. Thus, our preliminary work evaluated the substrate specificity of Tyc(Phe–AT) (taking advantage of its enantiospecificity) for racemates of (2S,3R)- and (2R,3S)-arylisoserine.

Structure-activity relationship analyses in earlier, independent studies showed that arylisoserine is necessary for the effective anticancer activity of paclitaxel. To access these activated CoA intermediates biosynthetically for use in a coupled enzyme assay with the paclitaxel pathway-specific 13-O-phenylpropanoyltransferase (BAPT), the CoA ligase function of Tyc(Phe-AT) was employed to convert various aryl- and non-aryl isoserine analogs to their CoA thioesters. We propose the products of the Tyc(Phe–AT) reaction can be transferred to baccatin III by a permissive BAPT. The isoserine substrates were synthesized by the Staudinger reaction that formed the Schiff base between benzaldehyde analogs and p-anisidine. This base was then reacted with acetoxyacetyl chloride in the presence of triethylamine. The amino and hydroxyl groups of the lactam product of this reaction were deprotected. Finally, hydrolysis of the lactam produced the isoserine analog. Tyc(Phe-AT) catalysis converted these analogs to their corresponding isoserinyl CoAs. All substrates in which the phenyl ring was substituted at ortho-(F, Cl, NO<sub>2</sub>), para- (F, Cl, Br, Me, OH, and NO<sub>2</sub>), or meta- (F, Cl, Br, Me, OH, CH<sub>3</sub>O and NO<sub>2</sub>) were converted to their CoA thioesters. Activity was also observed with the non-aromatic β-(cyclohexyl)isoserine and heteroaromatic β-(thiophenyl)isoserine analogs, but not with the aliphatic alkanyl groups (isopropyl-, and tert-butyl isoserine). This work provides a stepping stone towards novel biosynthesis of paclitaxel analogs with better efficacy than the parent drug.

This dissertation is dec destination." (Dan Mil	dicated to the journey: lman, Way of the Peac	"The journey is who	at brings us happine.	ss not the
		iv		

#### **ACKNOWLEDGEMENTS**

It is with immense gratitude that I acknowledge the support and help of my graduate research advisor Dr. Walker, without whom this thesis would have remained a dream. I also thank my thesis second reader Dr. Borhan for putting in extra effort in proofreading my thesis and providing great suggestions. Additionally, I appreciate my research committee members Dr. Tepe and Dr. Jones for sharing their pearls of wisdom with me during my early years in graduate school.

I would also like to thank the former members of Walker lab: Irosha for taking time to train me, Danielle for being a great friend, Getrude for being the big sister I needed when I was trying to find my way in graduate school, Mark, Washington, Sean, Dennis, Uday and Dilini. I also want to extend my gratitude to the current Walker lab members: Chelsea for fruitful discussions, Prakash and Tyler who create a friendly environment in the lab. I consider it an honor for the opportunity to mentor undergraduate students, Ashley and Aaron, and high school student Asha. Their hard work and dedication was evident and I am greatly indebted by their contribution towards my research project. I thank Dr. Jones and Lijun for their assistance with mass spectrometry, and also Dr. Holmes for his assistance with the NMR. I owe my deepest gratitude to the Chemistry department at MSU for their financial support and the opportunity to shape my teaching skills.

I wish to acknowledge the Forum for African Women Educationalists (FAWE) who saw the potential in me and put in their resources into my high school education. Without them, I may not have made it to the University of Nairobi. I cannot find words to express my gratitude to my dear mum, Mary Mukami. She instilled academic discipline, curiosity and spirit of hard work in me at a very tender age. I remember when she would challenge me to be the best student in my class with a promise of a gift at the end of the school year. Though at the time the drive was to receive the gift, I look back with a smile at how such childhood bait shaped my academic life. I can never forget how mum struggled to see me through my high school education and secured a full scholarship for me. I also extend my thanks to my dad, Muchiri, for his encouragement through-out the graduate school. I would like to also thank my siblings Lucas, Martha, Francis, Ben, Milly and Simon. They have been a great source of strength throughout my academic life. It gives me a great pleasure in acknowledging my primary school head teacher, Mr. Karanu, who has been a great motivation. He saw the great potential in me and challenged me to aim higher. I am glad he was present to witness the great achievement during my advanced degree commencement. Last but not least, I would like to thank my friends; Eric for his help in my thesis edits and comments, Waithira, my little sister for her love and support, Eunice, and the MSU-University Bible Fellowship church members for their constant prayers and encouragement.

# TABLE OF CONTENTS

LIST OF TABLES	xi
LIST OF FIGURES	xii
KEY TO ABBREVIATIONS	xix
1. INTRODUCTION	1
1.1. Chemotherapeutic Agents from Natural Products	1
1.2. Paclitaxel Discovery and Supply Shortage	
1.3. Paclitaxel Biosynthesis	
1.4. In Search for an Aminoacyl CoA Ligase	10
1.4.1. ANL Superfamily	
1.4.2. Tyrocidine Synthetase A: Member of NRPS Enzyme Family	14
1.4.2.1. Adenylation (A) Domain	16
1.4.2.2. Thiolation (T) Domain	
1.4.2.3. Epimerization (E) Domain	17
REFERENCES	
AMINOACYL COA AND AMINOACYL- <i>N</i> -ACETYLCYSTEAMINE	30
2.2. Experimental	
2.2.1. Substrates, Reagents, and General Instrumentation	
2.2.2. Expression of wild-type TycA cDNA	
2.2.3. Construction and Expression of the TycA–S563A Mutant	
2.2.4. Purification and Characterization of TycA and the TycA–S563A Mutant	
2.2.5. Synthesis of Phenylalanyl AMP	
2.2.6. Activity of wtTycA or $m$ TycA with ATP, and $\alpha$ –, $\beta$ –Phenylalanine, and (2 $R$ ,3 Phenylisoserine	
2.2.7. Synthesis of Product Standards	
2.2.7.1. Synthesis of [S–( $\alpha$ – and $\beta$ –Phenylalanyl)– $N$ –acetyl]cysteamine	
2.2.7.1. Synthesis of [S–( $\alpha$ – and $\beta$ –Phenylalanyl)]SNAC	
2.2.7.2. N-deprotection of [S=(\alpha = \text{and } \beta=r\tert{lenytatarry})]SNAC	
2.2.8. Activity and Kinetic Evaluation of wtTycA or $m$ TycA with $N$ -Acetylcysteam	
and Aminophenylpropanoates	
2.2.9. Kinetic Analysis of the <i>N</i> –acetylcysteamine Ligase Reaction Catalyzed by Ty	
TycA–S563A	
2.2.10. Activity and Kinetic Evaluation of wtTycA or mTycA as Ligases for Catalysis	
$\alpha$ — and $\beta$ —Aminophenylpropanoyl CoA Thioesters	
2.2.11. Kinetic Analysis of the CoA Ligase Reaction Catalyzed by TycA and TycA–	
S563A	

	2.3. F	Results and Discussion	52
	2.3.1.	Expression and Purification of the ATE Tridomain of wild-type and mutant	
		tycA	
	2.3.2.	Strategies used to Test the Activity of TycA with the Amino Acid Substrates	. 53
	2.3.3.	Incubation of TycA and TycA–S563A with <i>N</i> -Acetylcysteamine and Phenyl-	
		propanoates	
	2.3.4.	Kinetic Analyses of TycA and TycA–S563A with NAC	. 61
	2.3.5.	Assessment of TycA and TycA–S563A for CoA Ligase Activity	62
	2.3.6.	Kinetic Analyses of TycA and TycA–S563A with Phenylpropanoates and CoA.	. 66
	2.3.7.	Kinetic Analyses of TycA and TycA-S563A with Phenylpropanoates and ATP.	. 69
	2.3.8.	Comparing the Kinetic Parameters of TycA/TycA–S563A with Other CoA	
		Ligases	. 71
	2.4. C	Conclusion	. 72
	APPENI	DIX	. 74
	REFERE	ENCES	. 89
3.	TRU	NCATION OF TYROCIDINE SYNTHETASE A (TycA(Phe-ATE) to Tyc(Phe-	-A)
	and 7	Гус(Phe–AT), ACTIVITY EVALUATION, AND STEREOSPECIFICITY	
	STU	DIES IN THE BIOSYNTHESIS OF AMINOACYL COA THIOESTERS	. 94
	3.1. I	ntroduction	. 94
	3.2. E	Experimental	. 98
	3.2.1.	Substrates, Reagents, and General Instrumentation	. 98
	3.2.2.	Truncation and Subcloning of wt-tycA cDNA to Obtain tyc(phe-a) cDNA	. 98
		Tyc(Phe–A) Protein Expression and Purification	
	3.2.4.	Evaluation of Tyc(Phe–A) Activity with CoA and Aminophenylpropanoids	100
		Assessing Tyc(Phe-A) Substrate Binding by Tryptophan Fluorescence Quenchin	
		Studies	
	3.2.6.	Truncation of wt-tycA or tycA-S563A cDNA to Obtain tyc(phe-at) and tyc(phe-	_
		at(S563A)) Constructs	
	3.2.7.	Expression, Purification, and Characterization of Tyc(Phe–AT) Proteins	
		Activity Evaluation of Tyc(Phe–AT) and Tyc(Phe–AT(S563A)) with CoA and	
		Aminophenylpropanoids	104
	3.2.9.	Kinetic Evaluation of Tyc(Phe–AT) and Tyc(Phe–AT(S563A)) for CoA and	
		Aminophenylpropanoids	105
	3.2.10	. Stereospecificity of Tyc(Phe–AT) for Phenylisoserine Stereoisomers	
		0.1. Preparation of $(2R,3R)$ —Phenylisoserine	
		0.2. Preparation of (2S,3R)—Phenylisoserine	
		0.3. Evaluation of Tyc(Phe–AT) Activity for Phenylisoserine Stereoisomers	
		0.4. Kinetic Evaluation of Tyc(Phe–AT) for CoA and Phenylisoserine Stereo-	100
	2.2.1	isomers	108
	3 2 1	0.5. Inhibition Studies of $(2R,3S)$ -Phenylisoserine by the Enantiomer $(2S,3R)$ -	100
	5.2.1	Phenylisoserine	109
	3.3. F	Results and discussion	
		Construction and Expression of Tyc(Phe–A)	
		Activity of Tyc(Phe–A) with ATP, CoA, and Aminophenylpropanoids	

	3.3.3. Assessing Tyc(Phe–A) Substrate Binding by Tryptophan Fluorescence Quench Studies	
	3.3.4. Construction and Expression of Tyc(Phe–AT) and Tyc(Phe–AT(S563A))	
		. 114
	3.3.5. Activity and Kinetic Analysis of Tyc(Phe–AT) with ATP, CoA, and	115
	Aminophenylpropanoids	
	3.3.6.1. Contrasting Structural Features of Tyc(Phe–AT) Model and 4–Chloro-	11/
	benzoate:CoA Ligase	110
	3.3.6.2. Tyc(Phe–AT) Structure Model Alignment with Acetate:CoA Ligase	
	3.3.7. Substrate Stereospecificity of Tyc(Phe–AT)	
	3.3.7.1. Inhibition Studies of $(2R,3S)$ —Phenylisoserine by the Enantiomer $(2S,3R)$ —	
	Phenylisoserine	
	3.4. Conclusion	
	APPENDIX	
	REFERENCE	
		, 1 12
4.	SUBSTRATE SPECIFICITY STUDIES OF TYC(PHE-AT) WITH ISOSERINE	
•	ANALOGS IN THE BIOSYNTHESIS OF ISOSERINYL COA THIOESTERS	. 147
	4.1. Introduction	
	4.1.1. Paclitaxel Analogs and their Importance	
	4.1.2. Sources of Paclitaxel: An Historical Time Line	
	4.1.3. Catalytic Activity of Baccatin III 13–O–3–Amino–3–Phenylpropanoyltransfera	
	(BAPT) with Aminoacyl CoA Thioesters	. 151
	4.1.4. Tyrocidine Synthetase A Tyc(Phe–AT) Catalysis in Biosynthesis of Isoserinyl	CoA
	Analogs	
	4.2. Experimental	
	4.2.1. Substrates, Reagents, and General Instrumentation	. 156
	4.2.2. Synthesis of Isoserine Analogs	
	4.2.2.1. General Procedure 1: Synthesis of <i>N</i> –( <i>p</i> -Methoxyphenyl)benzylimines	
	4.2.2.2. General Procedure 2: Synthesis of 2-Azetidinones	
	4.2.2.3. General Procedure 3: Deprotection of Azetidinones	. 172
	4.2.2.4. General Procedure 4: Hydroxyl Deprotection of the 2-Azetidinones	. 182
	4.2.2.5. General Procedure 5: Hydrolysis of Azetidinone Ring	
	4.2.3. Synthesis of Pyridinyl Isoserine Analogs	
	4.2.3.1. General Procedure 6: Synthesis of Pyridinyl- <i>N</i> -benzhydryl Imine	. 195
	4.2.3.2. General Procedure 7: Synthesis of <i>N</i> -benzhydryl-3-acetoxy-4-	
	(pyridinyl)azetidin-2-one	. 197
	4.2.3.3. General Procedure 8: Lactam Ring Opening Along with Amine and Hydro	xyl
	Deprotection of N-benzhydryl-3-acetoxy-4-pyridinylazetidin-2-one	. 199
	4.2.4. Activity Assay for the Determination of the Substrate Specificity of	
	Tyc(Phe–AT)	
	4.2.5. Apparent Rates of Tyc(Phe–AT) with the Isoserine Substrates	. 201
	4.2.6. Kinetic Evaluation of Tyc(Phe–AT), CoA, and Racemic (2R,3S)-Phenyl-	
	isoserine	. 202
	4.3 Results and Discussion	202

	4.3.1. Synthesis of Isoserine Analogs via Staudinger Cycloaddition Reaction	202
	4.3.2. Relative Rates of Tyc(Phe–AT) for Isoserine Substrate Analogs	205
	4.3.3. Docking (2 <i>R</i> ,3 <i>S</i> )–Phenylisoserine into Grs1(Phe–A) Domain	208
	4.4. Conclusion	211
	4.5. Future Direction	212
	APPENDIX	215
	REFERENCES	258
_		
5.	PRELIMINARY SITE-DIRECTED MUTAGENESIS STUDIES AND FUTURE	264
	DIRECTION IN THE BIOSYNTHESIS OF AMINOACYL COA THIOESTERS	
	5.1. Introduction	
	5.1.2. Tyc(Phe–AT) Point Mutation Sites to Expand the Aryl Ring Binding Site	
	5.1.2. Tyc(File=AT) Foliat Mutation Sites to Expand the Aryl King Binding Site	
	5.2.1. Substrates, Reagents, and General Instrumentation	
	5.2.2. Tandem Site–Directed Mutagenesis of <i>tyc(phe–at)</i> cDNA	
	5.2.2.1 Mutation of Tyc(Phe–AT) to Tyc(Phe–AT(W227A, FFF $\rightarrow$ ARY)) and	200
	Tyc(Phe–AT(W227A))	268
	5.2.2.2. Mutation of Tyc(Phe–AT) to Tyc(Phe–AT(W227S, FFF $\rightarrow$ AQF)) and	200
	Tyc(Phe–AT(W227S))	269
	5.2.3. Protein Expression and Activity Assays of Tyc(Phe–AT) Mutants with	207
	Phenylisoserine Analogs and CoA	270
	5.2.4. Protein Purification of Tyc(Phe–AT) Mutants	
	5.2.5. Activity of Tyc(Phe–AT) Mutants with Isoserine Analogs	
	5.3. Results and Discussion	
	5.3.1. Protein Expression and Purification of Tyc(Phe–AT) Mutants	
	5.3.2. Activity Assays of Tyc(Phe–AT) Mutants with Phenylisoserine Analogs	
	5.3.2.1. Activity Evaluation of Tyc(Phe–AT(W227S)) in the Screen for Isoserine	
	Analogs in Isoserinyl CoA Biosynthesis	276
	5.4. Tyc(Phe–AT) and BAPT–Coupled Assays Towards the Biosynthesis of Precurso	
	Paclitaxel Analogs	
	REFERENCES	280

# LIST OF TABLES

Table 2.1. Steady state kinetic analysis of TycA and TycA–S563A with phenylpropanoids, CoA and <i>N</i> –acetylcysteamine
Table 2.2. Steady–state kinetic analysis of TycA and TycA–S563A with apparent saturation of phenylpropanoids and varying concentrations of ATP
Table 2.3. Ratio of $k_{\text{cat}}$ of phenylpropanoids in steady–state biosynthesis of aminoacyl AMP or aminoacyl CoA catalyzed by TycA or TycA–S563A
Table 2.4. Kinetic parameters of acyl CoA ligases from various microorganisms
Table 3.1. The dissociation constants for binding of (2 <i>S</i> )–α–phenylalanine ((2 <i>S</i> )–α–Phe) to Tyc(Phe–A), Tyc(Phe–AT), and Grs1(Phe–A)
Table 3.2. Steady–state kinetic analysis of Tyc(Phe–AT) and Tyc(Phe–AT(S563A)) with CoA in comparison to Tyc(Phe–ATE) and Tyc(Phe–ATE(S563A))
Table 3.3. Kinetic parameters of Tyc(Phe–AT) with phenylisoserine stereoisomers
Table 4.1. Cytotoxic activity of paclitaxel analogs in microtubule assembly and against B16 melanoma cells
Table 4.2. Relative rates of Tyc(Phe-AT) with aryl- and non-aryl isoserine and CoA
Table 5.1. The proposed mutations of F201, F202, and F206 of Tyc(Phe-AT) in tandem with W227 replacement residues
Table 5.2. The rates ( $v_{app}$ ) of Tyc(Phe–AT(W227S)) mutant in comparison to Tyc(Phe–AT) in the biosynthesis of isoserinyl CoA analogs

# LIST OF FIGURES

Figure 1.1.	Podophyllotoxin and its derivatives
Figure 1.2.	The vinca alkaloids; vinblastine and vincristine
Figure 1.3.	Camptothecin and the water soluble derivatives
Figure 1.4.	The structures of paclitaxel (Taxol®) and its analog, docetaxel (Taxotere®) 4
Figure 1.5.	The Holton methodology for the semisynthesis of paclitaxel via $\beta$ -lactam (A) and 10-DAB precursor (B)
Figure 1.6.	Biosynthetic pathway to paclitaxel starting from simple primary metabolite precursors to the baccatin III
Figure 1.7.	Biosynthesis of paclitaxel C–13 side chain (A) and the enzyme catalyzed transfer to the baccatin III (B)
Figure 1.8.	Synthesis of (2R,3S)-phenylisoserinyl CoA via the mixed anhydride intermediate11
Figure 1.9.	The tyrocidine synthetase cluster showing the three polypeptides; TycA, TycB, and
	TycC
Figure 1.10	D. Scheme showing the conversion of <i>apo-PCP</i> (or T domain) to <i>holo-PCP</i>
Figure 1.11	Schematic representation of the reactions catalyzed by various domains within a module in tyrocidine synthetase
Figure 2.1.	Scheme showing reactions catalyzed by TycA (Phe-ATE) domains
Figure 2.2.	The stabilization of thiol–α-carboxylate intermediate formed during epimerization reaction in NRPS enzymes
Figure 2.3.	Possible pathways for the epimerization at the alpha carbon
Figure 2.4.	Synthesis of (2 <i>R</i> ,3 <i>S</i> )–phenylisoserinyl CoA via the mixed anhydride intermediate (panel A, see <b>Figure 1.8</b> in Chapter 1 for full scheme) and the proposed biosynthetic route in the current study (panel B).
Figure 2.5.	$(N-\text{Boc})$ – $(S)$ – $\alpha$ –phenylalanyl–SNAC ( <b>B-2</b> ) and $(N-\text{Boc})$ – $(R/S)$ – $\beta$ –phenylalanyl–SNAC ( <b>B-3</b> )

Figure 2.6. Synthesis of (2S)–α–phenylalanyl–SNAC	. 42
Figure 2.7. (S)–α–Phenylalanyl SNAC ( <b>B-7</b> ) and β–Phenylalanyl SNAC·HCl salt ( <b>B-8</b> )	. 43
Figure 2.8. (2 <i>R</i> ,3 <i>S</i> )–Phenylisoserinyl SNAC	. 45
Figure 2.9. SDS-PAGE gel of fractions eluted from a Ni-affinity column containing TycA	
constructs	. 53
Figure 2.10. Radioactivity-guided assay of the phenylalanine adenylation domain of TycA	. 54
Figure 2.11. The exchange reaction, performed in the absence of thiolation activity, measures equilibrium exchange of $\gamma$ - <sup>18</sup> O <sub>4</sub> -ATP with <sup>16</sup> O <sub>4</sub> -pyrophosphate	
Figure 2.12. The proposed biosynthesis of aminoacyl CoAs using TycA	. 57
Figure 2.13. The LC–ESI–MS–MS spectra of aminoacyl SNACs	. 59
Figure 2.14. Molecular fragment ions profile resulting from LC–ESI–MS/MS of biosynthetic aminoacyl CoAs	. 63
Figure 2.15. The LC–ESI–MS–MS spectra of biosynthetic aminoacyl CoAs	. 64
Figure 2.16. Kinetic model for CoA thioesterification reaction catalyzed by TycA and TycA–S563A	
Figure I–1. MRM profile obtained by LC–ESI–MS/MS of biosynthetically derived α– phenylpropanoyl SNAC	. 75
Figure I–2. MRM profile obtained by LC–ESI–MS/MS of biosynthetically derived β– phenylpropanoyl SNAC	. 75
Figure I–3. MRM profile obtained by LC–ESI–MS/MS of biosynthetically derived (2 <i>S</i> ,3 <i>R</i> )– phenylisoserinyl SNAC	. 76
Figure I–4. MRM profile obtained by LC–ESI–MS/MS of biosynthetically derived α– phenylalanyl CoA	. 76
Figure I–5. MRM profile obtained by LC–ESI–MS/MS of biosynthetically derived β– phenylalanyl CoA	. 77
Figure I–6. MRM profile obtained by LC–ESI–MS/MS of biosynthetically derived (2 <i>R</i> ,3 <i>S</i> )–phenylisoserinyl CoA	
Figure I–7. The LC–ESI–MS analyses of authentic aminoacyl SNACs	. 78

Figure I–8. Total ion chromatograms obtained by LC–ESI–MS analysis (scan mode: <i>m/z</i> 100 to 1200) of the compounds in TycA assays
Figure I–9. Determination of kinetic parameters for A) $\alpha$ –phenylalanine, B) $\beta$ –phenylalanine, C) (2 <i>R</i> ,3 <i>S</i> )–phenylisoserine and D) CoA with wtTycA using Hannes Wolf plots . 81
Figure I–10. Determination of kinetic parameters for A) α–phenylalanine, B) β–phenylalanine, C) (2 <i>R</i> ,3 <i>S</i> )–phenylisoserine and D) <i>N</i> –acetylcysteamine with wtTycA using Hannes Wolf plots
Figure I–11. <sup>1</sup> H-NMR spectrum of ( <i>S</i> )–α–phenylalanyl SNAC standard
Figure I–12. <sup>13</sup> C-NMR spectrum of ( <i>S</i> )–α–phenylalanyl SNAC standard
Figure I–13. <sup>1</sup> H-NMR spectrum of β–phenylalanyl SNAC·HCl salt standard
Figure I–14. $^{13}$ C-NMR spectrum of $\beta$ –phenylalanyl SNAC·HCl salt standard
Figure I–15. <sup>1</sup> H-NMR spectrum of (2 <i>R</i> ,3 <i>S</i> )–phenylisoserinyl SNAC·standard
Figure I–16. <sup>13</sup> C-NMR spectrum of (2 <i>R</i> ,3 <i>S</i> )–phenylisoserinyl SNAC standard
Figure I–17. Trypsin digestion sequence analysis of TycA purified by Ni-affinity chromatography
Figure 3.1. Representation of reactions catalyzed by different adenylate forming enzymes 97
Figure 3.2. Deprotection of (2R,3R)–phenylisoserine
Figure 3.3. Deprotection of (2S,3R)–phenylisoserine
Figure 3.4. SDS–polyacrylamide gel electrophoresis (12% acrylamide) and Coomassie Blue staining of recombinantly expressed Tyc(Phe–A)
Figure 3.5. Plot of observed fluorescence change with increasing concentration of (2 <i>S</i> )–α– phenylalanine
Figure 3.6. SDS-polyacrylamide gel electrophoresis (12% acrylamide) and Coomassie blue staining of recombinantly expressed Tyc(Phe–AT)
Figure 3.7. Comparison of 4–ClBzCL with Tyc(Phe–AT) model
Figure 3.8. Comparison of active site of 4–ClBzCL with Tyc(Phe–AT) model
Figure 3.9. Comparison of active site of AcCL with Tvc(Phe–AT) model

Figure 3.10. Structure of paclitaxel	122
Figure 3.11. Grs1(Phe–A) active site (cyan) in complex with aminophenylpropanoids	124
Figure 3.12. Lineweaver–Burk plots for the inhibition of Tyc(Phe–AT) by (2 <i>S</i> ,3 <i>R</i> )–phenylisoserine	126
Figure II–1. Amino acid sequence variation in the highly conserved motifs in the acyl–adenyl enzyme family	
Figure II–2. Amino acid sequence alignment of close adenylation domain homologs of NRPS family	
Figure II–3. The amino acid sequence alignment of Tyc(Phe–AT), acetyl CoA and 4-chlorobenzoate:CoA ligase	132
Figure II–4. Spectra obtained by equilibrium fluorescence titration of (2 <i>S</i> )–phenylalanine to K <sup>+</sup> HEPES	134
Figure II–5. Spectra obtained by equilibrium fluorescence titration of (2 <i>S</i> )–phenylalanine at increasing concentrations (0 – 96 μM) to Tyc(Phe–A) (0.1 μM)	135
Figure II–6. Plot of observed fluorescence change with varying concentrations of AMP at fix concentration of Tyc(Phe–A)	
Figure II–7. Plot of observed fluorescence change with varying concentrations of (2S)–pheny alanine at fixed concentration of Tyc(Phe–AT)	
Figure II–8. Plot of observed fluorescence change with varying concentrations of AMP at fix concentration of Tyc(Phe–AT)	
Figure II–9. <sup>1</sup> H-NMR spectrum of (2 <i>R</i> ,3 <i>R</i> )–phenylisoserine	137
Figure II–10. <sup>13</sup> C NMR spectrum of (2 <i>R</i> ,3 <i>R</i> )–phenylisoserine	138
Figure II–11. <sup>1</sup> H-NMR spectrum of (2 <i>S</i> ,3 <i>R</i> )–phenylisoserine	139
Figure II–12. <sup>13</sup> C-NMR spectrum of (2 <i>S</i> ,3 <i>R</i> )–phenylisoserine	140
Figure II–13. Lineweaver-Burk plots for the inhibition of Tyc(Phe–AT) in the presence of (2S,3R)–phenylisoserine	141
Figure 4.1. The paclitaxel structure framework	147
Figure 4.2. Some of the paclitaxel analogs with modification at C–13	149

Figure 4.3.	The biosynthesis of paclitaxel in plants starting from geranylgeranyl diphosphate (GGDP)	150
Figure 4.4.	The proposed biosynthesis of paclitaxel	151
Figure 4.5.	A representative 11–step semisynthesis of paclitaxel analogs	153
Figure 4.6.	Synthesis of (2 <i>R</i> ,3 <i>S</i> )-phenylisoserinyl CoA via the mixed anhydride intermediate	154
Figure 4.7.	The reversible adenylation of ( <i>R/S</i> )–phenylalanine by Tyc(Phe–A) domain through ATP hydrolysis	
Figure 4.8.	Synthesis of <i>N</i> -protected imines from benzaldehyde analogs and <i>p</i> -anisidine	157
Figure 4.9.	Scheme showing the general synthesis of 2-azetidinones	161
Figure 4.10	). Scheme showing general method for deprotection of amine	172
Figure 4.11	. Scheme showing the general method for hydroxyl deprotection	182
Figure 4.12	2. Scheme showing the general method for the lactam ring hydrolysis	186
Figure 4.13	3. Scheme showing general synthesis of 2-pyridinylimines	195
Figure 4.14	Scheme showing the synthesis of pyridinyl-2-azetidinones	197
Figure 4.15	5. A scheme showing the synthesis of isoserine analogs	203
Figure 4.16	5. Synthesis of pyridinylisoserine isomers	204
Figure 4.17	7. Reaction mechanism for the formation of benzhydrylacetamide	205
Figure 4.18	3. (2R,3S)—phenylisoserine (green) docked into Grs1(Phe-A) active site	210
Figure 4.19	O. Synthesis of cabazetaxel (Jevtana®)	213
Figure III–	MS/MS fragment ion profile of the biosynthesized 3-F–phenylisoserinyl CoA	216
Figure III-	2. MS/MS fragment ion profile of the biosynthesized 3-Cl–phenylisoserinyl CoA	217
Figure III–	3. MS/MS fragment ion profile of the biosynthesized 3-Br–phenylisoserinyl CoA	218

Figure III–4. MS/MS fragment ion profile of the biosynthesized 3-Me–phenylisoserinyl CoA	. 219
Figure III–5. MS/MS fragment ion profile of the biosynthesized 3-NO <sub>2</sub> –phenylisoserinyl CoA	. 220
Figure III–6. MS/MS fragment ion profile of the biosynthesized 4-OMe–phenylisoserinyl CoA	. 221
Figure III–7. MS/MS fragment ion profile of the biosynthesized 4-OH–Phenylisoserinyl CoA	. 222
Figure III–8. MS/MS fragment ion profile of the biosynthesized thiophenylisoserinyl CoA	. 223
Figure III–9. MS/MS fragment ion profile of the biosynthesized cyclohexylisoserinyl CoA	. 224
Figure III–10. <sup>1</sup> H Homodecoupling NMR spectrum of 3-Hydroxy-4-(4-fluorophenyl)azetidin one	
Figure III–11. H <sub>2</sub> O/D <sub>2</sub> O exchange NMR spectrum of 3-Hydroxy-4-(4-fluorophenyl)azetidin- one	
Figure III–12. <sup>1</sup> H-NMR spectrum of phenylisoserine	. 227
Figure III–13. <sup>1</sup> H-NMR spectrum of <i>p</i> -F–phenylisoserine	. 228
Figure III–14. <sup>1</sup> H-NMR spectrum of <i>p</i> -Cl–phenylisoserine	. 229
Figure III–15. <sup>1</sup> H-NMR spectrum of <i>p</i> -Br–phenylisoserine	. 230
Figure III–16. <sup>1</sup> H-NMR spectrum of <i>p</i> -Me–phenylisoserine	. 231
Figure III–17. <sup>1</sup> H-NMR spectrum of <i>p</i> -OMe–phenylisoserine	. 232
Figure III–18. <sup>1</sup> H-NMR spectrum of <i>p</i> -OH–phenylisoserine	. 233
Figure III–19. <sup>1</sup> H-NMR spectrum of <i>p</i> -NO <sub>2</sub> –phenylisoserine	. 234
Figure III–20. <sup>1</sup> H-NMR spectrum of <i>m</i> -F–phenylisoserine	. 235
Figure III–21. <sup>1</sup> H-NMR spectrum of <i>m</i> -Cl–phenylisoserine	. 236
Figure III–22. <sup>1</sup> H-NMR spectrum of <i>m</i> -Br–phenylisoserine	. 237
Figure III–23. <sup>1</sup> H-NMR spectrum of <i>m</i> -Me–phenylisoserine	. 238

Figure III–24. <sup>1</sup> H-NMR spectrum of <i>m</i> -OMe–phenylisoserine	239
Figure III–25. <sup>1</sup> H-NMR spectrum of <i>m</i> -OH–phenylisoserine	240
Figure III–26. <sup>1</sup> H-NMR spectrum of <i>m</i> -NO <sub>2</sub> –phenylisoserine	241
Figure III–27. <sup>1</sup> H-NMR spectrum of <i>o</i> -F–phenylisoserine	242
Figure III–28. <sup>1</sup> H-NMR spectrum of <i>o</i> -Cl–phenylisoserine	243
Figure III–29. <sup>1</sup> H-NMR spectrum of <i>o</i> -Br–phenylisoserine	244
Figure III–30. <sup>1</sup> H-NMR spectrum of <i>o</i> -Me–phenylisoserine	245
Figure III–31. <sup>1</sup> H-NMR spectrum of <i>o</i> -OMe–phenylisoserine	246
Figure III–32. <sup>1</sup> H-NMR spectrum of <i>o</i> -NO <sub>2</sub> –phenylisoserine	247
Figure III–33. <sup>1</sup> H-NMR spectrum of trimethylisoserine	248
Figure III–34. <sup>1</sup> H-NMR spectrum of cyclohexylisoserine	249
Figure III–35. <sup>1</sup> H-NMR spectrum of thiopheneisoserine	250
Figure III–36. <sup>1</sup> H-NMR spectrum of isopropylisoserine	251
Figure III–37. <sup>1</sup> H-NMR spectrum of 2-pyridinylisoserine	252
Figure III–38. <sup>13</sup> C-NMR spectrum of 2-pyridinelisoserine	253
Figure III–39. <sup>1</sup> H-NMR spectrum of <i>N</i> -benzhydrylacetamide	254
Figure III–40. <sup>13</sup> C-NMR spectrum of <i>N</i> -benzhydrylacetamide	255
Figure III–41. <sup>1</sup> H-NMR spectrum of 3-pyridineisoserine	256
Figure III–42. LC-ESI-MS of intermediates and products obtained from the hydrolysis and deprotection of <i>N</i> -benzhydryl-3-acetoxy-4-(2-pyridinyl)azetidin-2-one	257
Figure 5.1. Tyc(Phe–AT) model (grey cartoon) in complex with phenylalanine	266
Figure 5.2. SDS–polyacrylamide gel electrophoresis (12% acrylamide) and Coomassie blue staining of recombinantly expressed Tyc(Phe–AT) mutants	275
Figure 5.3. Proposed Tyc(Phe–AT) and BAPT-coupled assays aimed at novel biosynthesis of paclitaxel analogs	

#### **KEY TO ABBREVIATIONS**

Ac<sub>2</sub>O, Acetic anhydride

AcCl, Acetyl chloride

AIDS, Acquired immune deficiency syndrome

AMP, Adenosine monophosphate

ANL, Acyl-CoA synthetase, non-ribosomal peptide synthetase, and luciferase enzymes

ATP, Adenosine triphosphate

BAPT, *Taxus* baccatin III 13α-O-3-amino-3-phenylpropanoyltransferase

Boc, tert-Butoxycarbonyl

*n*-BuLi, *n*-butyllithium

CAN, Cerium (IV) ammonium nitrate

CDCl<sub>3</sub>, Deuterated chloroform

cDNA, Complementary deoxyribonucleic acid

CoA, Coenzyme A

CoASH, Free coenzyme A thiol

D<sub>2</sub>O, Deuterated water

DAB, Deacetylbaccatin III

DBAT, 10-Deacetylbaccatin III-10β-O-acetyltransferase

DCC, Dicyclohexylcarbodiimide

DIPEA, N,N-Diisopropylethylamine

DMAP, 4-Dimethylaminopyridine

DMF, Dimethylformamide

DMSO, Dimethyl sulfoxide

E. coli, Escherichia coli

EDTA, Ethylenediaminetetraacetic acid

EE, Ethyl vinyl ether

ESI-MS/MS, Electrospray ionization tandem mass spectrometer

EtCOCl, Ethyl chloroformate

Et<sub>3</sub>SiCl, Chlorotriethylsilane

EtOAc, Ethyl acetate

FDA, U.S.A Food and Drug Administration

GGDP, Geranylgeranyl diphosphate

GGDPS, Geranylgeranyl diphosphate synthase

Grs1(Phe-A), Gramicidin synthetase 1 adenylation domain

HEPES, 4-(2-hydroxyethyl)-1-piperazineethanesulfonic acid

gHSQC, heteronuclear single quantum coherence 2-D NMR spectroscopic technique

HOAc, Acetic acid

HOBt, Hydroxybenzotriazole

HPLC, High performance liquid chromatography

HRMS, High resolution mass spectrometry

IC<sub>50</sub>, 50% inhibitory concentration

ED<sub>50</sub>, 50% Effective dosage

IPP, Isopentenyl diphosphate

IDPI, Isopentenyl diphosphate isomerase

IPTG, Isopropyl β–D–1–thiogalactopyranoside

 $k_{\rm cat}$ , catalytic turnover

 $K_{\rm M}$ , Michaelis constant

LB, Luria-Bertani medium

LC, Liquid chromatography

LDA, Lithium diisopropylamide

LiHMDS, Lithium bis(trimethylsilyl)amide

MEP, Methylerythritol phosphate pathway

MHz, Megahertz

MS, Mass Spectrometer

MRM, Multiple reaction monitoring

MWCO, Molecular weight cut off

Na<sub>2</sub>SO<sub>4</sub>, Sodium sulphate

NaHCO<sub>3</sub>, Sodium bicarbonate

NDTBT, 3'-N-Debenzoyl-2'-deoxytaxol N-benzoyltransferase

NMR, Nuclear Magnetic Resonance

NRPS, Non-ribosomal peptide synthetase

OD, Optical density

PAM, Phenylalanine aminomutase

PCF, Plant Cell Fermentation

PCP, Peptidyl carrier protein

PCR, Polymerase chain reaction

Tyc(Phe–ATE), Phenylalanine adenylation, thiolation and epimerization

PMP, para-methoxyphenyl

PPi, Inorganic phosphate

4'-Ppant, 4'-Phosphopantetheinyl

Q-ToF, quadrupole time of flight

RT, Room temperature

SAR, Structure-activity relationship

SDS-PAGE, Sodium dodecyl sulfate polyacrylamide gel electrophoresis

SNAC, N-acetylcysteamine

T. brevifolia, Taxus brevifolia

T. cuspidata, Taxus cuspidata

BuOH, Butanol

TES, Triethylsilyl

TFA, Trifluoroacetic acid

THF, Tetrahydrofuran

TIPS, Triisopropylsilyl

TLC, Thin layer chromatography

TMS, Trimethylsilyl

tRNA, Transfer ribonucleic acid

UPLC, Ultra performance liquid chromatography

UV, Ultraviolet

YT, Yeast extract and bacto tryptone medium

### 1. INTRODUCTION

# 1.1. Chemotherapeutic Agents From Natural Products

Natural products have historically been excellent leads for the discovery of biologically active compounds including therapeutics. For instance, 40% of all anticancer drugs developed before 2002 are natural products, while an additional 20% are synthetic compounds, based on natural product pharmacophore. Natural anticancer agents can be of microbial or plant origin. The microbial or more commonly referred to as antibiotics constitute the majority of these agents. The anthracycline antibiotics in use currently include doxorubicin, daunorubicin, epirubicin, and idarubicin. The bleomycin derivatives are used as glycosylated oligopeptide antibiotics, while other antibiotics such as pyrroloindole and phenoxazinone chromopeptide are commonly administered as mitomycin C, and actinomycin D, respectively in combination with other drugs. These antibiotics are important in the treatment of different cancers and have been extensively reviewed. 13,15,17,18

The plant-derived anticancer agents have attracted attention both in academia and commercial fields. <sup>19-22</sup> Their use as traditional medicine dates back to 1800s, <sup>22</sup> but the isolation and identification of their constituent active ingredients was not pursued until mid-1900. <sup>23,24</sup> Podophyllotoxin is probably the first documented anticancer agent of plant origin (**Figure 1.1**). <sup>23,25</sup> It is derived from the American mandrake or May apple (*Podophyllum peltatum* L) and was identified as a potent drug for the treatment of benign tumor, *Condylomata acuminate* in 1942. <sup>24</sup> Due to its toxicity, derivatives namely etoposide <sup>26</sup> and teniposide <sup>27</sup> were developed for therapeutic use. To overcome the solubility challenges associated with these derivatives, etoposide phosphate (Etopophos®)<sup>27</sup> was developed and approved for the treatment of Kaposi's

sarcoma, lung, testicular cancers, lymphoma, non-lymphocytic leukemia, and glioblastoma multiforme. <sup>28,29</sup>

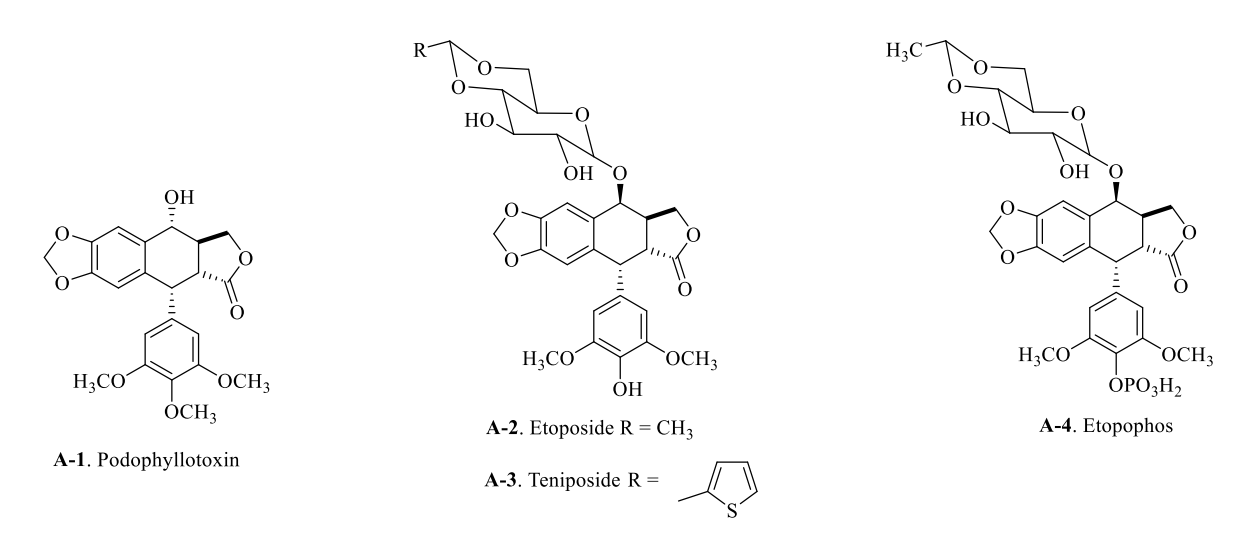


**Figure 1.1.** Podophyllotoxin and its derivatives

Additionally, early discoveries included the vinca alkaloids vinblastine and vincristine in 1958.<sup>30</sup> These drugs have continuously been used alongside other combinations as chemotherapeutic agents against non-small cell lung cancer, leukemia, lymphoma, Hodgkin's disease, bladder, brain, and breast cancers (**Figure 1.2**).<sup>31</sup> The vinca alkaloids prevent growth of cancerous cells by inhibiting microtubule formation during mitosis.<sup>32,33</sup>

Figure 1.2. The vinca alkaloids; vinblastine and vincristine

Later in 1966, the search for more potent anticancer agents from natural products led to the isolation of camptothecin by researchers, Wall and Wani.<sup>34</sup> This quinolone alkaloid was extracted from the bark and stem of camptotheca acuminate (the happy tree), a tree indigenous to China.<sup>34</sup> The seemingly common solubility challenge with the natural anticancer extracts was also observed with camptothecin in addition to severe adverse reactions.<sup>35</sup> These drawbacks halted the early development of camptothecin and its clinical trials. Nevertheless, due to its unique mechanism of action, namely inhibition of topoisomerase 1, <sup>36-39</sup> new interest in camptothecin led to the development of analogs that overcame the solubility and toxicity issues <sup>40</sup> (**Figure 1.3**). Currently, topotecan (Hycamtin<sup>®</sup>) and irinotecan (Camptosar<sup>®</sup>) are approved by FDA for use in ovarian, cervical, colon, and small cell lung cancers.<sup>41</sup>

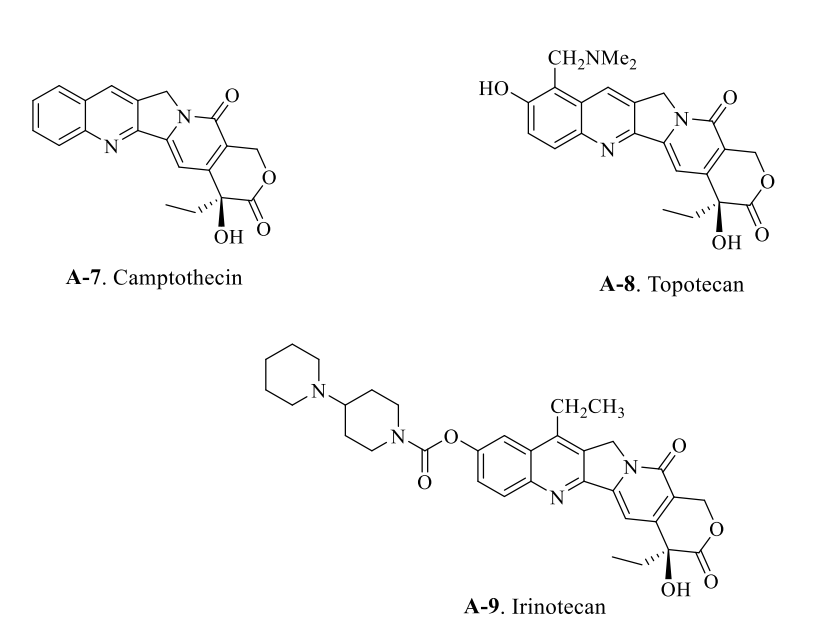


Figure 1.3. Camptothecin and the water soluble derivatives

Among the discoveries made from nature to date, the most interesting is perhaps paclitaxel (Taxol<sup>®</sup>).<sup>42</sup> It is a complex diterpenoid, with a phenylisoserine side chain and generally adorned with hydroxyl functionalities (**Figure 1.4**).<sup>42</sup> It is not surprising then, that it took ~30

years from discovery to commercialization.<sup>43-45</sup> The following sections will highlight important studies from discovery to the current status of paclitaxel and a proposal on a new approach towards its production.

### 1.2. Paclitaxel Discovery and Supply Shortage

The antineoplastic drug, paclitaxel (Taxol®) is one of the most important drugs in chemotherapy following its FDA approval in 1992. Initially, paclitaxel was used for the treatment of refractory ovarian cancer and refractory or anthracycline-resistant breast cancer. Over the years, paclitaxel and its analog, docetaxel (Taxotere®) (Figure 1.4) have found wide application in the treatment of various cancers including metastatic breast cancer, ovarian, and lung cancer, and also Aids-related Kaposi's sarcoma. Whereas other chemotherapy drugs, for example vinblastine and vincristine inhibit tubulin polymerization, paclitaxel has a unique mode of action where it promotes microtubule polymerization, thus arresting cell division and eventually leading to apoptosis of the target cells. Its unique mechanism of action prompted curiosity among the scientific community and partly contributed to its early development.

Figure 1.4. The structures of paclitaxel (Taxol®) and its analog, docetaxel (Taxotere®)

Initially, paclitaxel was extracted from the inner bark of the pacific yew tree, *Taxus brevifolia* at very low yields (0.02% w/w).<sup>54</sup> This means of supply raised concerns about its sustainability in addition to the labor intensive and high cost of production.<sup>54</sup> A supply shortage of paclitaxel in its early development prompted the need for alternative means of production. The initial approach was a semisynthetic process from 10-deacetylbaccatin III (10-DAB), which was discovered in European yew, *Taxus baccata*.<sup>55,56</sup> Several semisynthetic methods were developed including the coupling of a phenylisoserine precursor (β-lactam synthesized through six steps) to 10-DAB (**Figure 1.5**).<sup>57,58</sup> Bristol-Myers Squibb (BMS) adopted the semisynthesis method for commercial production of paclitaxel.<sup>59</sup> The application of semisynthesis method required use of environmentally harmful solvents and redundant protection/deprotection steps and was therefore abandoned for commercial production of paclitaxel.<sup>59</sup>

**Figure 1.5**. The Holton methodology for the semisynthesis of paclitaxel via β-lactam (A) and 10-DAB precursor (B).

In the search for a renewable and environmentally friendly production of paclitaxel, a lot of effort was geared towards the development of a biosynthetic process.<sup>60</sup> Ultimately, a

sustainable and environmentally safer Taxus plant cell fermentation (PCF) was developed by Phyton Biotech.<sup>60</sup> The first patent for PCF was filed in 1991 and produced paclitaxel at 1-3 mg·L.61 Currently, Phyton Biotech USA and SamyangGenex, South Korea are the two companies producing paclitaxel using PCF on an industrial scale.<sup>62</sup> PCF has been able to overcome challenges associated with its competitor methods, for example, production is independent of geographical and seasonal variations, it also provides uniform quality paclitaxel, and it is a renewable and environmentally friendly method. 63,64 However, there are still pertinent challenges associated with PCF including genetic instability, heterogeneous culture, low growth rates compared to bacterial cultures, variable yields, susceptibility to shear stresses in bioreactors, and aggregation.<sup>65</sup> Numerous proposals on how to overcome these drawbacks have been laid out and they mainly focus on molecular biological studies on taxane biosynthesis and how its accumulation affects metabolic profiles and gene expression in Taxus species cell cultures. 66 New taxane sources such as endophytic fungi of Taxus and Corylus avellana cell culture have also been identified and show promise in the biotechnological production of taxanes in the future.<sup>67</sup> While the semisynthetic method to produce the drug was considered environmentally harmful, it however avoided the likely rate-limiting biosynthetic steps occurring in planta<sup>68</sup> and proceeded with higher yields. The slow enzymatic steps in *Taxus* plants and derived cell cultures<sup>68</sup> likely contribute to the low production yields of paclitaxel. Besides the production challenges, paclitaxel also showed low solubility in water. <sup>69</sup> The discovery of a suitable formulation in a mixture of ethanol and Cremophor EL® (currently referred to as Kollipher EL<sup>®</sup>) proved effective during clinical trials and is still administered in this form.<sup>54,70</sup>

# 1.3. Paclitaxel Biosynthesis

The biosynthesis of paclitaxel in *Taxus* plants involves ~19 steps from geranylgeranyl diphosphate (GGDP), the universal diterpenoid precursor derived from deoxyxylulose phosphate pathway. The cyclization of GGDP by taxadiene synthase to the tricyclic taxane skeleton displayed by eight cytochrome P450-mediated oxygenations, three acyl CoA-dependent acylations, an oxidation at C9, and oxetane (D-ring) formation to provide baccatin III. This diterpene intermediate is further modified in five steps via the attachment of β-phenylalanine at C13 by a CoA-dependent acyltransferase, P450 hydroxylation at C2 and final *N*-benzoylation to produce paclitaxel (**Figures 1.6 and 1.7**). All the genes for the CoA thioester-dependent acyltransferases on the paclitaxel biosynthetic pathway were identified in previous studies. Among them are genes that code for 13-*O*-phenylpropanoyltransferase (BAPT) and *N*-benzoyltransferase enzymes, which have been characterized in the biosynthesis pathway.

Two benzoyltransferases and a 13-*O*-phenylpropanoyltransferase from *Taxus* were characterized separately in assays with a suitable paclitaxel precursor.<sup>80</sup> The benzoyl- and phenylpropanoyl CoA thioester co-substrates were synthesized by reaction of a mixed anhydride with CoA.<sup>80</sup> The β-phenylalanine and phenylisoserine needed protecting chemistry to cap the reactive amino or hydroxyl groups on the propanoid side chain before the CoA coupling step.<sup>80</sup> By application of these acyltransferases in the late-stage biosynthesis of paclitaxel, the biocatalytic method can be imagined to advance through direct side chain attachment to the baccatin III core (see **Figure 1.7**, bottom panel). Additionally, this biocatalytic conversion would also short-circuit the protecting group chemistries and hazardous solvents obligatory for the synthetic route.

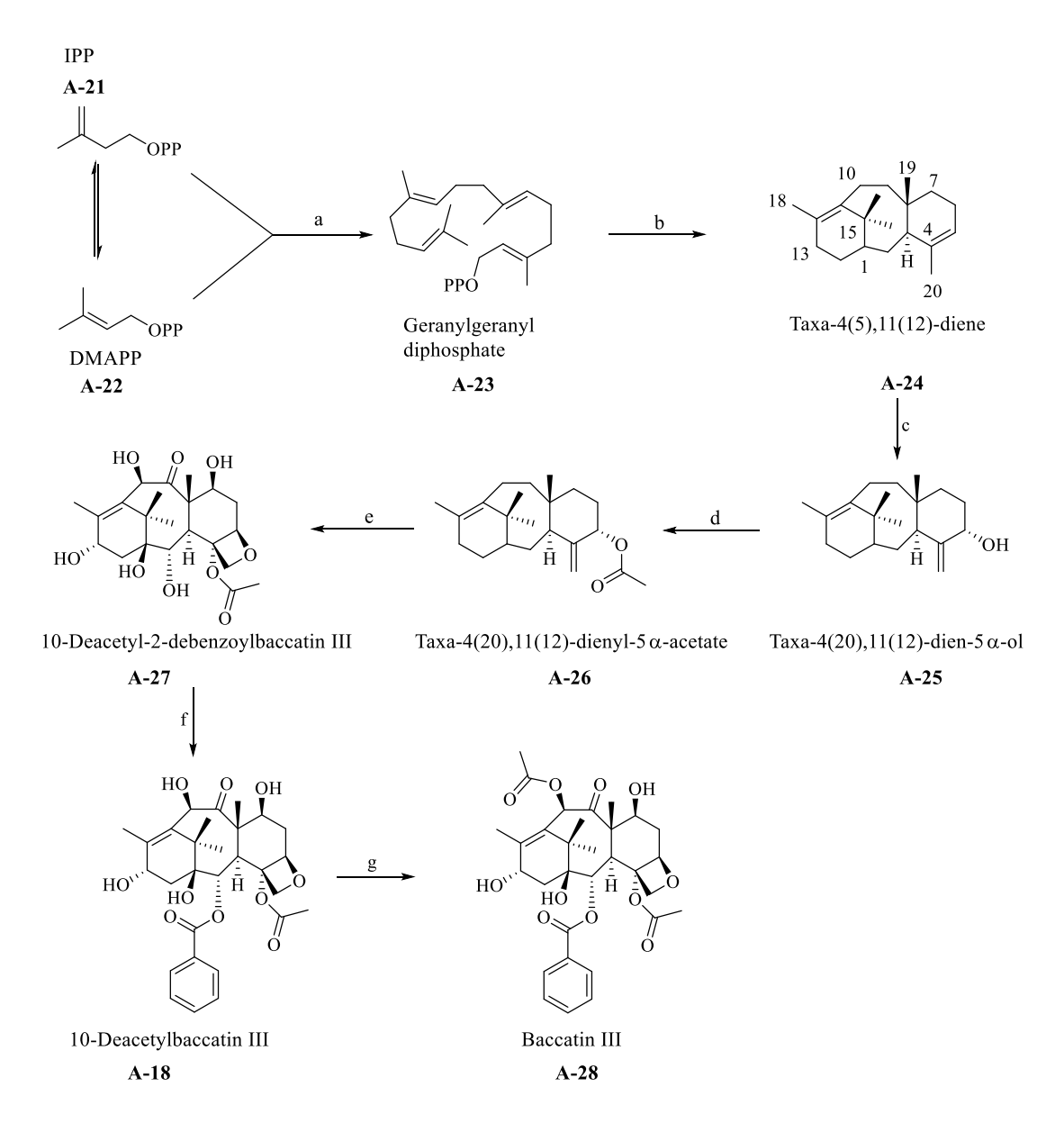


**Figure 1.6.** Biosynthetic pathway to paclitaxel starting from simple primary metabolite precursors to the baccatin III. The various enzyme catalyzed steps are shown: (a) geranylgeranyl diphosphate synthase, (b) GGDP cyclization by taxadiene synthase, (c) P450 oxygenase, (d) 5-O-acetylation by a taxa-5 $\alpha$ -ol acetyltransferase, (e) P450 oxygenases, (f) 2-O-benzoylation by a 2-O-debenzoylbaccatin III benzoyltransferase; (g) 10-O-acetylation by a 10-deacetylbaccatin III acyltransferase.

**Figure 1.7**. Biosynthesis of paclitaxel C-13 side chain (A) and the enzyme catalyzed transfer to the baccatin III (B); (h) the conversion of (2S)-α-phenylalanine to its (3R)-β isomer is catalyzed by an aminomutase (PAM); (i) phenylpropanoyl CoA is catalyzed by unidentified phenylalanyl CoA ligase in *Taxus* plants; (j) 13-*O*-acylation by a phenylpropanoyltransferase; (k) C-2'-oxidation by a P450 hydroxylase; (l) *N*-benzoylation by a taxane *N*-benzoyltransferase

# 1.4. In search for an Aminoacyl CoA Ligase

The protecting group chemistry used to synthesize the aminophenylpropanoyl CoA thioesters in the earlier paclitaxel biosynthetic studies<sup>80</sup> (**Figure 1.8**) can foreseeably be averted by employing a chemoselective carboxylate:CoA ligase during acyl CoA biosynthesis. Further, such a ligase

would avoid the solvent incompatibility of synthetic methods used to make acyl CoA thioesters when a hydrophobic acid anhydride is coupled with the hydrophilic CoA.

**Figure 1.8.** Synthesis of (2R,3S)—phenylisoserinyl CoA via the mixed anhydride intermediate. (i) CH<sub>2</sub>Cl<sub>2</sub>/THF, DMAP in CH<sub>2</sub>Cl<sub>2</sub>, benzyl chloroformate, rt, 1 h, 90% yield; (ii) CH<sub>3</sub>CN, DMAP in CH<sub>3</sub>CN, Boc<sub>2</sub>O, rt, 24 h, 20% yield; (iii) CH<sub>3</sub>OH, 6% Mg(OCH<sub>3</sub>)<sub>2</sub>, rt, 1 h, 80% yield; (iv) step (ii), 80% yield; (v) 2 M NaOH, 12 h; (vi) THF, ethyl chloroformate, rt, 1 h; (vii) CoASH in 0.4 M NaHCO<sub>3</sub>, *t*-BuOH, rt, 0.5 h; (viii) HCOOH, rt, 10% yield. Synthesis of α-, and β-phenylalanyl CoA were carried out similarly except for the 2-hydroxyl protection.

Earlier studies showed that *Taxus* 13-*O*-acyltransferase can attach a 3-amino-3-phenylpropanoyl by means of its synthetically-derived CoA thioester to the C13-hydroxyl of baccatin III to form an advanced precursor of paclitaxel. <sup>80</sup> The need to synthesize the 3-amino-3-phenylpropanoyl CoA thioesters is a major limitation towards the development of an *in vitro* biosynthetic approach to paclitaxel starting from baccatin III. To overcome this challenge, an alternative aminoacyl CoA ligase was proposed based on available literature as described in the following sections.

# 1.4.1. ANL Superfamily

Adenylation or adenylate forming enzymes are diverse in nature. They are involved in unique biological processes, for example biosynthesis of secondary metabolites, <sup>82</sup> lipid metabolism, <sup>83</sup> protein synthesis <sup>84</sup> and degradation, <sup>85</sup> DNA synthesis, <sup>86</sup> and CoA biosynthesis. <sup>87,88</sup> Over the years, a lot of research has been dedicated to identifying adenylation enzymes through mechanistic and structural studies. <sup>89-93</sup> The term ANL was coined to designate the three main subfamilies of adenylate-forming enzymes, namely <u>A</u>cyl CoA synthetases, <u>N</u>on-ribosomal peptide synthetases (NRPSs), and the <u>L</u>uciferase enzymes. <sup>94</sup>

The ANL enzymes catalyze two partial reactions; the initial adenylation half reaction starts with the binding of carboxylic acid and ATP to the enzyme active site, where the carboxylate attack on ATP–α-phosphate leads to the formation of acyl-adenylate intermediate. In the second half reaction, the acyl-AMP is attacked by a nucleophilic oxygen, sulfur, or nitrogen atom of an acceptor molecule leading to formation of an ester, thioester, or amide respectively. The acceptor molecule is either a small molecule such as CoA (in acyl CoA biosynthesis), a peptidyl carrier protein (PCP, also referred to as thiolation domain) in NRPSs or to the molecular oxygen in luciferase enzymes.

Besides the similar adenylation partial reaction mechanism in ANL superfamily, there is a high structural homology among many members. <sup>96</sup> The crystal structures of at least 16 proteins from ANL superfamily have been solved and used to identify core sequences that are highly conserved and the role they play in the catalysis. <sup>94</sup> Notably, the structures of these enzymes show a unique architecture; they have a large N-terminal and a small C-terminal domain. The roles of these two domains have been elucidated using gramicidin synthetase A (Grs1(Phe–A)) adenylation domain and acetyl CoA ligase structures. <sup>92,97</sup> It was shown that after the first half

reaction (shown with Grs1(Phe-A)), the enzyme adopts a different conformation for the second thiolation reaction through a 140° rotation of the C-terminal domain (shown with acetyl CoA ligase). 97 To validate this observation, a conserved Lys located at the C-terminal domain in the ANL superfamily was separately mutated to different residues in propionyl CoA synthetase and firefly luciferase. 98,99 A drastic reduction in enzyme activity for the first half acyl adenylation reaction was reported. 98,99 However, the Lys mutants in propionyl CoA synthetase converted propionyl-AMP to propionyl-CoA, hence further suggesting that the conserved Lys only catalyzes the first half reaction. 98 From the crystal structure, this Lys is located at 3 Å from the active site in Grs1(Phe-A). 92 Due to the close proximity to the carboxylate group of phenylalanine substrate, it was proposed that this residue is important in positioning the substrate at the right orientation for a nucleophilic attack on ATP α-phosphate. 92 However, in acetyl CoA ligase structure, the Lys at similar position was located 25 Å from the active site and was not shown to participate in the thiolation reaction. 97 The biochemical and structural data implicating the conserved Lys was suggested to support a novel catalytic strategy for ANL enzymes.<sup>94</sup> It has been proposed that the adenylate-forming enzymes adopt a Grs1(Phe-A)-like conformation in the first half adenylation reaction. Following the formation of the active acyl-adenylate intermediate, the enzyme adopts a different conformation for the second half reaction. 94-97

In NRPSs, it has been argued that the enzyme conformational changes also happen even though the thiol donor phosphopantetheine is covalently attached to the thiolation domain. <sup>94</sup> The crystal structure of surfactin A module (a NRPS enzyme), showed that the position of a serine residue on which the phosphopantetheine group (of PCP or thiolation domain) would attach was not positioned to allow shuttling of acyl group between domains in NRPS without a conformational change. <sup>100</sup> Therefore, the C-terminal domain would have to rotate to enable the

shuttling of the acyl moiety along the epimerization domain template to complete the catalytic reaction. 94,100

#### 1.4.2. Tyrocidine Synthetase A: Member of NRPS Enzyme Family

NRPSs are a family of enzymes involved in biosynthesis of important natural products, including antibiotics (e.g. tyrocidine, gramicidin S, penicillins, vancomycin, and bacitracin), <sup>101</sup> siderophores (e.g., enterobactin and mycobactin), <sup>102</sup> toxins (e.g. syringomycin and HC-toxin), <sup>103,104</sup> and immunosuppressive agents (e.g. rapamycin and cyclosporin). <sup>105-107</sup> Due to their importance and diversity, immense studies have been done to understand the biochemistry of this family of enzymes ranging from gene identity to structure elucidation. <sup>94,106,108,109</sup> NRPSs have been shown to consist of modules that are organized in an order corresponding to the amino acid sequence of the final product in a co-linear fashion (the so called co-linearity rule). <sup>108</sup> In this rule, each module is responsible for recognition, activation, modification (where necessary), and incorporation of a single amino acid into the growing peptide chain. <sup>108</sup>

Tyrocidine synthetase is a member of NRPS family and is naturally found in *Bacillus brevis* strain, a soil bacterium. It consists of ten modules designated TycA (contains module 1), TycB (contains modules 2 – 4), and TycC (contains modules 5 – 10). The starter module, TycA incorporates a D-phenylalanine, TycB incorporates three residues (L-proline, L-phenylalanine and D-phenylalanine) and TycC incorporates the remaining six residues (L-asparagine, L-glutamine, L-tyrosine, L-valine, ornithine, and L-leucine). The tyrocidine synthetase modules are further subdivided into domains, each responsible for one catalytic function (**Figure 1.9**). 110-112

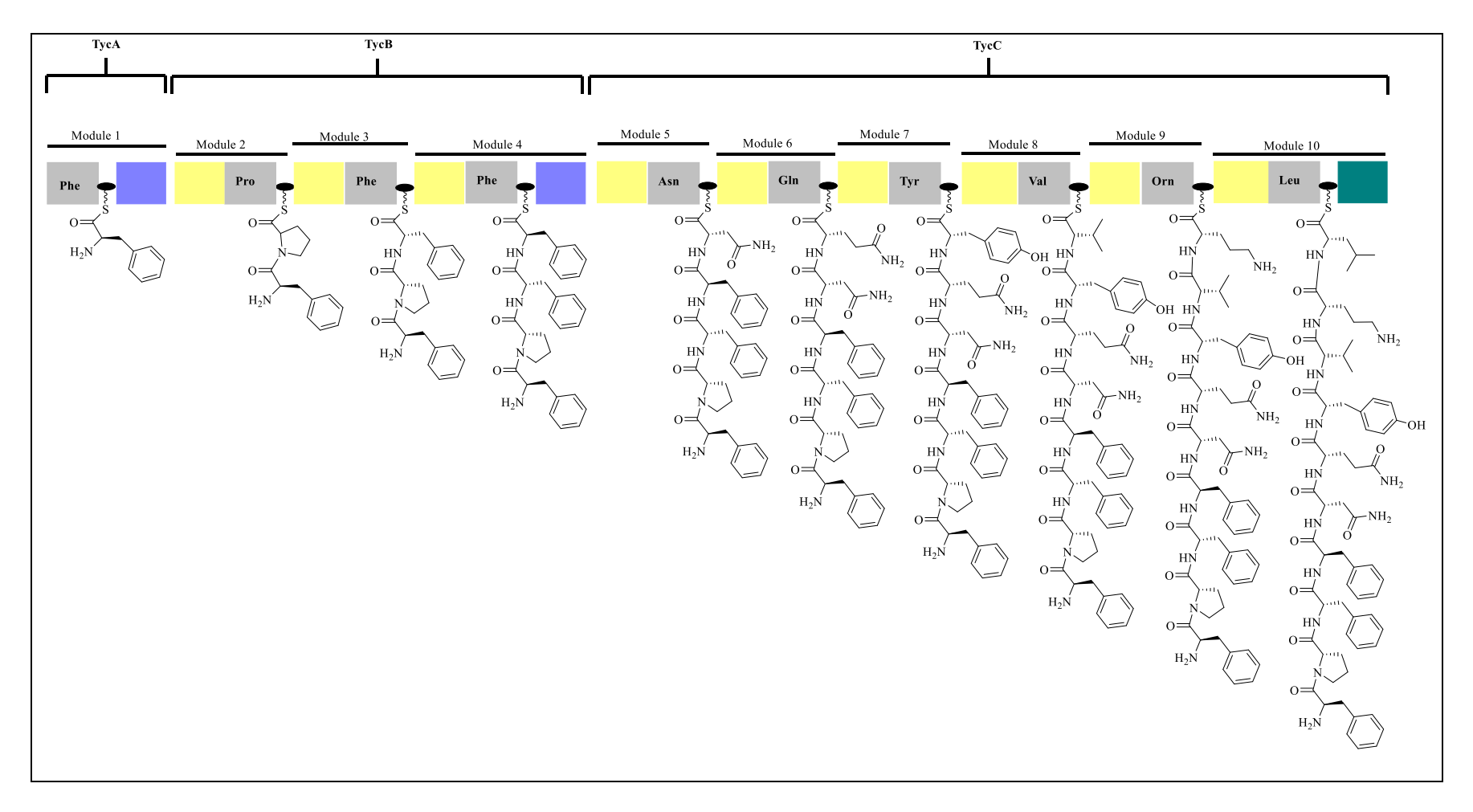


**Figure 1.9**. The tyrocidine synthetase cluster showing the three polypeptides; TycA, TycB, and TycC, that hosts one, three, and six modules respectively. Each of these modules contain necessary catalytic domains responsible for incorporation of a single amino acid residue into the growing peptide chain: Adenylation domain (**A**, grey), Thiolation domain (**T**, black oval), Condensation domain (**C**, yellow), Epimerization domain (**E**, blue), Thioesterase domain (**TE**, green). The figure is redrawn from Benoit & Florian (2009) with permission from John Wiley & Sons, copyright 2009.

#### 1.4.2.1. Adenylation (A) Domain

The A-domain (about 550 amino acids) bears the substrate recognition and activation site. A-domain activates its cognate amino acid into its adenylate form at the expense of ATP with loss of pyrophosphate (PPi). Due to its catalytic role and reaction mechanism, A-domain is classified under the ANL superfamily described in Section 1.4. He A-domains are structurally and functionally independent and catalyze the amino acid incorporation with similar specificity as the wild type enzyme (eg. TycA, consisting of adenylation, thiolation, and epimerization domains). Additionally, TycA adenylation domain exhibits broad substrate scope, a desirable feature in the synthesis of different aminoacyl—AMP derivatives. The aminoacyl—adenylate intermediates formed are then covalently bound to the enzyme through a thioester linkage to phophopantetheine moiety in the adjacent thiolation domain.

#### 1.4.2.2. Thiolation (T) Domain

Thiolation domains, also referred to as peptidyl carrier domains (PCP) are located downstream of the respective A-domain partner in tyrocidine synthetase cluster. <sup>116</sup> Each T-domain contains about 100 amino acids and hosts a conserved serine where a 4'-phosphopantetheine (4'-Ppant) cofactor is attached during post translational modification. <sup>114</sup> The conversion of T-domain from *apo* to *holo* form enzyme is mediated by a 4'-phosphopantetheine transferase that catalyzes the nucleophilic attack of a hydroxyl group of the highly conserved serine to the β-phosphate of CoA therefore transferring the Ppant moiety onto the T-domain (**Figure 1.10**). <sup>108</sup> The Ppant thiol attacks the aminoacyl-adenylate displacing the AMP to form a relatively stable aminoacyl-thioester intermediate (**Figure 1.11**).

HS 
$$\stackrel{\circ}{\underset{H}{\longrightarrow}}$$
  $\stackrel{\circ}{\underset{O}{\longrightarrow}}$   $\stackrel{\circ}{\underset{O}$ 

**Figure 1.10**. Scheme showing the conversion of *apo*-PCP (or T-domain) to *holo*-PCP. The 4'-Ppant-T (4'-phosphopantetheinyl transferase) catalyzes the nucleophilic attack of hydroxyl of a conserved serine residue (shown in the circle) on the α-phosphate of CoA hence transferring the Ppant moiety to the PCP (T-domain).

#### **1.4.2.3.** Epimerization (E) Domain

The E-domain belongs to a class of cofactor independent epimerases that catalyze the de- and reprotonation of  $C_{\alpha}$  of an enzyme bound aminoacyl–S-Ppant (in TycA) or peptidyl–S-Ppant (e.g in TycB, module 4). This domain is composed of ~450 amino acids and is embedded within each module that has been shown to convert an L to a D amino acid. At equilibrium, both L and D isomers are formed, but only the D isomer is accepted by the highly enantioselective condensation domain located on the adjacent module (**Figure 1.9**). As mentioned before, A- and T-domains are independent catalytic domains. On the contrary, the activity of E-domain relies on the presence of an upstream partner T-domain (**Figure 1.11**).

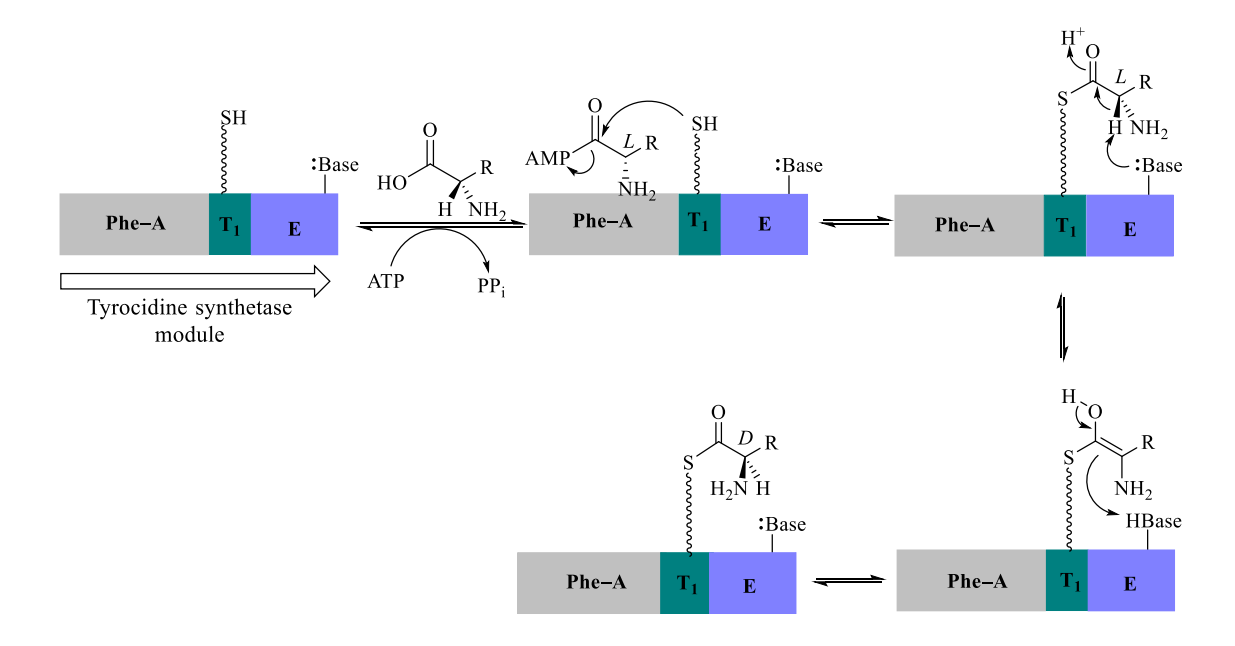


**Figure 1.11**. Schematic representation of the reactions catalyzed by various domains within a module in tyrocidine synthetase. Note: Epimerization (E) domain is present in modules 1 and 4 where the L amino acid is converted to the D isomer in tyrocidine synthetase. The 4'–Ppant precursor is shown as a wiggly line.

In NRPS enzymes, the chain elongation occurs through amide bond formation catalyzed by the condensation (C) domain.<sup>121</sup> The growing aminoacyl (or peptidyl) chain is covalently attached to the T-domain through a thioester bond and is transferred to the attacking aminoacyl residue which is in a thioester linkage to the downstream T-domain in the next module.<sup>121</sup> In tyrocidine synthetase, each elongation module has a CAT triad (**Figure 1.9**).<sup>108</sup> Once the necessary amino acid residues have been incorporated, the cyclization of the final product is catalyzed by the termination module referred to as thioesterase (TE) domain. The intramolecular cyclization of tyrosidine occurs when the amine group of D-phenylalanine, the first residue incorporated by TycA module attacks the thioester bond of the last residue (Leucine)<sup>122</sup> (see **Figure 1.9**).

Tyrocidine synthetase A (TycA) comprises of ATE domains that bind, activate and isomerize L-phenylalanine. Naturally, the A-domain of TycA has similar adenylation partial reaction as CoA ligases. The second partial thiolation reaction proceeds with different thiol donors (Ppant in TycA and CoA in acyl CoA ligases) that differentiate the two adenylases. The biosynthesis of paclitaxel in *Taxus* plants employs an aminoacyl CoA ligase in the pathway that remains unidentified. To develop and implement a novel semi-biosynthetic pathway towards paclitaxel production, there is a need to identify an alternative aminoacyl CoA ligase. TycA was selected as an ideal candidate due to the numerous similarities it shares with the acyl CoA ligases. Additionally, TycA activates phenylalanine which is structurally similar to the substrate needed for the biosynthesis of paclitaxel and its analogs. Furthermore, the broad substrate scope displayed further qualifies this adenylase as an ideal aminoacyl CoA ligase for investigation in the current study. The availability of structural information within the ANL super family provides a clue on the binding site architecture of close homologs which is handy in designing new substrates for TycA. P2.94,123

The projects aimed at elucidating the activity of TycA as a CoA ligase will be highlighted in the following three chapters. Chapter two will focus on characterization, activity assessment, and kinetic parameters of TycA (Phe–ATE) in the biosynthesis of aminophenylpropanoyl CoA products. Firstly, the development of TycA activity assays using *N*–acetylcysteamine as a thiol donor will be discussed. The comparison of TycA with other known aminoacyl CoA ligases will also be highlighted.

The focus of chapter three is dissecting TycA domains to understand their role in CoA ligase reaction and also the domains that are needed for maximum CoA ligase activity. The activity of TycA mutants (Phe–A and Phe–AT) with the aminophenylpropanoates will be

discussed. Additionally, the activity of these mutants will be analyzed using structural models that are based on close homologs of Tyc(Phe–A). Chapter four will focus on synthesis and characterization of isoserine analogs that are important motifs of paclitaxel derivatives. TycA substrate scope studies with the isoserine analogs will also be discussed. Chapter five will focus on engineering Tyc(Phe–AT) with the aim of expanding the substrate scope of this CoA ligase. Preliminary mutation studies will be discussed. In conclusion, future directions will be proposed based on the projects presented in the three chapters.

**REFERENCES** 

#### REFERENCES

- (1) Altmann, K.-H.; Gertsch, J. *Nat. Prod. Rep.* **2007**, *24*, 327.
- (2) Newman, D. J.; Cragg, G. M. J. Nat. Prod. **2007**, 70, 461.
- (3) Kingston, D. G. In Cancer Management in Man: Chemotherapy, Biological Therapy, Hyperthermia and Supporting Measures; Springer: 2011, p 3.
- (4) Weiss, R. B. In *Semin. Oncol.* 1992; Vol. 19, p 670.
- (5) Tacar, O.; Sriamornsak, P.; Dass, C. R. J. Pharm. Pharmacol. **2013**, 65, 157.
- (6) Arcamone, F. *Doxorubicin: anticancer antibiotics*; Elsevier, 2012.
- (7) Holowiecki, J.; Grosicki, S.; Giebel, S.; Robak, T.; Kyrcz-Krzemien, S.; Kuliczkowski, K.; Skotnicki, A. B.; Hellmann, A.; Sulek, K.; Dmoszynska, A. *J. Clin. Oncol.* **2012**, *30*, 2441.
- (8) Stock, W.; Johnson, J. L.; Stone, R. M.; Kolitz, J. E.; Powell, B. L.; Wetzler, M.; Westervelt, P.; Marcucci, G.; DeAngelo, D. J.; Vardiman, J. W. *Cancer* **2013**, *119*, 90.
- (9) Nagata, K.; Egashira, N.; Yamada, T.; Watanabe, H.; Yamauchi, Y.; Oishi, R. *Support. Care Cancer* **2012**, *20*, 951.
- (10) Minotti, G.; Menna, P.; Salvatorelli, E.; Cairo, G.; Gianni, L. *Pharmacol. Rev.* **2004**, *56*, 185.
- (11) Gardin, C.; Chevret, S.; Pautas, C.; Turlure, P.; Raffoux, E.; Thomas, X.; Quesnel, B.; de Revel, T.; de Botton, S.; Gachard, N. *J. Clin. Oncol.* **2013**, *31*, 321.
- (12) Arcamone, F.; Cassinelli, G. Curr. Med. Chem. **1998**, *5*, 391.
- (13) Arcamone, F.; Animati, F.; Capranico, G.; Lombardi, P.; Pratesi, G.; Manzini, S.; Supino, R.; Zunino, F. *Pharmacol. Ther.* **1997**, *76*, 117.
- (14) Sikic, B. I.; Rozencweig, M.; Carter, S. K. *Bleomycin chemotherapy*; Elsevier, 2013.
- (15) Crooke, S. T.; Bradner, W. T. Cancer Treat. Rev. **1976**, *3*, 121.
- (16) Verweij, J.; Pinedo, H. M. *Anti-cancer drugs* **1990**, *1*, 5.

- (17) Farber, S.; D'Angio, G.; Evans, A.; Mitus, A. J. Urol. **2002**, 168, 2560.
- (18) Demain, A. L.; Vaishnav, P. *Microbial Biotech.* **2011**, *4*, 687.
- (19) Cragg, G. M.; Newman, D. J. J. Ethnopharmacol. **2005**, 100, 72.
- (20) Pezzuto, J. M. Biochem. Pharmacol. 1997, 53, 121.
- (21) Newman, D. J.; Cragg, G. M. J. Nat. Prod. 2007, 70, 461.
- (22) Hartwell, J. Lloydia 1967, 30, 379.
- (23) Kelly, M.; Hartwell, J. L. J. Natl. Cancer Inst. 1954, 14, 967.
- (24) Kaplan, I. New Orleans Med. Surg. J. 1942, 94, 1941.
- (25) Imbert, T. F. *Biochimie* **1998**, *80*, 207.
- (26) Hande, K. Eur. J. Cancer **1998**, 34, 1514.
- (27) Gordaliza, M.; García, P. A.; Miguel del Corral, J. M.; Castro, M. A.; Gómez-Zurita, M. A. *Toxicon* **2004**, *44*, 441.
- (28) Damayanthi, Y.; Lown, J. W. Curr. Med. Chem. 1998, 5, 205.
- (29) Bohlin, L.; Rosen, B. *Drug Discov. Today* **1996**, *1*, 343.
- (30) Noble, R. L. *Biochem. Cell Biol.* **1990**, *68*, 1344.
- (31) DeVita, V. T.; Lawrence, T. S.; Rosenberg, S. A. *Cancer: principles and practice of oncology-advances in oncology*; Lippincott Williams & Wilkins, 2010; Vol. 1.
- (32) Coderch, C.; Morreale, A.; Gago, F. Curr. Med. Chem.: Anti-Cancer Agents **2012**, 12, 219.
- (33) Moudi, M.; Go, R.; Yien, C. Y. S.; Nazre, M. Int. J. Prev. Med. 2013, 4, 1231.
- (34) Wall, M. E.; Wani, M.; Cook, C.; Palmer, K. H.; McPhail, A.; Sim, G. *J. Am. Chem. Soc.* **1966**, 88, 3888.
- (35) Wall, M. E.; Wani, M. C. Cancer Res. 1995, 55, 753.
- (36) Gallo, R. C.; Whang-Peng, J.; Adamson, R. H. J. Natl. Cancer. Inst. 1971, 46, 789.

- (37) Pommier, Y.; Pourquier, P.; Urasaki, Y.; Wu, J.; Laco, G. S. *Drug Resist. Update* **1999**, 2, 307.
- (38) Hsiang, Y.-H.; Hertzberg, R.; Hecht, S.; Liu, L. *J. Biol. Chem.* **1985**, 260, 14873.
- (39) Staker, B. L.; Hjerrild, K.; Feese, M. D.; Behnke, C. A.; Burgin, A. B.; Stewart, L. *Proc. Natl. Acad. Sci. U. S. A.* **2002**, *99*, 15387.
- (40) Luzzio, M. J.; Besterman, J. M.; Emerson, D. L.; Evans, M. G.; Lackey, K.; Leitner, P. L.; McIntyre, G.; Morton, B.; Myers, P. L.; Peel, M. *J. Med. Chem.* **1995**, *38*, 395.
- (41) Pommier, Y. Nat. Rev. Cancer **2006**, 6, 789.
- (42) Wani, M. C.; Taylor, H. L.; Wall, M. E.; Coggon, P.; McPhail, A. T. *J. Am. Chem. Soc.* **1971**, *93*, 2325.
- (43) Itokawa, H.; Lee, K.-H. *Taxus: the genus Taxus*; CRC Press, 2003.
- (44) DeVita, V. T. N. Engl. J. Med. 2001, 344, 1335.
- (45) Viúdez, A.; Ramírez, N.; Hernández-García, I.; Carvalho, F. L.; Vera, R.; Hidalgo, M. *Crit. Rev. Oncol. Hematol.*, *92*, 166.
- (46) Kingston, D. In Anticancer Agents from Natural Products; CRC Press: 2005.
- (47) McGuire, W. P.; Rowinsky, E. K.; Rosenshein, N. B.; Grumbine, F. C.; Ettinger, D. S.; Armstrong, D. K.; Donehower, R. C. *Ann. Intern. Med.* **1989**, *111*, 273.
- (48) Markman, M.; Mekhail, T. M. Expert Opin. Pharmaco. 2002, 3, 755.
- (49) Hudis, C. Eur. J. Cancer Supplement **2003**, 1, 1.
- (50) Nowak, A.; Wilcken, N.; Stockler, M.; Hamilton, A.; Ghersi, D. *Lancet Oncol.* **2004**, *5*, 372.
- (51) Ramalingam, S.; Belani, C. P. Expert Opin. Pharmaco. 2004, 5, 1771.
- (52) Cai, J.; Zheng, T.; Masood, R.; Smith, D. L.; Hinton, D. R.; Kim, C. N.; Fang, G.; Bhalla, K.; Gill, P. S. *Sarcoma* **2000**, *4*, 37.
- (53) Schiff, P. B.; Fant, J.; Horwitz, S. B. *Nature* **1979**, 277, 665.
- (54) Suffness, M. Taxol: science and applications; CRC press, 1995; Vol. 22.

- (55) Sénilh, V.; Blechert, S.; Colin, M.; Guénard, D.; Picot, F.; Potier, P.; Varenne, P. *J. Nat. Prod.* **1984**, *47*, 131.
- (56) Denis, J. N.; Greene, A. E.; Guenard, D.; Gueritte-Voegelein, F.; Mangatal, L.; Potier, P. J. Am. Chem. Soc. 1988, 110, 5917.
- (57) Holton, R. A.; Biediger, R. J.; Boatman, P. D. *Taxol: science and applications* **1995**, 97.
- (58) Suffness, M. Taxol®: Science and applications; CRC press, 1995; Vol. 22.
- (59) Patel, R. N. Annu. Rev. Microbiol. 1998, 52, 361.
- (60) Tabata, H. Curr. Drug Targets **2006**, 7, 453.
- (61) Leone, L.; Roberts, S. In *Natural Products and Cancer Drug Discovery*; Koehn, F. E., Ed.; Springer New York: 2013, p 193.
- (62) Howat, S.; Park, B.; Oh, I. S.; Jin, Y.-W.; Lee, E.-K.; Loake, G. J. *N. Biotechnol.* **2014**, *31*, 242.
- (63) Malik, S.; Cusidó, R. M.; Mirjalili, M. H.; Moyano, E.; Palazón, J.; Bonfill, M. *Process Biochem.* **2011**, *46*, 23.
- (64) Smetanska, I. In *Food Biotechnol.*; Stahl, U., Donalies, U. B., Nevoigt, E., Eds.; Springer Berlin Heidelberg: 2008; Vol. 111, p 187.
- (65) Roberts, S.; Kolewe, M. *Nat. Biotech.* **2010**, 28, 1175.
- (66) Cusido, R. M.; Onrubia, M.; Sabater-Jara, A. B.; Moyano, E.; Bonfill, M.; Goossens, A.; Angeles Pedreño, M.; Palazon, J. *Biotechnol. Adv.* **2014**, *32*, 1157.
- (67) Miele, M.; Mumot, A.; Zappa, A.; Romano, P.; Ottaggio, L. *Phytochem. Rev.* **2012**, *11*, 211.
- (68) Bohlmann, J.; Keeling, C. I. *Plant J.* **2008**, *54*, 656.
- (69) Rose, W. Taxol: Science and Applications, Pharmacology and Toxicology **1995**, 8, 209.
- (70) Tewari, K.; Monk, B. *The 21st Century Handbook of Clinical Ovarian Cancer* **2015**, 165.
- (71) Rohmer, M.; Knani, M.; Simonin, P.; Sutter, B.; Sahm, H. *Biochem. J* **1993**, 295, 517.

- (72) Eisenreich, W.; Menhard, B.; Hylands, P. J.; Zenk, M. H.; Bacher, A. *Proc. Natl. Acad. Sci. U.S.A* **1996**, *93*, 6431.
- (73) Koepp, A. E.; Hezari, M.; Zajicek, J.; Vogel, B. S.; LaFever, R. E.; Lewis, N. G.; Croteau, R. *J. Biol. Chem.* **1995**, *270*, 8686.
- (74) Hezari, M.; Lewis, N. G.; Croteau, R. Arch. Biochem. Biophys. **1995**, 322, 437.
- (75) Floss, H. G.; Mocek, U. *Biosynthesis of taxol*; CRC Press: Boca Raton, FL, 1995.
- (76) Fleming, P. E.; Mocek, U.; Floss, H. G. J. Am. Chem. Soc. **1993**, 115, 805.
- (77) Jennewein, S.; Rithner, C. D.; Williams, R. M.; Croteau, R. B. *Proc. Natl. Acad. Sci. U. S. A.* **2001**, *98*, 13595.
- (78) Fleming, P. E.; Knaggs, A. R.; He, X.-G.; Mocek, U.; Floss, H. G. *J. Am. Chem. Soc.* **1994**, *116*, 4137.
- (79) Jennewein, S.; Wildung, M. R.; Chau, M.; Walker, K.; Croteau, R. *Proc. Natl. Acad. Sci. U. S. A.* **2004**, *101*, 9149.
- (80) Walker, K.; Fujisaki, S.; Long, R.; Croteau, R. *Proc. Natl. Acad. Sci. U. S. A.* **2002**, *99*, 12715.
- (81) Walker, K.; Long, R.; Croteau, R. *Proc. Natl. Acad. Sci. U. S. A.* **2002**, 99, 9166.
- (82) Sieber, S. A.; Marahiel, M. A. Chem. Rev. 2005, 105, 715.
- (83) Watkins, P. A. *Prog. Lipid Res.* **1997**, *36*, 55.
- (84) Ibba, M.; Söll, D. Annu. Rev. Biochem. **2000**, 69, 617.
- (85) Schulman, B. A.; Harper, J. W. Nat. Rev. Mol. Cell Biol. 2009, 10, 319.
- (86) Shuman, S. J. Biol. Chem. **2009**, 284, 17365.
- (87) Pankiewicz, K.; Chen, L.; Petrelli, R.; Felczak, K.; Gao, G.; Bonnac, L.; Yu, J.; Bennett, E. *Curr. Med. Chem.* **2008**, *15*, 650.
- (88) Webb, M. E.; Smith, A. G.; Abell, C. Nat. Prod. Rep. **2004**, 21, 695.
- (89) Kim, Y. S.; Kang, S. W. *Biochem. J* **1994**, 297, 327.
- (90) Lipmann, F. J. Biol. Chem. 1944, 155, 55.
- (91) Conti, E.; Franks, N. P.; Brick, P. Structure **1996**, 4, 287.

- (92) Conti, E.; Stachelhaus, T.; Marahiel, M. A.; Brick, P. Embo J. 1997, 16, 4174.
- (93) Babbitt, P. C.; Kenyon, G. L.; Martin, B. M.; Charest, H.; Slyvestre, M.; Scholten, J. D.; Chang, K. H.; Liang, P. H.; Dunaway-Mariano, D. *Biochemistry* **1992**, *31*, 5594.
- (94) Gulick, A. M. ACS Chem. Biol. 2009, 4, 811.
- (95) Reger, A. S.; Wu, R.; Dunaway-Mariano, D.; Gulick, A. M. *Biochemistry* **2008**, 47, 8016.
- (96) Linne, U.; Schäfer, A.; Stubbs, M. T.; Marahiel, M. A. *FEBS Lett.* **2007**, *581*, 905.
- (97) Reger, A. S.; Carney, J. M.; Gulick, A. M. *Biochemistry* **2007**, *46*, 6536.
- (98) Horswill, A. R.; Escalante-Semerena, J. C. *Biochemistry* **2002**, *41*, 2379.
- (99) Branchini, B. R.; Murtiashaw, M. H.; Magyar, R. A.; Anderson, S. M. *Biochemistry* **2000**, *39*, 5433.
- (100) Tanovic, A.; Samel, S. A.; Essen, L.-O.; Marahiel, M. A. *Science* **2008**, *321*, 659.
- (101) Luo, L. S.; Burkart, M. D.; Stachelhaus, T.; Walsh, C. T. J. Am. Chem. Soc. **2001**, 123, 11208.
- (102) Gehring, A. M.; Mori, I.; Walsh, C. T. *Biochemistry* **1998**, *37*, 2648.
- (103) Guenzi, E.; Galli, G.; Grgurina, I.; Gross, D. C.; Grandi, G. *J. Biol. Chem.* **1998**, 273, 32857.
- (104) Walton, J. D. *Phytochemistry* **2006**, *67*, 1406.
- (105) Schwecke, T.; Aparicio, J. F.; Molnar, I.; König, A.; Khaw, L. E.; Haydock, S.; Oliynyk, M.; Caffrey, P.; Cortes, J.; Lester, J. B. *Proc. Natl. Acad. Sci. U. S. A.* **1995**, *92*, 7839.
- (106) Stachelhaus, T.; Marahiel, M. A. FEMS Microbiol. Lett. 1995, 125, 3.
- (107) Dittmann, J.; Wenger, R. M.; Kleinkauf, H.; Lawen, A. J. Biol. Chem. **1994**, 269, 841.
- (108) Marahiel, M. A.; Stachelhaus, T.; Mootz, H. D. Chem. Rev. 1997, 97, 2651.
- (109) Stachelhaus, T.; Mootz, H. D.; Marahiel, M. A. Chem. Biol. **1999**, 6, 493.

- (110) Mootz, H. D.; Marahiel, M. A. J. Bacteriol. 1997, 179, 6843.
- (111) Mittenhuber, G.; Weckermann, R.; Marahiel, M. A. J. Bacteriol. 1989, 171, 4881.
- (112) Pfeifer, E.; Pavela-Vrancic, M.; von Doehren, H.; Kleinkauf, H. *Biochemistry* **1995**, *34*, 7450.
- (113) Stachelhaus, T.; Marahiel, M. A. J. Biol. Chem. 1995, 270, 6163.
- (114) Stachelhaus, T.; Huser, A.; Marahiel, M. A. Chem. Biol. 1996, 3, 913.
- (115) Schaffer, M. L.; Otten, L. G. J. Mol. Catal. B-Enzym. 2009, 59, 140.
- (116) Villiers, B. R. M.; Hollfelder, F. Chembiochem 2009, 10, 671.
- (117) Gocht, M.; Marahiel, M. A. J. Bacteriol. 1994, 176, 2654.
- (118) Samel, S. A.; Czodrowski, P.; Essen, L.-O. *Acta Crystallogr.*, *Sect. D: Biol. Crystallogr.* **2014**, *70*, 1442.
- (119) Stachelhaus, T.; Walsh, C. T. *Biochemistry* **2000**, *39*, 5775.
- (120) Linne, U.; Doekel, S.; Marahiel, M. A. Biochemistry 2001, 40, 15824.
- (121) Stachelhaus, T.; Mootz, H. D.; Bergendahl, V.; Marahiel, M. A. *J. Biol. Chem.* **1998**, *273*, 22773.
- (122) Trauger, J. W.; Kohli, R. M.; Mootz, H. D.; Marahiel, M. A.; Walsh, C. T. *Nature* **2000**, *407*, 215.
- (123) Wu, R.; Reger, A. S.; Lu, X.; Gulick, A. M.; Dunaway-Mariano, D. *Biochemistry* **2009**, *48*, 4115.

This Chapter is adapted (Muchiri, R.; Walker, Kevi	from our published in D. <i>Chem. Biol.</i> <b>2</b> 0	d work in the <b>012</b> , <i>19</i> , 679).	Journal of (	Chemistry &	k Biology
		20			

# 2. TYROCIDINE SYNTHETASE A (TycA) CATALYSIS IN THE BIOSYNTHESIS OF AMINOACYL COA AND AMINOACYL-N-ACETYLCYSTEAMINE

#### 2.1. Introduction

Tyrocidine synthetase A (TycA or Phe–ATE) is a member of the broad acyl-adenylate-forming enzyme family that includes numerous CoA ligases, including those that transfer CoA to acetate<sup>1</sup>, fatty acid,<sup>2</sup> coumarate,<sup>3</sup> *O*-succinylbenzoate, carnitine, bile acid, and benzoate.<sup>4,5</sup> During the CoA ligase catalysis, the acyl-adenylate intermediate, formed by nucleophilic attack of carboxylate substrate on α-phosphate group of ATP, serves as the acyl donor to the thiol group of CoA. Though alkanoyl-, alkenyl-, and aroyl CoA ligases have been extensively studied,<sup>6-10</sup> only few studies have been reported for the aminoacyl CoA ligases.<sup>11-13</sup>

TycA belongs to a non-ribosomal peptide synthetase (NRPS) family of enzymes that are characterized by a unique set of modular proteins. <sup>14</sup> Each module is responsible for incorporating a single amino acid substrate into a growing polypeptide chain through assistance of structurally independent domains that activate and condense the carboxyl substrate. <sup>15</sup> TycA consists of Adenylation (A), Thiolation (T), and Epimerization (E) domains (designated Phe–ATE). The Adomain recognizes and binds the amino acid, and then uses the cosubstrate ATP to adenylate the carboxylate of the substrate to form the aminoacyl adenylate. <sup>16</sup> The activated acyl moiety is then transferred to the sulfhydryl group of 4'-phosphopantetheine (Ppant) cofactor that is covalently bound to the adjacent thiolation domain. The latter cofactor is added during posttranslational modification of the apoprotein. <sup>17</sup>

Previous studies showed that Ppant is covalently tethered to a serine residue within a highly conserved motif within the thiolation domain, characterized by the term 'CoreT' residues

(GG[H,D]S[L,I].<sup>18</sup> The posttranslational modification is catalyzed by a CoA-dependent 4'-phosphopantetheinyl transferase. The Ppant cofactor is critical in tethering the acyl intermediate as a thioester in Tyc(Phe–ATE).<sup>17</sup> The covalently attached thioester intermediate is epimerized by the epimerization domain and acyl moiety is subsequently transferred to the downstream modules (**Figure 2.1**).<sup>19</sup> The E domains of NRPS catalyze isomerization reactions that involve catalytic transfer of protons that inverts stereochemistry.<sup>18</sup> This type of reaction traditionally follows the "minimal number rule", which defines reaction classes that use or may be thought to use one catalytic residue where theoretically two or more could be employed. For this rule, there is a dual economy in the use of catalytic groups for the epimerization reaction.<sup>20</sup>

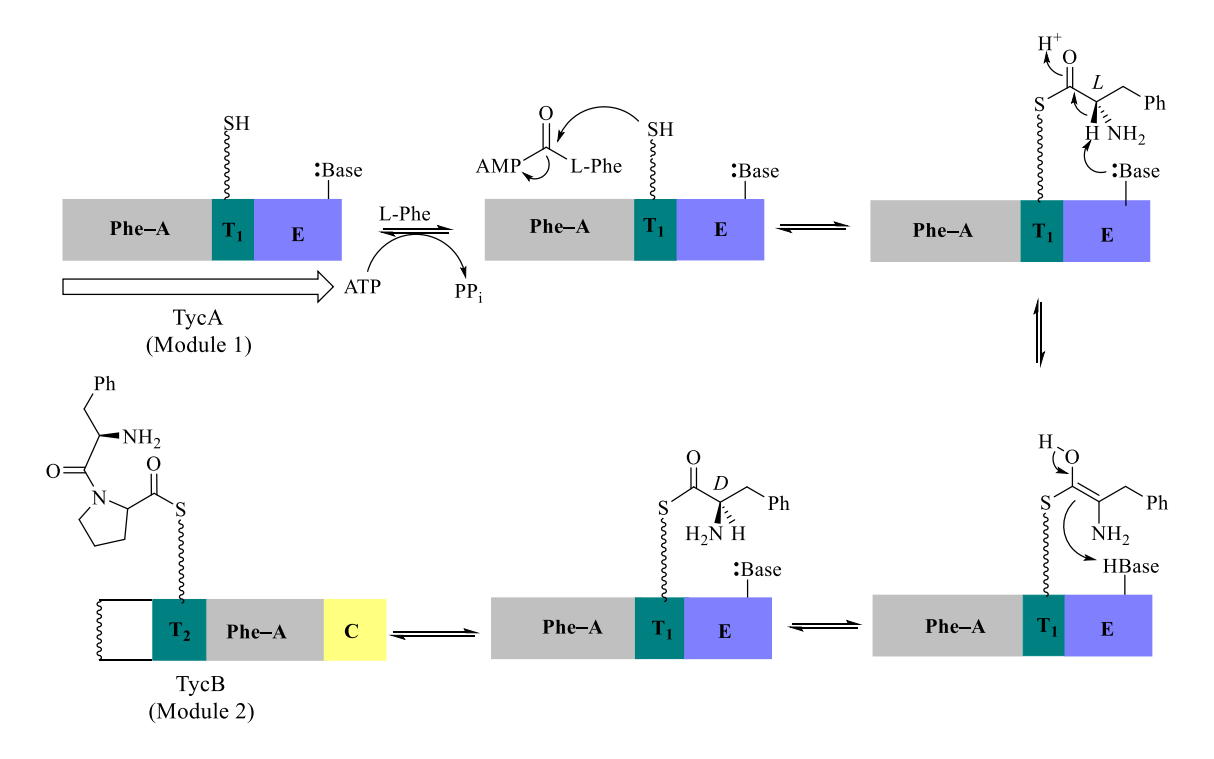


**Figure 2.1.** Scheme showing reactions catalyzed by TycA (Phe–ATE) domains. Domains shown are: Adenylation (**A**), Thiolation (**T**) [phosphopantetheinyl arm (squiggly line)] and the Epimerization (**E**) domains. The dipeptide intermediate is shown in the downstream TycB (module 2) comprised of the Condensation (**C**), Adenylation (**A**) and Thiolation (**T**) domains.

In NRPS epimerization domains, the cleavage of the  $C_{\alpha}$ -H bond yield an  $C_{\alpha}$ -carbanion intermediate that is envisioned to be stabilized by resonance, forming a planar thio- $\alpha$ -

carboxylate anion. Reprotonation on either face of the thiol carboxylate forms the L- or D- amino acid species (**Figure 2.2**). <sup>18,21</sup>

**Figure 2.2**. The stabilization of thiol- $\alpha$ -carboxylate intermediate formed during epimerization reaction in NRPS enzymes.

Two alternative enzyme catalysis mechanism are described to explain this proton transfer step.  $^{18}$  One mechanism employs two bases where one removes the  $C_{\alpha}$ -proton from the substrates and the conjugate acid of the second enzymatic base delivers a proton back to the opposite face (**Figure 2.3A**). By contrast, a one-base mechanism uses a single enzymatic base to both deprotonate and reprotonate the aminoacyl-S-Ppant (**Figure 2.3B**). To differentiate between these two mechanisms in gramicidin synthetase A (Grs1) epimerization domain, radiolabeled L- $[2-^3H]$ -phenylalanine was used as the substrate. In this study, there could be no label retained after epimerization to the D-phenylalanyl-S-phosphopantetheinyl-acyl enzyme product. The mechanistic evaluation of the epimerization step between L-phenylalanine to D-phenylalanine on the gramicidin synthetase pathway therefore supported a two base mechanism.  $^{18}$ 

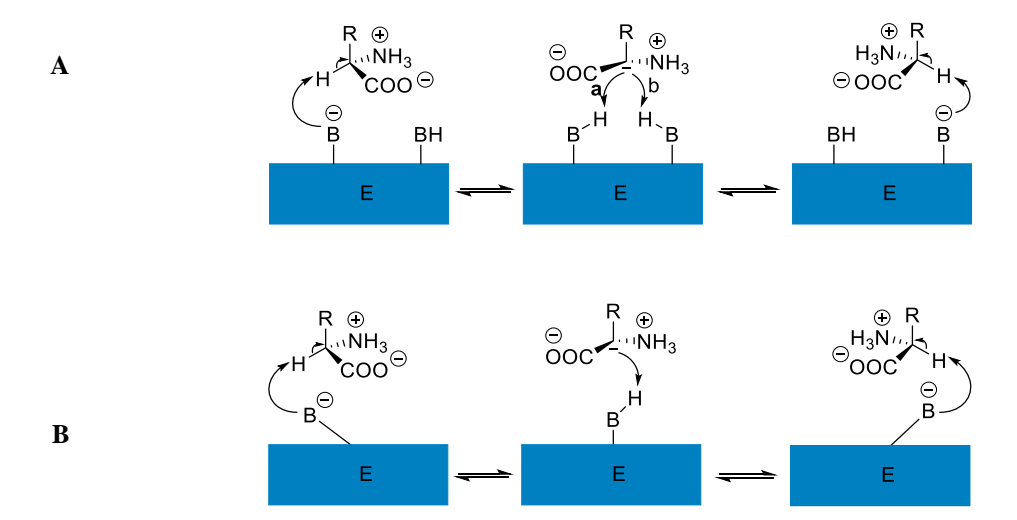


**Figure 2.3**. <u>Possible pathways for the epimerization at the alpha carbon:</u> **A)** Two base mechanism where one active site base abstracts the proton from the substrate and a second active site base donates a proton. **B)** One base mechanism for epimerization where only one residue abstracts and donates the proton.

On the tyrocidine NRPS pathway, the final product is formed through iterative processes on the three separate catalytic modules (TycA, TycB and TycC). Generally, the adenylation, thioesterification, and epimerization (where necessary) reaction cycle is repeated with the insertion of a condensation step that forms an amide bond between amino acid residues.<sup>22</sup> Despite the wealth of mechanistic information on the chemistry of the adenylation domains on NRPS pathways, overviewed in the previous discussion, application of this information towards making tyrocidine and gramicidin analogs is limited.<sup>23-26</sup> In earlier studies, the mechanistic similarities between CoA ligases and the A-domains of NRPSs were elucidated.<sup>27</sup> In one study, the enterobactin A-domain on the enterobactin NRPS pathway in *Escherichia coli* was shown to use CoA and pantetheine in thiol dependent release of PPi in place of the pendent Ppant moiety of the thiolation domain.<sup>28</sup> It remained unclear in this study whether the thiol surrogates were binding the active site during the catalysis of the thioester or were non-enzymatically scavenging the acyl-adenylate intermediate released from the active site. Encouraged by the earlier study where the A-domain of an NRPS pathway could apparently utilize CoA to form activated

thioesters, TycA (Phe–ATE) was examined to evaluate whether it could enzymatically catalyze the production of acyl CoAs under steady state conditions. The "CoA ligase"-like mechanism of TycA prompted us to explore this phenylpropanoid adenylation enzyme towards adenylating phenylisoserine for the potential production of phenylisoserinyl CoA that likely appears on the biosynthetic pathway of the anticancer drug paclitaxel (Taxol). 12 In earlier studies, the phenylpropanoyltransferase was characterized with amino phenylpropanoyl CoA substrates that were synthesized using a mixed anhydride and CoA.<sup>29</sup> This synthesis involved eight steps that required protection/deprotection of the amine group and was challenged by the solvent incompatibility of the hydrophobic acid anhydride intermediate and the hydrophilic CoA in the synthesis method (Figure 2.4). The protection/deprotection chemistry and the use of nonenvironmental friendly and expensive solvents and reagents can be avoided by employing a chemoselective carboxylate CoA ligase. To evaluate the substrate specificity and kinetics of the Tyc(Phe-AT) domains of the TycA module, the conserved serine residue on the T-domain was mutated to prevent enzyme bound phosphopantetheinylation of the substrate and decouple the activity of the Tyc(Phe-AT) from downstream epimerization domain. In addition, the earlier study indirectly assessed the formation of a thioester using exchange of <sup>32</sup>PPi into ATP to measure the reversible formation of an acyl AMP. Herein, electrospray ionization mass spectrometry was employed to directly evaluate the formation of the aminoacyl CoA and also evaluate the release, if any, of the aminoacyl AMP intermediate.

#### (A) Previous studies

#### (B) This study

**Figure 2.4**. Synthesis of (2*R*,3*S*)-phenylisoserinyl CoA via the mixed anhydride intermediate (panel A, see **Figure 1.8** in Chapter 1 for full scheme) and the proposed biosynthetic route in the current study (panel B).

### 2.2. Experimental

#### 2.2.1. Substrates, Reagents, and General Instrumentation

Bovine serum albumin was obtained from Thermo Scientific (Rockford, IL), N–Boc–(S)– $\alpha$ –phenylalanine and N–acetylcysteamine were purchased from Sigma Aldrich, N–Boc–(R,S)– $\beta$ –phenylalanine was obtained from Alfa Aesar, (Ward Hill, MA), N–Boc–(2R,3S)–phenylisoserine was obtained from PepTech Corp. (Burlington, MA), CoA was purchased from American Radiolabeled Chemicals Inc. (St. Louis, MO). All other reagents were obtained from Sigma–Aldrich and were used without further purification, unless noted otherwise.

A Varian Inova-300 or a Varian UnityPlus500 instrument was used to acquire <sup>1</sup>H- and <sup>13</sup>C-NMR. A Q-ToF Ultima electrospray ionization high resolution mass spectrometer (ESI–MS, Waters, Milford, MA) with a Waters 2795 HPLC and Quattro–Premier ESI–MS coupled with Acquity® UPLC system were used for mass spectral analysis.

## 2.2.2. Expression of wild-type TycA cDNA

A cDNA clone of wild-type tyrocidine synthetase A (TycA) was obtained as a gift from Florian Hollfelder (University of Cambridge, UK). Cloned cDNA tycA was inserted into a pSU18 vector, and the plasmid was designated pSU18–TycA–His encoding expression for a C–terminal His6–epitope. The plasmid was used to transform E. coli BL21 (DE3) that was grown in 2xYT medium (100 mL), containing Bacto Tryptone (1.6 g), Bacto Yeast Extract (1.0 g), NaCl (0.5 g), and chloramphenicol (20 mg·mL<sup>-1</sup>) at 37 °C for 12 h. A 10–mL aliquot of the seed culture was used to inoculate 2×YT medium (5 × 1 L). The bacteria were grown at 37 °C to OD600 ~0.6, at which time isopropyl  $\beta$ –D–1–thiogalactopyranoside (IPTG) was added to a final concentration of 0.5 mM, and the culture was grown for 4 h at 30 °C. The cells were pelleted by centrifugation (30 min, 4000g) at 4 °C, resuspended in Binding buffer (20 mM Tris–HCl buffer containing 0.5 M NaCl and 5 mM imidazole at pH 7.8), lysed by sonication (Misonix XL 2020 sonicator, Misonix, Inc. Farmingdale, NY), and then centrifuged at 15,000g for 0.5 h. The supernatant was decanted and centrifuged at 149,000g for 2 h to remove cell wall debris and light membranes.

### 2.2.3. Construction and Expression of the TycA–S563A Mutant

A S563A amino acid mutation was incorporated into the wild-type TycA clone by site—directed mutagenesis. The oligonucleotide primer pair used to incorporate the point mutation (underlined) was as follows: Forward primer S563A–For: 5'–TTA CTC GCT CGG CGG AGA TGC GAT CCA AGC GAT CCA GGT CG–3'; Reverse primer S563A–Rev: 5'–CGA CCT GGA TCG CTT GGA TCG CAT CTC CGC CGA GCG AGT AA–3'. The correct synthesis of the mutant cDNA was verified by DNA sequencing. The resultant plasmid encoding a C–terminal His–tag (designated pSU18–TycA–S563A–His) was used to transform *E. coli* BL21 (DE3) cells. A 10–

mL culture of *E. coli* transformed with the PSU18 vector was grown in 2xYT medium at 37 °C with chloramphenicol (20 mg·mL<sup>-1</sup>) selection for 12 h. The 10–mL inoculum was transferred to a new batch of 2×YT medium (1 L), as described previously for the expression of the wild–type *tycA* clone. The bacteria were grown at large–scale at 37 °C to OD<sub>600</sub> ~0.6, and the cDNA expression was induced by IPTG, and the culture was grown for 4 h at 30 °C. The cells were pelleted by centrifugation (30 min, 4000*g*) at 4 °C, resuspended in Binding buffer, lysed by sonication, and the corresponding soluble protein fraction was clarified by centrifugation as described earlier to remove cell-wall debris and light membranes.

#### 2.2.4. Purification and Characterization of TycA and the TycA–S563A Mutant

Crude soluble enzyme was separately isolated from bacteria expressing the wild-type *tycA* or *tycA*–S563A. Each fraction contained ~15 mg total protein as estimated by the Bradford protein assay. These fractions were independently loaded onto a nickel–nitrilotriacetic acid affinity column (Qiagen, Valencia, CA) and eluted according to the protocol described by the manufacturer. The column was washed with increasing concentration of imidazole (20 – 250 mM) in Binding buffer. SDS–PAGE slabs were loaded with aliquots from each fraction that eluted off the nickel-affinity column and stained with Coomassie Blue. Fractions that contained >95% pure protein corresponding to a molecular weight consistent with that of TycA and TycA–S563A at 123 kDa were combined. The enzymes eluted in ~50 mM imidazole (100 mL) were separately loaded into a Centriprep size–selective (100,000 MWCO) centrifugal filtration unit (Millipore, Billerica, MA). The protein solutions were concentrated to 1 mL, and the buffer was exchanged with the Assay buffer (50 mM HEPES containing 100 mM NaCl and 1 mM EDTA at pH 8.0) over several dilution/concentration cycles. The final purity of the enzyme was estimated

by SDS-PAGE with Coomassie Blue staining. The final protein concentration was determined by Beer's Law and measuring the absorbance of the protein solution at  $A_{280}$  on a NanoDrop ND1000 Spectrophotometer (Thermo Scientific, Wilmington, DE). The extinction coefficient  $(\varepsilon_{280} = 142685 \text{ M}^{-1} \text{ cm}^{-1})$  and the molecular weight of TycA and TycA-S563A were 122675 g·mol<sup>-1</sup> and 122,675 g·mol<sup>-1</sup>, respectively). The purified protein was stored at 5 mg/mL at -80 °C. The protein sequence of the isolated TycA recombinant protein was confirmed by LC/electrospray ionization tandem mass spectrometry analysis at the Michigan State University Proteomics Facility (Appendix I, **Figure I-11**).

### 2.2.5. Synthesis of Phenylalanyl AMP

Authentic phenylalanyl Amp was synthesized by a previously described procedure. Briefly, to (2S)-phenylalanine (330.4 mg, 2.0 mmol, 1.04 equiv) and adenosine monophosphate (666.6 mg, 1.92 mmol, 1 equiv) were added distilled water (3.2 mL) and pyridine (10.4 mL) in a glass-stoppered round bottom flask. The solution was acidified with 8 N HCl (0.25 mL) and stirred at 0 °C for 15 min. A solution of N, N'-dicyclohexylcarbodiimide (10.3 g, 50 mmol) dissolved in pyridine (12 mL) was then added, and the reaction was stirred for 4 h. The reaction was terminated by the addition of ice-cold acetone (150 mL), and after 1 min, the precipitate of crude (2S)-phenylalanyl adenylate was rapidly sunction filtered through 55 mm grade filter paper (Whatman, England) on a Büchner funnel. The filter cake was washed with ice-cold acetone/ethyl alcohol  $(60:40, 3 \times 5 \text{ mL})$ , then with ice-cold diethyl ether (5 mL), and air-dried on the filter. The crude product was suspended in ice-cold water (10 mL), rapidly vacuum filtered, and the insoluble particulates were washed with ice-cold water  $(3 \times 5 \text{ mL})$ . All of the filtrates were combined, and 8N HCl was added to adjust the pH to 3. Cold ethanol (100 mL) was then

added and the solution was stored at 4 °C for 18 h. The resultant precipitate was separated by centrifugation, washed with ethanol, and the sample was lyophilized to a residue (309 mg). The sample was judged to be 32% pure by LC–MS and was dissolved in  $D_2O$  and analyzed by NMR.  $^1H$ -NMR (500 MHz)  $\delta$ : 3.56 (m, 1H, C $\alpha$ -H), 4.18 (m, 2H, ribose 5'-H), 4.27 (m, 1H, ribose 4'-H), 4.43 (m, 2H, PheCH<sub>2</sub>), 6.04 (d, 1H, 1'-H), 7.09 (s, 5H, aromatic H), 8.20 (s, 1H, 3'-H), 8.42 (s, 1H, 8'-H).  $^{13}C$ -NMR (125 MHz)  $\delta$ : 167.0, 152.0, 149.0, 147.0, 144.0, 131.0, 130.0, 129.0, 120, 89.0, 75.0, 65.0, 56.0, 35.0.

# 2.2.6. Activity of wtTycA or mTycA with ATP and $\alpha$ -, $\beta$ -Phenylalanine, and (2R,3S)-Phenylisoserine

Substrates (S)— $\alpha$ —phenylalanine, (R)— $\beta$ —phenylalanine, and (2R,3S)—phenylisoserine (each at 1 mM) were separately incubated at 31 °C in single stopped—time (1 h) reactions containing 100 mM HEPES (pH 8.0), ATP (1 mM), MgCl<sub>2</sub> (3 mM) and TycA or TycA–S563A (20  $\mu$ g). Various control reactions were carried out in parallel under the same conditions used for assays containing enzyme, where TycA, TycA–S563A, ATP, or amino acid was omitted from the assay. The reactions were quenched by acidification to pH ~2 (10% formic acid in distilled water) and lyophilized to dryness. The resultant samples were separately dissolved in aqueous 0.01 M formic acid (100  $\mu$ L) and analyzed using a Quattro–Premier XE Mass Spectrometer coupled with Acquity® UPLC system fitted with a C18 Ascentis Express column (2.5 × 50 mm, 2.7  $\mu$ m) at 30 °C. An aliquot (10  $\mu$ L) of each sample was loaded onto the column and the analytes were eluted with a solvent gradient of acetonitrile (Solvent A) and 0.05% triethylamine in distilled water (Solvent B) (held at 2.5% Solvent A for 3.17 min, increased to 100% Solvent A over 5 sec with a 2–min hold, and then returned to 2.5% Solvent A over 5 sec with a 50–sec hold) at a flow

rate of 0.4 mL/min. The effluent from the column was directed to the mass spectrometer set to negative ion mode electrospray ionization with a scan range of m/z 50 – 1000.

After identifying productive substrates for TycA and TycA-S563A in the screen for AMP adenylases function, substrates (S)- $\alpha$ -phenylalanine and (R)- $\beta$ -phenylalanine (each at 1 mM) were separately incubated (at 31 °C) in 100 μL reactions containing 100 mM HEPES (pH 8.0), MgCl<sub>2</sub> (3 mM), and TycA or TycA-S563A (20 µg) and ATP (0.5, 1 or 2 mM), and the reactions were acid quenched (10% formic acid) at various time points (1, 5, 10, 15, 20, 30, 60, 90 and 120 min) to establish steady-state conditions. At the end of each reaction and prior to mass spectrometry analysis, acetyl CoA (1 µM) was added as the internal standard to each sample to correct for variations of the analyte. The products of the enzyme-catalyzed reaction were quantified by a liquid chromatography multiple reaction monitoring (MRM) mass spectrometry technique<sup>32</sup> on the Ouattro-Premier XE Mass Spectrometer coupled with Acquity® UPLC system fitted with a C18 Ascentis Express column (2.5  $\times$  50 mm, 2.7  $\mu$ m) at 30 °C. An aliquot (5 µL) of each sample was loaded onto the column and the analytes were eluted as described before, with a solvent gradient of acetonitrile (Solvent A) and 0.05% triethylamine in distilled water (Solvent B) (held at 2.5% Solvent A for 3.17 min, increased to 100% Solvent A over 5 sec with a 2-min hold, and then returned to 2.5% Solvent A over 5 sec with a 50-sec hold) at a flow rate of 0.4 mL/min.

The effluent from the chromatography column was directed to the mass spectrometer where the first quadrupole mass analyzer (in negative ion mode) was set to select for the  $[M - H]^-$  ion of a biosynthesized acyl AMP product. The selected ion was then directed to a collision gas chamber where the collision energy was optimized to maximize the abundance of a single signature fragment ion (m/z 134, the adenine fragment of the adenosine moiety) in negative ion

mode. This ion was resolved in the second quadrupole mass analyzer by MRM of the adenine transition ion fragment (m/z 134). The peak area of ion m/z 134 for each biosynthetic phenylpropionyl–AMP ester was converted to concentration units using linear regression of a dilution series of authentic adenine (at six intervals from 0.01 to 20  $\mu$ M) plotted against the corresponding ion abundance (m/z 134, in negative ion mode). The initial velocity ( $v_0$ ) of phenylpropionyl–AMP production was used to calculate  $K_{\rm M}$  and  $k_{\rm cat}$  according to the Michaelis–Menten equation ( $R^2$  was typically between 0.90 and 0.99).

### 2.2.7. Synthesis of Product Standards

### 2.2.7.1. Synthesis of $[S-(\alpha-\text{ and }\beta-\text{Phenylalanyl})-N-\text{acetyl}]$ cysteamine

**Figure 2.5**.  $(N-Boc)-(S)-\alpha$ —phenylalanyl SNAC (**B-2**) and  $(N-Boc)-(R/S)-\beta$ —phenylalanyl SNAC (**B-3**).

[S–((2S)– $\alpha$ – and (3R/S)– $\beta$ –phenylalanyl)–N–acetyl]cysteamine (i.e., (2S)– $\alpha$ – and (3R/S)– $\beta$ –phenylalanyl SNAC) were synthesized according to a reported procedure, with some modifications (**Figure 2.6**). <sup>33</sup>

**Figure 2.6**. Synthesis of (2S)–α–phenylalanyl SNAC. (i) a) DCC, HOBt, DIPEA, THF, rt. 45 min, b) *N*-acetylcysteamine, rt. 12 h. (ii) TFA/DCM, 0 °C, 4 h.

Generally, to N-Boc-(2S)- $\alpha$ - or N-Boc-(3R/S)- $\beta$ -phenylalanine (530 mg, 2 mmol) dissolved in tetrahydrofuran (15 – 18 mL) were added N,N'-dicyclohexylcarbodiimide (372.2 mg, 2 mmol), 1-hydroxybenzotriazole monohydrate (255.2 mg, 2 mmol), and N,Ndiisopropylethylamine (258.5, 8 mmol) at 24 °C. After 45 min, N-acetylcysteamine (NAC) (238 mg, 2 mmol) was added to the reaction, and the solution was stirred for ~12 h. The contents of the reaction mixture were gravity filtered (42.5 mm filter paper, Whatman, Stockton, NJ), and the filtrate was concentrated under vacuum. The resultant residue was then dissolved in ethylacetate (8 mL), and extracted with an equal volume of 10% aqueous NaHCO<sub>3</sub>. The aqueous layer was separated, and the organic layer was extracted twice more with 10% aqueous NaHCO<sub>3</sub>. The organic fraction was dried (Na<sub>2</sub>SO<sub>4</sub>), filtered, and the solvent was removed under vacuum. The resultant crude product was purified by silica gel flash chromatography (3 - 5%) gradient of methanol in chloroform). The fractions containing the product, as judged by the thin layer chromatography (TLC) ( $R_f = 0.15$  and 0.12 for N-Boc- $\alpha$ -phenylalanyl SNAC and N-Boc-(R/S)- $\beta$ -phenylalanyl SNAC, respectively) were combined separately and concentrated to afford N-Boc-α-phenylalanyl SNAC (552 mg, 75% isolated yield).  $^{1}$ H-NMR (500 MHz, DMSO- $d_6$ ) δ: 1.32 (s, 9H, methyl-H of Boc), 1.80 (s, 3H, H-1), 2.79 (dd,  $J = 13.7, 10.0, Hz, 1H, H_b-7$ ), 2.87  $(t, J = 6.0 \text{ Hz}, 2H, H_a - 4, H_b - 4), 3.05 \text{ (dd}, J = 13.9, 5.0 \text{ Hz}, 1H, H_a - 7), 3.15 \text{ (q, } J = 6.0, 2H, H_a - 3), 3.15 \text{ (q, } J = 6.0, 2H, H_a - 3), 3.15 \text{ (q, } J = 6.0, 2H, H_a - 3), 3.15 \text{ (q, } J = 6.0, 2H, H_a - 3), 3.15 \text{ (q, } J = 6.0, 2H, H_a - 3), 3.15 \text{ (q, } J = 6.0, 2H, H_a - 3), 3.15 \text{ (q, } J = 6.0, 2H, H_a - 3), 3.15 \text{ (q, } J = 6.0, 2H, H_a - 3), 3.15 \text{ (q, } J = 6.0, 2H, H_a - 3), 3.15 \text{ (q, } J = 6.0, 2H, H_a - 3), 3.15 \text{ (q, } J = 6.0, 2H, H_a - 3), 3.15 \text{ (q, } J = 6.0, 2H, H_a - 3), 3.15 \text{ (q, } J = 6.0, 2H, H_a - 3), 3.15 \text{ (q, } J = 6.0, 2H, H_a - 3), 3.15 \text{ (q, } J = 6.0, 2H, H_a - 3), 3.15 \text{ (q, } J = 6.0, 2H, H_a - 3), 3.15 \text{ (q, } J = 6.0, 2H, H_a - 3), 3.15 \text{ (q, } J = 6.0, 2H, H_a - 3), 3.15 \text{ (q, } J = 6.0, 2H, H_a - 3), 3.15 \text{ (q, } J = 6.0, 2H, H_a - 3), 3.15 \text{ (q, } J = 6.0, 2H, H_a - 3), 3.15 \text{ (q, } J = 6.0, 2H, H_a - 3), 3.15 \text{ (q, } J = 6.0, 2H, H_a - 3), 3.15 \text{ (q, } J = 6.0, 2H, H_a - 3), 3.15 \text{ (q, } J = 6.0, 2H, H_a - 3), 3.15 \text{ (q, } J = 6.0, 2H, H_a - 3), 3.15 \text{ (q, } J = 6.0, 2H, H_a - 3), 3.15 \text{ (q, } J = 6.0, 2H, H_a - 3), 3.15 \text{ (q, } J = 6.0, 2H, H_a - 3), 3.15 \text{ (q, } J = 6.0, 2H, H_a - 3), 3.15 \text{ (q, } J = 6.0, 2H, H_a - 3), 3.15 \text{ (q, } J = 6.0, 2H, H_a - 3), 3.15 \text{ (q, } J = 6.0, 2H, H_a - 3), 3.15 \text{ (q, } J = 6.0, 2H, H_a - 3), 3.15 \text{ (q, } J = 6.0, 2H, H_a - 3), 3.15 \text{ (q, } J = 6.0, 2H, H_a - 3), 3.15 \text{ (q, } J = 6.0, 2H, H_a - 3), 3.15 \text{ (q, } J = 6.0, 2H, H_a - 3), 3.15 \text{ (q, } J = 6.0, 2H, H_a - 3), 3.15 \text{ (q, } J = 6.0, 2H, H_a - 3), 3.15 \text{ (q, } J = 6.0, 2H, H_a - 3), 3.15 \text{ (q, } J = 6.0, 2H, H_a - 3), 3.15 \text{ (q, } J = 6.0, 2H, H_a - 3), 3.15 \text{ (q, } J = 6.0, 2H, H_a - 3), 3.15 \text{ (q, } J = 6.0, 2H, H_a - 3), 3.15 \text{ (q, } J = 6.0, 2H, H_a - 3), 3.15 \text{ (q, } J = 6.0, 2H, H_a - 3), 3.15 \text{ (q, } J = 6.0, 2H, H_a - 3), 3.15 \text{ (q, } J = 6.0, 2H, H_a - 3), 3.15 \text{ (q, } J = 6.0, 2H, H_a - 3), 3.15 \text{ (q, } J = 6.0, 2H, H_a - 3), 3.15 \text{ (q, } J = 6.0, 2H, H_a - 3), 3.15 \text{ (q, } J = 6.0, 2H,$  $H_b-3$ ), 4.23 (dd, J=7.2, 5.0 Hz, 1H, H-6), 7.20 – 7.27 (m, 5H, aromatic protons), 7.67 (d, J=

8.30 Hz, 1H, OC(O)NH); 8.04 (t, J = 5.0 Hz, 1H, C(O)NH). <sup>13</sup>C-NMR (125 MHz, DMSO– $d_6$ )  $\delta$ : 202.33, 169.91, 155.97, 138.20, 129.78, 128.86, 127.10, 79.34, 62.97, 42.85, 38.79, 28.83, 24.20, 23.22. N–Boc–(R/S)– $\beta$ –phenylalanyl SNAC (487 mg, 66% isolated yield). <sup>1</sup>H-NMR (500 MHz, DMSO– $d_6$ )  $\delta$ : 1.74 (s, 9H, methyl–H of Boc), 2.07 (s, 3H, H–1), 2.84 (ddd, J = 12.0, 6.0, 6.0Hz, 2H, H<sub>a</sub>–4, H<sub>b</sub>–4), 3.08 (q, J = 6.0, 2H, H<sub>a</sub>–3, H<sub>b</sub>–3), 3.29 (dd, J = 15.0, 9.0 Hz, 1H, H<sub>a</sub>–6), 3.40 (dd, J = 15.0, 5.5, 1H, H<sub>b</sub>–6), 4.64 (m, 1H, H–7), 7.37 – 7.51 (m, 5H, aromatic protons), 8.02 (t, J = 5.5 Hz, 1H, C(O)NH); 8.63 (bs, 1H, OC(O)NH). <sup>13</sup>C-NMR (125 MHz, DMSO– $d_6$ )  $\delta$ : 196.49, 169.89, 155.35, 143.11, 128.99, 127.75, 127.04, 78.67, 51.93, 50.72, 38.86, 28.89, 28.68, 23.22.

#### 2.2.7.2. *N*-deprotection of [S– $(\alpha$ – and $\beta$ –Phenylalanyl)]SNAC

**Figure 2.7**. (S)–α–Phenylalanyl SNAC (**B-7**) and β–Phenylalanyl SNAC·HCl salt (**B-8**)

To remove the Boc groups, N–Boc–(S)– $\alpha$ – and N–Boc–(R/S)– $\beta$ –phenylalanyl SNAC were separately dissolved in dichloromethane (4 mL), and trifluoroacetic acid was added dropwise over 4 h at 0 °C. The reaction progress was monitored by normal–phase thin layer chromatography (5% MeOH in CHCl<sub>3</sub>) until complete. Excess trifluoroacetic acid was removed prior to isolating the (S)– $\alpha$ –phenylalanyl SNAC by concentrating the reaction volume to 2 mL under vacuum, diluting 2–fold in dichloromethane, and then concentrating to 1 – 2 mL. This

dilution/concentration cycle was repeated three times, after which, the solvent was removed completely. To the residue containing (S)–α–phenylalanyl SNAC was added ethylacetate and dilute aqueous NaOH at 0 °C to partition the (S)–α–phenylalanyl SNAC and aqueous soluble contaminants, respectively. The organic layer was decanted and then removed under vacuum. Water (2 mL) was added to the remaining residue to which 1 M HCl (2 mL) was added at 0 °C. Ethylacetate was added  $(2 \times 2 \text{ mL})$  to extract any remaining t-butanol and SNAC, and the organic layer was decanted. The water fraction was lyophilized to yield (S)- $\alpha$ -phenylalanyl SNAC as the hydrochloride salt isolated at ~31% yield (90 mg), based on the N-Boc-protected starting material. <sup>1</sup>H-NMR (500 MHz, DMSO- $d_6$ )  $\delta$ : 1.78 (s, 3H, CH<sub>3</sub>), 2.69 (dd, J = 13.6, 10.0 Hz, 1H,  $H_b-7$ ), 2.80 (t, J=6.0 Hz, 2H,  $H_a-4$ ,  $H_b-4$ ), 2.96 (dd, J=13.6, 5.0 Hz, 1H,  $H_a-7$ ), 3.12  $(q, J = 6.0, 2H, H_a - 3, H_b - 3), 3.62 (dd, J = 8.7, 5.0 Hz, 1H, H - 6), 7.17 - 7.29 (m, 5H, aromatic)$ protons), 8.02 (t, J = 5.0 Hz, 1H, C(O)NH). <sup>13</sup>C-NMR (125 MHz, DMSO– $d_6$ )  $\delta$ : 204.13, 168.15, 136.78, 128.32, 127.16, 125.30, 61.74, 39.51, 37.22, 26.64, 21.53. The exact mass was determined in the positive ion mode on a Quadrupole Time-of-Flight Tandem Mass Spectrometer: observed m/z = 267.1164; calculated m/z = 267.1167 for  $C_{13}H_{19}N_2O_2S$ .

After deprotection of (N-Boc)–(R/S)– $\beta$ –phenylalanyl SNAC, excess trifluoroacetic acid was removed prior to isolating the product, as described above, except the residue was dissolved in 1 M HCl (2 mL, at 0 °C) to exchange the trifluoroacetate salt for the hydrochloride salt of the product. The sample was lyophilized to dryness, resulting in the hydrochloride salt of (R/S)– $\beta$ –phenylalanyl SNAC (48 mg, ~88.1% yield). <sup>1</sup>H-NMR (500 MHz, DMSO– $d_6$ )  $\delta$ : 1.74 (s, 3H, CH<sub>3</sub>), 2.84 (ddd, J = 12.0, 6.0, 6.0 Hz, 2H, H<sub>a</sub>–4, H<sub>b</sub>–4), 3.08 (q, J = 6.0 Hz, 2H, H<sub>a</sub>–3, H<sub>b</sub>–3), 3.31 (dd, J = 15.0, 9.0 Hz, 1H, H<sub>a</sub>–6), 3.45 (dd, J = 15.0, 5.5 Hz, 1H, H<sub>b</sub>–6), 4.63 (m, 1H, H–7), 7.35 – 7.60 (m, 5H, aromatic protons), 8.06 (t, J = 5.5 Hz, 1H, C(O)NH), 8.73 (bs, 3H, H<sub>3</sub>N).

<sup>13</sup>C-NMR (125 MHz, DMSO– $d_6$ ) δ: 196.47, 169.98, 137.06, 129.58, 129.37, 128.40, 51.64, 48.07, 38.57, 28.92, 23.18. The exact mass was determined in the positive ion mode on a Quadrupole Time–of–Flight Tandem Mass Spectrometer: observed m/z = 267.1173; calculated m/z = 267.1167 for C<sub>13</sub>H<sub>19</sub>N<sub>2</sub>O<sub>2</sub>S.

### 2.2.7.3. Synthesis of [(2R,3S)-Phenylalanyl]–N-acetylcysteamine

Figure 2.8. (2R,3S)–Phenylisoserinyl SNAC.

N–Boc–(2R,3S)–Phenylisoserinyl SNAC was synthesized according to the procedure described for the  $\alpha$ – and  $\beta$ –phenylalanyl SNAC thioesters. To N–Boc–(2R,3S)–phenylisoserine (100 mg, 0.36 mmol) dissolved in tetrahydrofuran (~6 mL) were added N,N′–dicyclohexylcarbodiimide (74.27 mg, 0.36 mmol), 1–hydroxybenzotriazole monohydrate (48.64 mg, 0.36 mmol), and N,N′–diisopropylethylamine (23.29 mg, 0.72 mmol) and stirred at 24 °C. After 45 min, NAC (85.61 mg, 0.72 mmol) was added to the reaction, and the solution was stirred for ~12 h. The reaction work up and purification were done as described above, resulting in crude N–Boc–(2R,3S)–phenylisoserinyl SNAC (40 mg, 29% yield), which was used for the N–Boc deprotection without further purification. To remove the Boc groups, N–Boc–(2R,3S)–phenylisoserinyl was dissolved in dichloromethane (4 mL), and trifluoroacetic acid was added dropwise over 3 h at 0 °C. The reaction progress was monitored by normal–phase TLC (5% methanol in chloroform) until complete. The work up was done according to the procedure

described for β–phenylalanyl SNAC resulting in (2R,3S)–phenylisoserinyl SNAC (20 mg, ~24% isolated yield). <sup>1</sup>H-NMR (500 MHz, DMSO– $d_6$ ) δ: 1.79 (s, 3H, CH<sub>3</sub>), 2.81 (m, 2H, H<sub>a</sub>–4, H<sub>b</sub>–4), 3.15 (m, 2H, H<sub>a</sub>–3, H<sub>b</sub>–3), 4.39 (d, J = 5.0 Hz, 1H, H–6), 4.45 (m, 1H, H–7), 7.40 – 7.47 (m, 5H, aromatic protons), 8.09 (t, J = 5.6 Hz, 1H, C(O)NH), 8.52 (br.d, J = 5.0 Hz, 2H, NH<sub>2</sub>). <sup>13</sup>C-NMR (125 MHz, DMSO– $d_6$ ) δ: 202.06, 170.14, 135.25, 129.51, 129.16, 128.77, 78.24, 57.09, 38.38, 28.33, 23.24. The exact mass was determined in the positive ion mode on a Quadrupole Time–of–Flight Tandem Mass Spectrometer: observed m/z = 283.1108; calculated m/z = 283.1116 for C<sub>13</sub>H<sub>19</sub>N<sub>2</sub>O<sub>3</sub>S.

# 2.2.8. Activity and Kinetic Evaluation of wtTycA or mTycA with NAcetylcysteamine and Aminophenylpropanoates

Substrates (S)— $\alpha$ —phenylalanine, (R)— $\beta$ —phenylalanine, and (2R,3S)—phenylisoserine (each at 1 mM) were separately incubated at 31 °C in single stopped—time (1 h) reactions containing 100 mM HEPES (pH 8.0), ATP (1 mM), MgCl<sub>2</sub> (3 mM), N—acetylcysteamine (1 mM), and TycA or TycA—S563A (100  $\mu$ g). Various control reactions were carried out in parallel under the same conditions used for the enzyme assay, where TycA or TycA—S563A, ATP, or N—acetylcysteamine was omitted from separate assays. The reactions were quenched by acidifying to pH ~2 (6 M HCl) and lyophilized to dryness. The resultant residues were separately dissolved in aqueous 0.01 M HCl (100  $\mu$ L) and analyzed using a Quadrupole Time—of—Flight Tandem Mass Spectrometer coupled with 2795 HPLC system fitted with a reverse—phase Halo C18 column (5 cm × 2.1 mm). An aliquot (10  $\mu$ L) of each sample was loaded onto the column (at 30 °C) and the analytes were eluted with a solvent gradient of 0 – 15% of acetonitrile (Solvent A) and 0.1% formic acid in distilled water (Solvent B) at a flow rate of 0.2 mL/min.

# 2.2.9. Kinetic Analysis of the *N*-acetylcysteamine Ligase Reaction Catalyzed by TycA or TycA-S563A

Substrates (S)- $\alpha$ -phenylalanine, (R)- $\beta$ -phenylalanine, and (2R,3S)-phenylisoserine (each at 1 mM) were separately incubated with TycA-S563A (20 µg) in the presence of Nacetylcysteamine (1 mM), ATP (1 mM), and Mg<sup>2+</sup> (3 mM) to establish steady-state conditions with respect to protein concentration and time at 31 °C. Under steady-state conditions, either (S)-phenylalanine, (R)- $\beta$ -phenylalanine, or (2R,3S)-phenylisoserine at 5, 10, 20, 40, 80, 160, 250, 500, 1000, and 2000 μM was separately incubated with TycA or TycA-S563A (20 μg), ATP (1 mM), Mg<sup>2+</sup> (3 mM), and N-acetylcysteamine (1 mM) in duplicate, single stopped-time (20 min) 100 μL assays. The reactions were quenched by acidifying to pH ~2 (10% formic acid in distilled water), and (N-Boc)-α-phenylalanyl SNAC or (N-Boc)-β-phenylalanyl SNAC (1  $\mu$ M) were added as an internal standard when (S)-phenylalanine or (R)- $\beta$ -phenylalanine was used as the substrate, respectively. The samples were analyzed on a Quattro-Premier XE Mass Spectrometer coupled with Acquity® UPLC system fitted with a C18 Ascentis® Express column  $(2.5 \times 50 \text{ mm}, 2.7 \mu\text{m})$  at 30 °C. An aliquot (5  $\mu$ L) of each sample was loaded onto the column and the analytes were eluted with a solvent gradient of acetonitrile (Solvent A) and 0.05% triethylamine in distilled water (Solvent B) (held at 2.5% Solvent A for 3.17 min, increased to 100% Solvent A over 5 sec with a 2-min hold, and then returned to 2.5% Solvent A over 5 sec with a 50-sec hold) at a flow rate of 0.4 mL/min. In brief, the effluent from the chromatography column was directed to the Quattro Premier ESI mass spectrometer, in multiple reaction monitoring (MRM) scan mode, to quantify the biosynthetic acyl SNAC products. The monitored fragment ions were m/z 120.06, 131.10, and 105.95 for (S)- $\alpha$ -phenylalanyl, (R)- $\beta$ -phenylalanyl, and (2R,3S)-phenylisoserinyl SNAC, respectively. A standard curve was used to convert the

peak area under the curve of the monitored fragment ion to concentration for each biosynthetic phenylpropionyl SNAC. Authentic (S)- $\alpha$ -phenylalanyl, (R/S)- $\beta$ -phenylalanyl and (2R,3S)-phenylisoserinyl SNAC were used to construct the standard curves by correlating the peak area under the curve of the monitored ion to concentration of the standard (at 0.16, 0.32, 0.63, 1.3, 2.5, 5, 10, 20, 40, 80, 160 and 320  $\mu$ M) using linear regression analysis. The initial velocity  $(v_0)$  production of (S)- $\alpha$ -phenylalanyl, (R/S)- $\beta$ -phenylalanyl, and (2R,3S)-phenylisoserinyl SNAC was plotted against substrate concentration and fit by non-linear regression to the Michaelis-Menten equation  $(R^2$  was typically 0.99) to calculate the Michaelis parameters  $(K_M$  and  $k_{cat})$ .

The  $K_{\rm M}$  values of TycA and TycA–S563A for N–acetylcysteamine was assessed by incubating each enzyme separately with (S)– $\alpha$ –phenylalanine (1 mM), MgCl<sub>2</sub> (3 mM), ATP (1 mM), and N–acetylcysteamine at 5, 10, 20, 40, 80, 160, 250, 500, 1000, and 2000  $\mu$ M at 31 °C for 20 min. The reactions were quenched by acidifying to pH ~2 (10% formic acid in distilled water), and internal standard (N–Boc)– $\alpha$ –phenylalanyl SNAC (1  $\mu$ M) was added to each sample to correct for variations of the analyte. The SNAC thioester products of the enzyme-catalyzed reaction were quantified by a liquid chromatography multiple reaction monitoring (MRM) mass spectrometry technique, and the monitored fragment ion (m/z 120.06) derived from the SNAC thioester analytes in the effluent were quantified identically to the procedure described earlier. The initial velocity  $(v_0)$  production of (R)– $\beta$ –phenylalanyl SNAC made in separate assays was plotted against substrate concentration and fit by non–linear regression to the Michaelis–Menten equation  $(R^2$  was typically between 0.97 and 0.99) to calculate the Michaelis constant  $(K_{\rm M})$ .

# 2.2.10. Activity and Kinetic Evaluation of wtTycA or mTycA as Ligases for Catalysis of $\alpha$ - and $\beta$ -Aminophenylpropanoyl CoA Thioesters

Similar experiments were done as described above for the N-acetylcysteamine ligase screen study, except CoA (1 mM) was used in place of N-acetylcysteamine with the substrates (S)- $\alpha$ phenylalanine, (R)- $\beta$ -phenylalanine and (2R,3S)-phenylisoserine in different 1 mL assays. The enzyme assays for this study contained 100 mM HEPES (pH 8.0), (S)-phenylalanine (1 mM), ATP (1 mM), MgCl<sub>2</sub> (3 mM), CoA (1 mM), and TycA or TycA-S563A (100 µg), and were incubated at 31 °C for 1 h. Various control reactions were carried out in parallel under the same conditions used for assays containing enzyme, where TycA, TycA-S563A, ATP, or CoA was omitted from the assay. The reactions were quenched by acidifying to pH ~2 (6 M HCl) and lyophilized to dryness. The resultant samples were separately dissolved in aqueous 0.01 M HCl (100 μL) and analyzed using a Quadrupole Time-of-Flight Tandem Mass Spectrometer coupled with a 2795 HPLC system fitted with a reverse-phase Halo C18 column (5 cm × 2.1 mm) at 30 °C. An aliquot (10 µL) of each sample was loaded onto the column and the analytes were eluted with a solvent gradient of 0 - 15% of acetonitrile (Solvent A) and 0.1% formic acid in distilled water (Solvent B) at a flow rate of 0.2 mL/min. The effluent from the column was directed to the mass spectrometer set to negative ion mode with a scan range of m/z 200 – 1000 atomic mass units. Authentic phenylalanyl CoA was used as a model to identify the diagnostic ion cleavage transitions of the three acyl CoA products.

# 2.2.11. Kinetic Analysis of the CoA Ligase Reaction Catalyzed by TycA and TycA-S563A

After identifying productive substrates for TycA and TycA–S563A in the screen for CoA ligase function, substrates (S)- $\alpha$ -phenylalanine, (R)- $\beta$ -phenylalanine, and (2R,3S)-phenylisoserine (each at 1 mM) were separately incubated in 100 µL reactions containing 100 mM HEPES (pH 8.0), ATP (1 mM), MgCl<sub>2</sub> (3 mM), CoA (1 mM), and TycA or TycA–S563A (50 μg or 20 μg) to establish steady–state conditions with respect to protein concentration and time at 31 °C. Under steady-state conditions, (S)-phenylalanine, (R)- $\beta$ -phenylalanine, and (2R,3S)phenylisoserine at 5, 10, 20, 40, 80, 160, 250, 500, 1000, and 2000 µM were separately incubated with TycA or TycA-S563A (20 µg) for 30 min. At the end of each reaction and prior to mass spectrometry analysis, acetyl CoA (1 µM) was added as the internal standard to each sample to correct for variations of the analyte. The products of the enzyme-catalyzed reaction were quantified by a liquid chromatography MRM mass spectrometry technique on the Quattro-Premier XE Mass Spectrometer coupled with Acquity® UPLC system fitted with a C18 Ascentis Express column (2.5  $\times$  50 mm, 2.7 µm) at 30 °C. An aliquot (5 µL) of each sample was loaded onto the column and the analytes were eluted with a solvent gradient of acetonitrile (Solvent A) and 0.05% triethylamine in distilled water (Solvent B) (held at 2.5% Solvent A for 3.17 min, increased to 100% Solvent A over 5 sec with a 2-min hold, and then returned to 2.5% Solvent A over 5 sec with a 50-sec hold) at a flow rate of 0.4 mL/min. The effluent from the chromatography column was directed to the mass spectrometer where the first quadrupole mass analyzer (in negative ion mode) was set to select for the molecular ion of a biosynthesized acyl CoA product. The selected ion was then directed to a collision gas chamber wherein the collision energy was optimized to maximize the abundance of a single signature fragment ion (m/z) 408.31) monitored in the second quadrupole mass analyzer (in negative ion mode). The monitored ion was derived by a fragmentation reaction in the CoA moiety that is characteristic of acyl CoA thioesters analyzed by this MRM method. The peak area under the curve of the monitored fragment ion m/z 408.31 corresponding to each biosynthetic phenylpropionyl CoA thioester was converted to concentration by comparing the peak area of the same ion produced by authentic CoA (at 0.048, 0.098, 0.20, 0.39, 0.78, 1.6, 3.1, 6.3, 12.5, 25, 50, 100  $\mu$ M) using linear regression analysis. The initial velocity ( $v_0$ ) production of (S)- $\alpha$ -phenylalanyl, (R)- $\beta$ -phenylalanyl and (2R,3S)-phenylisoserinyl CoA made in separate assays was plotted against substrate concentration and fit by non-linear regression to the Michaelis-Menten equation ( $R^2$  was between 0.85 and 0.99) to calculate the Michaelis parameters ( $K_M$  and  $k_{cat}$ ).

The  $K_{\rm M}$  values of TycA and TycA–S563A for CoA were assessed by incubating each enzyme separately with (S)– $\alpha$ –phenylalanine (1 mM), MgCl<sub>2</sub> (3 mM), ATP (1 mM), and CoA at 0.05, 0.1, 0.2, 0.4, 0.8, 1.6, 3.2, 6.4, 12.8, and 25.6  $\mu$ M at 31 °C for 20 min. At the end of each reaction and prior to mass spectrometry analysis, acetyl CoA (1  $\mu$ M) was added as the internal standard to each sample to correct for variations of the analyte. The products of the enzyme-catalyzed reaction were quantified by a liquid chromatography MRM mass spectrometry technique, and the monitored fragment ion (m/z 408.31) derived from the CoA thioester analytes in the effluent were quantified identically to the procedure described earlier herein. The initial velocity ( $v_0$ ) production of (S)– $\alpha$ –phenylalanyl CoA made in separate assays was plotted against substrate concentration and fit by non–linear regression to the Michaelis–Menten equation ( $R^2$  was typically between 0.92 and 0.98) to calculate the Michaelis constant ( $K_{\rm M}$ ).

#### 2.3. Results and Discussion

## 2.3.1. Expression and Purification of the ATE Tridomain of Wild-type and Mutant tycA

To test the TycA tridomain module as a potential CoA ligase, the wild-type tycA cDNA encoding the A-, T-, and E-domains was subcloned into a pSU18 vector and heterologously expressed as a His6-fusion in E. coli BL21(DE3). In addition, Ser563 of TycA was changed to Ala563 (TycA–S563A) since the T-domain of a functional TycA module requires covalent attachment of 4'-Ppant to a conserved serine by the 4'-Ppant transferase enzyme. This mutation was envisaged to prevent phosphopantetheinylation of the conserved serine residue by E. coli BL21, known to contain a phosphopantetheinyl transferase gene. The T-domain mutant TycA-S563A was expressed similarly. The isolated soluble enzymes were Ni-affinity purified to ~95%, based on SDS-PAGE analysis with Coomassie Blue staining, and the apparent molecular mass (123 kDa) was consistent with the theoretical value (Figure 2.9). Wild-type TycA and the S563A mutant (TycA-S563A) were expressed, isolated, and purified from a 5-L bacterial culture, resulting in ~15 mg of protein used for activity assays. In this preliminary study, the stereochemistry of the aminophenylpropanoyl side chain of the biosynthetic CoA and SNAC thioesters was not evaluated. Thus, it is unknown if the E-domain of TycA or TycA-S563A racemized a chiral center(s) of the CoA thioester products.

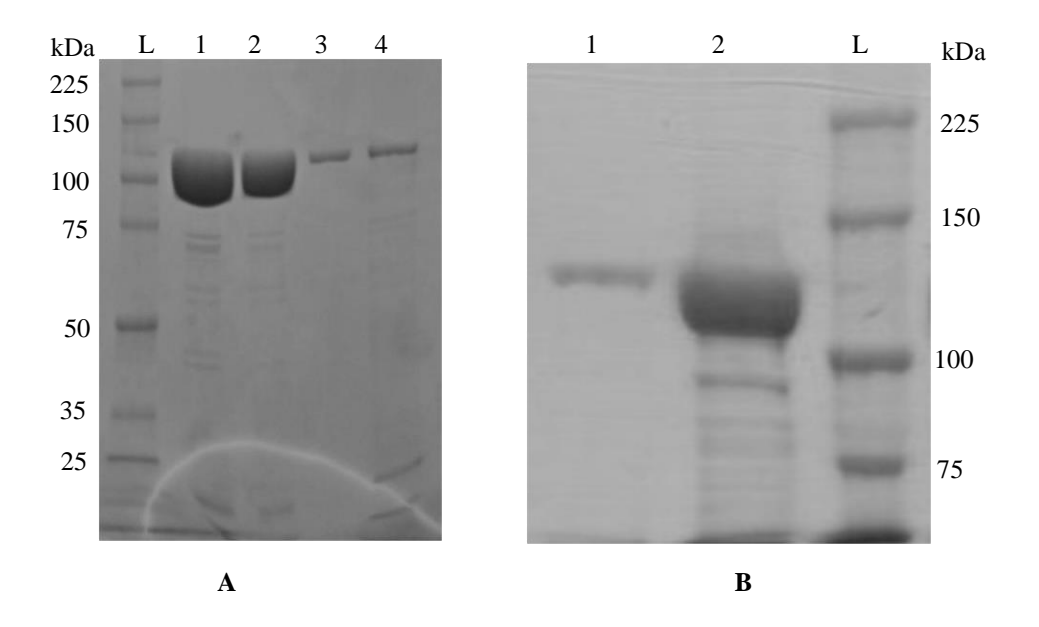


**Figure 2.9**. SDS-PAGE gel of fractions eluted from a Ni-affinity column containing TycA constructs. **A**) TycA-S563A mutant. Lane L: Molecular weight standards. A profile of the protein eluted in Binding buffer contained the following: Lane 1: 50 mM imidazole (fraction 1); Lane 2: 50 mM imidazole (fraction 2); Lane 3: 100 mM imidazole (fraction 3); and Lane 4: 200 mM imidazole (fraction 4). **B**) SDS-PAGE gel (7% acrylamide) of fractions eluted from a Ni-affinity column that contained the wild type TycA. Lane L: Molecular weight standards; Lanes 1 and 2 are profiles of protein eluted under the same conditions described previously for mTycA. Binding buffer: (0.5 M NaCl, 20 mM Tris-HCl, 5 mM imidazole, pH 7.8).

#### 2.3.2. Strategies used to Test the Activity of TycA with the Amino Acid Substrates

Numerous different assays have been developed to explore the adenylation step of ATP-dependent adenylation and thioesterification of aminoacyl substrates by TycA domain and the analogous Grs1 domain on the pathways to tyrocidines A – D and gramicidin. Radioactive assays were principally employed for members of this acyl-adenylation family, including assays for NRPS domains and CoA ligases. Since a bonafide end product is not derived from the amino acyl substrate for these partial biosynthetic reactions comprising a subset of the complete module matrix on NRPS pathways, creative cofactor/byproduct exchange assays were developed to assess the catalysis of the NRPS candidates. In an earlier study, the amino acid specificity of the adenylation domain of TycA was studied in a dynamic exchange assay using radioactive <sup>32</sup>PPi

and unlabeled ATP.<sup>34,35</sup> This assay relies on the dynamic reversibility of the amino acid adenylation (aminoacyl AMP), inorganic diphosphate (PPi) and ATP formed during catalysis. As the reaction progresses towards equilibrium, <sup>32</sup>PPi hydrolyzes the acyl AMP intermediate, forming AT<sup>32</sup>P. The specific activity of this end product was measured to assess the activity of TycA (**Figure 2.10**). This classical radiolabeled <sup>32</sup>PPi /ATP exchange assay has limitations: the costs of the <sup>32</sup>PPi and disposal of the radioactive material are high and  $t_{1/2}$  of <sup>32</sup>PPi is short (~14 days). Radiolabeled assay was also used in a benzoyl–CoA ligase assay.<sup>36</sup> In this study, radiolabeled benzoic acid, putative CoA ligase, and CoA were incubated together. At the completion of the reaction, the unreacted radiolabeled benzoic acid was separated by solvent extraction; the remaining radioactivity in the aqueous phase suggested the amount of biosynthesized benzoyl–CoA.

**Figure 2.10**. <u>Radioactivity-guided assay of the phenylalanine adenylation domain of TycA</u>. \*The reverse reaction forces the formation of radioactive ATP by addition of excess <sup>32</sup>PPi. This radioactive ATP is measured in the ATP-PPi exchange assay.

Another PPi/ATP exchange assay to characterize an adenylation enzyme uses  $\gamma^{-18}O_4$ -ATP pyrophosphate exchange as outlined in **Figure 2.11**.<sup>37</sup> In this assay, mass sensitive observation of PPi exchange was key in the detection of adenylation domain catalyzed mass shifts on either side of the exchange equation. As back exchange is favored by using PPi in excess, the authors introduced a heavy atom label in the starting material as  $\gamma^{-18}O_4$ -ATP. The

time-dependent formation of  $\gamma$ - $^{16}O_4$ -ATP and disappearance of  $\gamma$ - $^{18}O_4$ -ATP with an adenylase was measured by MALDI-ToF MS.

**Figure 2.11.** The exchange reaction, performed in the absence of thiolation activity, measures equilibrium exchange of  $\gamma^{-18}O_4$ -ATP with  $^{16}O_4$ -pyrophosphate. The newly formed  $\gamma^{-16}O_4$ -ATP is measured using MALDI–ToF to indirectly analyze and quantify the adenylation domain-catalyzed acyl adenylate product.

Another assay employed acyl CoA ligase<sup>11</sup> to characterize the acyl CoA formation by measuring the amount of AMP formed. The AMP analysis was done using a spectrophotometric HPLC method and authentic AMP standard.

In addition, studies on the gramicidin synthetase pathway analyzed the phenylalanyl adenylate intermediate by UV–HPLC.<sup>38</sup> The chromatographically isolated product was analyzed by MALDI–ToF MS. In the same study, the first evidence was provided for a covalently bound thioester (L–[<sup>14</sup>C]phenylalanyl–S–Ppant) and the isomer (D–[<sup>14</sup>C]phenylalanyl–S–Ppant) adducts on the gramicidin pathway. L–[<sup>14</sup>C]Phenylalanine substrate was incubated with wild-type *holo*–Grs1, containing the 4'–phosphopantetheinyl group, and the H753A mutant (with an inactive epimerization domain), in two separate assays. The time-course analysis for the phenylalanyl adenylate showed that about 75% of the initial L–[<sup>14</sup>C]Phe (450 mCi/mmol) was

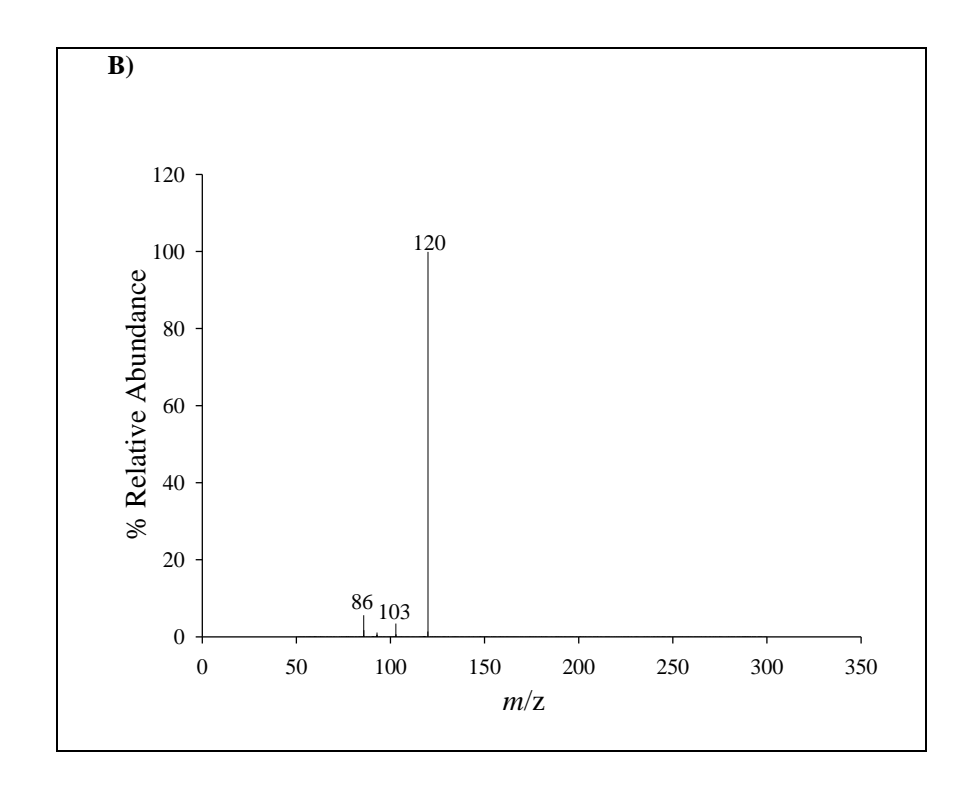
converted to L-[14C]Phe-AMP over 500 ms. The [14C]phenylalanyl-S-Ppant enzyme complexes were hydrolyzed by incubation with potassium hydroxide and extracted with methanol, followed by centrifugation to get rid of the enzyme. This product was then analyzed after the reaction reached equilibrium; ~85% of substrate L-[14C]Phe was converted to enzyme bound forms. 38 These previous studies with acyl adenylase enzyme family heavily relied on indirect assay methods to test for the formation of acyl adenylate intermediates or acyl CoA products. The PPi/ATP exchange assay provided information about the reversible formation of acyl adenylate intermediates. The assay was uninformative about the second half reaction catalyzed by adenylation domain. Secondly, direct analysis of acyl AMP formation is challenging due to slow release of this intermediate into the solution. As mentioned previously, studies on TycA showed that phenylalanyl AMP is formed when a TycA mutant, lacking a functional Ppant group was incubated with (S)-phenylalanine. This intermediate is proposed to be labile yet remains tightly bound in the TycA active site.<sup>38</sup> It is therefore proposed that the acyl AMP intermediate is susceptible to attack by a nucleophile added to the assay. The formation of the aminoacyl adenylate intermediate could be determined indirectly. Therefore, based on these initial studies, a hypothesis was proposed stating that the adenylation domain could potentially function as a potential amino phenylpropanoid:CoA ligase (Figure 2.12). In the current study, mass spectrometry was used to assess if TycA could make CoA thioesters of  $\alpha$ - and  $\beta$ -phenylalanine and (2R,3S)-phenylisoserine via their corresponding adenylate intermediate. To test this hypothesis, assays were developed for non-radiative detection of phenylpropanoyl AMP intermediates of TycA catalysis and for the CoA ligase function of TycA.

**Figure 2.12**. The proposed biosynthesis of aminoacyl CoAs using TycA. The TycA domains shown are: adenylation (A), thiolation domain (T) (without the Ppant group) and the epimerization (E) domain. CoA serves as a surrogate thiol donor to form the acyl CoA products.

# 2.3.3. Incubation of TycA and TycA-S563A with N-Acetylcysteamine and Phenylpropanoates

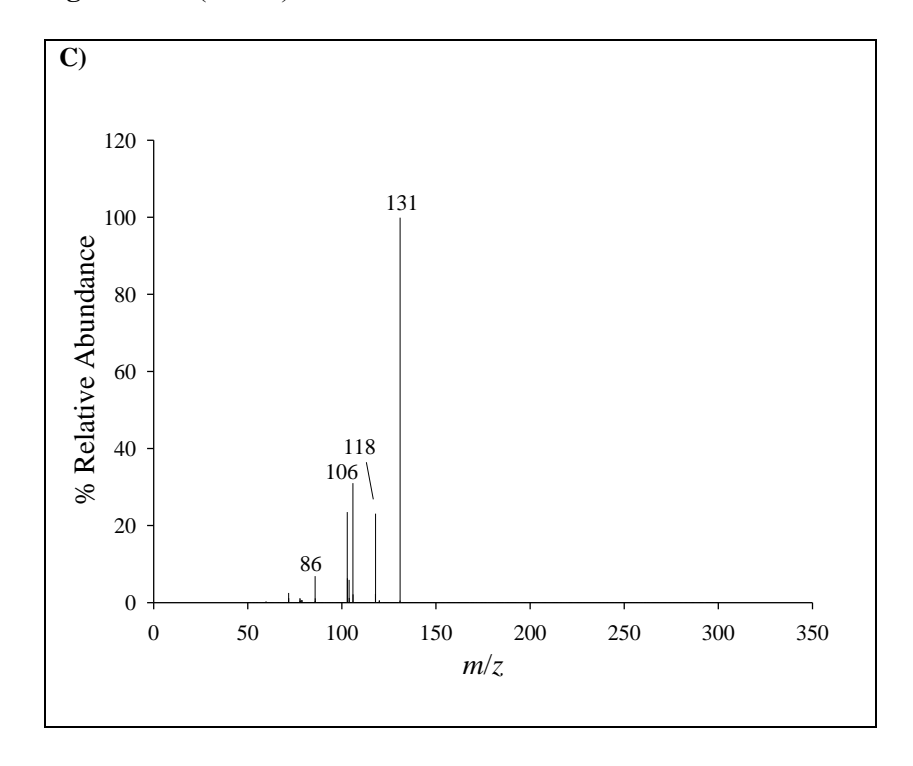
4'-Phosphopantetheinyl (i.e., the cysteamine amide of pantothenic acid) is attached posttranslationally to the T-domain of a functional TycA module. On the natural pathway, the thiol group of the phosphopantetheinyl serves as a nucleophile that reacts with the phenylalanyl AMP to form an intermediary pendent thioester on the tyrocidine pathway. In the present study, N-acetylcysteamine (NAC, the terminal fragment of CoA) was explored as a surrogate of TycA and TycA-S563A when incubated with (S)- $\alpha$ -phenylalanine, (R)- $\beta$ -phenylalanine, and (2R,3S)-phenylisoserine. N-acetylcysteamine was chosen for the initial activity development to conserve the expensive CoA, which was the ultimate thiol donor of interest.

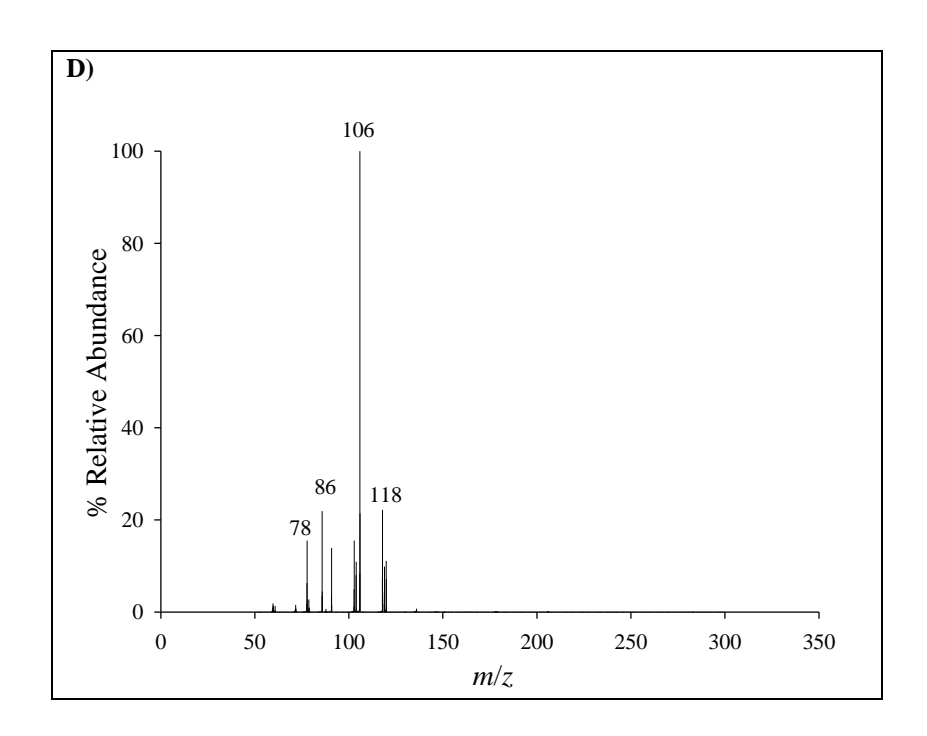
A mixture of TycA or TycA–S563A and N–acetylcysteamine (1 mM) was incubated with (S)- $\alpha$ -phenylalanine, (R)- $\beta$ -phenylalanine, or (2R,3S)-phenylisoserine for 1.5 h. The products of each assay were analyzed by LC-ESI-MS in scan mode. The first-stage mass spectrometer (positive ion mode) was set to select for the  $[M + H]^+$  ions consistent with  $\alpha$ - or  $\beta$ -phenylalanyl (m/z 267, eluting at 4.49 and 3.01 min, respectively) and <math>(2R,3S)-phenylisoserinyl-Nacetylcysteamine (i.e., phenylisoserinyl SNAC) (m/z 283, eluting at 2.32 min) (Appendix, Figures I-1, I-2, and I-3). These ions were directed to an inert gas collision chamber, and the resulting fragment ions were analyzed by the second-stage mass spectrometer set to positive ion scan mode (Figure 2.13). The sample in which TycA or TycA-S563A and NAC were incubated separately with  $(S)-\alpha$ -phenylalanine,  $(R)-\beta$ -phenylalanine, and (2R,3S)-phenylisoserine contained an analyte that generated fragment ions consistent with the respective phenylpropanoyl SNAC (Figure 2.13). The MS and MS/MS data for each biosynthetic SNAC matched those of authentic standards (see Appendix I, Figure I–7). Control assays that lacked the enzyme catalyst from the assay mixture, but included the necessary cofactors and phenylpropanoate substrate did not yield a detectable molecular ion consistent with the mass of  $\alpha$ - or  $\beta$ -phenylalanyl SNAC nor phenylisoserinyl SNAC.



**Figure 2.13**. The LC–ESI–MS–MS spectra of aminoacyl SNACs. m/z 267, 267, and 283 ([M + H]<sup>+</sup>) correspond to molecular ion of biosynthetic (S)– $\alpha$ –phenylalanyl SNAC (B), (R)– $\beta$ –phenylalanyl SNAC (C), and (2R,3S)–phenylisoserinyl SNAC (D). The fragments corresponding to the ions in the spectrum are shown in top panel (A).

**Figure 2.13**. (cont'd)





### 2.3.4. Kinetic Analyses of TycA and TycA–S563A with NAC

The  $k_{\text{cat}}$  and  $K_{\text{M}}$  values were calculated for TycA or TycA-S563A by incubating each catalyst separately with a dilution series of (S)- $\alpha$ -phenylalanine, (R)- $\beta$ -phenylalanine, or (2R,3S)phenylisoserine substrates in the presence of N-acetylcysteamine (1 mM) and the necessary reagents and cofactors. The reaction products were analyzed by a quantitative LC-ESI-MRM method, as before. In brief, the relative amount of each biosynthetic acyl SNAC was determined by the ion abundance of the transition ions  $[M + H]^+ \rightarrow m/z$  120,  $[M + H]^+ \rightarrow m/z$  131, and  $[M + H]^+ \rightarrow m/z$  106 for (S)- $\alpha$ -phenylalanyl, (R)- $\beta$ -phenylalanyl, and (2R,3S)-phenylisoserinyl SNAC thioesters, respectively. The transition ion abundance was converted to concentration units by linear regression analysis by charting the relationship between ion abundance and concentration of authentic phenylpropanoyl SNAC (the synthesis procedure is described in the experimental section) that matched the biosynthesized product. Analysis of the catalytic parameters for TycA and TycA-S563A with varying concentrations of NAC followed a similar trend as when incubated with CoA and the phenylpropanoates (described below). TycA was more catalytically efficient (6-fold higher) when NAC was incubated with (R)- $\beta$ -phenylalanine compared with the other phenylpropanoates (Table 2.1). The  $K_{\rm M}$  values of TycA–S563A were higher for all the phenylpropanoate and NAC cosubstrates compared with the  $K_{\mathrm{M}}$  values of TycA. The 15-fold slower turnover of (R)- $\beta$ -phenylalanine by TycA-S563A to its SNAC thioester caused the catalytic efficiency of the mutant enzyme to fall 30-fold lower compared with that of TycA for the same reaction. In addition, the efficiency of TycA–S563A for (S)– $\alpha$ – phenylalanine was increased 2.5-fold over that of TycA for the same substrate, due to its superior  $k_{\text{cat}}$  (Table 2.1). Despite the higher  $k_{\text{cat}}$  of TycA-S563A compared with that of TycA for the conversion of (2R,3S)-phenylisoserine to its acyl SNAC, the  $K_{\rm M}$  of TycA-S563A was 3.9-fold

greater than that of TycA for the same reaction. Thus, these latter parameters reduced the  $k_{\text{cat}}/K_{\text{M}}$  of TycA–S563A by 3.3-fold compared with that of TycA for the conversion of (2R,3S)–phenylisoserine to its SNAC thioester. The  $K_{\text{M}}$  for TycA and TycA–S563A with NAC were calculated by incubating each catalyst separately with a dilution series of NAC in the presence of (S)– $\alpha$ –phenylalanine at apparent saturation, Mg<sup>2+</sup>, and ATP. The catalytic efficiency of TycA was 2.5-fold higher than that of TycA–S563A incubated under the same conditions with varying concentrations of NAC.

### 2.3.5. Assessment of TycA and TycA–S563A for CoA Ligase Activity

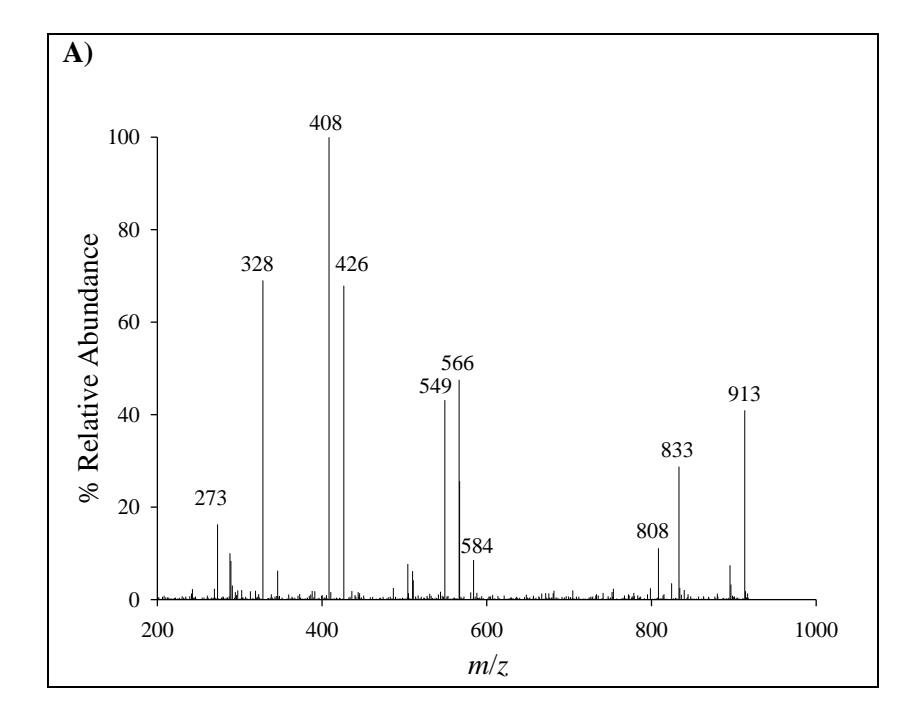
(S)–α–Phenylalanine, (R)–β–phenylalanine, and (2R,3S)–phenylisoserine were added separately to reaction mixtures containing heterologously expressed TycA or TycA–S563A with ATP, MgCl<sub>2</sub>, and CoA. The product mixtures were screened by LC–ESI–mass spectrometry in scan mode. The ESI–MS ion profiles in negative ion mode contained a diagnostic, negative molecular ion [M – H]<sup>-</sup> consistent with the value calculated for each putative α–phenylalanyl (m/z 913, eluting at 2.67 min), β–phenylalanyl (m/z 913, eluting at 2.47 min), and (2R,3S)–phenylisoserinyl CoA (m/z 929, eluting at 2.26 min) (Appendix, **Figures I–4, I–5 and I–7**).

To confirm the identity of the phenylpropanoyl CoA thioesters, the molecular ions were evaluated further by tandem MS/MS analysis by collision-induced dissociation of the  $[M - H]^-$  ion. The analytes in each of the samples incubated separately with (S)- $\alpha$ -phenylalanine, (R)- $\beta$ -phenylalanine, and (2R,3S)-phenylisoserine produced fragment ions consistent with the corresponding CoA thioesters (**Figures 2.14 and 2.15**). Control assays lacking TycA or TycA-S563A, ATP, or CoA from the appropriate enzyme assay mixture did not yield a detectable [M - R]-[M - R]-[

H] ion consistent with the mass of  $\alpha$ -phenylalanyl,  $\beta$ -phenylalanyl, nor phenylisoserinyl CoA, as expected for a ATP/Mg<sup>2+</sup> – dependent CoA ligase (see Appendix, **Figure I–8**).

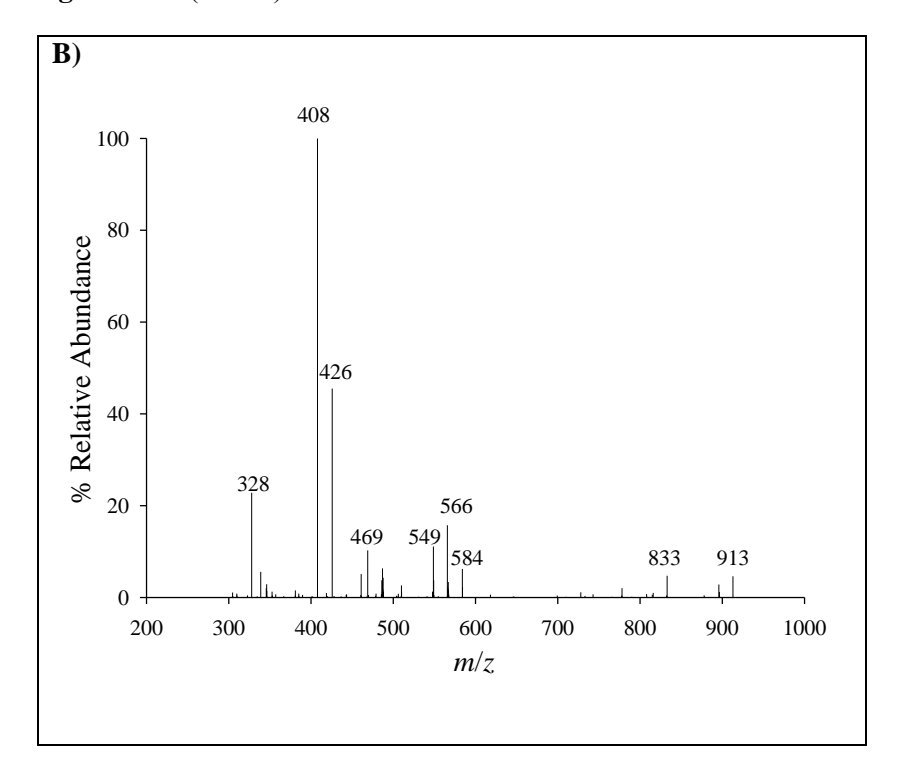
**Figure 2.14.** Molecular fragment ions profile resulting from LC–ESI–MS/MS of biosynthetic aminoacyl CoAs: (S)– $\alpha$ –phenylalanyl CoA (m/z 913), (R)– $\beta$ –phenylalanyl CoA (m/z 913), and (2R,3S)–phenylisoserinyl CoA (m/z 929).

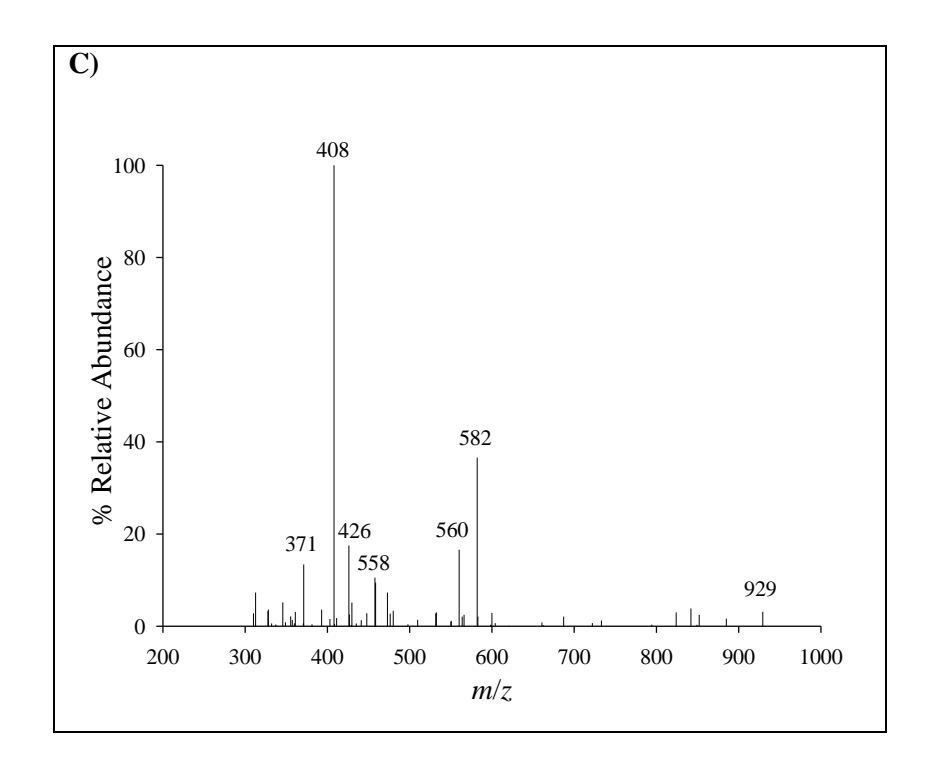
Figure 2.14. (cont'd)



**Figure 2.15**. The LC-ESI-MS-MS spectra of biosynthetic aminoacyl CoAs. m/z 913, 913, and 929 are ions corresponding to the biosynthetic (S)- $\alpha$ -phenylalanyl CoA (A), (R)- $\beta$ -phenylalanyl CoA (B), and (2R,3S)-phenylisoserinyl CoA (C). The molecular fragments corresponding to the ions in the spectrums are shown in **Figure 2.14** above.

**Figure 2.15**. (cont'd)





### 2.3.6. Kinetic Analyses of TycA and TycA–S563A with Phenylpropanoates and CoA

The kinetic parameters of TycA and TycA-S563A were calculated by separately incubating each catalyst with a varying concentration of (S)- $\alpha$ -phenylalanine, (R)- $\beta$ -phenylalanine, or (2R,3S)phenylisoserine substrates in the presence of necessary cofactors and Mg2+. Aliquots from reactions containing TycA or TycA-S563A were quenched by acidification to pH 2. The resulting CoA thioester products were analyzed by a quantitative LC-ESI-MRM method to detect the  $[M-H]^- \rightarrow m/z$  408 transition, common to each phenylpropanoyl CoA used in this study. The abundance of the transition ion was converted to concentration units by linear regression (using CoA as the quantitation standard). The catalytic efficiencies of TycA with CoA and each amino acid were within the same order of magnitude as when SNAC was used. The higher  $k_{\text{cat}}$  of TycA for (R)- $\beta$ -phenylalanine over the other amino acids tested coupled with a  $K_{\text{M}}$ value similar to that for the other phenylpropanoate substrates resulted in a 5- and 10- fold higher catalytic preference of TycA for (R)- $\beta$ -phenylalanine than for (S)- $\alpha$ -phenylalanine and (2R,3S)phenylisoserine, respectively. The  $K_{\rm M}$  of TycA–S563A followed a similar trend as that of TycA and was slightly lower when incubated with the natural substrate (S)- $\alpha$ -phenylalanine compared to the non-natural (R)- $\beta$ -phenylalanine, yet had a nearly 6-fold higher  $K_{\rm M}$  for (2R,3S)phenylisoserine (**Table 2.1**). The catalytic efficiency of TycA–S563A with (R)– $\beta$ –phenylalanine was highest among the amino phenylpropanoates tested. Similarly, the kinetic parameters for TycA and TycA-S563A with a dilution series of CoA were calculated by incubating each catalyst separately in the presence of (S)- $\alpha$ -phenylalanine at 1 mM. The resulting CoA thioester product was analyzed by a quantitative LC-ESI-MRM method, as before. The  $K_{\rm M}$  value of TycA was 2- fold higher compared to the mutant, hence resulting in a 2.5-fold lower catalytic efficiency of TycA for CoA compared to TycA–S563A.

**Table 2.1.** Steady state kinetic analysis of TycA and TycA–S563A with phenylpropanoids, CoA, and *N*–acetylcvsteamine.

CoA, and N-acetylcysteamine							
TycA							
Substrate	$K_{\rm M}$ ( $\mu$ M)	$k_{\rm cat}({\rm min}^{-1})$	$k_{\rm cat}/K_{\rm M}~({\rm s}^{-1}\cdot{\rm M}^{-1})$				
(S)–α–Phenylalanine	$41.9 \pm 2.0$	$0.25 \pm 0.01$	$99.4 \pm 6.2$				
(R)–β–Phenylalanine	$50.6 \pm 7.9$	$1.6 \pm 0.3$	$527 \pm 129$				
(2R,3S)–Phenylisoserine	$89.3 \pm 15.0$	$0.25 \pm 0.02$	$46.7 \pm 8.7$				
CoA <sup>a</sup>	$1976 \pm 175$	$0.75 \pm 0.05$	$6.3 \pm 0.7$				
TycA-S563A							
(S)–α–Phenylalanine	$33.9 \pm 4.0$	$0.69 \pm 0.08$	$339 \pm 56$				
(R)–β–Phenylalanine	$62.3 \pm 1.0$	$3.00 \pm 0.04$	$803 \pm 17$				
(2R,3S) –Phenylisoserine	191 ± 10	$0.43 \pm 0.01$	$37.5 \pm 2.1$				
CoA <sup>a</sup>	$804 \pm 26$	$0.90 \pm 0.08$	$18.7 \pm 1.8$				
TycA with NAC							
Substrate	$K_{\rm M}$ ( $\mu$ M)	$k_{\rm cat}$ (min <sup>-1</sup> )	$k_{\text{cat}}/K_{\text{M}} (\text{s}^{-1} \cdot \text{M}^{-1})$				
(S)–α–Phenylalanine	$27.0 \pm 6.5$	$0.05 \pm < 0.01$	$30.8 \pm 9.7$				
(R)–β–Phenylalanine	$30.4 \pm 3.9$	$0.36 \pm 0.06$	$197 \pm 42$				
(2R,3S) –Phenylisoserine	$132 \pm 56$	$0.19 \pm 0.01$	$24.0 \pm 10.3$				
NAC <sup>a</sup>	$153 \pm 22$	$0.09 \pm < 0.01$	$9.8 \pm 1.8$				
TycA–S563A with NAC							
(S)–α–Phenylalanine	$37.8 \pm 1.6$	$0.20 \pm 0.002$	$88.1 \pm 3.8$				
(R)–β–Phenylalanine	$58.9 \pm 6.4$	$0.024 \pm 0.001$	$6.8 \pm 0.8$				
(2R,3S) –Phenylisoserine	$512 \pm 43$	$0.31 \pm 0.05$	$10.1 \pm 1.8$				
NAC <sup>a</sup>	$268 \pm 4$	$0.10 \pm < 0.01$	$6.2 \pm 0.6$				

<sup>&</sup>lt;sup>a</sup>Kinetic parameters for CoA or NAC were determined with (S)–α–phenylalanine as cosubstrate.

The kinetic parameters calculated for TycA show different behavior with the three phenylpropanoate substrates with CoA. Based on the  $K_{\rm M}$  of TycA, the enzyme binds the natural substrate (S)- $\alpha$ -phenylalanine and surrogate substrate (R)- $\beta$ -phenylalanine nearly the same, but ~2-fold better than (2R,3S)-phenylisoserine (**Table 2.1**). These data suggested that TycA prefers substrates with an amino group at  $C_{\alpha}$  or  $C_{\beta}$ , but not phenylisoserine, containing both a  $C_{\alpha}$ -hydroxyl and  $C_{\beta}$ - amino group. For (2R,3S)-phenylisoserine, the stereochemistry of the  $C_{\beta}$ -amino group is oriented identical to the amino group of (R)- $\beta$ -phenylalanine, while the  $C_{\alpha}$ -

hydroxyl group is oriented opposite to that of the  $C_{\alpha}$ -amino group of (S)- $\alpha$ -phenylalanine. Thus, the hydroxyl group likely affects binding either sterically, electrostatically, or through unfavorable H-bonding that alters the trajectory of the substrate.

Initial studies had showed that E. coli contained a 4'-Ppant acyltransferase that catalyzed the posttranslational modification of peptide synthetases with the cofactor 4'-Ppant. Therefore, the TycA catalyzed aminoacyl CoA biosynthesis reaction would likely compete with the internal thioesterification by the pantetheine thiol donor. Therefore, to remove any residual competitive thioesterification by the native Ppant thiol, an S563A mutation was made to prevent 4'phosphopantetheinylation. The turnover  $(k_{cat})$  of TycA-S563A was only slightly greater than TycA with each phenylpropanoate substrate and CoA as the thiol donor, suggesting that CoA access was unimpeded by the 4'-Ppant arm at the reaction center of Tyc(Phe-A). The increase in  $k_{\text{cat}}$  of TycA–S563A with substrates  $\beta$ –phenylalanine and (2R,3S)–phenylisoserine was offset by a nearly equal increase in  $K_{\rm M}$  (suggesting poorer binding) compared with TycA, resulting in similar catalytic efficiency of the catalysts with these substrates. Considering the catalytic efficiency of TycA did not vary by more than 3-fold over TycA-S563A suggested that CoA at 1 mM was perhaps higher than the slight amount, if any, TycA holoenzyme containing the covalent Ppant in the T-domain. Thus, CoA likely attacks the phenylpropanoate phosphoric acid anhydride in the A-domain of TycA without much competition from the pendent thiol prosthetic group. TycA was therefore considered operationally similar to TycA-S563A and principally in its apoenzyme form.

The  $K_{\rm M}$  of TycA for each phenylpropanoate substrate with NAC at apparent saturation was different, but approximately the same order of magnitude as when CoA was used. This suggested that NAC (a smaller, structural mimic of CoA) did not affect binding of the

phenylpropanoate to the Tyc(Phe–A) (**Table 2.1**). The  $K_{\rm M}$  values suggested  $\alpha$ –phenylalanine bound the best to TycA and (2R,3S)–phenylisoserine the worst in the presence of NAC, similar to when CoA was the cosubstrate. Further, the  $k_{\rm cat}$  values of TycA were faster for CoA turnover than the rates for NAC under steady state reaction conditions (**Table 2.1**). The  $k_{\rm cat}/K_{\rm M}$  of TycA with each phenylpropanoate and CoA ranged between 1.5- and 3-fold higher than when NAC was the thiol donor, suggesting that CoA is more catalytically competent than NAC. However, the efficiency of TycA (with NAC) was highest for (R)– $\beta$ –phenylalanine, followed by (S)– $\alpha$ –phenylalanine, and then by (2R,3S)–phenylisoserine. This trend was similar to (but the values were lower than) that for the phenylpropanoids when CoA was used in place of NAC (**Table 2.1**). This further suggested the two stereogenic functional groups of phenylisoserine are somehow affecting the thioesterification catalysis.

### 2.3.7. Kinetic Analyses of TycA and TycA–S563A with Phenylpropanoates and ATP

The chemical syntheses of authentic amino phenylpropanoyl–AMPs for use as quantitation standards were low yielding; therefore, the biosynthetic acyl AMPs were quantified by LC–ESI–MRM for kinetic analyses and adenosine was used as the standard (the abundant molecular ion fragment of amino phenylpropanoyl–AMPs quantified using the MRM method corresponds to adenine). The catalytic efficiency value of TycA for the conversion of (S)– $\alpha$ –phenylalanine and (R)– $\beta$ –phenylalanine (ATP in the assays was at apparent saturation) to (S)– $\alpha$ –phenylalanyl and (R)– $\beta$ –phenylalanyl AMP was ~2- and 15-fold lower, respectively, than the catalytic efficiency values for the conversion of the same substrates to their corresponding amino phenylpropanoyl CoAs (**Table 2.2**). A similar trend was observed for TycA–S563A, where the catalytic efficiency

was ~7- and 46-fold lower, respectively, for the conversion of the same substrates to their AMP anhydrides than the values for the conversion to the corresponding CoA thioesters. Phenylisoserinyl—AMP was below the limits of detection in similar assays.

**Table 2.2.** Steady state kinetic analysis of TycA and TycA–S563A with apparent saturation of phenylpropanoids and varying concentrations of ATP

TycA						
Substrate	$k_{\rm cat}  ({\rm min}^{-1})$	$k_{\rm cat}/K_{\rm M}~({\rm s}^{-1}\cdot{\rm M}^{-1})$				
(S)–α–Phenylalanine	$0.13 \pm 0.01$	$51.7 \pm 1.7$				
$(R)$ – $\beta$ –Phenylalanine	$0.10 \pm 0.01$	$32.9 \pm 0.14$				
(2R,3S)–Phenylisoserine	a	a				
TycA-S563A						
Substrate						
(S)–α–Phenylalanine	$0.09 \pm 0.01$	$44.2 \pm 0.20$				
(R)–β–Phenylalanine	$0.06 \pm 0.01$	$16.1 \pm 1.2$				
(2R,3S)–Phenylisoserine	a	a				

<sup>&</sup>lt;sup>a</sup>Phenylisoserinyl–AMP was below limits of detection in the LC–ESI–MS.

The slower steady-state production rate of the amino phenylpropanoate—AMPs detected in solution did not account for the production rate of the corresponding amino phenylpropanoyl CoAs (**Table 2.1**). The greater catalytic efficiency for CoA thioester production over amino phenylpropanoyl AMP biosynthesis confirmed that CoA displaced AMP from the amino phenylpropanoyl AMP in complex with TycA or TycA–S563A, at steady state, and not from the acyl AMP intermediate in solution to form the thioesters. Previously, aminoacyl AMP formation was studied using Grs1 under single turn over reaction conditions. It was reported that about 74 – 84% of the amino acids were enzyme bound, but in the absence of the T domain the increase of aminoacyl AMP in solution was only 20%. This suggested that the acyl AMPs were labile and were rapidly transferred to the covalently-linked Ppant group. However, in the absence of Ppant, the acyl AMPs are tightly bound to the active site and the leak rate into the solution is slow.  $^{21,38}$  In the current study, the ratio of  $k_{cat(CoA)}/k_{cat(AMP)}$  was greater than one for all the substrates tested

which shows that the formation of acyl CoA did not arise from non catalytic reaction of CoA with the acyl AMP in solution, but rather that CoA binds to the TycA active site (**Table 2.3**, **Figure 2.16**).

**Table 2.3**. Ratio of  $k_{\text{cat}}$  of phenylpropanoids in steady–state biosynthesis of aminoacyl AMP or aminoacyl CoA catalyzed by TycA or TycA–S563A.

Substrate	$k_{\text{cat(CoA)}} (\text{min}^{-1})$ $k_{\text{cat(ATP)}} (\text{min}^{-1})$		$k_{\text{cat(CoA)}}/k_{\text{cat(ATP)}}$	
(S)–α–Phenylalanine	$0.25 \pm 0.01$	$0.13 \pm 0.01$	1.92	
(R)–β–Phenylalanine	$1.6 \pm 0.3$	$0.10 \pm 0.01$	16.0	
(2R,3S)–Phenylisoserine	$0.75 \pm 0.05$	a	>>1	
T				
Substrate				
(S)–α–Phenylalanine	$0.69 \pm 0.08$	$0.09 \pm 0.01$	7.67	
(R)–β–Phenylalanine	$3.00 \pm 0.04$	$0.06 \pm 0.01$	50.0	
(2R,3S)–Phenylisoserine	$0.43 \pm 0.01$	a	>>1	

<sup>&</sup>lt;sup>a</sup>Phenylisoserinyl-AMP was below limits of detection in the LC-ESI-MS.

[E] + AmPheprop + ATP 
$$\stackrel{Mg^{2+}}{=}$$
 [E·AmPheprop-yl-AMP]  $\stackrel{K_{cat}^{CoA}}{=}$  0.25 - 3.0 min<sup>-1</sup> [AmPheprop-yl-CoA] + E [AmPheprop-yl-AMP]  $\stackrel{K_{cat}^{CoA}}{=}$  [AmPheprop-yl-CoA]  $\stackrel{K_{cat}^{ATP}}{=}$  0.06 - 0.13 min<sup>-1</sup>

**Figure 2.16**. <u>Kinetic model for CoA thioesterification reaction catalyzed by TycA and TycA–S563A</u>. **E** is TycA, **E·AmPheprop-yl–AMP** is aminophenylpropanoyl–AMP anhydride TycA complex.

## 2.3.8. Comparing the Kinetic Parameters of TycA/TycA-S563A with Other CoA Ligases

Compared to the  $K_{\rm M}$  values of bacterial CoA ligases for CoA (100 – 940  $\mu$ M) and acyl substrates (10 – 6000  $\mu$ M), those of TycA and TycA–S563A for CoA (1976 and 804  $\mu$ M, respectively) are

about same order of magnitude, whereas the carboxylate substrates (34 – 132 μM) were more variable (refer to **Tables 2.1 and 2.4**). CoA ligases on catabolic pathways in various bacteria convert, for example, propionate,<sup>39</sup> benzoate, <sup>40</sup> and 4–chlorobenzoate<sup>41</sup> to their corresponding CoA thioesters with superior catalytic efficiency (1.65 × 10<sup>6</sup>, 3.96 × 10<sup>7</sup>, 1.02 × 10<sup>7</sup> s<sup>-1</sup>·M<sup>-1</sup>, respectively) compared to those on secondary metabolic pathways (<2,500 s<sup>-1</sup>·μM<sup>-1</sup>) such as for TycA (used in tyrocidines A–D biosynthesis, described here as CoA ligase), phenylacetate:CoA ligase from *Penicillium chrysogenum*,<sup>11</sup> and cinnamate:CoA ligase from *Streptomyces coelicolor*.<sup>42</sup> The role of cinnamoyl–CoA is as yet undefined; however, it may play a role in biosynthesis because *Streptomyces* sp. are known to produce a variety of secondary products.<sup>42</sup>

**Table 2.4**. Kinetic parameters of acyl CoA ligases from various microorganisms.

CoA Ligase (CL) (Organism)	Substrate	$K_{\rm M}(\mu{ m M})$	$k_{\rm cat}$ (min <sup>-1</sup> )	$k_{\rm cat}/K_{\rm M}$ $({\rm s}^{\text{-1}}\cdot{ m M}^{\text{-1}})$	Ref
Propionyl-CL (Salmonella enterica)	propionate	20	1980	$1.65 \times 10^{6}$	
	CoA	215	2520	$1.98 \times 10^{5}$	40
Benzoate-CL (Pseudomonas st. KB 740)	benzoate	11	26,000	$3.94 \times 10^{7}$	43
	CoA	100	NL	NL	
Phenylacetate-CL (Penicillium chrysogenum)	phenylacetate	6100	84	230	44
	CoA	940	NL	NL	
Cinnamate-CL (Streptomyces coelicolor)	cinnamate	190	28.5	2500	45
	CoA	NL	NL	NL	
4-Chlorobenzoate-CL ( <i>Alcaligenes</i> sp. AL3007)	4-Cl-benzoate	0.9	552	$1.02 \times 10^{7}$	41
	CoA	310	NL	$3.00 \times 10^{4}$	

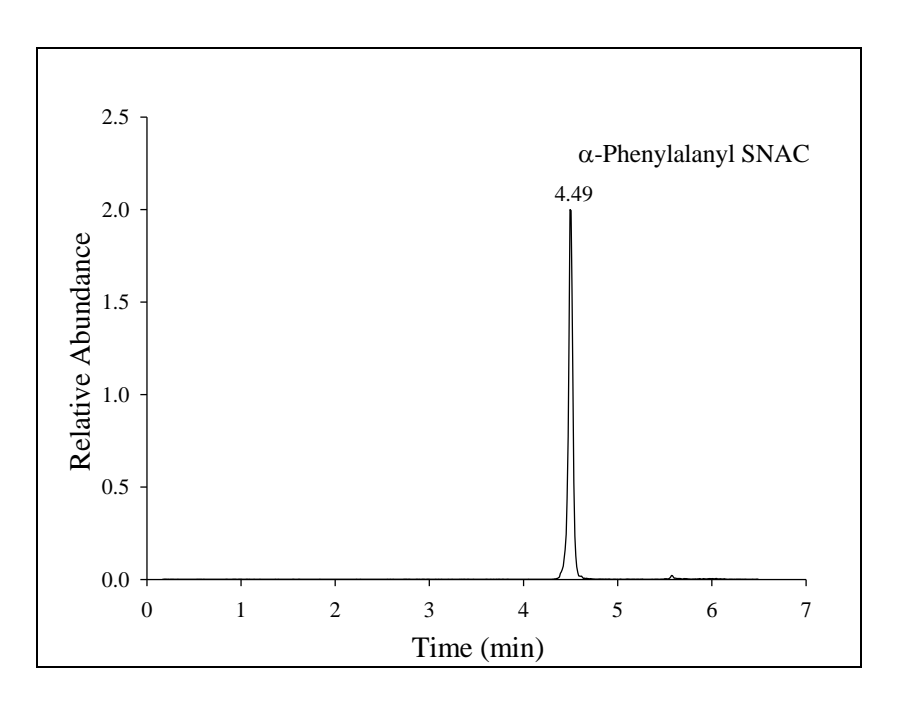
NL: no listing

#### 2.4. Conclusion

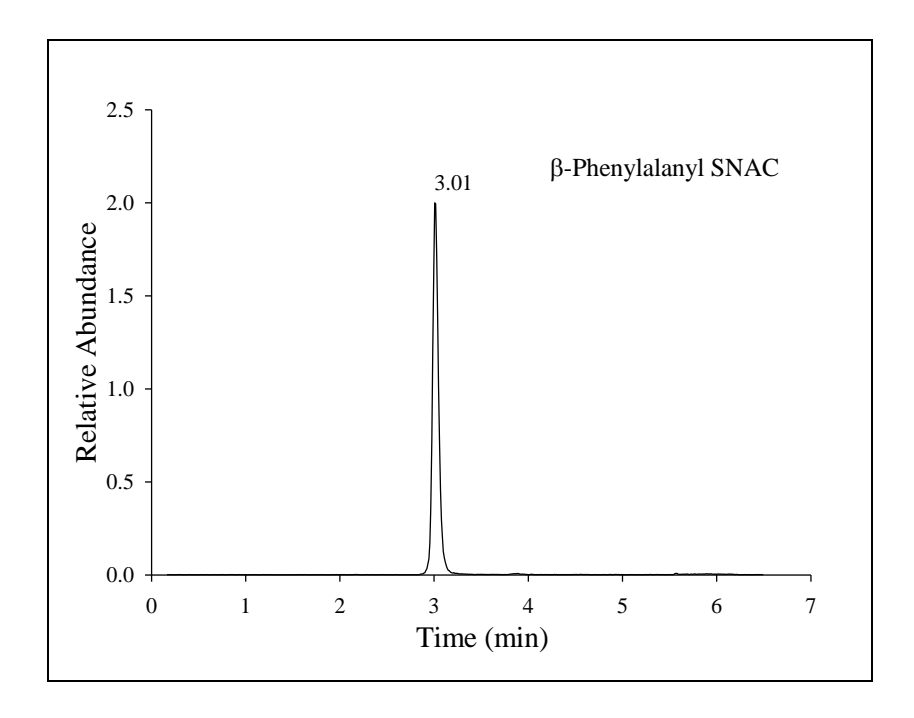
The importance of acyl CoA substrates has been demonstrated in the biosynthesis of key therapeutic compounds such as tetracyclin, macrolides, actinorhodin,<sup>46</sup> erythromycin, rifamycin,<sup>47</sup> rapamycin,<sup>48</sup> and paclitaxel.<sup>43,49,50</sup> Though most of the known CoA ligases utilize an

alkyl/alkenyl carboxylate substrate, less information is known for the amino phenylpropanoid CoA ligases. One study explored a phenylpropanoate: CoA ligase and found that it could transfer CoA to β-phenylalanine.<sup>11</sup> This limited knowledge on amino acid CoA ligases for use in biocatalytically modifying bioactive secondary metabolites, warrants further discovery of new routes to access these acyl CoA substrates. This study highlighted the acyl CoA ligase activity of an NRPS adenylation domain; whereas in earlier studies, the catalytic transfer of CoA was suspected as fortuitous, non-catalyzed event. The ability of TycA to catalyze the synthesis of the aminoacyl CoA intermediates on the paclitaxel biosynthetic pathway opens exploration towards designing novel paclitaxel analogs. TycA catalyzed the production of  $\alpha$ -phenylalanyl,  $\beta$ phenylalanyl, and (2R,3S)-phenylisoserinyl CoA under similar assay conditions. This biosynthetic method has an advantage over the conventional methods that have been challenged by reactions involving multiple steps that require protection/deprotection of the amine group and is challenged by the solvent incompatibility of the hydrophobic acid anhydride intermediate and the hydrophilic CoA in the synthesis method. Also, for the first time, the biosynthesis of (2R,3S)-phenylisoserinyl CoA has been demonstrated in this study. In addition, this study showed that besides CoA or a pendent Ppant group, TycA can also use the small thiol donor Nacetylcysteamine (NAC) in the ligase reaction to make acyl SNACs. The acyl SNACs have been used extensively as surrogate substrates to interrogate the substrate specificity of NPRS catalysts, 51,52 PKS-catalyzed pathways, 53-56 and transformations on the mitomycin C pathway, 57 and also in interrogating proofreading mechanism that releases stalled intermediates from PKs.<sup>58</sup> Biocatalytic production of acyl SNACs would thus bypass the protection/deprotection chemistry required in some thioester syntheses.

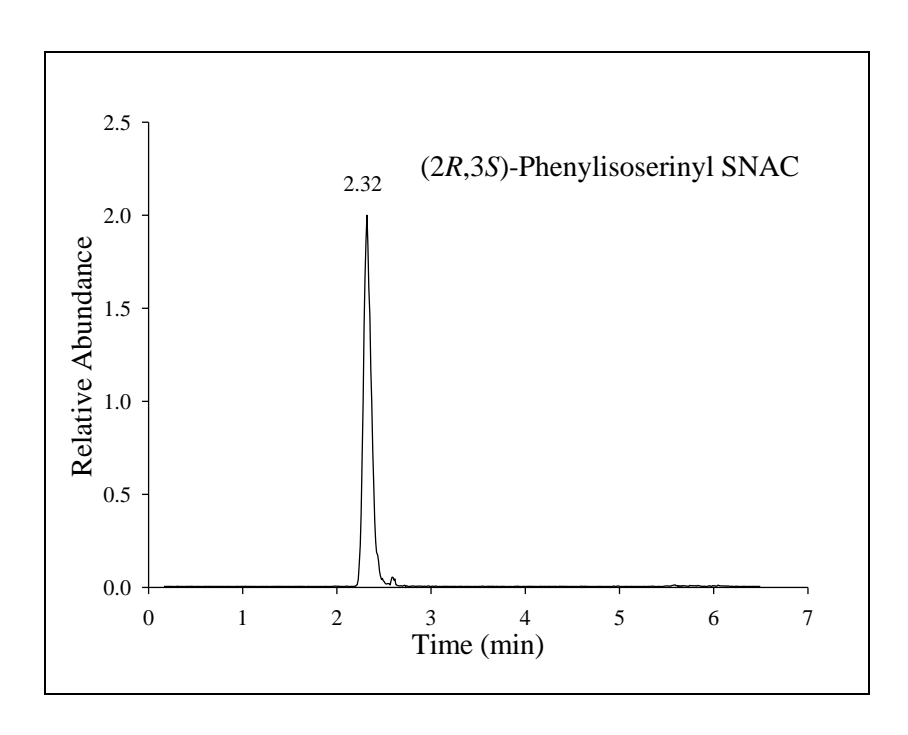
### APPENDIX



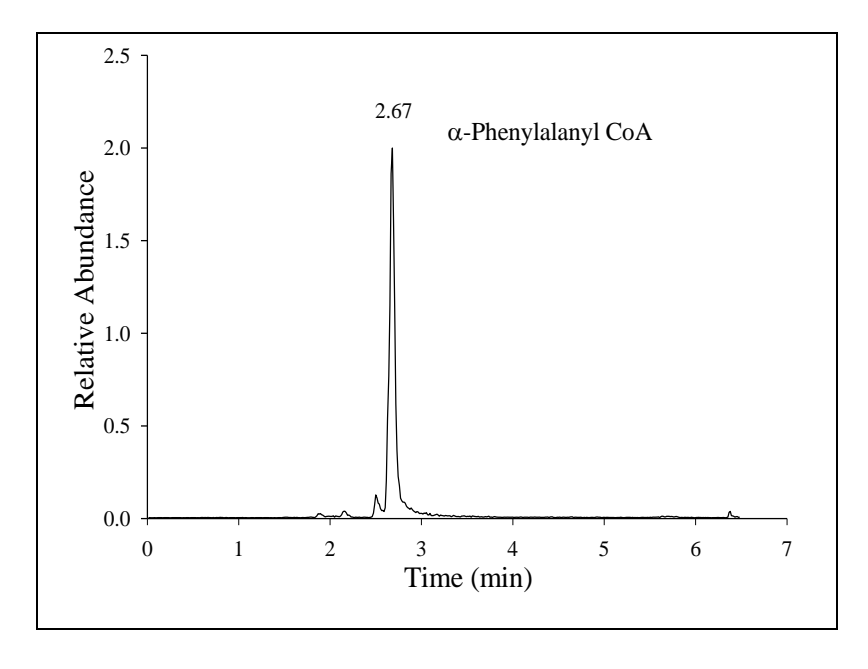
**Figure I–1**. MRM profile obtained by LC–ESI–MS/MS of biosynthetically derived α–phenylpropanoyl SNAC  $[M + H]^+ \rightarrow m/z$  120.



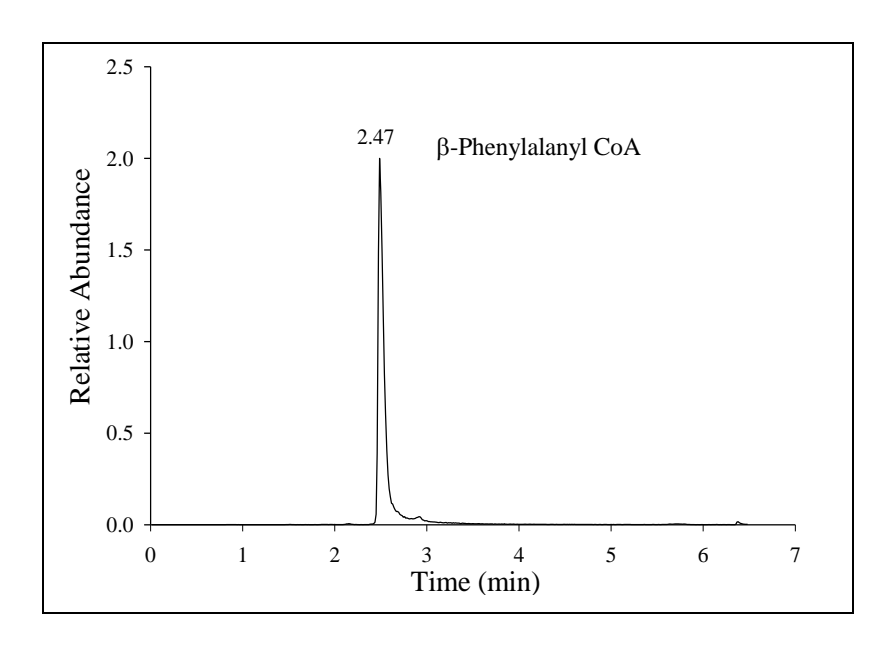
**Figure I–2**. MRM profile obtained by LC–ESI–MS/MS of biosynthetically derived β–phenylpropanoyl SNAC  $[M + H]^+ \rightarrow m/z$  131.



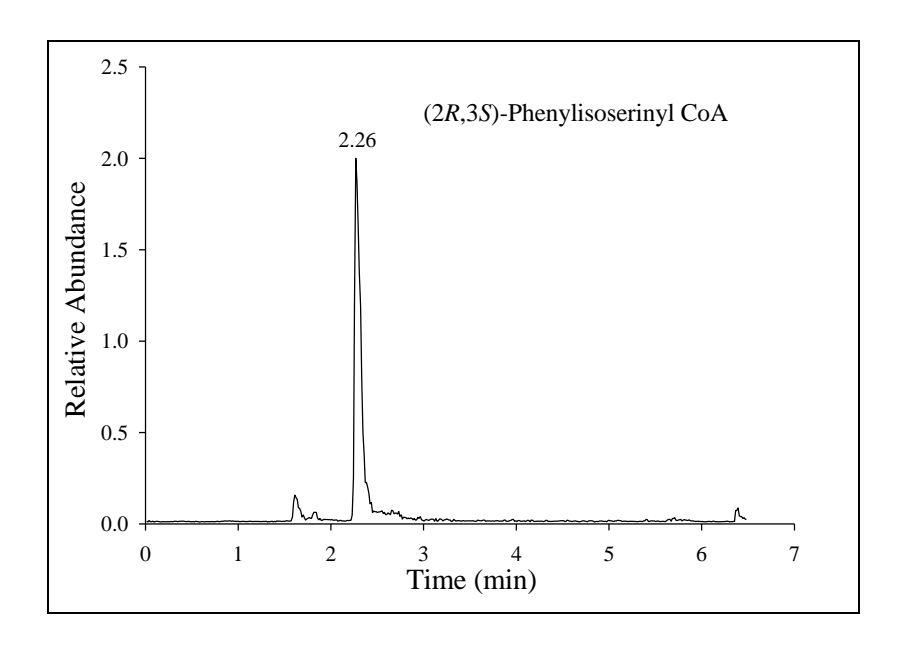
**Figure I–3**. MRM profile obtained by LC–ESI–MS/MS of biosynthetically derived (2*S*,3*R*)– phenylisoserinyl SNAC  $[M + H]^+ \rightarrow m/z$  131.



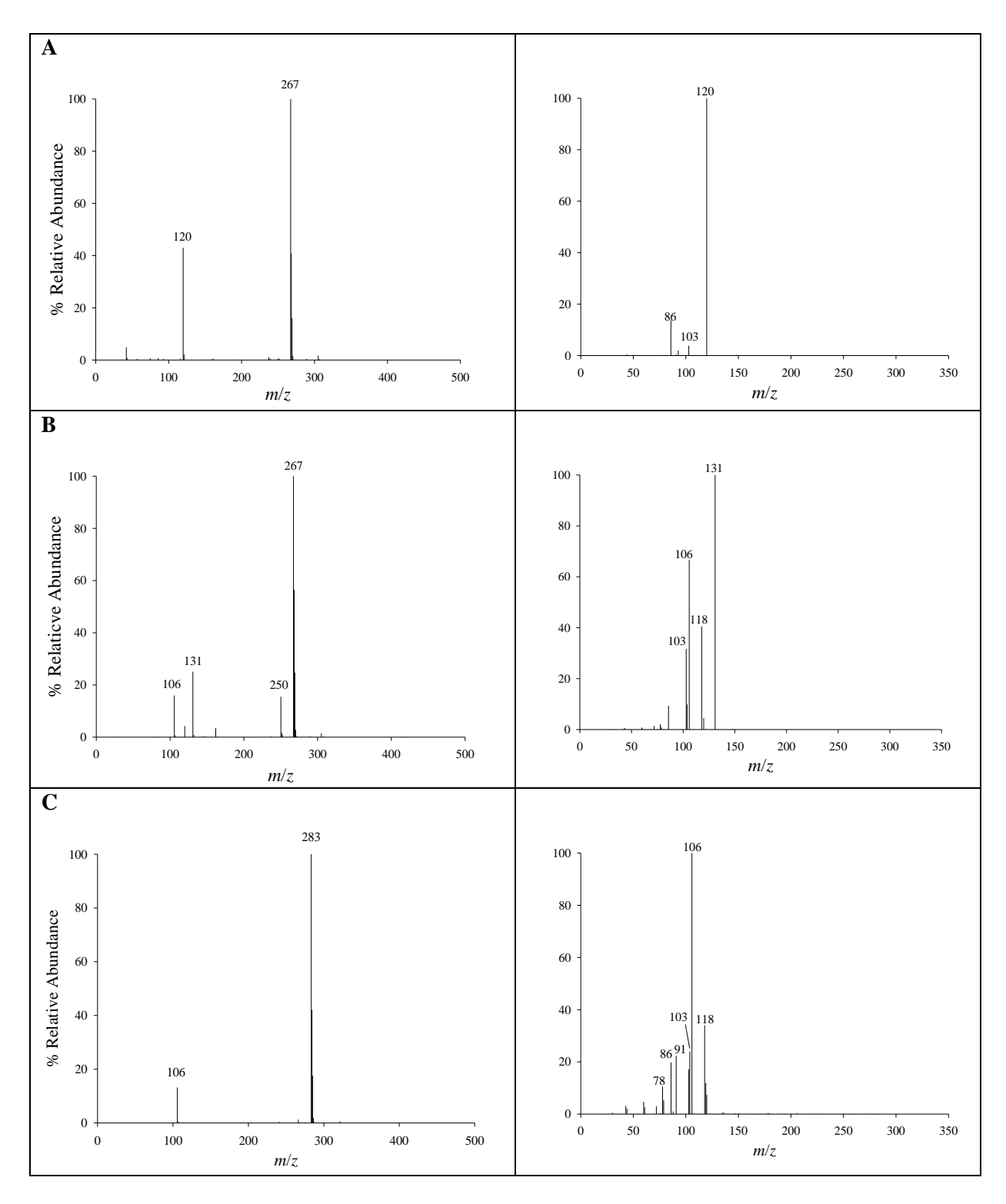
**Figure I–4**. MRM profile obtained by LC–ESI–MS/MS of biosynthetically derived  $\alpha$ –phenylalanyl CoA [M – H] $^{-}$   $\rightarrow$  m/z 408.



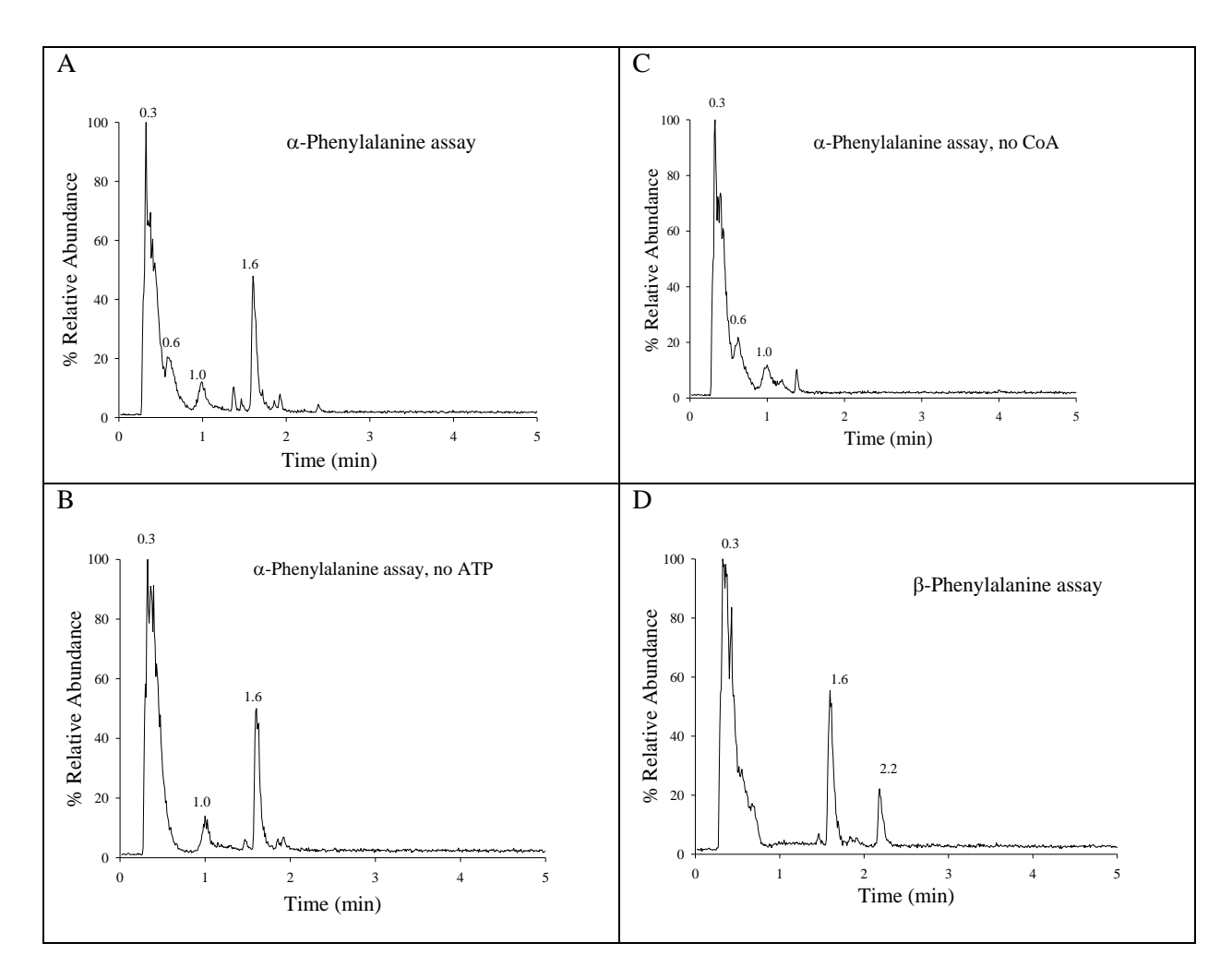
**Figure I–5**. MRM profile obtained by LC–ESI–MS/MS of biosynthetically derived β–phenylalanyl CoA  $[M-H]^- \rightarrow m/z$  408.



**Figure I–6**. MRM profile obtained by LC–ESI–MS/MS of biosynthetically derived (2R,3S)– phenylisoserinyl CoA [M – H] $^- \rightarrow m/z$  408.



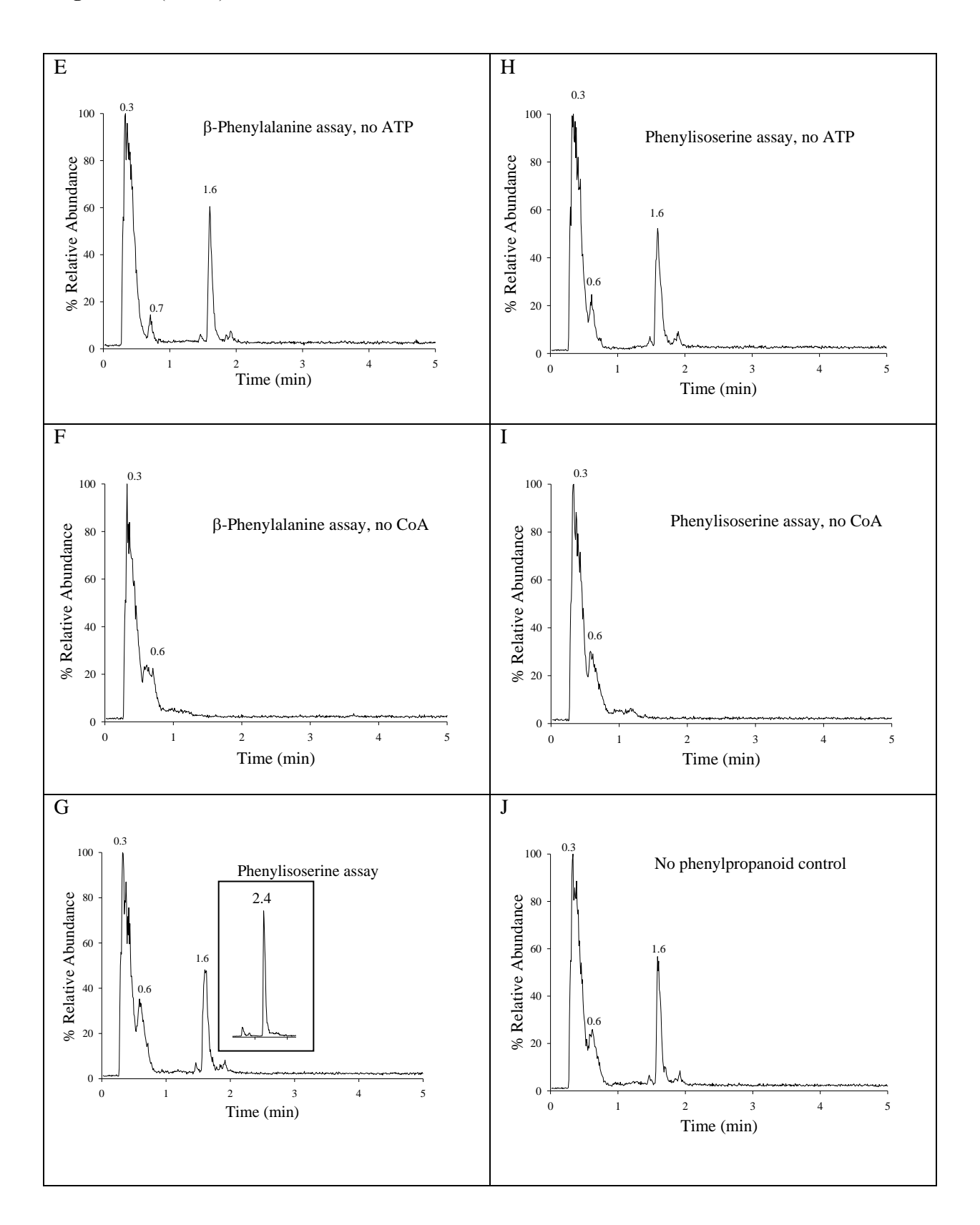
**Figure I–7**. The LC–ESI–MS analyses of authentic aminoacyl SNACs. The total ion profile of the LC–ESI–MS analyses (left column) and the fragment ions derived by MS/MS of the corresponding  $[M + H]^+$  molecular ion (right column) of authentic **A**) (S)– $\alpha$ –phenylalanyl SNAC, molecular ion ( $[M + H]^+$ , m/z 267.1), **B**) (R)–R–phenylalanyl SNAC, molecular ion ( $[M + H]^+$ , R) (R)–phenylalanyl SNAC ( $[M + H]^+$ , R) (R)–phenylalanyl SNAC ( $[M + H]^+$ , R) (R)–phenylalanyl SNAC ( $[M + H]^+$ ), R) (R)–phenylalanyl SNAC ( $[M + H]^+$ ), R) (R)–phenylalanyl SNAC ( $[M + H]^+$ ), R)–phenylalanyl SNAC ( $[M + H]^+$ )

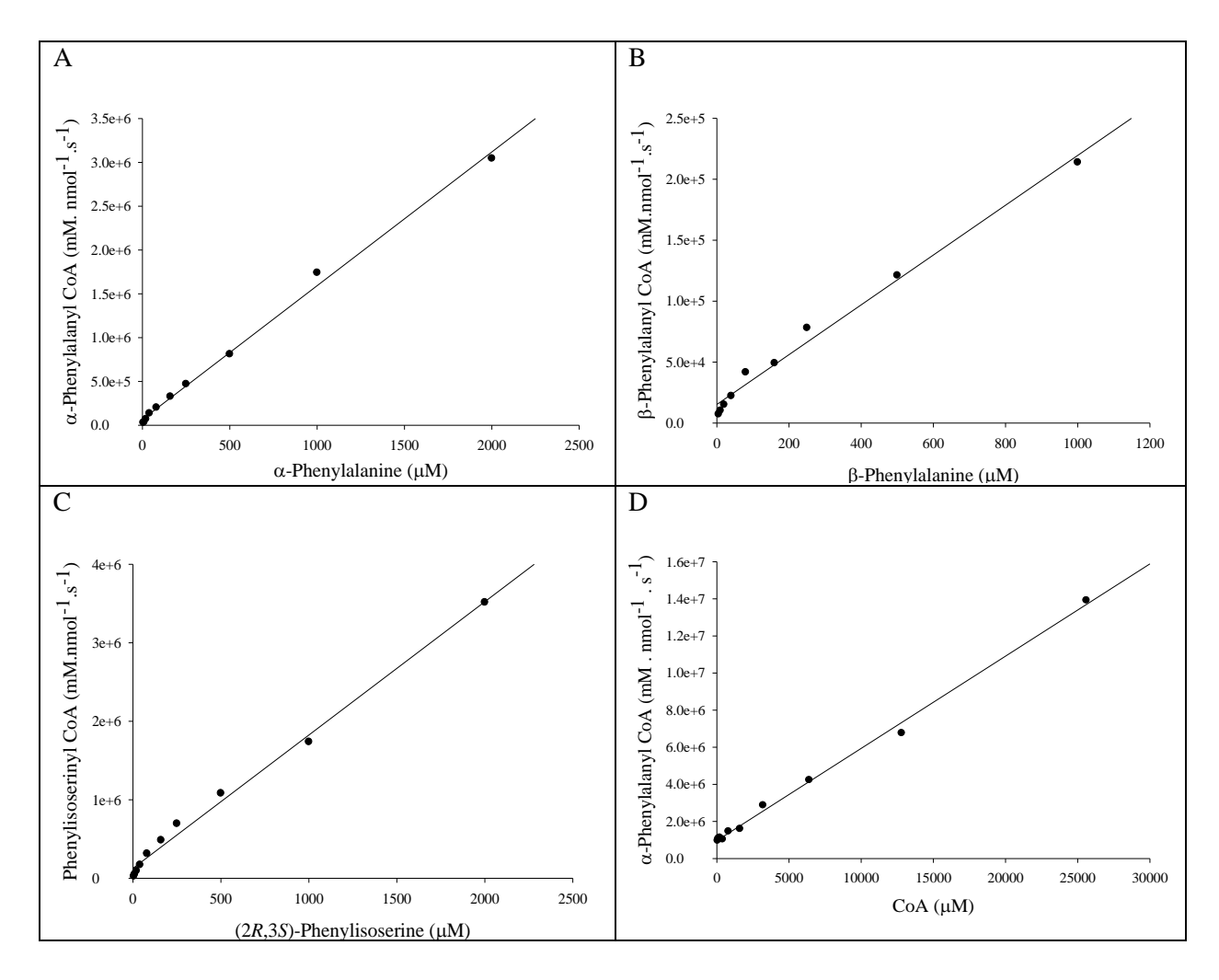


**Figure I–8**. Total ion chromatograms obtained by LC–ESI–MS analysis (scan mode: m/z 100 to 1200) of the compounds in TycA assays (incubated for 30 min at 31 °C) containing the enzyme (100 μg), ATP (1 mM, 100 nmol in 0.1 mL), CoA (1 mM), Mg<sup>2+</sup> (3 mM) and **A**) α–Phenylalanine, **D**) β–Phenylalanine or **G**) (2R,3S)–Phenylisoserine (each at 1 mM). Control assays: **B**, **E**, and **H** lacked ATP, **C**, **F**, and **I** lacked CoA, and **J** lacked phenylpropanoid substrate. The identity of the individual peaks was determined by selected-ion monitoring (post-run) of the [M – H]<sup>-</sup> ions of each analyte and comparison to the retention time and fragment ions of authentic standards.

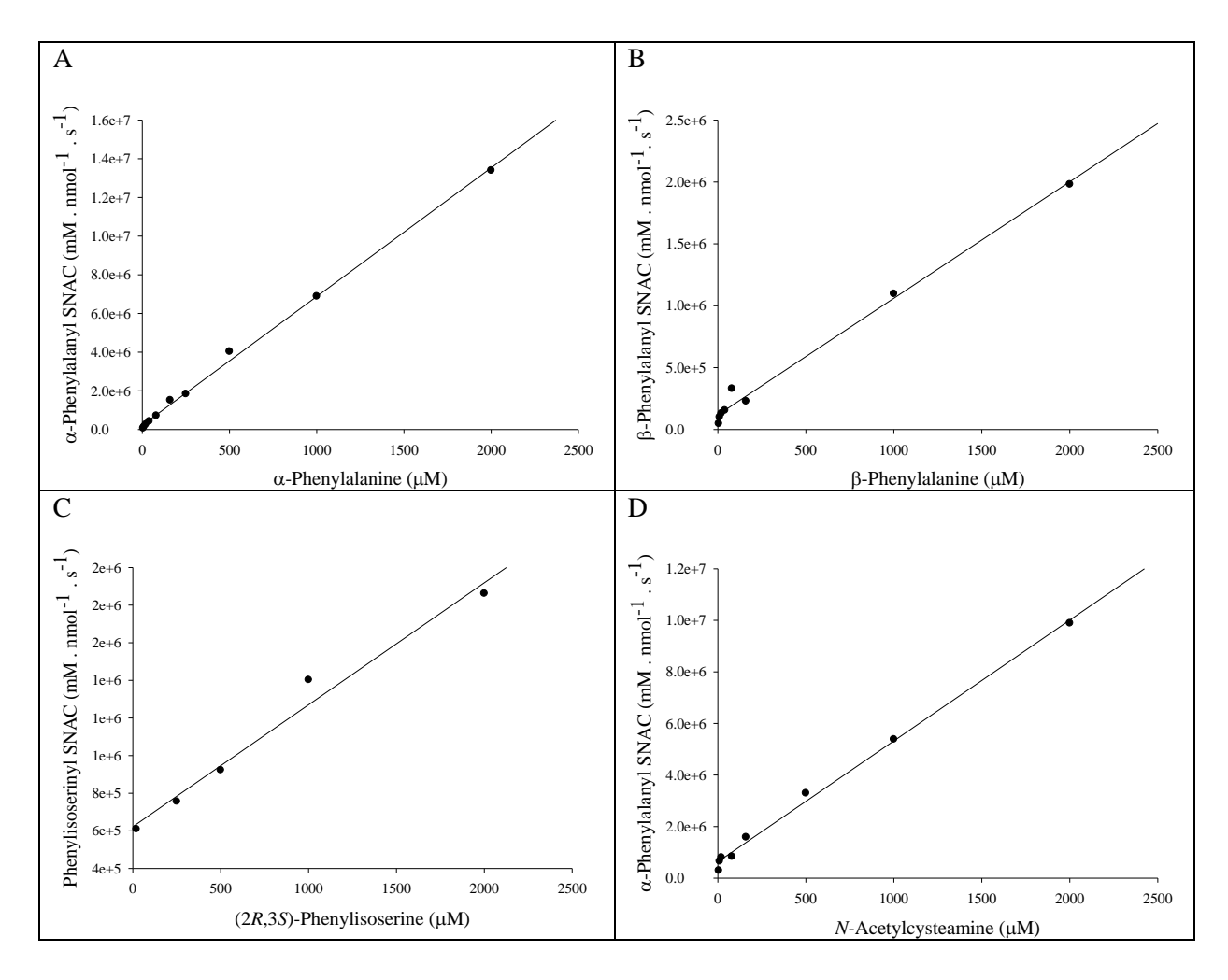
**Retention times**: Hepes buffer (0.3 min); AMP and ADP (0.3 to 0.6 min); ATP and (2*S*,3*R*)–phenylisoserine (0.6 min);  $\beta$ –phenylalanine (0.7 min);  $\alpha$ –phenylalanine (1.0 min); CoA (1.6 min); unknown contaminant – an adenylate phosphate compound that lacked the pantetheine side chain by LC–MS/MS analysis – in the CoA stock from the manufacturer (1.8 min);  $\alpha$ –phenylalanyl CoA (2.0 min);  $\beta$ –phenylalanyl CoA (2.2 min); phenylisoserinyl CoA (2.4 min – extracted peak ion). Proportions of ATP, ADP, and AMP, respectively, in product mixture of reaction represented in **A**) 79, 18, and 3 nmol; **C**) 82, 17, and 1 nmol; **D**) 82, 9, and 10 nmol; **F**) 75, 21, and 3 nmol; **G**) 85, 14, and 1 nmol; **I**) 87, 13, and below limits of detection; **J**) 89, 10, and below limits of detection.

Figure I–8. (cont'd)





**Figure I–9.** Determination of kinetic parameters for A) α–phenylalanine, B) β–phenylalanine, C) (2R,3S)–phenylisoserine, and D) CoA with wtTycA using Hannes Wolf plots. Conditions: 20 μg wtTycA, Hepes buffer, 100 mM, pH 8.0, 1 mM ATP, 3 mM MgCl<sub>2</sub> and 1 mM CoA (except when varying CoA; α–phenylalanine was used at 1 mM concentration).



**Figure I–10.** Determination of kinetic parameters for A) α-phenylalanine, B) β-phenylalanine, C) (2R,3S)-phenylisoserine, and D) N-acetylcysteamine with wtTycA using Hannes Wolf plots. Conditions: 20 μg wtTycA, Hepes buffer (100 mM, pH 8.0), 1 mM ATP, 3 mM MgCl<sub>2</sub> and 1 mM N-acetylcysteamine (except when varying N-acetylcysteamine; α-phenylalanine was used at 1 mM concentration).

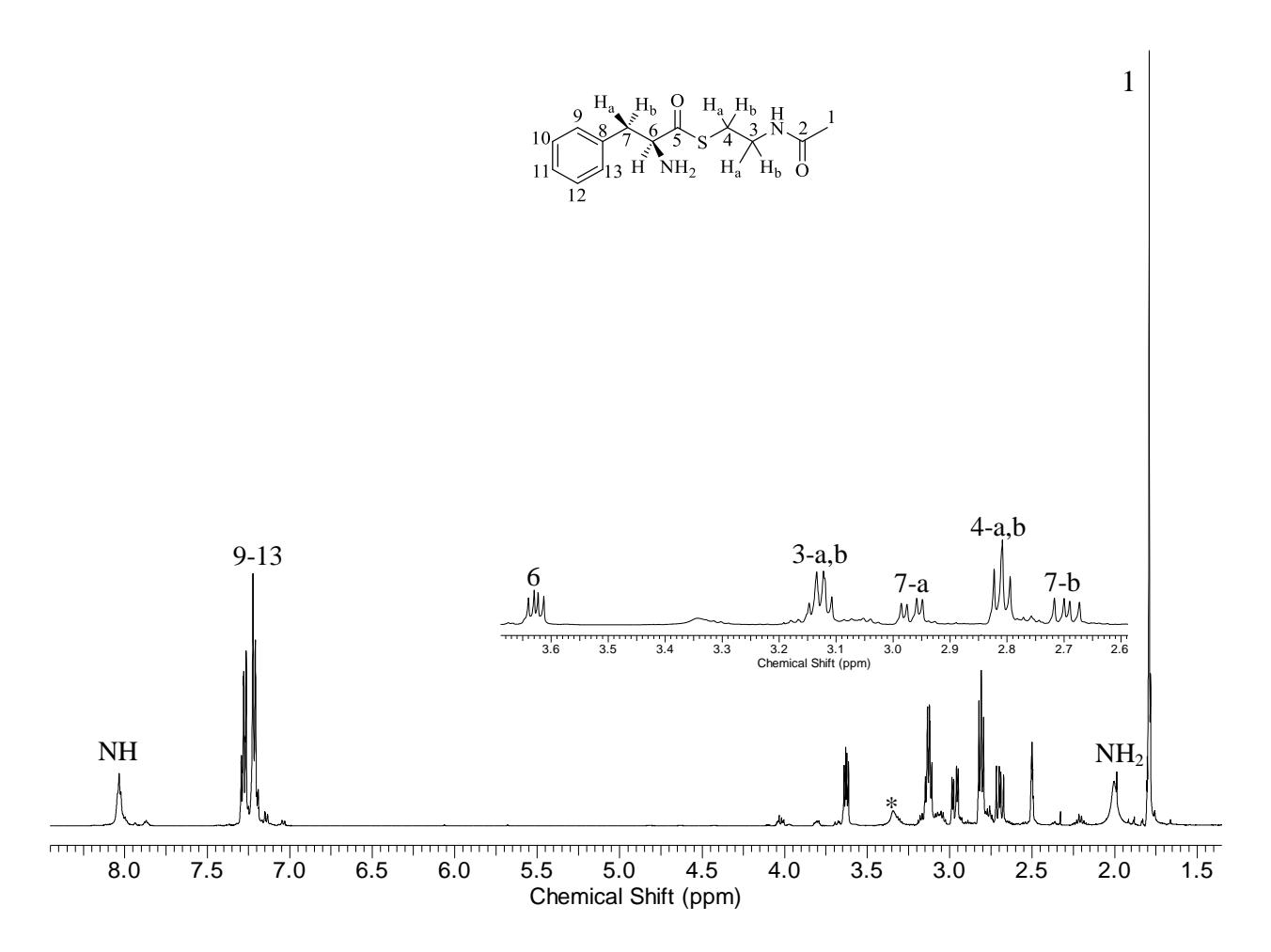


**Figure I–11**.  ${}^{1}$ H-NMR spectrum of (*S*)– $\alpha$ –phenylalanyl SNAC standard. DMSO– $d_6$  was used as solvent.

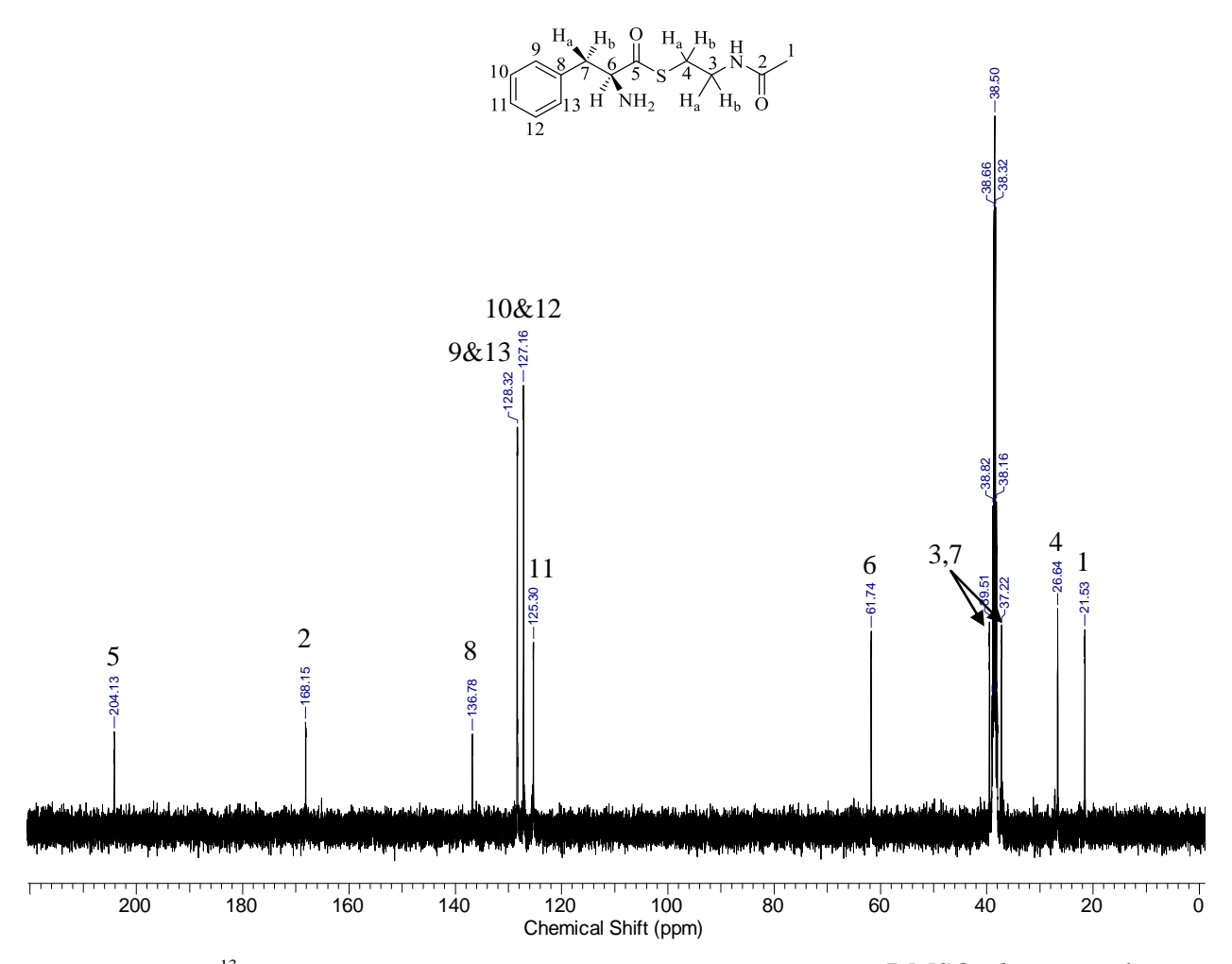


**Figure I–12**.  $\frac{^{13}\text{C-NMR}}{^{13}\text{C-NMR}}$  spectrum of (*S*)– $\alpha$ –phenylalanyl SNAC standard. DMSO– $d_6$  was used as solvent.

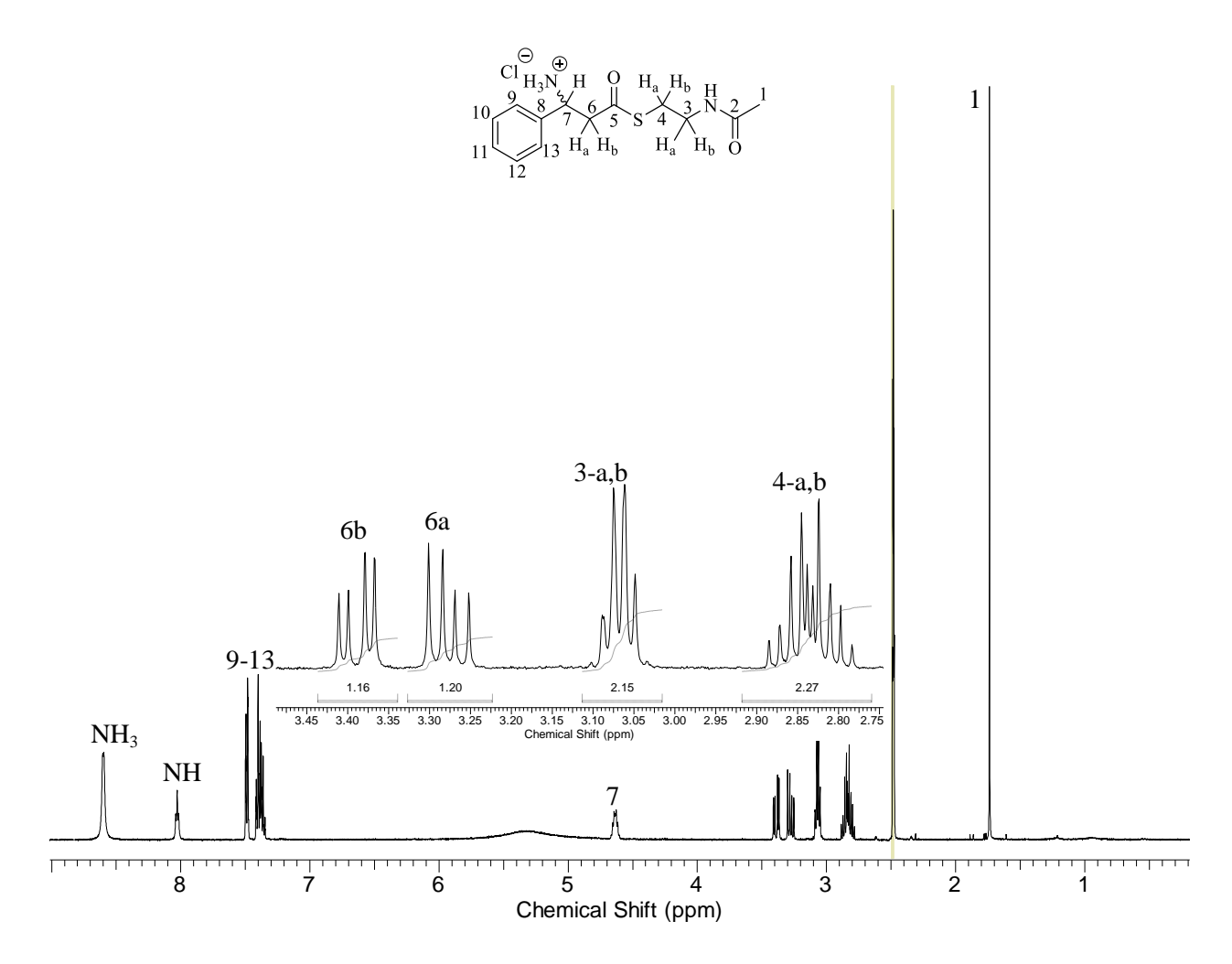


**Figure I–13**.  ${}^{1}$ H-NMR spectrum of β–phenylalanyl SNAC·HCl salt standard. DMSO– $d_6$  was used as solvent.

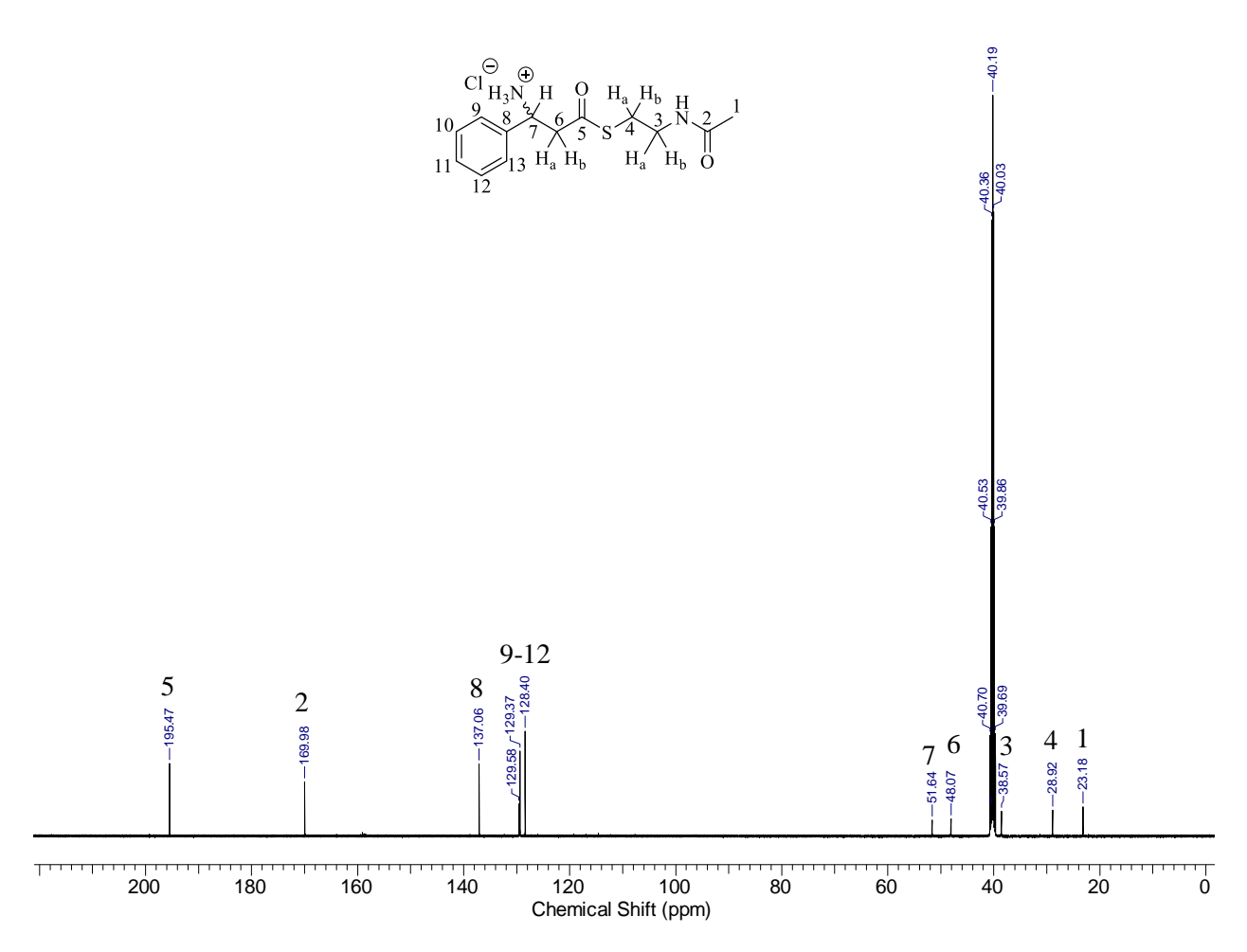


**Figure I–14**.  $^{13}$ C-NMR spectrum of β–phenylalanyl SNAC·HCl salt standard. DMSO– $d_6$  was used as solvent.

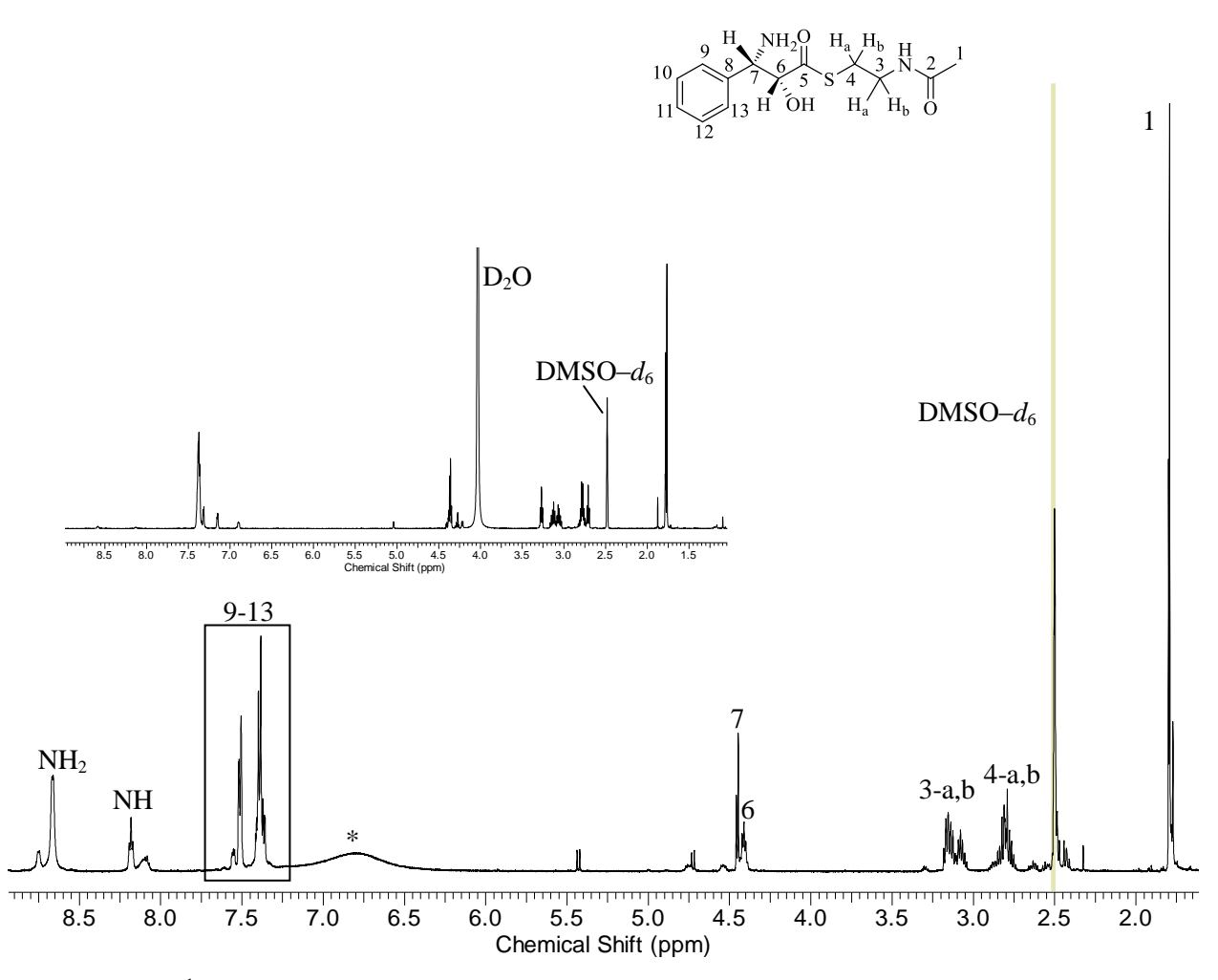


**Figure I–15**. <u>H-NMR spectrum of (2*R*,3*S*)—phenylisoserinyl SNAC standard. The inset shows H/D exchange NMR spectrum.</u>

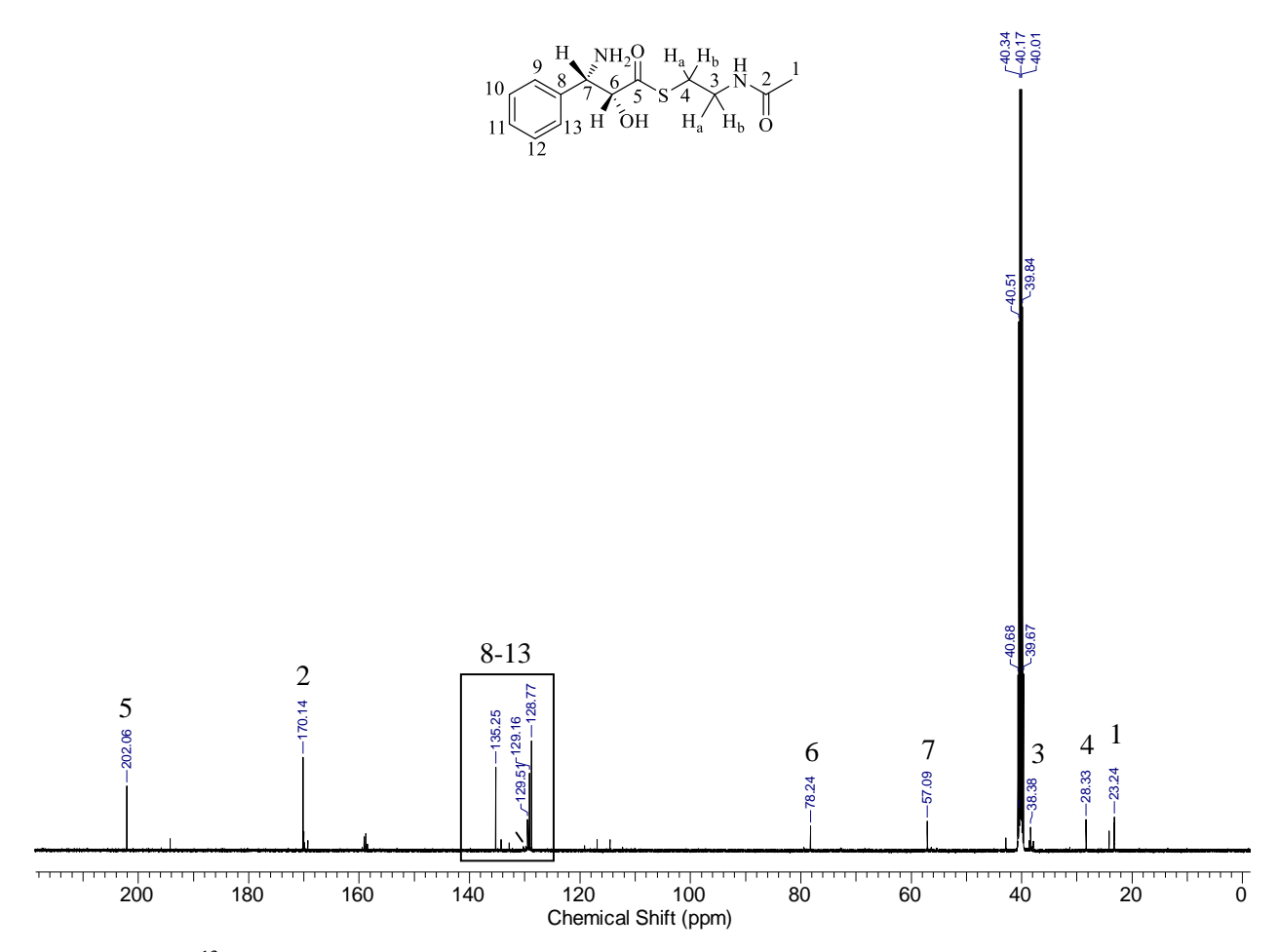


**Figure I–16.**  $\underline{^{13}\text{C-NMR}}$  spectrum of (2R,3S)–phenylisoserinyl SNAC standard. DMSO– $d_6$  was used as solvent.



**Figure I–17**. Trypsin digestion sequence analysis of TycA purified by Ni-affinity chromatography. Assembly of the peptide fragment sequences and comparison to the sequence of the wtTycA (Accession No. AAC45928) deposited in GenBank shows 59% coverage (sequenced residues highlighted in yellow). During the acrylamide purification, methionine and cysteine (green highlight) are oxidized and acrylamide-modified to methionine sulfone and S-alkylated, respectively.<sup>59</sup>

**REFERENCES** 

#### REFERENCES

- (1) Starai, V. J.; Escalante-Semerena, J. C. Cell Mol. Life Sci. 2004, 61, 2020.
- (2) Hisanaga, Y.; Ago, H.; Nakagawa, N.; Hamada, K.; Ida, K.; Yamamoto, M.; Hori, T.; Arii, Y.; Sugahara, M.; Kuramitsu, S.; Yokoyama, S.; Miyano, M. *J. Biol. Chem.* **2004**, *279*, 31717.
- (3) Ehlting, J.; Shin, J. J. K.; Douglas, C. J. *Plant J.* **2001**, *27*, 455.
- (4) Kawaguchi, K.; Shinoda, Y.; Yurimoto, H.; Sakai, Y.; Kato, N. *FEMS Microb. Lett.* **2006**, 257, 208.
- (5) Chang, K.-H.; Xiang, H.; Dunaway-Mariano, D. *Biochemistry* **1997**, *36*, 15650.
- (6) Scholten, J. D.; Chang, K.-H.; Babbitt, P. C.; Charest, H.; Sylvestre, M.; Dunaway-Mariano, D. *Science* **1991**, *253*, 182.
- (7) Baldock, M. I.; Denger, K.; Smits, T. H.; Cook, A. M. *FEMS Microbiol. Lett.* **2007**, *271*, 202.
- (8) Knights, K.; Drogemuller, C. Curr. Drug Metab. 2000, 1, 49.
- (9) Knobloch, K.-H.; Hahlbrock, K. Arch. Biochem. Biophys. 1977, 184, 237.
- (10) Schomburg, D.; Stephan, D. In *Enzyme Handbook 17*; Springer: 1998, p 293.
- (11) Koetsier, M. J.; Jekel, P. A.; Wijma, H. J.; Bovenberg, R. A. L.; Janssen, D. B. *FEBS Lett.* **2011**, *585*, 893.
- (12) Muchiri, R.; Walker, Kevin D. *Chem. Biol.* **2012**, *19*, 679.
- (13) Linne, U.; Schäfer, A.; Stubbs, M. T.; Marahiel, M. A. FEBS Lett. 2007, 581, 905.
- (14) Marahiel, M. A.; Stachelhaus, T.; Mootz, H. D. Chem. Rev. 1997, 97, 2651.
- (15) Gocht, M.; Marahiel, M. A. J. Bacteriol. **1994**, 176, 2654.
- (16) Conti, E.; Stachelhaus, T.; Marahiel, M. A.; Brick, P. *Embo J.* **1997**, *16*, 4174.
- (17) Stachelhaus, T.; Huser, A.; Marahiel, M. A. Chem. Biol. **1996**, *3*, 913.
- (18) Stachelhaus, T.; Walsh, C. T. *Biochemistry* **2000**, *39*, 5775.

- (19) Linne, U.; Doekel, S.; Marahiel, M. A. *Biochemistry* **2001**, *40*, 15824.
- (20) Hanson, K. R.; Rose, I. A. Acc. Chem. Res. 1975, 8, 1.
- (21) Luo, L. S.; Burkart, M. D.; Stachelhaus, T.; Walsh, C. T. J. Am. Chem. Soc. **2001**, 123, 11208.
- (22) Fisch, K. M. RSC Adv. 2013, 3, 18228.
- (23) Winnick, R. E.; Winnick, T. *Biochim. Biophys. Acta* **1961**, *53*, 461.
- (24) Okuda, K.; Edwards, G. C.; Winnick, T. *J Bacteriol.* **1963**, 85, 329.
- (25) Mach, B.; Reich, E.; Tatum, E. *Proc. Natl. Acad. Sci. U. S. A.* **1963**, *50*, 175.
- (26) Fujikawa, K.; Sakamoto, Y.; Suzuki, T. J.; Kurahashi, K. *Biochim. Biophys. Acta, Nucleic Acids and Protein Synth.* **1968**, *169*, 520.
- (27) Arora, P.; Goyal, A.; Natarajan, V. T.; Rajakumara, E.; Verma, P.; Gupta, R.; Yousuf, M.; Trivedi, O. A.; Mohanty, D.; Tyagi, A.; Sankaranarayanan, R.; Gokhale, R. S. *Nat. Chem. Biol.* **2009**, *5*, 166.
- (28) Ehmann, D. E.; Shaw-Reid, C. A.; Losey, H. C.; Walsh, C. T. *Proc. Natl. Acad. Sci. U. S. A.* **2000**, *97*, 2509.
- (29) Walker, K.; Fujisaki, S.; Long, R.; Croteau, R. *Proc. Natl. Acad. Sci. U. S. A.* **2002**, *99*, 12715.
- (30) Bradford, M. M. Anal. Biochem. 1976, 72, 248.
- (31) Owczarek, A.; Safro, M.; Wolfson, A. D. *Biochemistry* **2008**, *47*, 301.
- (32) Anderson, L.; Hunter, C. L. *Mol. Cell. Proteomics* **2006**, *5*, 573.
- (33) Ehmann, D. E.; Trauger, J. W.; Stachelhaus, T.; Walsh, C. T. *Chem. Biol.* **2000**, *7*, 765.
- (34) Villiers, B. R. M.; Hollfelder, F. *Chembiochem* **2009**, *10*, 671.
- (35) Schaffer, M. L.; Otten, L. G. J. Mol. Catal. B-Enzym. 2009, 59, 140.
- (36) Beuerle, T.; Pichersky, E. Arch. Biochem. Biophys. **2002**, 400, 258.
- (37) Phelan, V. V.; Du, Y.; McLean, J. A.; Bachmann, B. O. *Chem. Biol.* **2009**, *16*, 473.

- (38) Luo, L. S.; Walsh, C. T. *Biochemistry* **2001**, *40*, 5329.
- (39) Horswill, A. R.; Escalante-Semerena, J. C. Biochemistry 2002, 41, 2379.
- (40) Altenschmidt, U.; Oswald, B.; Fuchs, G. J. Bacteriol. 1991, 173, 5494.
- (41) Wu, R.; Reger, A. S.; Lu, X.; Gulick, A. M.; Dunaway-Mariano, D. *Biochemistry* **2009**, *48*, 4115.
- (42) Kaneko, M.; Ohnishi, Y.; Horinouchi, S. J. Bacteriol. 2003, 185, 20.
- (43) Nevarez, D. M.; Mengistu, Y. A.; Nawarathne, I. N.; Walker, K. D. *J. Am. Chem. Soc.* **2009**, *131*, 5994.
- (44) Walker, K.; Long, R.; Croteau, R. *Proc. Natl. Acad. Sci. U. S. A.* **2002**, 99, 9166.
- (45) Admiraal, S. J.; Walsh, C. T.; Khosla, C. *Biochemistry* **2001**, *40*, 6116.
- (46) Malpartida, F.; Hopwood, D. A. *Nature* **1984**, *309*, 462.
- (47) Weissman, K. J.; Leadlay, P. F. Nat. Rev. Microbiol. 2005, 3, 925.
- (48) Khosla, C.; Gokhale, R. S.; Jacobsen, J. R.; Cane, D. E. *Annu. Rev. Biochem.* **1999**, *68*, 219.
- (49) Nawarathne, I. N.; Walker, K. D. J. Nat. Prod., 73, 151.
- (50) Ondari, M. E.; Walker, K. D. J. Am. Chem. Soc. 2008, 130, 17187.
- (51) Lautru, S.; Challis, G. L. *Microbiology* **2004**, *150*, 1629.
- (52) Yeh, E.; Kohli, R. M.; Bruner, S. D.; Walsh, C. T. *ChemBioChem* **2004**, *5*, 1290.
- (53) Jacobsen, J. R.; Hutchinson, C. R.; Cane, D. E.; Khosla, C. *Science* **1997**, 277, 367.
- (54) Cane, D. E.; Yang, C. C. J. Am. Chem. Soc. **1987**, 109, 1255.
- (55) Harmrolfs, K.; Brünjes, M.; Dräger, G.; Floss, H. G.; Sasse, F.; Taft, F.; Kirschning, A. *ChemBioChem* **2010**, *11*, 2517.
- (56) Bravo-Rodriguez, K.; Ismail-Ali, A. F.; Klopries, S.; Kushnir, S.; Ismail, S.; Fansa, E. K.; Wittinghofer, A.; Schulz, F.; Sanchez-Garcia, E. *ChemBioChem* **2014**, *15*, 1991.

- (57) Chamberland, S.; Grüschow, S.; Sherman, D. H.; Williams, R. M. *Org. Lett.* **2009**, *11*, 791.
- (58) Jensen, K.; Niederkrüger, H.; Zimmermann, K.; Vagstad, Anna L.; Moldenhauer, J.; Brendel, N.; Frank, S.; Pöplau, P.; Kohlhaas, C.; Townsend, Craig A.; Oldiges, M.; Hertweck, C.; Piel, J. *Chem. Biol.* **2012**, *19*, 329.
- (59) Nguyen, D. N.; Becker, G. W.; Riggin, R. M. J. Chromatogr. A 1995, 705, 21.

3. TRUNCATION OF TYROCIDINE SYNTHETASE A (TycA(Phe–ATE)) to

Tyc(Phe–A) AND Tyc(Phe–AT), ACTIVITY EVALUATION, AND

STEREOSPECIFICITY STUDIES IN THE BIOSYNTHESIS OF

AMINOACYL COA THIOESTERS

#### 3.1. Introduction

Non-ribosomal peptide synthetases (NRPSs) are multimodular peptide synthetases comprising structurally and functionally independent domains on a single polypeptide chain.<sup>1</sup> These enzymes are expressed sequentially from the contiguous DNA template.<sup>2</sup> Previous NRPSs studies revealed that the catalytic modules within the polypeptide chain contain adenylation (A) domain, thiolation (T) domain,<sup>3</sup> and a modifying domain which can be an epimerization (gramicidin and tyrocidine),<sup>3</sup> *N*-methylation (in cyclosporine A),<sup>4</sup> *N*-formylation (in anabaenopeptilide 90–A),<sup>5</sup> oxidation (in bleomycin and epothiline),<sup>6</sup> and reduction (versiniabactin and pyochelin).<sup>7</sup>

The adenylation and thiolation domains are responsible for aminoacyl adenylation and thioesterification on a specific 4'–phosphopantetheine prosthetic group, respectively. The thioester intermediate is then modified as needed by the corresponding modifying domain. For example, in tyrocidine synthetase A (TycA) module, the  $C_{\alpha}$  of the activated phenylalanyl–phosphopantetheine intermediate is epimerized by the epimerization (E) domain prior to the transfer of the activated phenylalanine to the first domain of the adjacent module (also referred to as the chain elongation module). The elongation modules studied so far contain domains that participate in substrate activation (A domain), thioesterification (T–domain), modification (where necessary), and condensation (C domains).

Individual domains that make up the modules in NRPSs have been isolated as stable enzymes, with some of them retaining activity independently of the partner domains. 11-13 Generally, the catalytic independence of the various domains within a module has been demonstrated through deletion studies. For example, gramicidin synthetase 1 (Grs1) module on the gramicidin biosynthesis pathway was mutated to leave the adenylation and thiolation domains (designated herein as Grs1(Phe–AT)). 12 The deletion in Grs1 caused no reduction in the adenylation of the natural substrate (S)–phenylalanine compared to the wild type reactivity based on ATP/PPi exchange assay. 12 Also, the Grs1(Phe–AT) was able to form a T–domain–linked 4'–phosphopantetheinyl (4'–Ppant) thioester. A further deletion of 100 amino acid residues at the C terminal end of Grs1 (Grs1(Phe–AT) to Grs1(Phe–A)) could only activate the (S)–phenylalanine to its adenylate form, which was not covalently bound to the enzyme, hence suggesting loss of T–domain activity. 12

The NRPSs domain independence has also been studied using tyrocidine synthetase A (TycA). Firstly, the (*S*)–phenylalanyl-AMP intermediate was generated by addition of TycA A–domain (Tyc(Phe–A)) to an assay containing (*S*)–phenylalanine and ATP.<sup>11</sup> When the thiolation domain was added into this reaction mixture, a covalently bound (*S*)–phenylalanine-S–Ppant thioester on the T–domain was observed albeit in small amounts.<sup>11</sup> This study suggested that independent domains can perform their respective catalytic activity without a need for a covalent peptide bond joining them.

In the current study, it was hypothesized that the catalytic efficiency of TycA, which already uses aminophenylpropanoate substrates, would improve by eliminating thiolation and epimerization domains through mutagenesis. It was expected that CoA would serve as a thiol donor in place of 4'–Ppant to access aminophenylpropanoyl CoAs biosynthetically. Additionally,

deletion of E-domain would prevent any possibility of epimerization of aminoacyl CoA products.

CoA has been described as a Ppant surrogate in the TycA catalyzed aminoacyl CoA biosynthesis (Chapter 2). 14 Additionally, CoA is not a natural substrate for TycA, and hence to rationalize how CoA is able to serve as a thiol donor in a reaction catalyzed by Tyc(Phe-A) and/or Tyc(Phe-AT) described herein, homology modeling of Tyc(Phe-AT) on the structure of Grs1(Phe-A) and comparison of the resulting model to acyl CoA structures will be discussed. Based on their similar reaction mechanism and presence of conserved peptide motifs, the acyl CoAs and NRPSs have been classified into a superfamily of adenylate forming enzymes<sup>15</sup> (Figure 3.1). Specifically, there is an AMP binding motif that is conserved in all members of this family (SGXTGKPKG)<sup>16,17</sup> (See appendix, **Figure II-1**). The amino acid sequence identity between these acyl adenylate forming enzymes is low (20 - 30%). However, many members of this family share high structural homology. 15 Crystal structures of different enzymes in this family have been solved, including oxidoreductase luciferase from *Photinus pyralis* (PDB code: 1LCI), <sup>18</sup> Grs1(Phe–A domain) from *Bacillus brevis* (PDB code: 1AMU), <sup>19</sup> DhbE from *Bacillus* subtilis (PDB code: 1MDF),<sup>20</sup> acetate:CoA ligase from Salmonella enterica (PDB code: 1PG4),<sup>21</sup> 4-chlorobenzoate:CoA ligase from Alcaligenes sp. (PDB code: 3CW9), 22 benzoate:CoA ligase from Burkholderia xenovorans (PDB code: 2V7B), <sup>23</sup> and malonyl CoA ligase from Streptomyces coelicolor (PDB code: 3NYR).<sup>24</sup> Analysis of the crystal structures of adenylate forming family shows high similarities, for example, the overall folds of firefly luciferase and acetate:CoA ligase were shown to be very similar to those of NRPSs A-domains. 15,20

Acyl CoA ligases

$$R \stackrel{\bigcirc}{\longrightarrow} R \stackrel{ATP}{\longrightarrow} R \stackrel{O}{\longrightarrow} AMP \stackrel{CoA}{\longrightarrow} R \stackrel{O}{\longrightarrow} CoA$$

tRNA-synthetases

$$R \stackrel{\bigcirc}{\longrightarrow} R \stackrel{ATP}{\longrightarrow} R \stackrel{O}{\longrightarrow} AMP \stackrel{3'OH-tRNA}{\longrightarrow} R \stackrel{O}{\longrightarrow} tRNA$$

Thiol-template synthetases

Firefly luciferase

**Figure 3.1.** Representation of reactions catalyzed by different adenylate forming enzymes.

Generally, the A-domains of NRPSs share sequence identities of ~30 – 60%, thus making the Grs1(Phe–A) domain structure an archetype for most amino acid activating A-domains in NRPSs.<sup>20</sup> With the wealth of information on amino acid sequence, structure, and function of acyl adenylate enzyme family, it is possible to understand the CoA thioesterification reaction catalyzed by TycA domains. In the study described herein, Tyc(Phe–AT) was modeled on Grs1(Phe–A) structure and compared to acetate:CoA and 4–chlorobenzoate:CoA ligase in complex with CoA.

## 3.2. Experimental

### 3.2.1. Substrates, Reagents, and General Instrumentation

*N*–Boc–(2*R*,3*R*)–phenylisoserine and (2*S*,3*R*)–*N*–benzoyl–3–phenylisoserine were obtained from Peptech (Bedford, MA). The DNA oligo primers were purchased from IDT (Commercial Park Coralville, Iowa). The DNA polymerase was obtained from New England BioLabs (Ipswich, MA). A Varian Inova-300 or a Varian UnityPlus500 instrument was used to acquire <sup>1</sup>H- and <sup>13</sup>C-NMR. A Q–ToF Ultima electrospray ionization high resolution mass spectrometer (ESI–MS, Waters, Milford, MA) with a Waters 2795 HPLC and Quattro–Premier XE coupled with Acquity<sup>®</sup> UPLC system were used for mass spectrometry analysis.

## 3.2.2. Truncation and Subcloning of wt-tycA cDNA to Obtain tyc(phe-a) cDNA

The *tycA* cDNA encoding the adenylation domain Tyc(Phe–A) was amplified by PCR from the original expression vector pSU18 to install terminal restriction sites for subcloning into pET28a (Novagen), designated pET28a–Tyc(Phe–A)–His. The PCR was performed using Pfu turbo® DNA Polymerase and 10× reaction buffer (New England Biolabs, Ipswich, MA) following the manufacturer's protocol. The oligonucleotides used are as follows (bold, restriction sites): 5′– *NcoI* Forward primer – GAG AAA TTA ACC ATG GTA GCA AAT CAG GCC-3′ and 5′– *SalI* reverse primer – TGT GTC GAC GCC CAG CTT GAC GAA ATA AGA TGG –3′. The *tyc(phe–a)* cDNA was digested using *NcoI* and *SalI* restriction enzymes, and T4 ligase (New England Biolabs, Ipswich, MA) was used to insert the cDNA into pET28a vector that was digested similarly. The fusion sites between the vector and the *tyc(phe–a)* gene were confirmed by DNA sequencing (MSU Research Technology Support Facility: Genomics, East Lansing, MI).

## 3.2.3. Tyc(Phe–A) Protein Expression and Purification

The plasmid Tyc(Phe–A)–His encoding a C–terminal His–tag was used to transform *E. coli* BL21 (DE3) cells. A 10–mL culture of *E. coli* transformed with the pET28a vector was grown in LB medium at 37 °C supplemented with kanamycin (50 mg·mL<sup>-1</sup>) for 12 h. The 10–mL inoculum was transferred to a new batch of LB medium (1 L). The bacteria were grown at 37 °C to OD<sub>600</sub> ~0.6, and the cDNA expression was induced by isopropyl  $\beta$ –D–1–thiogalactopyranoside (IPTG), and the culture was grown further for 18 h at 16 °C. The cells were pelleted by centrifugation (30 min, 4000*g*) at 4 °C, resuspended in Binding buffer (20 mM Tris–HCl buffer containing 0.5 M NaCl and 5 mM imidazole at pH 7.8), lysed by sonication (Misonix sonicator, Farmingdale, NY), and the corresponding soluble protein fraction was clarified by centrifugation at 15,000*g* for 0.5 h. The supernatant was then decanted and centrifuged at 135,000*g* for 1.5 h to remove cell-wall debris and light membranes.

The crude Tyc(Phe–A)–His in the soluble fraction was purified by nickel–nitrilotriacetic acid (Ni-NTA) affinity chromatography (Qiagen, Valencia, CA) and eluted according to the protocol described by the manufacturer. The column was eluted with increasing concentration of imidazole (20 – 250 mM) in Binding buffer. Fractions containing Tyc(Phe–A)–His were identified by SDS–PAGE analysis and Coomassie Blue staining. The Tyc(Phe–A) fractions eluting at 50 and 100 mM imidazole were combined (75 mL) and concentrated (1 mL) by size-selective centrifugation (Centriprep 30,000 MWCO unit; Millipore, Billerica, MA). The buffer was exchanged with the Assay buffer (50 mM HEPES containing 100 mM NaCl and 1 mM EDTA at pH 8.0) over five dilution/concentration cycles. Enzyme purity was estimated by SDS–PAGE with Coomassie Blue staining. The protein concentration (35 mg/mL) was determined by measuring the *A*<sub>280</sub> absorbance on a NanoDrop ND1000 Spectrophotometer (Thermo Scientific,

Wilmington, DE). The calculated extinction coefficient and molecular weight of Tyc(Phe–A) were  $\epsilon_{280} = 60405~\text{M}^{-1}~\text{cm}^{-1}$  and 58.06~kDa, respectively. The purified protein was stored at -80 °C.

### 3.2.4. Evaluation of Tyc(Phe–A) Activity with CoA and Aminophenylpropanoids

Substrates (S)- $\alpha$ -phenylalanine, (R)- $\beta$ -phenylalanine, and (2R,3S)-phenylisoserine (each at 1 mM) were separately incubated at 31 °C in single stopped-time (1 h) reactions containing 100 mM HEPES (pH 8.0), ATP (1 mM), MgCl<sub>2</sub> (3 mM), CoA or N-acetylcysteamine (1 mM), and Tyc(Phe-A) (100 µg). Various control reactions were done in parallel under the same conditions used for assays containing enzyme, except Tyc(Phe-A), ATP, or CoA was omitted. The reactions were quenched by acidifying to pH ~2 (10% formic acid) and lyophilized to dryness. The resultant samples were separately dissolved in 100 µL dH<sub>2</sub>O (pH 4.0) and analyzed using a Quattro-Premier XE Mass Spectrometer coupled to an Acquity® UPLC system fitted with a C18 Ascentis Express column ( $2.5 \times 50$  mm,  $2.7 \mu m$ ) at 30 °C. An aliquot ( $10 \mu L$ ) of each sample was loaded onto the column, and the analytes were eluted with a solvent gradient of acetonitrile (Solvent A) and 0.05% triethylamine in distilled water (Solvent B) (held at 2.5% Solvent A for 3.17 min, increased to 100% solvent A over 5 sec with a 2-min hold, and then returned to 2.5% Solvent A over 5 sec with a 50-sec hold) at a flow rate of 0.3 mL/min. The effluent from the column was directed to the mass spectrometer set to negative ion mode with a scan range of m/z 200 – 1000 atomic mass units. During the development of an LC-ESI-MS-MS method for the analysis of the aminophenylpropanoyl CoA products, a common diagnostic fragment ion (m/z, 408) was identified. Authentic  $\beta$ -phenylalanyl CoA was used to validate the observed LC-ESI-MS-MS profile of the biosynthetic products.

# 3.2.5. Assessing Tyc(Phe–A) Substrate Binding by Tryptophan Fluorescence Quenching Studies

Aliquots of (2S)-phenylalanine, between 0 – 96 µM were added to a solution containing Tyc(Phe-A) at 0.1 µM. The excitation wavelength was set at 280 nm and the emission spectra were recorded from 300 – 420 nm. The fluorescence intensity was recorded after every addition of (S)-phenylalanine as an average of three readings. In the control experiment, K<sup>+</sup>HEPES was titrated to 2.0 mL Tyc(Phe–A) (0.1 µM) and the readings were recorded similarly to those of the ligand. The equilibrium fluorescence titration experiments and control, where Tyc(Phe-A) was omitted, were repeated using a fixed excitation wavelength at 280 nm and fixed emission wavelength at 340 nm. Similar fluorescence titration experiments were done using a fixed concentration of Tyc(Phe-A) (0.1 µM) and (2S)-phenylalanine (at 96 µM) with varying concentration of AMP  $(0 - 96 \mu M)$  in K<sup>+</sup>HEPES (pH 7.5). The fluorescence intensity obtained for the control experiment in the absence of Tyc(Phe-A) was subtracted from that of the test samples containing the enzyme and ligand ((S)-phenylalanine). The fluorescence change observed at 340 nm was plotted vs the ligand concentration and equation 1 was applied in the curve analysis using KaleidaGraph program to obtain the binding constants ( $K_d$ ) (Figure 3.5 and Appendix, **Figures II–7 – II–9**).

## 3.2.6. Truncation of wt-tycA or tycA-S563A cDNA to Obtain tyc(phe-at) and tyc(phe-at(S563A)) Constructs

In Chapter two, the full length *tycA* (also identified as *tyc(phe–ate)* and single point mutant *tycA–* S563A are described. The latter encoded Tyc(Phe–ATE(S563A)) that removed the serine residue needed for covalent 4'–phosphopantetheinylation in the native reaction. The full-length *tyc(phe–ate)* 

ate) cDNA encoding Tyc(Phe–ATE) and tyc(phe–ate(S563A)) encoding Tyc(Phe–ATE(S563A)) were truncated to encode Tyc(Phe–AT) and Tyc(Phe–AT(S563A)). Briefly, tycA or tycA(S563A) was amplified by PCR with the following oligonucleotides (bold, restriction sites): 5'–NcoI Forward primer – GAG AAA TTA ACC ATG GTA GCA AAT CAG GCC–3' and SalI reverse primer 5'–CGC AAG CTT GTC GAC GCC GCT TTT TCT CGT CGT GCT CTT GAC–3' to generate the fragment Tyc(Phe–AT) and install terminal restriction sites for subcloning from the original expression vector pSU18 into pET28a (Novagen). The PCR was performed using Pfu turbo® DNA polymerase and 10× reaction buffer from New England Biolabs (Ipswich, MA) following the manufacturer's protocol. The resultant tyc(phe–at) and tyc(phe–at(S563A)) fragments were individually digested using NcoI and SalI restriction enzymes. T4 ligase (New England Biolabs, Ipswich, MA) was used to separately insert the cDNA into pET28a vector that was digested similarly. The fusion sites between the vector and the tyc(phe–at) or tyc(phe–at(S563A)) gene were confirmed by DNA sequencing (MSU Research Technology Support Facility; Genomics, East Lansing, MI).

### 3.2.7. Expression, Purification, and Characterization of Tyc(Phe–AT) Proteins

The resultant tyc(phe-at) and tyc(phe-at(S563A)) plasmids encoding a C-terminal His-tag (designated Tyc(Phe-AT)-His and Tyc(Phe-AT(S563A))-His, respectively) were separately used to transform  $E.\ coli$  BL21 (DE3) cells. Five 10-mL cultures of the two  $E.\ coli$  transformant were separately grown in LB medium supplemented with 50  $\mu$ g·mL kanamycin at 37 °C for 12 h as described above. A 10-mL aliquot of each seed culture expressing Tyc(Phe-AT)-His and Tyc(Phe-AT(S563A))-His was used to inoculate LB medium (5 × 1 L for each transformant). The bacteria were grown at 37 °C to OD<sub>600</sub> ~0.6, then IPTG was added to a final concentration of

0.5 mM, and the culture was grown for 18 h at 16 °C. The cells were pelleted by centrifugation (30 min, 4000*g*) at 4 °C, resuspended in Binding buffer (20 mM Tris–HCl buffer containing 0.5 M NaCl and 5 mM imidazole at pH 7.8), lysed by sonication, and then centrifuged at 15,000*g* for 0.5 h. The supernatant was decanted and centrifuged at 135,000*g* for 1.5 h to remove cell wall debris and light membranes.

Crude soluble protein isolated from bacteria expressing the Tyc(Phe-AT) and Tyc(Phe-AT(S563A)) was estimated by the Bradford protein assay at ~50 mg and ~75 mg total protein, respectively.<sup>26</sup> These fractions were independently loaded onto a Ni-NTA affinity column (Qiagen, Valencia, CA) and eluted according to the protocol described by the manufacturer. The column was eluted with increasing concentration of imidazole (20 – 250 mM) in Binding buffer. Fractions containing the His-tagged enzymes were identified by SDS-PAGE analysis and Coomassie Blue staining. Fractions eluting in 50 - 100 mM imidazole were combined and showed >95% pure protein corresponding to a molecular weight consistent with that of the calculated molecular weight for Tyc(Phe-AT) or Tyc(Phe-AT(S563A)) at 69.57 kDa. The enzyme solutions (100 mL) for each enzyme were separately concentrated to 1 mL by sizeselective centrifugation (Centriprep 30,000 MWCO unit; Millipore, Billerica, MA). The buffer was exchanged with the Assay buffer (50 mM HEPES containing 100 mM NaCl and 1 mM EDTA at pH 8.0) over five dilution/concentration cycles. Enzyme purity was estimated by SDS-PAGE with Coomassie Blue staining. The concentration of each protein (35 and 28 mg/mL for Tyc(Phe–AT) and Tyc(Phe–AT(S563A)), respectively) was determined by measuring the  $A_{280}$ absorbance on a NanoDrop ND1000 Spectrophotometer (Thermo Scientific, Wilmington, DE). The calculated extinction coefficient and molecular weight of either Tyc(Phe-AT) or Tyc(PheAT(S563A) was  $\epsilon_{280} = 60405~\text{M}^{-1}~\text{cm}^{-1}^{27}$  and 69.57 kDa, respectively. The purified proteins were stored at -80 °C.

## 3.2.8. Activity Evaluation of Tyc(Phe–AT) and Tyc(Phe–AT(S563A)) with CoA and Aminophenylpropanoids

Substrates  $\alpha$ -phenylalanine,  $\beta$ -phenylalanine, and (2R,3S)-phenylisoserine (each at 1 mM) were separately incubated at 31 °C in single stopped-time (1 h) assays containing 100 mM HEPES (pH 8.0), ATP (1 mM), MgCl<sub>2</sub> (3 mM), CoA (1 mM), and Tyc(Phe–AT) or Tyc(Phe– AT(S563A)) (100 µg). Various control reactions were done in parallel under the same conditions used for assays containing enzyme, where Tyc(Phe-AT) or Tyc(Phe-AT(S563A)), ATP, or amino acid was omitted from the assay. The reactions were quenched by acidification to pH ~2 (10% formic acid in dH<sub>2</sub>O) and lyophilized to dryness. The resultant samples were separately dissolved in 100 µL dH<sub>2</sub>O (pH 4.0) and analyzed using a Quattro-Premier XE Mass Spectrometer coupled to an Acquity<sup>®</sup> UPLC system fitted with a C18 Ascentis Express column  $(2.5 \times 50 \text{ mm}, 2.7 \mu\text{m})$  at 30 °C. An aliquot (10  $\mu$ L) of each sample was loaded onto the column and the analytes were eluted with a solvent gradient of acetonitrile (Solvent A) and 0.05% triethylamine in distilled water (Solvent B) (held at 2.5% Solvent A for 3.17 min, increased to 100% Solvent A over 5 sec with a 2-min hold, and then returned to 2.5% Solvent A over 5 sec with a 50-sec hold) at a flow rate of 0.4 mL/min. The effluent from the column was directed to the mass spectrometer set to negative ion mode with a scan range of m/z 50 – 1000 atomic mass units.

# 3.2.9. Kinetic Evaluation of Tyc(Phe–AT) and Tyc(Phe–AT(S563A)) for CoA and Aminophenylpropanoids

After identifying productive substrates for Tyc(Phe–AT) or Tyc(Phe–AT(S563A)), (R)– $\beta$ – phenylalanine, and (2R,3S)-phenylisoserine (each at 1 mM) were separately incubated in 1 mL reactions containing 100 mM HEPES (pH 8.0), ATP (1 mM), MgCl<sub>2</sub> (3 mM), CoA (1 mM), and Tyc(Phe-AT) or Tyc(Phe-AT(S563A)) (100 µg) to establish steady-state conditions with respect to protein concentration and time at 31 °C. Under steady-state conditions, (R)- $\beta$ phenylalanine and (2R,3S)-phenylisoserine at 5 - 2000  $\mu$ M were separately incubated with Tyc(Phe–AT) or Tyc(Phe–AT(S563A)) (20 µg) for 15 min. At the end of each reaction and prior to mass spectrometry analysis, acetyl CoA (1 µM) was added as the internal standard to each sample to correct for losses during workup. The biosynthetic products were quantified by a LC-ESI-MRM (liquid chromatography electro-spray multiple reaction monitoring) mass spectrometry on the Quattro-Premier XE Mass Spectrometer coupled to an Acquity® UPLC system fitted with a C18 Ascentis Express column (2.5 × 50 mm, 2.7 µm) at 30 °C. An aliquot (5 µL) of each sample was loaded onto the column and the analytes were eluted with a solvent gradient as described in Section 3.2.8. The effluent from the column was directed to the mass spectrometer where the first quadrupole mass analyzer (in negative ion mode) was set to select for the molecular ion of a biosynthesized acyl CoA product. The selected ion was then directed to a collision gas chamber wherein the collision energy was optimized to maximize the abundance of a signature fragment ion (m/z 408.31, derived by a fragmentation reaction in theCoA moiety of the acyl CoA) monitored in the second quadrupole mass analyzer in negative ion mode. The peak area under the curve of the monitored fragment ion m/z 408.31 corresponding to each biosynthetic phenylpropionyl CoA thioester was converted to concentration by comparison

to a standard curve of authentic CoA (0.048 – 100  $\mu$ M). The initial velocity ( $v_o$ ) production of (R)– $\beta$ –phenylalanyl–, and (2R,3S)–phenylisoserinyl CoA made in separate assays was plotted against substrate concentration and fit by non–linear regression to the Michaelis–Menten equation ( $R^2$  was typically between 0.90 and 0.99) to calculate the  $K_M$  and  $k_{cat}$ .

The  $K_{\rm M}$  values of Tyc(Phe–AT) and Tyc(Phe–AT(S563A)) for CoA was assessed by incubating each enzyme separately with (R)– $\beta$ –phenylalanine, MgCl<sub>2</sub> (3 mM), ATP (1 mM), and CoA varied between 5 – 2000  $\mu$ M at 31 °C for 15 min. At the end of each reaction and prior to mass spectrometry analysis, acetyl CoA (1  $\mu$ M) was added as the internal standard to each sample. The products of the enzyme-catalyzed reactions were quantified by a LC–MRM mass spectrometry, and the monitored fragment ion (m/z 408.31) derived from the CoA thioester analytes in the effluent were quantified identically to the procedure described earlier in this Section. The initial velocity ( $\nu_0$ ) production of (R)– $\beta$ –phenylalanyl CoA made in separate assays was plotted against substrate concentration and fit by non–linear regression to the Michaelis–Menten equation ( $R^2$  was 0.9) to calculate  $K_{\rm M}$ .

### 3.2.10. Stereospecificity of Tyc(Phe–AT) for Phenylisoserine Stereoisomers

### 3.2.10.1. Preparation of (2R,3R)-Phenylisoserine

$$\begin{array}{c|c} O \\ \hline O \\$$

Figure 3.2. Deprotection of (2R,3R)-phenylisoserine

The N-Boc-(2R,3R)-phenylisoserine was deprotected as previously reported. 28 Briefly, to 5 mg

(0.018 mmol) of the *N*–Boc–(2*R*,3*R*)–phenylisoserine in a 25-mL round bottom flask was added dichloromethane (1 mL). To the solution stirred at 0 °C was added dropwise TFA:DCM (1:1 v/v, 1 mL total) until all the starting material was deprotected (monitored by TLC; 1:3:6 acetic acid: dH<sub>2</sub>O: *t*-butanol). The reaction was concentrated under vacuum to 1 mL, then diluted 2-fold in dichloromethane, and concentrated to 1 mL. This dilution/concentration cycle was repeated three times, and then the solvent was removed completely. The residue was dried under vacuum to obtain a white solid (3.2 mg, 0.018 mmol, 100% yield) which was judged to be 100% pure by  $^{1}$ H-NMR analysis.  $^{1}$ H-NMR (500 MHz, D<sub>2</sub>O)  $\delta$ : 4.78 – 4.82 (m, H-2 & H-3), 7.41 – 7.42 (m, aromatic protons).  $^{13}$ C-NMR (126 MHz, D<sub>2</sub>O)  $\delta$ : 173.31 (C1), 131.50 (C4), 129.70 (C7), 128.90 (C5 & C9), 127.89 (C6 & C8), 70.38 (C2), 55.87 (C3).

## 3.2.10.2. Preparation of (2S,3R)-Phenylisoserine

O  
NH O  
OH 
$$\frac{7 \text{ N HCl}}{95 \text{ °C}, 24 \text{ h}}$$
 OH  
ether extraction  $\frac{5}{8}$  OH

Figure 3.3. Deprotection of (2S,3R)-phenylisoserine

To a 25 mL round-bottom flask, 5 mg (0.018 mmol) of (2S,3R)–N–benzoyl–3–phenylisoserine and 7 N HCl (1 mL) were added and the reaction stirred under reflux for 24 h. The reaction was then cooled down to room temperature and diethyl ether was added to remove benzoic acid, leaving the product in the aqueous layer, which was lyophilized to obtain (2S,3R)–phenylisoserine (2.2 mg, 0.012 mmol, 57% yield at >98% purity by  $^{1}$ H-NMR analysis).  $^{1}$ H-NMR (500 MHz, D<sub>2</sub>O)  $\delta$ : 4.56 (d, J = 6.36 Hz, H-2), 4.64 (d, J = 6.36 Hz, H-3), 7.41 – 7.53 (m,

aromatic protons). <sup>13</sup>C-NMR (126 MHz, D<sub>2</sub>O) δ: 176.30 (C1), 133.44 (C4), 129.27 (C7), 128.98 (C5 & C9), 127.17 (C6 & C8), 73.35 (C2), 57.42 (C3).

## 3.2.10.3. Evaluation of Tyc(Phe–AT) Activity for Phenylisoserine Stereoisomers

(2R,3S)–, (2R,3R)–, and (2S,3R)–Phenylisoserine (each at 1 mM) were separately incubated at 31 °C in single stopped–time (1 h) assays, containing 100 mM HEPES (pH 8.0), ATP (1 mM), MgCl<sub>2</sub> (3 mM), CoA (1 mM), and Tyc(Phe–AT) (100  $\mu$ g). The assays were quenched by acidifying to pH ~2 (10% formic acid) and lyophilized to dryness. The resultant samples were separately dissolved in 100  $\mu$ L dH<sub>2</sub>O (pH 4.0) and analyzed by LC–ESI–MRM as described in Section 3.2.9.

## 3.2.10.4. Kinetic Evaluation of Tyc(Phe–AT) for CoA and Phenylisoserine Stereoisomers

The kinetic parameters of Tyc(Phe–AT) for (2R,3R)–phenylisoserine were determined to provide a basis of comparison with the (2R,3S)–phenylisoserine isomer (described in Section 3.2.9). (2R,3R)–Phenylisoserine (at 1 mM) was incubated in a 1–mL reaction containing 100 mM HEPES (pH 8.0), ATP (1 mM), MgCl<sub>2</sub> (3 mM), CoA (1 mM), and Tyc(Phe–AT) (100  $\mu$ g·mL) to establish steady-state conditions with respect to protein concentration and time at 31 °C. Aliquots (100  $\mu$ L) were taken at various time points between 0 – 2 h and quenched with 10% formic acid (5  $\mu$ L). Acetyl CoA (1  $\mu$ M) was added as the internal standard and the samples were analyzed as described in Section 3.2.8. The kinetic assays with (2R,3R)–phenylisoserine were done similarly to the procedure described for (2R,3S)–phenylisoserine in Section 3.2.9.

## 3.2.10.5. Inhibition Studies of (2R,3S)-Phenylisoserine by the Enantiomer (2S,3R)-Phenylisoserine

The inhibition of Tyc(Phe–AT) by the (2S,3R)–phenylisoserine was determined by incubating (2R,3S)–phenylisoserine at varying concentrations (0.01 - 2 mM), ATP (1 mM), CoA (1 mM), and MgCl<sub>2</sub> (3 mM). A fixed concentration of (2S,3R)–phenylisoserine (0.25 mM) and Tyc(Phe–AT)  $(20 \mu\text{g})$  were added to each of the assay and the reaction incubated at 31 °C for 30 min. The assays were quenched by acidifying to pH ~2 (10% formic acid) and analyzed by LC–ESI–MRM as described in Section 3.2.9.

#### 3.3. Results and Discussion

## **3.3.1.** Construction and Expression of Tyc(Phe–A)

The *tyc(phe–a)* cDNA encoding the Tyc(Phe–A) domain was heterologously expressed as a C-terminal His6-fusion in *E. coli* BL21(DE3). The solubly-expressed enzyme was isolated and Ni-affinity purified to 98% for use in the activity assays. The Tyc(Phe–A) protein from both the soluble and insoluble fractions was analyzed by SDS–PAGE and Coomasie–blue staining (**Figure 3.4**).

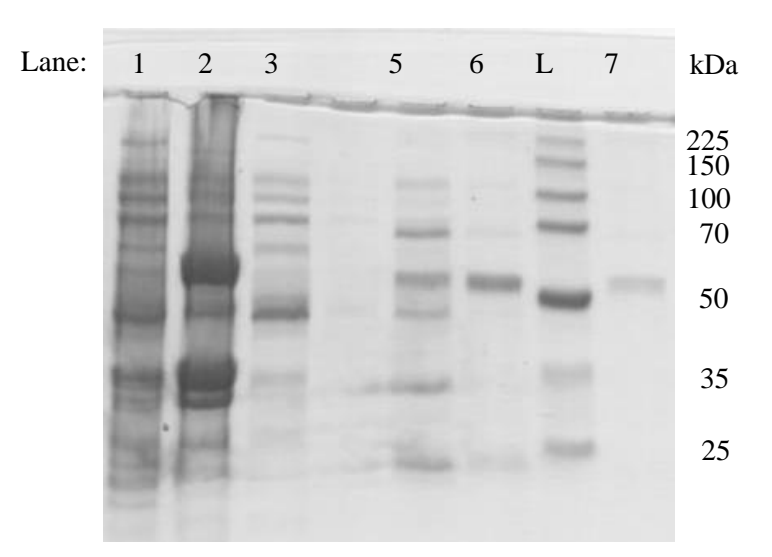


**Figure 3.4.** SDS-polyacrylamide gel electrophoresis (12% acrylamide) and Coomassie-Blue staining of recombinantly expressed Tyc(Phe-A) isolated from *E. coli* BL21(DE3). Lane 1: whole cell contents before IPTG induction; Lane 2: whole cell contents after IPTG induction. The profile of the soluble protein eluted from Ni-affinity resin chromatography with Binding buffer contained the following; Lane 3: flow-through; Lane 5: 50 mM imidazole (fraction 1); Lane 6: 100 mM imidazole (fraction 2); L: Molecular weight standard; Lane 7: 200 mM imidazole (fraction 3).

## 3.3.2. Activity of Tyc(Phe-A) with ATP, CoA, and Aminophenylpropanoids

In a previous study, the Tyc(Phe–A) domain was reported as active when its stand-alone thiolation (T) domain Tyc(Phe–T) complement was added to the reaction mixture that included ATP and [\frac{14}{C}]-α-phenylalanine.\frac{11}{1} The phenylalanine was thioesterified by the pendent pantetheinyl thiol donor on the holo–Tyc(Phe–T) domain. This study confirmed the formation of a phenylalanyl–AMP intermediate. This earlier study suggested that Tyc(Phe–A) is an active stand-alone domain that catalyzed phenylalanine adenylation.

In the current study, it was hypothesized that CoA would serve as a thiol donor based on similarities to the Tyc(Phe–T)–bound 4'–Ppant moiety. The enzyme activity of Tyc(Phe–A) was tested in separate assays containing ATP (1 mM), MgCl<sub>2</sub> (3 mM), CoA (1 mM), and either  $\alpha$ –,  $\beta$ –phenylalanine, or (2*R*,3*S*)–phenylisoserine. *N*–acetylcysteamine was also used as a thiol donor in place of CoA in separate assays under similar conditions. Control reactions were done in

parallel under the same conditions except Tyc(Phe-A), ATP, or CoA was omitted. No aminoacyl CoA nor aminoacyl-N-acetylcysteamine was detected by ESI mass spectrometer for either  $\alpha$ phenylalanine,  $\beta$ -phenylalanine, or (2R,3S)-phenylisoserine. Thus, CoA binding was either affected by the absence of thiolation domain, or the expressed Tyc(Phe-A) was inactive. To address these arguments, a tryptophan fluorescence quenching technique was used to assess indirectly the functional expression of the Tyc(Phe-A) truncation. In addition, Tyc(Phe-AT) and Tyc(Phe–AT(S563A)) were expressed to assess the dependence of the CoA thioesterification on The S563A mutant thiolation domain. was constructed eliminate phosphopantetheinylation of the T-domain, and thus eliminate competition between the pendent thiol and the diffusible CoA added to the activity assay.

## 3.3.3. Assessing Tyc(Phe–A) Substrate Binding by Tryptophan Fluorescence Quenching Studies

In principle, fluorescence quenching is observed when molecular contact between a fluorophore and a quencher molecule occurs. The contact can be as a result of diffusive encounter (dynamic quenching) or due to complex formation (static quenching).<sup>29</sup> When a contact between the quencher and the fluorophore (which is in the excited state) is established, its excited electron in the LUMO (lowest unoccupied molecular orbital) returns to ground state. The fluorophore is unable to emit light and the energy is dissipated as heat.<sup>29</sup> The fluorescence quenching technique has been exploited to study protein conformation changes and interactions with other molecules.<sup>30,31</sup> Tryptophan fluorescence is highly sensitive to its local environment and is affected by any changes to the protein conformation as a result of ligand binding. Therefore,

tryptophan has been used as a probe to study protein dynamics and intermolecular interactions including protein-ligand binding.<sup>30,31</sup>

Previously, a tryptophan quenching titration experiment was used to determine the binding constants of amino acids to Grs1, a homolog of TycA.  $^{32,33}$  Increase in tryptophan quenching within Grs1 (Phe–A domain) in the presence of varying concentrations of acrylamide showed a linear correlation.  $^{33}$  This observation led to the conclusion that a single tryptophan residue was involved in the quenching, which was presumed to be W239.  $^{33}$  This previous study prompted the application of equilibrium tryptophan fluorescence quenching to determine the binding outcome of (2S)– $\alpha$ –phenylalanine to the Tyc(Phe–A) domain examined herein. Equation 1 shows the relationship between the change in the observed fluorescence  $(\Delta F_{obs})$ , the ligand dissociation constant  $K_d$ , and the maximum observed difference in tryptophan fluorescence quenching when the ligand is saturating  $(\Delta F_{max})$ .  $\Delta F_{obs} = F_0 - F_{[S]}$ ; where  $F_0$  is the fluorescence emission without the ligand and  $F_{[S]}$  is the quenched fluorescence reading of Tyc(Phe–A) at ligand concentration [S]. The  $K_d$  of Tyc(Phe–A)  $(0.1 \ \mu\text{M})$  for (2S)– $\alpha$ –phenylalanine was  $4.0 \pm 1.0 \ \mu\text{M}$  with a  $\Delta F_{max}$  of 24.3.

$$\Delta F_{obs} = \frac{\Delta F_{max}[S]}{K_{d} + [S]}$$
 Equation 1

Similar equilibrium titrations were repeated with Tyc(Phe–AT), (a functional aminoacyl CoA ligase). The similar  $K_d$  value of 4.0  $\pm$  1.0  $\mu$ M for Tyc(Phe–AT) agreed with that for Tyc(Phe–A) suggesting that (2S)– $\alpha$ –phenylalanine could bind the Tyc(Phe–A) active site.

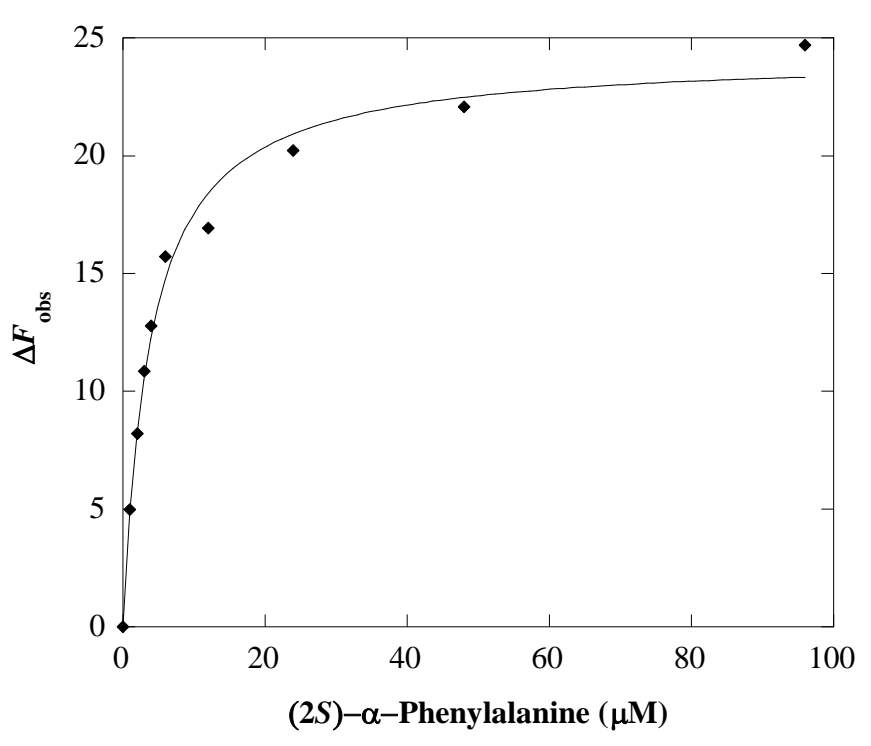


**Figure 3.5**. Plot of observed fluorescence change with increasing concentration of (2S)- $\alpha$ -phenylalanine (0 – 96  $\mu$ M) titrated to 0.1  $\mu$ M Tyc(Phe-A) (in K<sup>+</sup>HEPES, pH 7.5, 25 °C). The curve was fit by the nonlinear regression curve defined by equation 1.

In an earlier study, analysis of the Grs1(Phe–A) domain (62% sequence similarity with Tyc(Phe–A)) reported a dissociation constant for (2S)– $\alpha$ –phenylalanine of 6.0  $\pm$  1.0  $\mu$ M<sup>32</sup> which is similar to that determined in the current study (**Table 3.1**). These results suggest that the inability of Tyc(Phe–A) to catalyze aminoacyl CoA biosynthesis stem from its failure to bind CoA in a catalytically competent orientation for nucleophilic displacement of AMP from the adenylate intermediate as discussed in Section 3.3.6.

**Table 3.1**. The dissociation constants for binding of (2S)– $\alpha$ –phenylalanine ((2S)– $\alpha$ –Phe) to Tyc(Phe–A), Tyc(Phe–AT), and Grs1(Phe–A).

Substrate	$K_{ m d}  (\mu  m M)$		
	Tyc(Phe–A))	Tyc(Phe–AT)	Grs1(Phe–A) <sup>32</sup>
(2S)–α–Phe	$4.0 \pm 1.0$	$4.0 \pm 1.0$	$6.0 \pm 1.0$
$(2S)$ - $\alpha$ -Phe + AMP	$8.0 \pm 1.0$	$7.0 \pm 1.0$	*ND

<sup>\*</sup>Not determined

In a previous study, a standalone A domain (EntE), that belongs to the NRPS enzyme family was shown to activate dihydroxybenzoate to its adenylate anhydride.<sup>34</sup> The earlier study evaluate whether CoA would act as a surrogate of the native 4'-Ppant. The formation of dihydroxybenzoyl CoA was analyzed indirectly by measuring the formation of PPi using a continuous spectrophotometric assay. A dearth of PPi (that confirmed the production of dihydroxybenzoyl CoA) was detected, suggesting that the product formed fortuitously and nonenzymatically in solution.<sup>34</sup> A similar conclusion was derived from earlier studies in which Tyc(Phe-A) and Tyc(Phe-T) domains were expressed separately and mixed as untethered standalone domains with  $\alpha$ -phenylalanine and ATP. Similar to the results for the EntE study, only a small amount of Tyc(Phe-T) was thioesterified. Based on the results from the previous EntE and Tyc(Phe–T) thioesterification studies, it could be imagined that in the current study, Tyc(Phe-A) catalyzes the adenylation of α-phenylalanine. Thereafter, CoA merely nonenzymatically thioesterifies (2S)–α-phenylalanine by reaction with the AMP anhydride intermediate when it dissociates from the enzyme. Since no observable CoA thioester product was obtained in reactions with Tyc(Phe-A) and the needed cofactors, even with detection by an LC-ESI-MRM method, it is evident that CoA binds to the Tyc(Phe-ATE) or Tyc(Phe-AT) active site, where it forms acyl thioesters, and this binding is interrupted in the absence of Tyc(Phe–T) domain, as discussed in the next Section (3.3.4).

### 3.3.4. Construction and Expression of Tyc(Phe–AT) and Tyc(Phe–AT(S563A))

The wild-type *tycA* cDNA encoding the A-, T-, and E-domains was truncated to test the activity of Tyc(Phe–AT) didomain for aminoacyl CoA biosynthesis. In addition, a mutant Tyc(Phe–AT(S563A)) derived from Tyc(Phe–AT) was expressed to eliminate the native pantetheinylation

of S563; this way, the only thiol/nucleophile would be the one added exogenously. The apparent molecular mass (69.5 kDa) of the expressed Tyc(Phe–AT) and Tyc(Phe–AT(S563A)) on SDS–PAGE was consistent with the theoretical value (**Figure 3.6**).

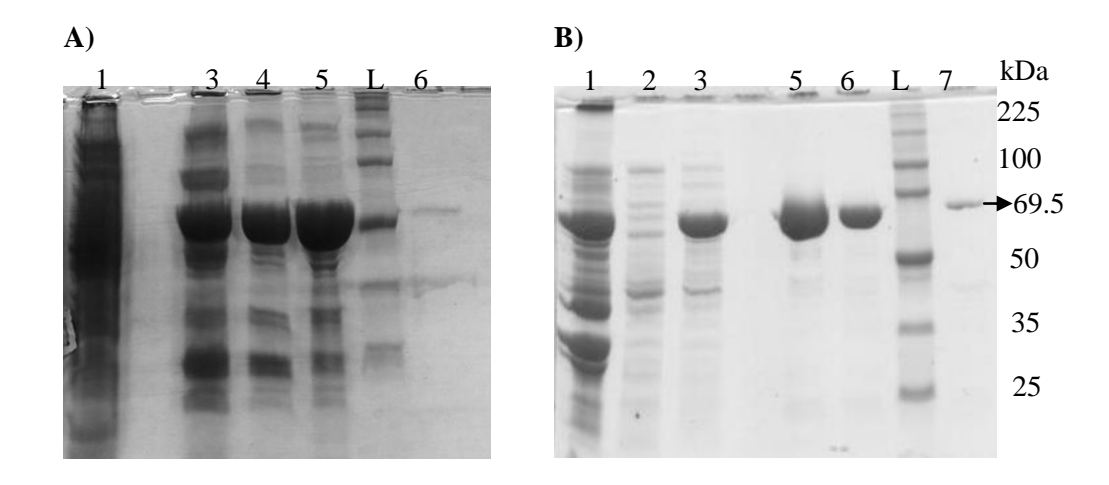


**Figure 3.6.** SDS-polyacrylamide gel electrophoresis (12% acrylamide) and Coomassie blue staining of recombinantly expressed Tyc(Phe–AT) (**A**) and Tyc(Phe–AT(S563A)) (**B**) which were separately isolated from *E. coli* BL21(DE3). **A**) Lane 1 shows the soluble cell crude lysate before purification. The profile of the soluble protein eluted from nickel–affinity resin chromatography with Binding buffer contained the following; Lane 3: 20 mM imidazole wash; Lane 4: 50 mM imidazole (fraction 1); Lane 5: 100 mM imidazole (fraction 2); L: Molecular weight standard; Lane 6: 200 mM imidazole (fraction 3). **B**) Lane 1: 10 mM imidazole wash; Lane 2: 20 mM imidazole wash; Lane 3: 50 mM imidazole (fraction 1); Lane 5: 100 mM imidazole (fraction 2); Lane 6: 200 mM imidazole (fraction 3); Lane 7: 250 mM imidazole (fraction 4).

## 3.3.5. Activity and Kinetic Analysis of Tyc(Phe–AT) with ATP, CoA, and Aminophenylpropanoids

Tyc(Phe–AT) and Tyc(Phe–AT(S563A)) were incubated with CoA, cofactors, and separately with (S)– $\alpha$ –, (R)– $\beta$ –phenylalanine, or (2R,3S)–phenylisoserine. Analysis of the assay products by LC–MS method showed a mass profile matching that of authentic phenylalanyl CoA. The results reveal that truncation of Tyc(Phe–AT) and Tyc(Phe–AT(S563A)) enhanced turnover rates for the three substrates examined compared to Tyc(Phe–ATE). The  $k_{cat}$  of (R)– $\beta$ –phenylalanine was

the most improved with either catalyst by 7-fold compared to the wild-type Tyc(Phe–ATE), whereas the  $K_{\rm M}$  was within the same range for both wild type Tyc(Phe–ATE) and the truncated version Tyc(Phe–AT).

**Table 3.2**. Steady–state kinetic analysis of Tyc(Phe–AT) and Tyc(Phe–AT(S563A)) with CoA in comparison to Tyc(Phe–ATE) and Tyc(Phe–ATE(S563A))

Tyc(Phe-AT)					
Substrate	$K_{\rm M}$ ( $\mu$ M)	$k_{\rm cat}  ({\rm min}^{-1})$	$k_{\rm cat}/K_{\rm M}~({\rm s}^{-1}\cdot{\rm M}^{-1})$		
(R)–β–phenylalanine	$45.9 \pm 2.60$	$14.6 \pm 0.500$	$4018 \pm 119$		
(2R,3S)–Phenylisoserine	440 ± 62.1	$1.51 \pm 0.170$	$33.5 \pm 1.70$		
CoA <sup>a</sup>	$208 \pm 57.2$	$10.4 \pm 2.00$	$838 \pm 74.0$		
Tyc(Phe-AT(S563A))					
$(R)$ – $\beta$ –phenylalanine	$32.6 \pm 4.70$	$22 \pm 4.10$	$11244 \pm 485$		
(2R,3S)–Phenylisoserine	$348 \pm 140$	$1.06 \pm 0.570$	$50.6 \pm 8.20$		
CoA <sup>a</sup>	$687 \pm 250$	$31.4 \pm 8.30$	$762 \pm 87.0$		
Tyc(Phe–ATE)					
$(R)$ – $\beta$ –phenylalanine	$50.6 \pm 7.90$	$1.6 \pm 0.300$	$527 \pm 129$		
(2R,3S)–Phenylisoserine	$89.3 \pm 15.0$	$0.25 \pm 0.020$	$46.7 \pm 8.70$		
$CoA^b$	$1976 \pm 175$	$0.75 \pm 0.050$	$6.3 \pm 0.700$		
Tyc(Phe–ATE(S563A))					
$(R)$ – $\beta$ –phenylalanine	$62.3 \pm 1.00$	$3.00 \pm 0.04$	$803 \pm 17.0$		
(2R,3S)–Phenylisoserine	$191 \pm 10.0$	$0.43 \pm 0.01$	$37.5 \pm 2.10$		
CoA <sup>b</sup>	$804 \pm 26.0$	$0.90 \pm 0.08$	$18.7 \pm 1.80$		

<sup>&</sup>lt;sup>a</sup>Kinetic measurements for CoA were done in the presence of (R)–β–phenylalanine, ATP, and MgCl<sub>2</sub>. <sup>b</sup>Kinetic measurements for CoA were performed in the presence of (S)–α–phenylalanine, ATP, and MgCl<sub>2</sub>. All values are expressed as means  $\pm$  standard deviations of triplicates. The kinetic values of Tyc(Phe–ATE) and Tyc(Phe–ATE(S563A)) are listed for comparison to those of Tyc(Phe–AT) and Tyc(Phe–AT(S563A)).

Similarly, (2R,3S)—phenylisoserine showed a gain in turnover rate with both Tyc(Phe–AT) (6-fold increase) and Tyc(Phe–AT(S563A)) (2.5-fold increase) compared to the Tyc(Phe–ATE) and Tyc(Phe–ATE(S563A)) respectively. Tyc(Phe–AT(S563A)) displayed the highest  $k_{\text{cat}}$  value when incubated with CoA (35-fold increase) compared to the Tyc(Phe–ATE(S563A)) counterpart. Additionally, Tyc(Phe–AT) showed a 4-fold improvement in  $k_{\text{cat}}$  with CoA compared to the wild type Tyc(Phe–ATE). The catalytic efficiency ( $k_{\text{cat}}/K_{\text{M}}$ ) of Tyc(Phe–AT) for CoA improved 10 orders-of-magnitude over that of Tyc(Phe–ATE) due mainly to lower  $K_{\text{M}}$ 

value ( $208 \pm 57.2 \,\mu\text{M}$ ). The same increase in catalytic efficiency of Tyc(Phe–AT) and Tyc(Phe–AT(S563A)) at 8-fold and 14-fold, respectively due mainly to a 7-fold increase in  $k_{\text{cat}}$  for (R)– $\beta$ –phenylalanine was also observed. The catalytic efficiency of Tyc(Phe–AT) for (2R,3S)–phenylisoserine was lower compared to that of Tyc(Phe–ATE) due to a higher  $K_{\text{M}}$  value despite the 6-fold greater  $k_{\text{cat}}$  (**Table 3.2**). Overall, the catalytic efficiencies of Tyc(Phe–AT) and Tyc(Phe–AT(S563A)) were superior to those for the wild-type Tyc(Phe–ATE) and Tyc(Phe–ATE(S563A)) counterparts, respectively for the three substrates. These results suggest that eliminating the epimerization (E) domain likely improved product dissociation from the multidomain enzyme as evidenced by the improved turnover rates (**Table 3.2**). In addition, the possibility of epimerization of aminoacyl CoA products was eliminated.

### 3.3.6. Tyc(Phe–AT) Secondary Structure Model and Comparison with CoA Ligases

Previous studies showed that the secondary structures of acetate:CoA ligase (AcCL, from *Salmonella enterica*, PDB code: 1PG4), Grs1(Phe–A PDB code: 1AMU), and DhbE (a free standing adenylation domain from *Bacillus subtilis*, PDB code: 1MDF) are similar, <sup>15</sup> while their amino acid sequence homology is only moderate (19 – 25% similar). <sup>15</sup> It is well known that Tyc(Phe–AT) normally thioesterify α–phenylalanine with a pantetheinyl side chain covalently linked to the T–domain through a phosphate ester bond. By contrast, CoA ligases use diffusible CoA in the bulk medium to thioesterify the acyl substrates. <sup>35</sup> Phosphopantetheine is a precursor of CoA and, by comparison lacks the adenine moiety at the 4'–phosphate terminus. In the current study, Tyc(Phe–A) did not biosynthesize aminoacyl CoA, when CoA was used as a cosubstrate with the three amino acid substrates described herein, whereas Tyc(Phe–AT) was active. To help explain how CoA served as a thiol donor in the reaction catalyzed by Tyc(Phe–AT) and not

Tyc(Phe–A), homology models of Tyc(Phe–A) and Tyc(Phe–AT) (SWISS model program)<sup>36</sup> were built on the structure of Grs1(Phe–A) (65% amino acid sequence identity). It should be noted that the amino acid residues of the phenylalanine binding pockets of Tyc(Phe–AT) and Grs1(Phe–A) are 100% identical. The resulting Tyc(Phe–AT) model was compared to 4–chlorobenzoate:CoA (4–ClBzCL; PDB code: 3CW9) and acetate:CoA (AcCL, PDB code: 1PG4) ligases (**Figure 3.7**). Tyc(Phe–AT) model was superimposed on the structure of 4–ClBzCL and AcCL separately (**Figure 3.7**). There are key features common to Tyc(Phe–AT) and both ligases used herein. The residues used to bind the carboxylate substrate, ATP, and Mg<sup>2+</sup> and those used to catalyze the reaction are highly conserved. In addition, both Tyc(Phe–AT) model and 4–ClBzCL have a channel that accommodates pantetheine chain which is mainly surrounded by hydrophobic and a few hydrophilic residues (**Figure 3.8**).

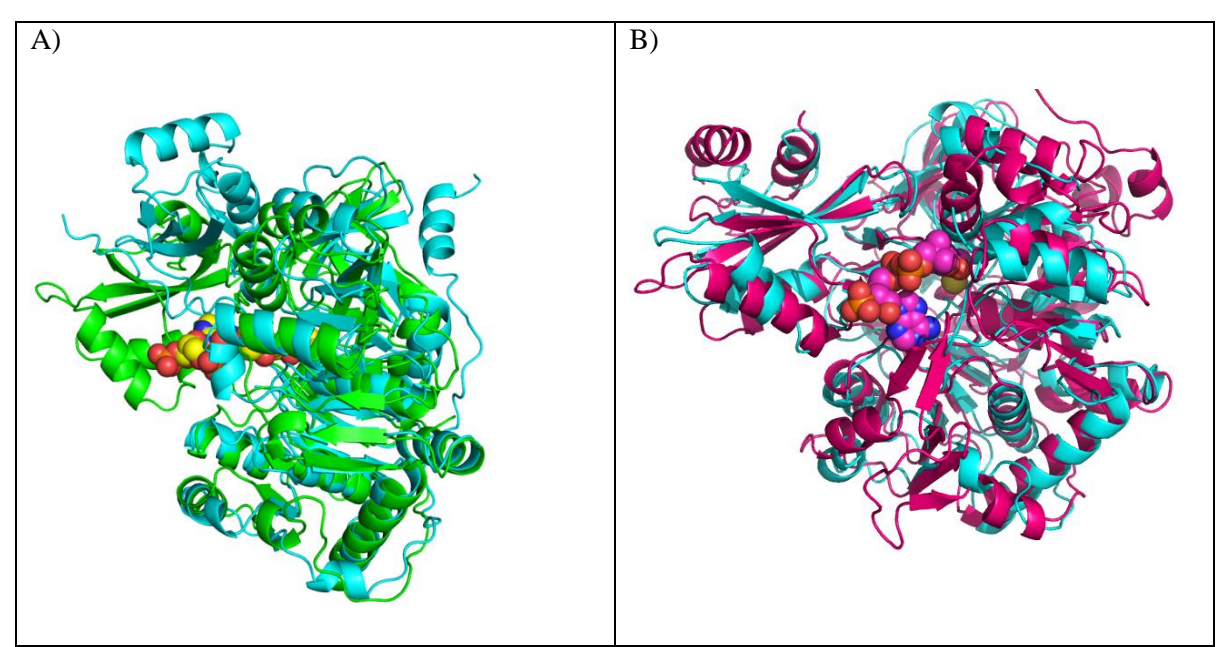


**Figure 3.7**. Comparison of 4–ClBzCL with Tyc(Phe–AT) model. A) Overlay of Tyc(Phe–AT) model (cyan ribbon) and 4–ClBzCL (green ribbon) in complex with CoA (carbon skeleton shown as yellow spheres). The amino acid sequence alignment between the two proteins show 21% sequence identity. B) Overlay of Tyc(Phe–AT) model (cyan ribbon) and AcCL (magenta ribbon) in complex with CoA (hot pink spheres). Tyc(Phe–AT) shows 19% amino acid sequence identity to AcCL.

# 3.3.6.1. Contrasting Structural Features of Tyc(Phe–AT) Model and 4–Chlorobenzoate:CoA Ligase

Key differences are seen between Tyc(Phe–AT) and the CoA ligases, for instance the binding site of the structures of Tyc(Phe–AT) and 4–ClBzCL are noticed. Specifically, the key residues that form favorable interactions with the adenosyl moiety in 4–ClBzCL (S407, W440, K477, R475, D472, F473, and R87) align the CoA binding pocket around the adenosyl group and also form favorable electrostatic contacts with the 5′–diphosphate bridge. Tyc(Phe–AT) residues at the same position (I424, A457, S491, L489, A486, Y487, and E110) are largely hydrophobic that likely do not form favorable interactions with the polar diphosphatidyl adenosyl moiety.

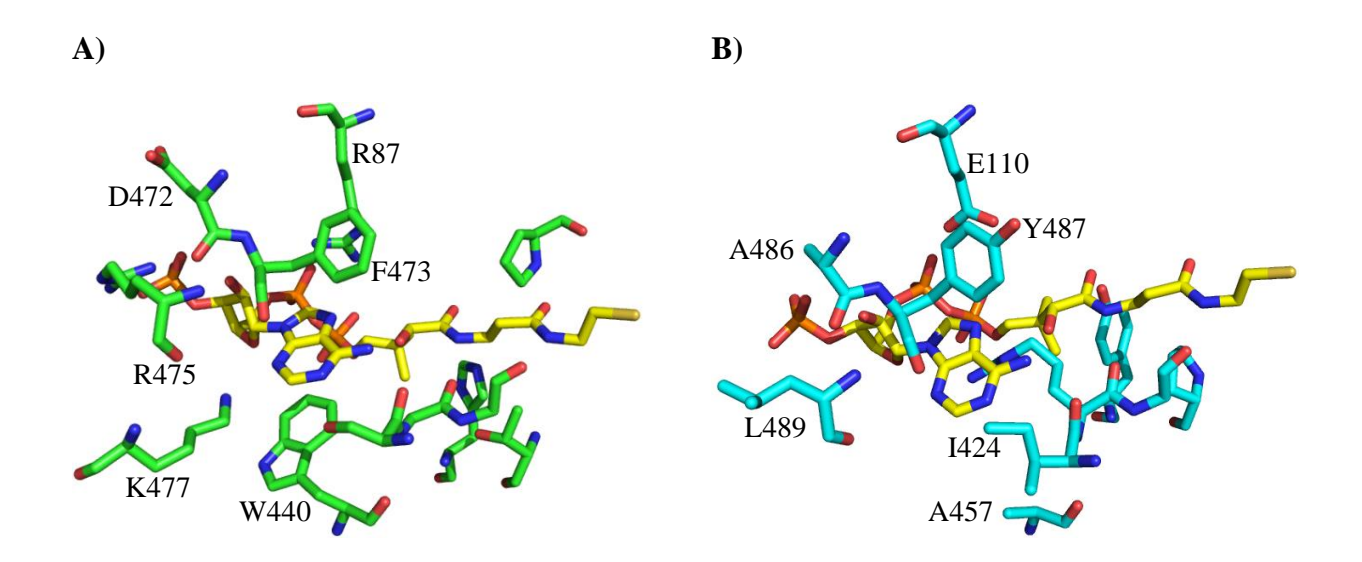


**Figure 3.8**. Comparison of active site of 4–ClBzCL with Tyc(Phe–AT) model. **A)** Shown are residues (green sticks) that constitute the binding pocket of CoA (yellow) in 4–ClBzCL. **B)** Shown are residues (cyan) that surround the proposed binding channel for CoA (yellow) in Tyc(Phe–AT) model.

### 3.3.6.2. Tyc(Phe–AT) Structure Model Alignment with Acetate:CoA Ligase

Comparison of Tyc(Phe–AT) model to that of AcCL structure shows similar residues oriented around the adenosyl group of CoA. In AcCL, the adenine ring of CoA forms  $\pi$ -stacking

interactions with the peptide backbone between G164 and G165 (Figure 3.9A). The other residues that contribute to the hydrophobic environment are F163 and I196 (Figure 3.9A). Additionally, the 5'-diphosphate on the adenosyl of CoA forms favorable interactions with the side chain of R191 whereas 3'-phosphate interacts with R584 and R194 (Figure 3.9A). The pantetheine chain is supported by interaction between the carbon skeleton and hydrophobic residues (G524 and A357) and also the hydrogen bonding of the two amines with polar residues (S523 and H525). In Tyc(Phe-AT), the adenine binding site is surrounded by hydrophilic residues D108, E110 and R428 which are not positioned for a favorable  $\pi$ -stacking interaction with the adenine. Also, the 3'-phosphate binds at the surface of Tyc(Phe-AT) and lacks important H-bonding interactions. Thus, the differences in binding site architecture around the adenosyl moiety most likely contribute to unfavorable binding of CoA to Tyc(Phe-AT). However, the pantetheine binding channel consists of residues similar to those of the AcCL and the 4-ClBzCL. These observations shed light on how the acyl adenylate enzymes are tailored to suite their respective catalytic reactions; the acyl CoA ligases need a framework to support the binding site of adenine moiety of CoA, whereas Tyc(Phe–AT) requires a channel that binds only the pantetheinyl moiety.

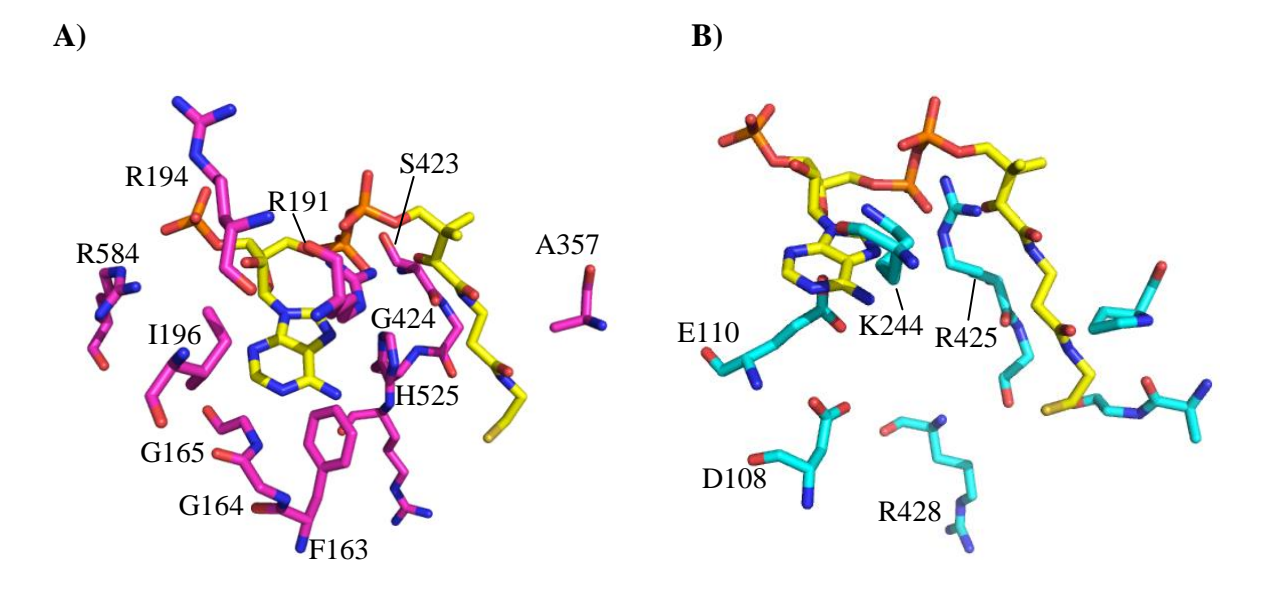


**Figure 3.9**. Comparison of active site of AcCL with Tyc(Phe–AT) model. **A**) Shown are residues (magenta) that contribute to CoA (yellow) binding interactions in AcCL. **B**) Shown are residues (cyan) that constitute the proposed CoA binding pocket in Tyc(Phe–AT).

In AcCL and the 4–ClBzCL, the adenine of CoA is bound on the surface of the protein, and the pantetheinyl moiety is directed into the active site through a hydrophobic channel (**Figures 3.8A** and **3.9A**). The T-domain of the Tyc(Phe–AT) model was excluded by the SWISS modeling program, since the Grs1(Phe–A) structure upon which it was modeled also lacked the conjugate T–domain. These jettisoned residues likely have an added role in binding CoA (see Appendix, **Figure II–3**). The T–domain residues must help CoA to bind Tyc(Phe–AT), as evidenced by the lack of aminoacyl CoA biosynthetic activity by Tyc(Phe–A), which lacked the T–domain as described herein (Section 3.3.1).

### 3.3.7. Substrate Stereospecificity of Tyc(Phe–AT)

The A-domain of Tyc(Phe-ATE) has broad substrate specificity for both S and R amino acids.<sup>37</sup> Specifically, both S- and R-phenylalanine are converted with similar efficiency to a pendent

thioester via an AMP anhydride. Thereafter, the E-domain epimerizes the *S*-phenylalanine to the *R*-isomer at a ratio of 1:2 in favor of *R*-phenylalanine. However, only the *R*-isomer proceeds along the catalytic chain to form the downstream dipeptide bond with proline on the biosynthetic pathway to tyrocidines A – D in *Bacillus brevis* (Chapter 2, Figure 2.1). <sup>37,38</sup> Generally, for NRPS family members, the A-domains are known to be highly promiscuous, <sup>1,37,39,40</sup> and the E-domains are gatekeepers and play a major role in substrate selectivity and stereospecificity. <sup>41-43</sup> However, the interest of using Tyc(Phe-ATE) in the studies described herein was to identify phenylisoserine:CoA ligase that could be used in the biosynthesis of phenylisoserinyl CoA, an important substrate for a 13–*O*–3–amino–3–phenylpropanoyltransferase (BAPT) on the paclitaxel biosynthetic pathway. <sup>44</sup>

The (2R,3S) stereochemistry of the phenylisoserinyl moiety at C-13 of paclitaxel is important for its biological activity (**Figure 3.10**). It was thus necessary to assess the stereospecificity of Tyc(Phe-AT) for the phenylisoserine diastereoisomers before this 'CoA ligase' could be employed in the semi-biosynthesis of paclitaxel or its analogs.

Figure 3.10. Structure of paclitaxel

Tyc(Phe–AT) turned over (2R,3R) isomer at a 2-fold slower rate  $(k_{\text{cat}} = 0.78 \text{ min}^{-1})$  than the (2R,3S)-isomer  $(k_{\text{cat}} = 1.5 \text{ min}^{-1})$ ; the latter has the stereochemistry of the natural side chain

of paclitaxel. The CoA thioester of (2S,3R)-phenylisoserine was below the limits of detection (**Table 3.3**). In order to elucidate the differences observed in the Tyc(Phe–AT) stereospecificity studies, the (2R,3S)-, (2R,3R)-, and (2S,3R)-phenylisoserine isomers were docked into the Grs1(Phe–A) crystal structure using Autodock Vina program<sup>46</sup> (**Figure 3.11B** – **D**). The residues for phenylpropanoyl binding in Grs1(Phe–A) are identical to those used by Tyc(Phe–A), thus the ligand coordinates established by the Grs1(Phe–A) chassis were deemed representative of Tyc(Phe–A).

**Table 3.3**. Kinetic parameters of Tyc(Phe–AT) with phenylisoserine stereoisomers

Substrate	$K_{\rm M}(\mu{ m M})$	$k_{\rm cat}({\rm min}^{\text{-1}})$
(2R,3S)–Phenylisoserine	$440 \pm 62.1$	$1.51 \pm 0.17$
(2R,3R)–Phenylisoserine	$375 \pm 68.8$	$0.780 \pm 0.13$
*(2S,3R)–Phenylisoserine		

<sup>\*</sup>The kinetic constants of Tyc(Phe–AT) for (2*S*,3*R*)–phenylisoserine were not obtained as the CoA product was below the detection limit of the LC–ESI–MS.

The docking conformations of the phenylisoserine isomers were compared to that of (2*S*)-phenylalanine in complex with Grs1(Phe-A) structure (PDB: 1AMU) (**Figure 3.11A – D**). The trajectory of (2*S*)-phenylalanine is established in the active site through a hydrogen bonding interaction between the amino group of the substrate and D235, and a salt bridge between the carboxylate and K517 (**Figure 3.11 A**). The phenyl ring is surrounded by common hydrophobic residues (A236, W239, I299, A322, I330, and C331) in the structures. However, a major difference between phenylalanine and the docked phenylisoserine isomers is the carbon skeleton around the rotatable bond between *ipso* carbon of phenyl ring and C-3. This rotation orients the isoserine moiety in a conformation that enables favorable interactions in the active site. In (2*R*,3*S*)-phenylisoserine (**Figure 3.11 B**), H-bonding interaction between C2-OH and active site D235 is observed. The C3-NH<sub>2</sub> forms polar interaction through hydrogen bonding with D235,

while the carboxylate group continues to interact with K517 but gains an additional interaction with G324.

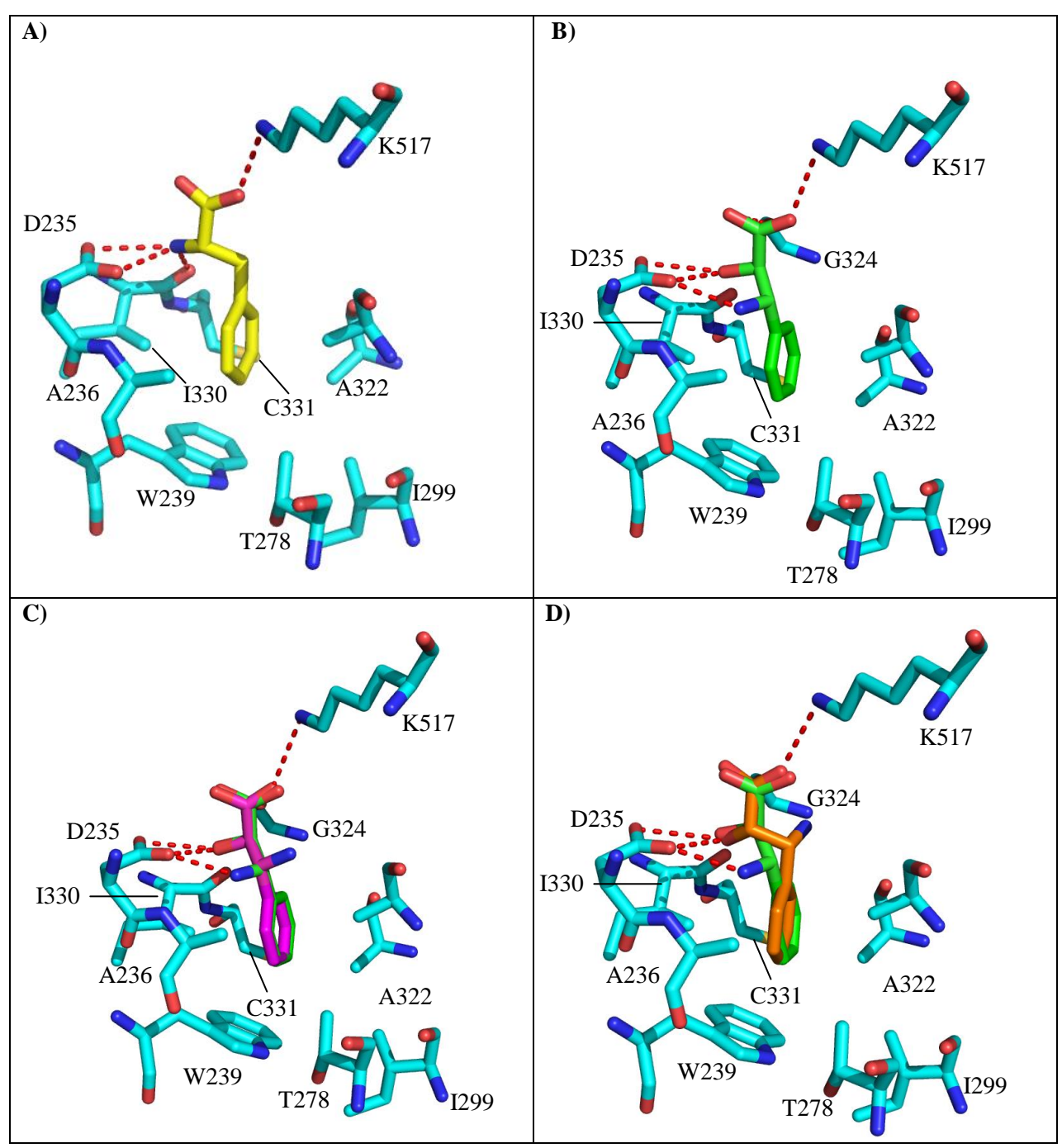


**Figure 3.11.** Grs1(Phe–A) active site (cyan) in complex with aminophenylpropanoids: **A**) (2S)–phenylalanine (yellow). **B**) (2R,3S)–phenylisoserine (green), **C**) (2R,3R)–phenylisoserine (magenta) and (2R,3S)–phenylisoserine (green) superimposed, and **D**) (2S,3R)–phenylisoserine (orange) and (2R,3S)–phenylisoserine (green) superimposed.

Similar hydrogen bonding interaction between C2–OH and active site D235 is seen for (2R,3R)-phenylisoserine (**Figure 3.11 C**). However, the C3–NH<sub>2</sub> is oriented in the opposite direction and the H-bonding contact with D235 is lost. Interestingly, this difference does not affect the binding of (2R,3R)-isomer since the  $K_{\rm M}$  (375 ± 68.8  $\mu$ M) is similar to that of (2R,3S)-phenylisoserine (440 ± 62.1  $\mu$ M). The catalytic rate of Tyc(Phe–AT) however, is 2-fold lower for (2R,3R)-phenylisoserine, compared to that for (2R,3S)-phenylisoserine. The binding of (2S,3R)-phenylisoserine to the active site shows a different orientation of the phenyl ring compared to (2R,3S)-phenylisoserine (**Figure 3.11 D**). Also, the C3–NH<sub>2</sub> binds in a different site, away from D235 (the ligand that contributes to the H-bonding). The loss of Tyc(Phe–AT) activity with (2S,3R)-phenylisoserine could be due to the different orientation of the phenyl ring in the binding pocket in addition to the lack of H-bonding between the C3–NH<sub>2</sub> and active site D235.

### 3.3.7.1. Inhibition Studies of (2R,3S)-Phenylisoserine by the Enantiomer (2S,3R)-Phenylisoserine

In the presence of (2S,3R)—phenylisoserine at 250  $\mu$ M, the  $K_{\rm M}$  of Tyc(Phe–AT) for (2R,3S)—phenylisoserine was 500  $\mu$ M which was nearly identical to the  $K_{\rm M}$  (436  $\mu$ M) of Tyc(Phe–AT) in the absence of the inhibitor. The  $k_{\rm cat}$  however, decreased by 15-fold (**Figure 3.12**) and the  $K_{\rm I}$  (92.0  $\mu$ M) was calculated using **Equation 3.2**.

$$v_{max}' = v_{max}(1+[I]/K_I)$$
 Equation 3.2

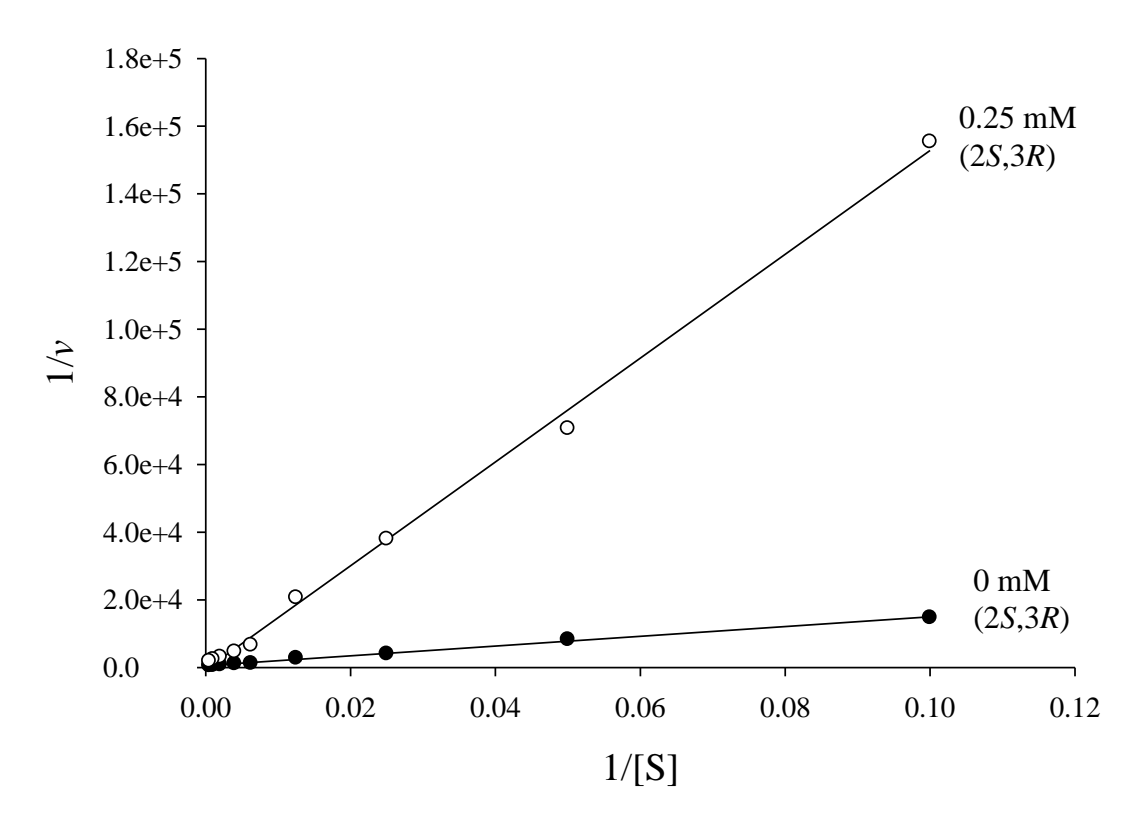


**Figure 3.12**. Lineweaver–Burk plots for the inhibition of Tyc(Phe–AT) by (2S,3R)–phenylisoserine. The  $K_{\rm M}$  value of (2R,3S)–phenylisoserine without inhibitor was 436  $\mu$ M, and  $k_{\rm cat}$  was 1.5 min<sup>-1</sup>. In the presence of (2S,3R)–phenylisoserine  $(25 \, \mu\text{M})$ , the  $K_{\rm M}$  was 500  $\mu$ M and the  $k_{\rm cat}$  was 0.10 min<sup>-1</sup>.

The results indicate a non-competitive inhibition of Tyc(Phe-AT) by (2S,3R)—phenylisoserine suggesting that this inhibitor binds allosterically to a site other than the active site and affects the catalytic turnover.

#### 3.4. Conclusion

Numerous studies on NRPS modules have dissected substrate recognition and the mechanisms of acylation, thioesterification, <sup>3,5,9,12,48-53</sup> and epimerization catalyzed by the domains. <sup>32,39,54-58</sup> This information was useful for identifying an NRPS module Tyc(Phe–ATE) (i.e TycA) that could function as a CoA ligase and thioesterify phenylisoserine, a paclitaxel pathway intermediate, to

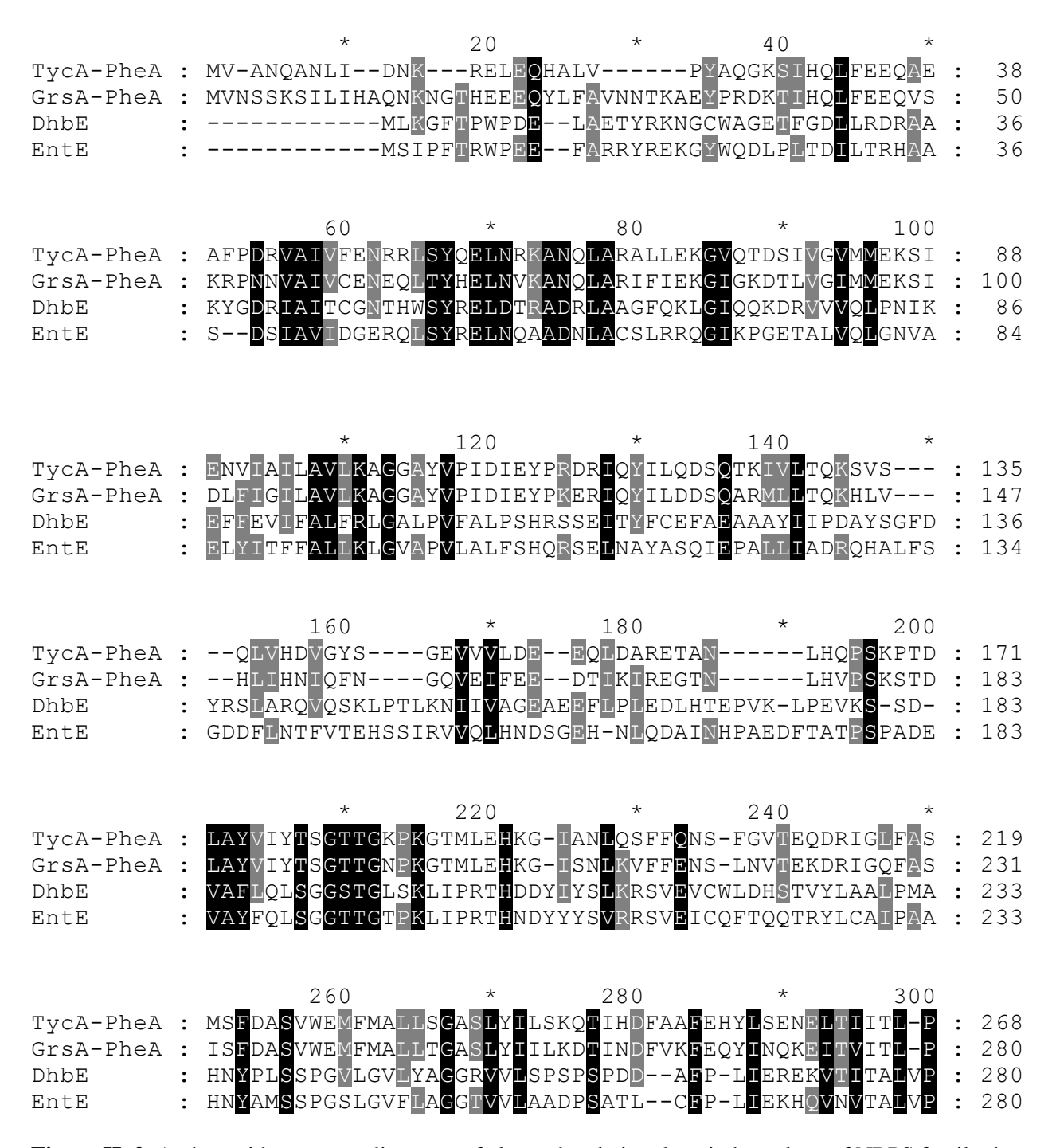
its biologically relevant CoA thioester. The design and biochemical validation of Tyc(Phe–AT) mutants gave us access to catalysts that biosynthesized aminoacyl CoAs at a superior rate (~7fold for (R)- $\beta$ -phenylalanine and (2R,3S)-phenylisoserine) compared to the wild-type Tyc(Phe-ATE) enzymes. The ability of Tyc(Phe–AT) to catalyze the CoA ligase-like reaction traces back to the structural and sequence similarities with acyl CoA ligases. The alignment of Tyc(Phe–AT) model on either acetate:CoA or 4-chlorobenzoate:CoA ligase showed some similarities in the residues lining the active sites where carboxylate, ATP, Mg<sup>2+</sup>, and pantetheine arm of CoA binds. However, striking differences were observed with the composition of residues around adenosyl binding cavity – CoA ligases have residues that support the binding of adenosyl moiety (for example W440, K447, R475, D472, F473 and R87 in 4-clorobenzoate:CoA ligase) whereas Tyc(Phe-AT) consists of residues that are not suitable for favorable  $\pi$ -stacking with the adenosyl moiety or electrostatic interactions with the phosphate groups. The binding affinity and catalytic efficiency of Tyc(Phe-AT) could likely improve upon changing the residues near the adenosyl terminus of CoA (A457, S491, L498, A486, Y487 and E110) to those found in CoA ligases.

Tyc(Phe–AT) was stereospecific for phenylisoserine diastereomers (2R,3S)–phenylisoserine –  $(k_{rel} = 1.0)$ , followed by (2R,3R) –  $(k_{rel} = 0.5)$ , and then (2S,3R) –  $(k_{rel} = 0)$ . Molecular docking of (2R,3S)–phenylisoserine into the active site of Tyc(Phe–AT) homolog (Grs1(Phe–A)) showed that the C2–OH and C3–NH<sub>2</sub> substituents formed favorable polar contacts through H-bonding with D234, while the phenyl ring of the substrate formed hydrophobic interactions in the aryl ring binding pocket. The findings from this study will enable Tyc(Phe–AT) to be used in the development of a biosynthetic route towards paclitaxel and its analogs containing (2R,3S)–arylisoserines.

#### **APPENDIX**

<u>Protein</u>	Motif I	<b>Motif II</b>	<b>Motif III</b>
CoA ligases 4-Chlorobenzoate CL	<sup>161</sup> T <b>SG</b> T <b>TG</b> LP <b>K</b> G <sup>170</sup>	<sup>302</sup> YGT <b>TE</b> <sup>306</sup>	<sup>376</sup> YRTS <b>D</b> <sup>380</sup>
Coumarate CL	TSGTTGPPKG	YGS <b>TE</b>	YRT <b>GD</b>
4–Hydroxybenzoate CL	S <b>SG</b> S <b>TG</b> RP <b>K</b> G	IGS <b>TE</b>	TKS <b>GD</b>
O-Succinatebenzoate CL	T <b>sg</b> t <b>tg</b> pq <b>k</b> a	FGM <b>TE</b>	FNT <b>GD</b>
Acetate CL	T <b>sg</b> s <b>tg</b> kp <b>k</b> g	YWQ <b>TE</b>	YFT <b>GD</b>
Acetyl CL	TSGTTGNPKG	WGM <b>TE</b>	FST <b>GD</b>
Thiol-template acyl-adenylate Grs1 TycA	e forming enzymes  190 TSGSTGNPKG <sup>199</sup> 178 TSGTTGKPKG <sup>187</sup>	YGP <b>TE</b> YGP <b>TE</b>	YRT <b>GD</b> 376  YRT <b>GD</b> 380
EntE	SGGTTGTPKL	FGMA <b>E</b>	YCS <b>GD</b>
Luciferase enzymes			
Luciferase <sup>a</sup> Luciferase <sup>b</sup>	<sup>198</sup> S <b>SG</b> S <b>TG</b> LP <b>K</b> G <sup>207</sup> S <b>SG</b> T <b>TG</b> LP <b>K</b> G	<sup>340</sup> YGL <b>TE</b> <sup>344</sup> FGL <b>TE</b>	418LHS <b>GD</b> 422 LHS <b>GD</b>

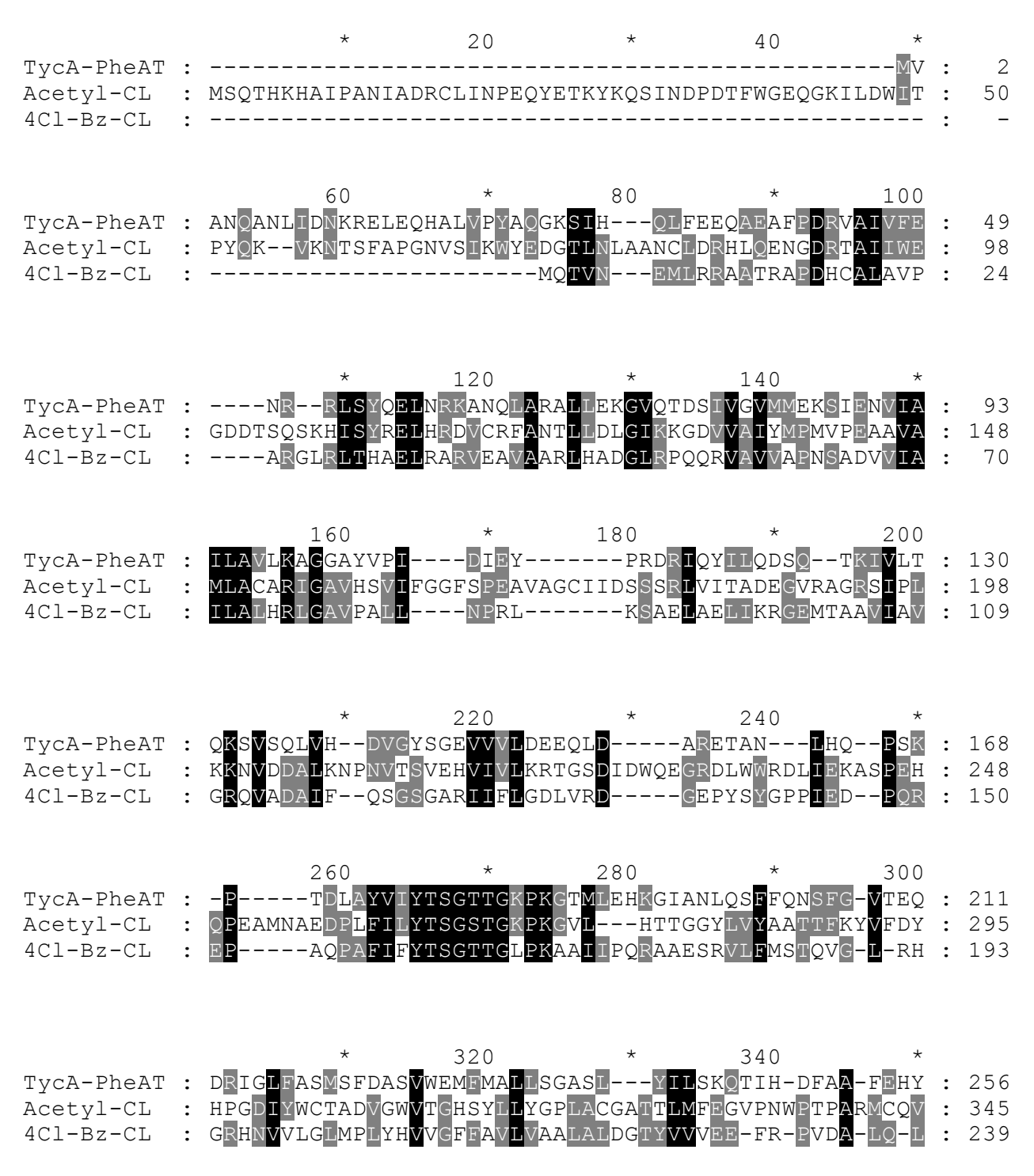
**Figure II–1.** Amino acid sequence variation in the highly conserved motifs in the acyl–adenylate enzyme family. CL is CoA ligase, 4–chlorobenzoate CL is from *Pseudomonas* sp., coumarate CL is from *Mycobacterium leprae*, 4–hydroxybenzoate CL is from *Rhodopseudomas palustris*, *O*–succinatebenzoate CL is from *Staphylococcus aureus*, acetate CL is from *Neurospora crassa*, acetyl CL is from *Pseudomonas olevorns*, TycA and Grs1 are from *Bacillus brevis*, EntE is adenylation domain from enterobactin synthetase from *E. coli*. <sup>a</sup>Luciferase is from *Photinus pyralis* and <sup>b</sup>Luciferase is from the green-emitting strain of the click beetle.



**Figure II–2**. Amino acid sequence alignment of close adenylation domain homologs of NRPS family that show 16 – 61% amino acid sequence identity. The residues that are conserved across all sequences are highlighted in black, whereas the residues conserved in some of the sequences are highlighted in grey.

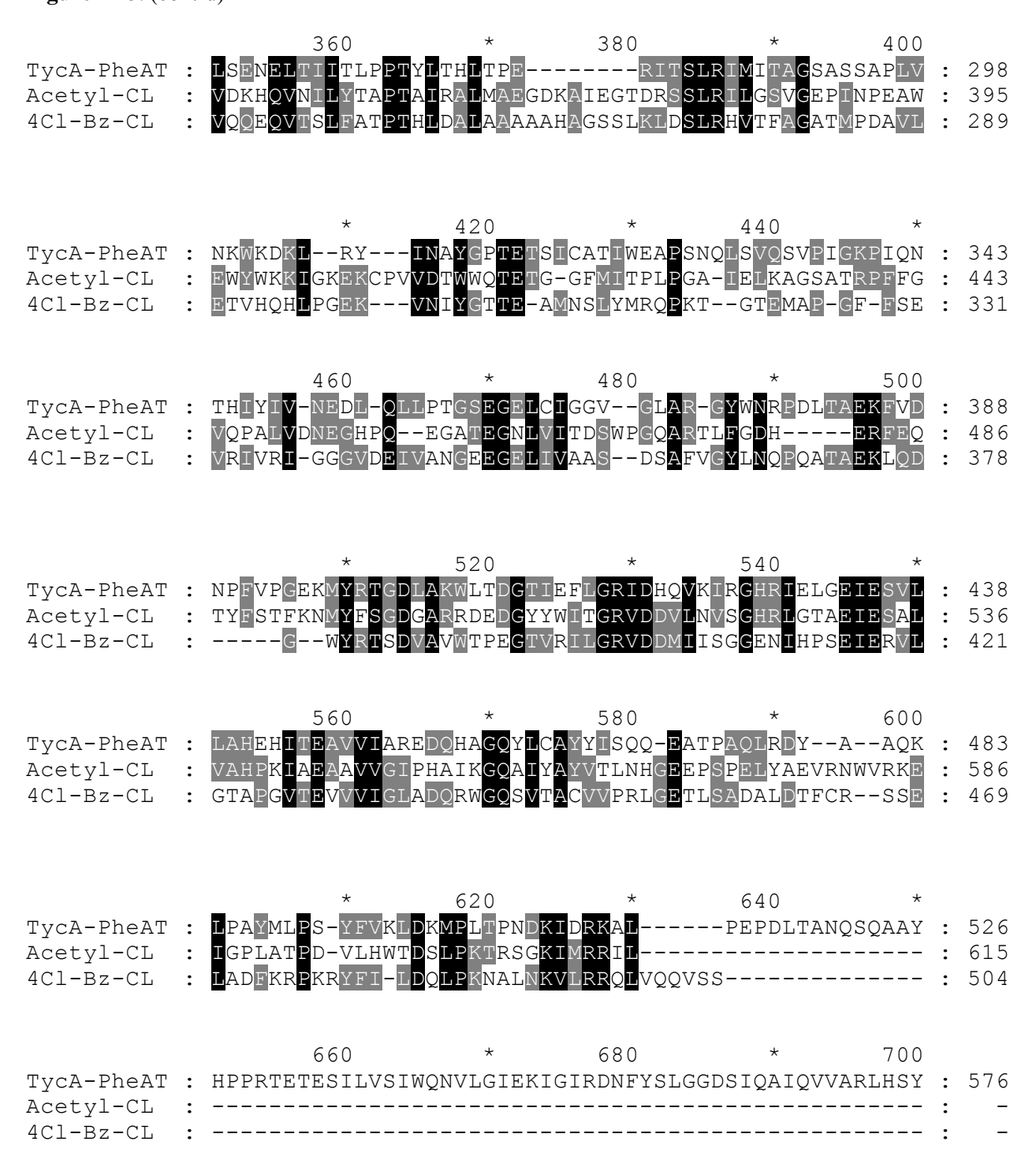
### Figure II–2. (cont'd)

TycA-PheA GrsA-PheA DhbE EntE	: : : :	* PTYLTHLTPER- PTYVVHLDPER- PLAMVWMDAASSRRI PAVSLWLQALTEGESRA	ILSIQTLI DDLSSLQVLQ	TAGSATSPSLV QVGGAKFSAEA	/NKWKEK <mark>VTY</mark> ARRVKAVFGCTL	IN : QQ :		309 321 328 330
TycA-PheA GrsA-PheA DhbE EntE	: : :	360 AYGPTETSICATIWEAR AYGPTETTICATTWVAT VFGMAEGLVNYTRLDDR VFGMAEGLVNYTRLDDR	rketi-g-hs Peeiivntog	SVPIGAPIQNTÇ SKPM-SPYDESI	HIYIVNEDLQLL QIYIVDENLQLK RVWDDHDRDV	SV : KP :		358 369 375 377
TycA-PheA GrsA-PheA DhbE EntE	: : : :	* GSEGELCIGGVGLARGY GEAGELCIGGEGLARGY GETGHLLTRGPYTIRGY GEVGRLMTRGPYTFRGY	YWKRPELTSÇ YYK <mark>AE</mark> EHNA	QKFVD <mark>n</mark> pfvpge Asftedgf	EKLYKTGD <mark>Q</mark> ARW	LS : TR :	: 4	408 419 419 421
TycA-PheA GrsA-PheA DhbE EntE	: : : :	460 DGTIEFLGRIDHQVKIR DGNIEYLGRIDNQVKIR DGYIVVEGRAKDQINRO EGYITVQGREKDQINRO	RGHRV <mark>ELEEV</mark> GGEKVAAEEV	ÆSILLKHMYIS ÆNHLLAHPAVI	TEAVVIAREDOH. SETAVSVHKDHO. IDAAMVSMPDOF:	EQ : LG :	: 4	458 469 469 471
TycA-PheA GrsA-PheA DhbE EntE	: : : :	* QYLCAYYISQQEATPA- PYLCAYFVSEKHIPLE- ERSCVFIIPRDEAPKAA EKSCAYLVVK-EPLRAV	-QLRQFSSEE AELKAFLREF	C-LPTYMIPSYE RGLAAYKIPD		-P :		505 511 504 505
	:	560 	TFGMRVDYE	CAPRNEIEETL\	 /TIWQDVLGSHH	НН : :	:	- 561 -
TycA-PheA	: :	*	620  	* 	-: - -: 563 (: 539	•		



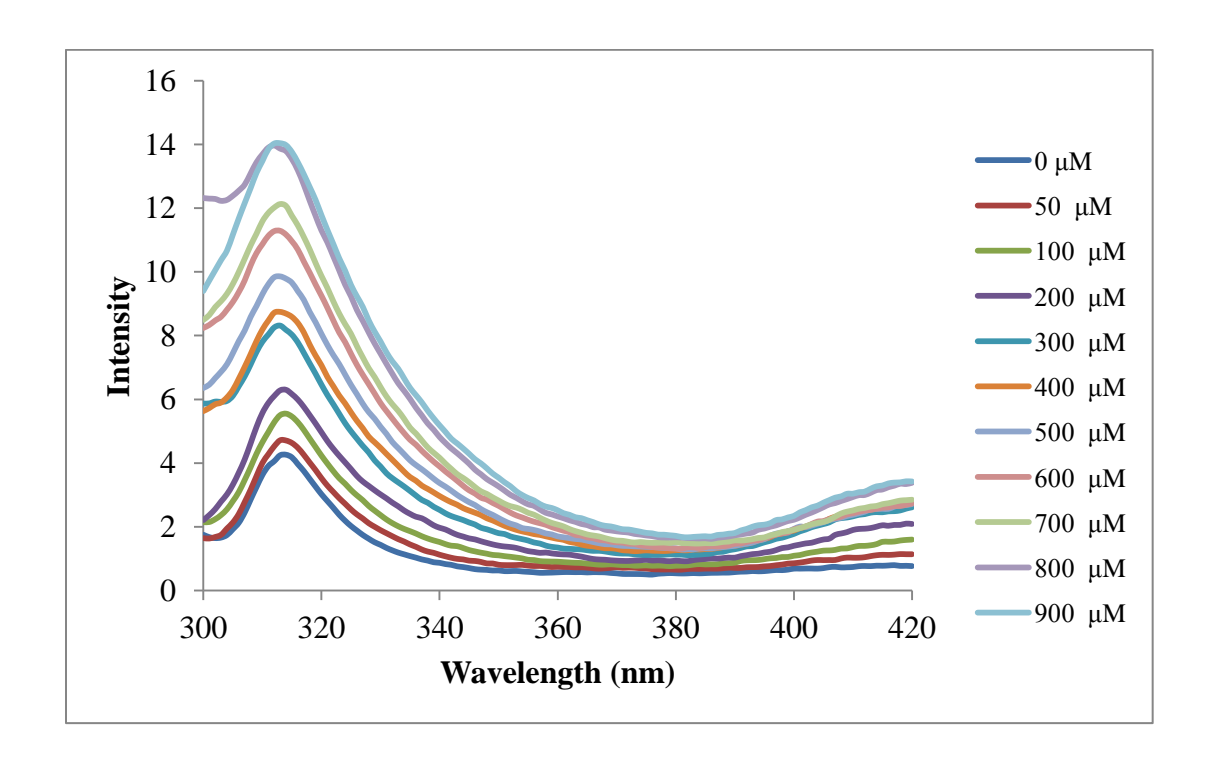
**Figure II–3.** The amino acid sequence alignment of Tyc(Phe–AT), acetyl CoA and 4-chlorobenzoate:CoA ligase are shown. The overall sequence identity of Tyc(Phe–AT) to acetyl CoA and 4-chlorobenzoate:CoA ligase is 19 and 21% respectively. The Tyc(Phe–AT) residues that are not aligned to either CoA ligase (residues numbered 639 to 740) belong to thiolation domain.

Figure II-3. (cont'd)



#### Figure II–3. (cont'd)

		*	720	*	740	*	
Acetyl-CL	:	QLKLETKDLLNYP				-RKIAA	621 620 -
		760	*	780			
TycA-PheAT Acetyl-CL 4Cl-Bz-CL		GDTSNLGDTSTLA	 DPGVVEKLLEEK 	QAIAMPS :	- 652 -		



**Figure II–4.** Spectra obtained by equilibrium fluorescence titration of (2S)–phenylalanine to K $^+$ HEPES, pH 7.5, 25  $^{\circ}$ C. This assay lacked the enzyme and was used as the control experiment. The emission wavelength was scanned from 300 to 420 nm using a fixed excitation wavelength of 280 nm.

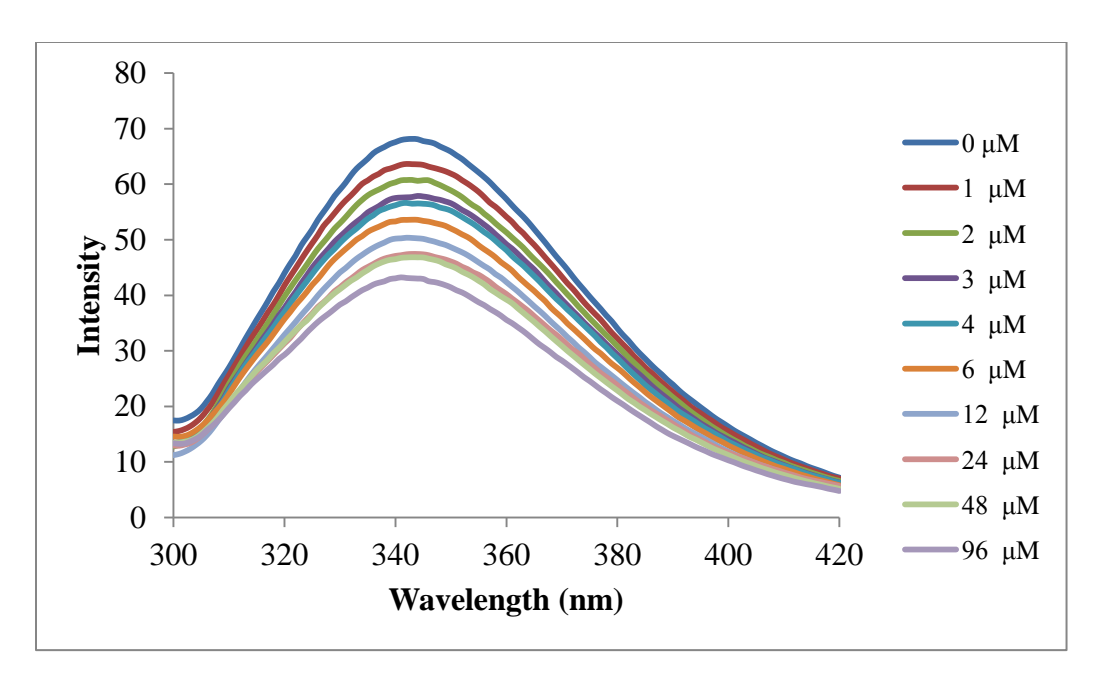


**Figure II–5**. Spectra obtained by equilibrium fluorescence titration of (2S)–phenylalanine at increasing concentrations (0 – 96  $\mu$ M) to Tyc(Phe–A) (0.1  $\mu$ M (in 50 mM K<sup>+</sup>Hepes buffer, pH 7.5 at 25 °C)). The emission wavelength was scanned from 300 to 420 nm using a fixed excitation wavelength of 280 nm.

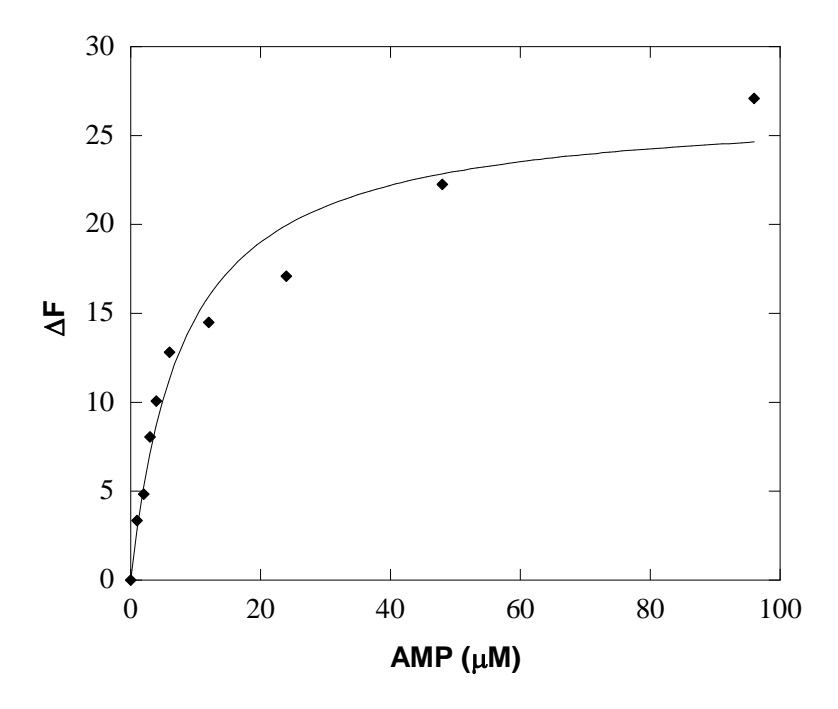


**Figure II–6.** Plot of observed fluorescence change with varying concentrations of AMP at fixed concentration of Tyc(Phe–A) (in K<sup>+</sup>HEPES, pH 7.5, 25  $^{\circ}$ C) containing 96  $\mu$ M (2S)–phenylalanine. The curve was fitted using equation 1 in KaleidaGraph program.

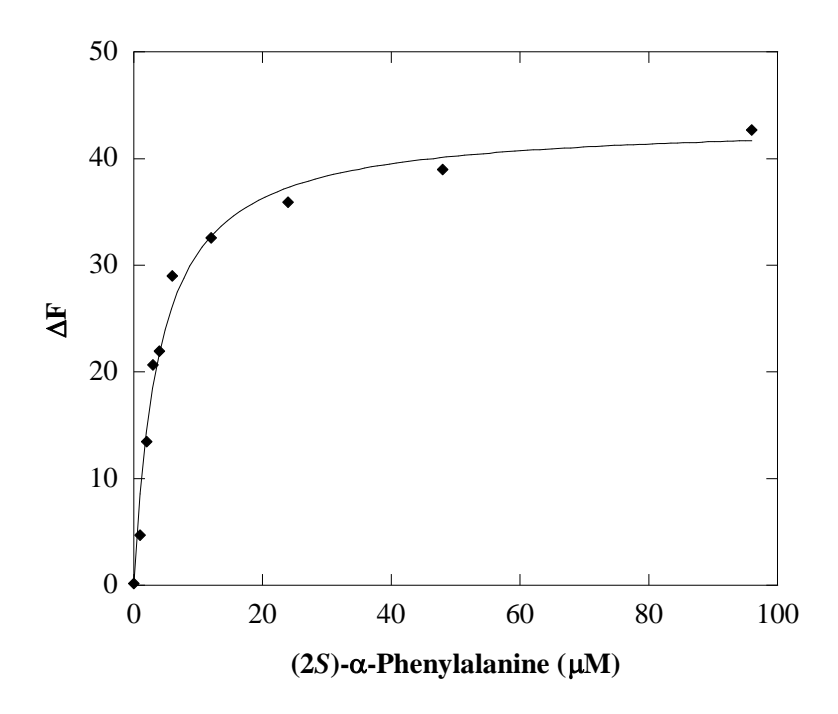


**Figure II–7.** Plot of observed fluorescence change with varying concentrations of (2S)–phenylalanine at fixed concentration of Tyc(Phe–AT) (in K<sup>+</sup>HEPES, pH 7.5, 25 °C). The curve was fitted using equation 1 in KaleidaGraph program.

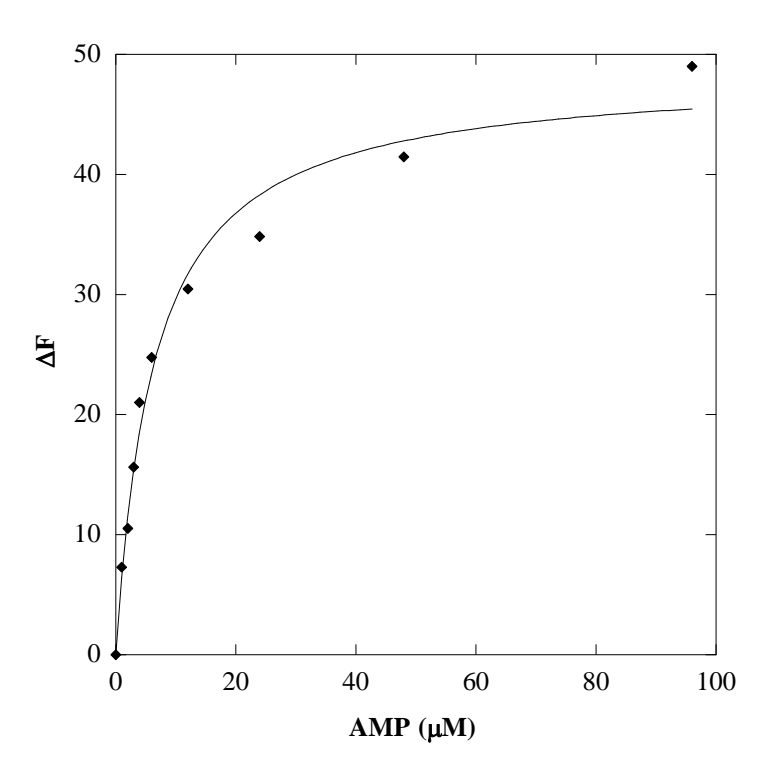


**Figure II–8**. Plot of observed fluorescence change with varying concentrations of AMP at fixed concentration of Tyc(Phe–AT) (in K<sup>+</sup>HEPES, pH 7.5, 25 °C) containing 96 μM (2S)–phenylalanine. The curve was fitted using equation 1 in KaleidaGraph program.

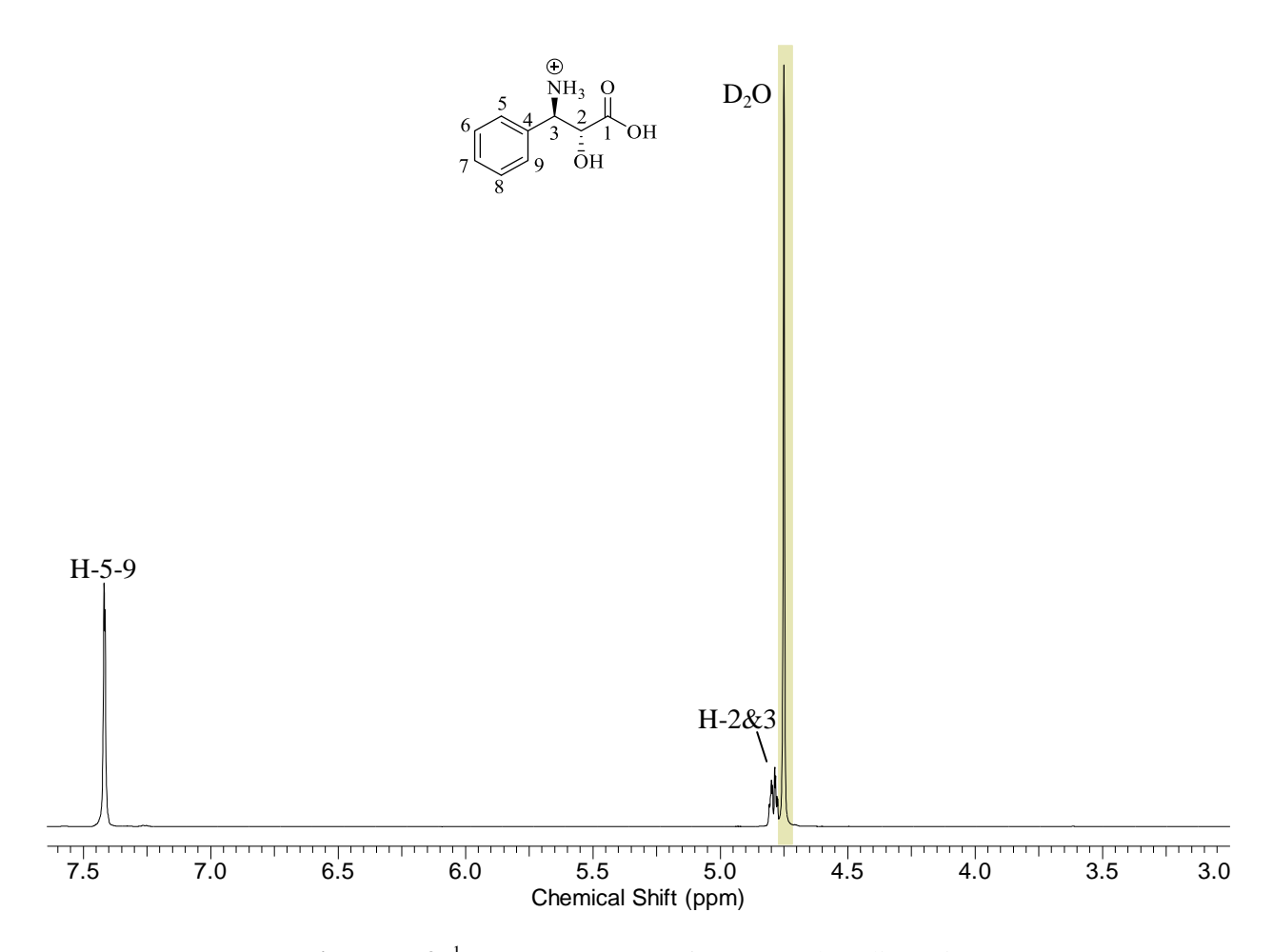


**Figure II–9**. <sup>1</sup>H-NMR spectrum of (2*R*,3*R*)–phenylisoserine

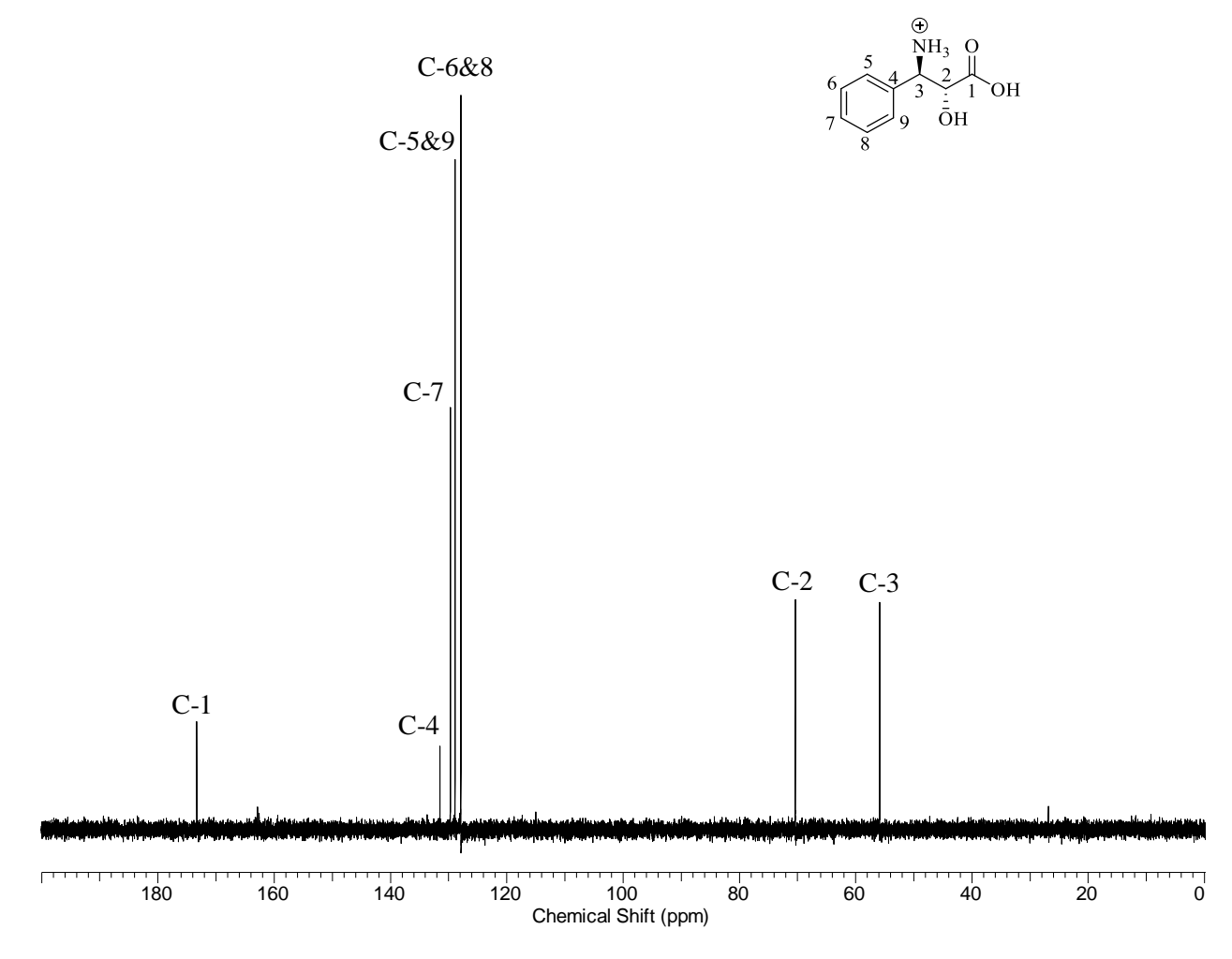


**Figure II–10**. <sup>13</sup>C-NMR spectrum of (2*R*,3*R*)–phenylisoserine

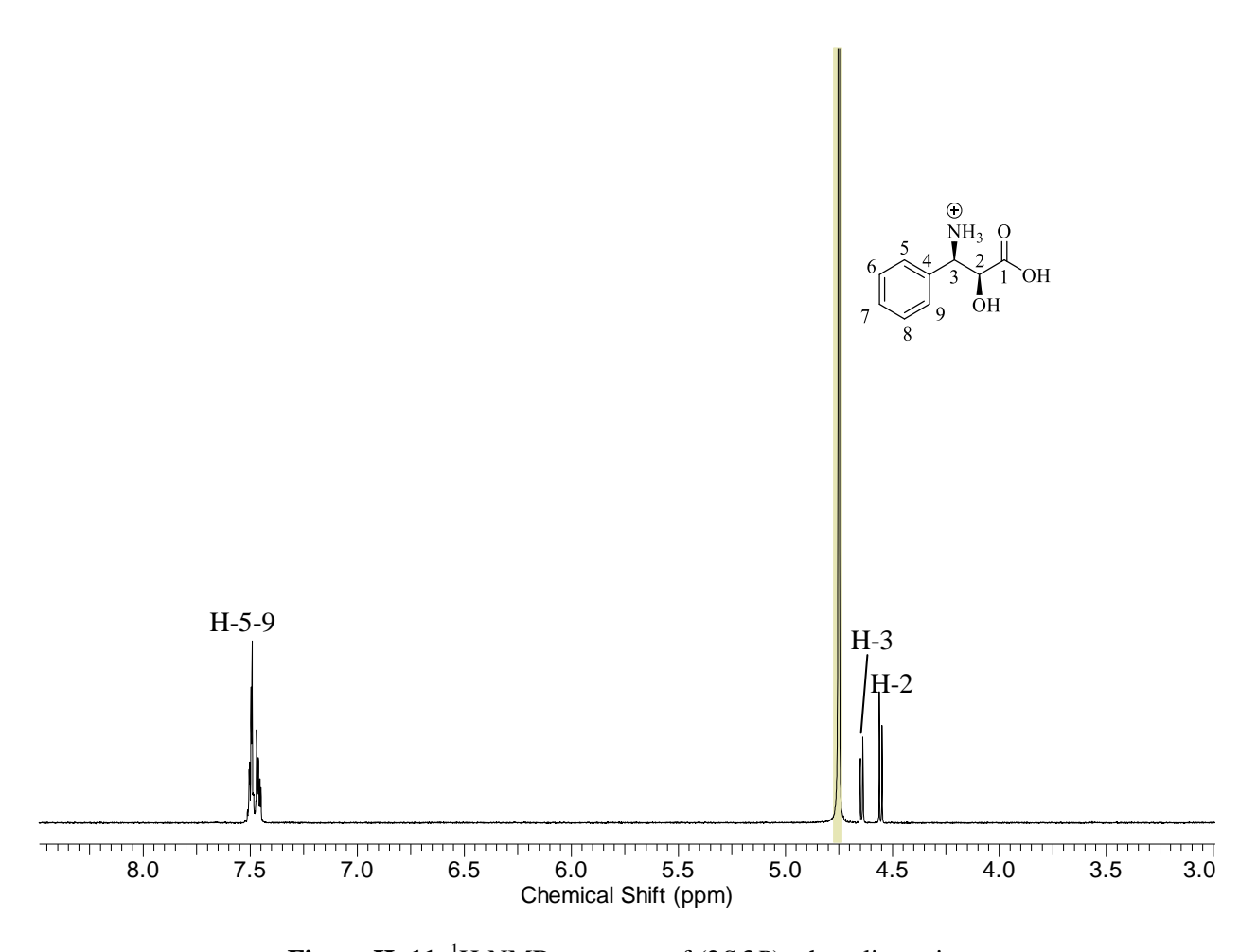


**Figure II–11**. <sup>1</sup>H-NMR spectrum of (2*S*,3*R*)–phenylisoserine

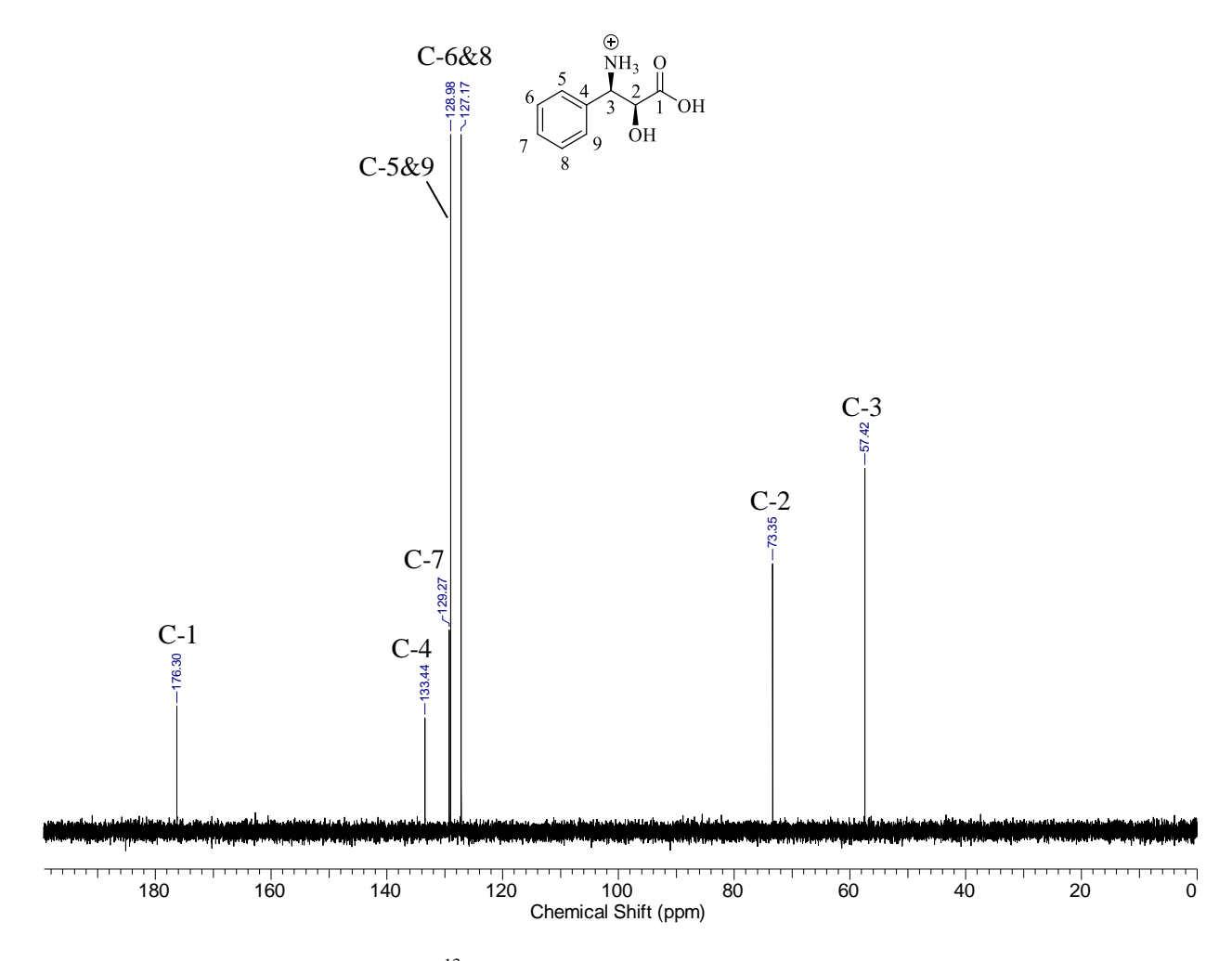


**Figure II–12**. <sup>13</sup>C-NMR spectrum of (2*S*,3*R*)–phenylisoserine

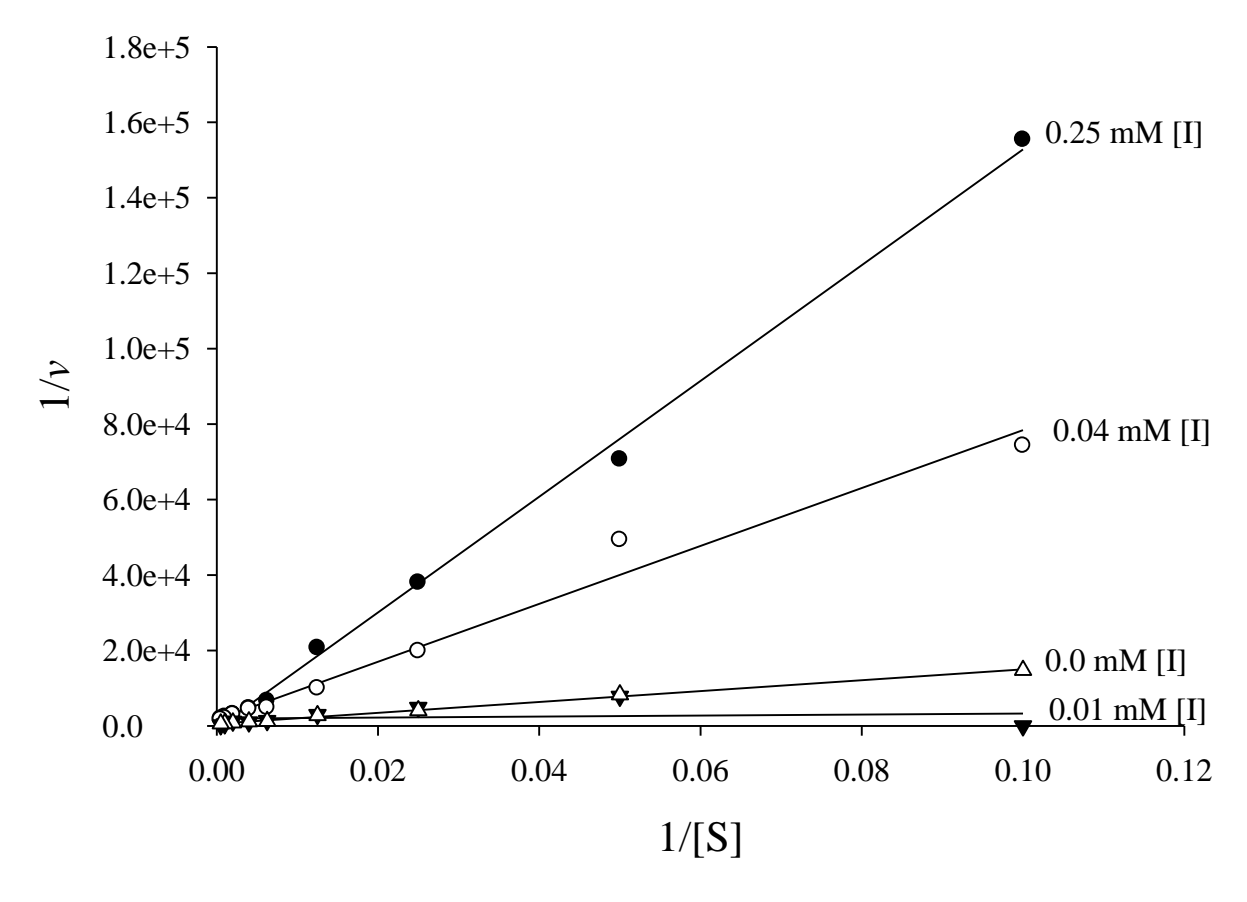


**Figure II–13**. Lineweaver-Burk plots for the inhibition of Tyc(Phe–AT) in the presence of (2S,3R)–phenylisoserine at 0 mM, 0.01 mM, 0.04 mM, and 0.25 mM. (2R,3S)–phenylisoserine was used as the substrate at varying concentrations (0.001-2 mM).

**REFERENCES** 

#### **REFERENCES**

- (1) Finking, R.; Marahiel, M. A. Annu. Rev. Microbiol. 2004, 58, 453.
- (2) Schwarzer, D.; Finking, R.; Marahiel, M. A. *Nat. Prod. Rep.* **2003**, *20*, 275.
- (3) Marahiel, M. A.; Stachelhaus, T.; Mootz, H. D. Chem. Rev. **1997**, 97, 2651.
- (4) Sieber, S. A.; Marahiel, M. A. Chem. Rev. 2005, 105, 715.
- (5) Rouhiainen, L.; Paulin, L.; Suomalainen, S.; Hyytiäinen, H.; Buikema, W.; Haselkorn, R.; Sivonen, K. *Mol. Microbiol.* **2000**, *37*, 156.
- (6) Schneider, T. L.; Shen, B.; Walsh, C. T. *Biochemistry* **2003**, *42*, 9722.
- (7) Rausch, C.; Hoof, I.; Weber, T.; Wohlleben, W.; Huson, D. *BMC Evol. Biol.* **2007**, *7*, 78.
- (8) Hur, G. H.; Vickery, C. R.; Burkart, M. D. Nat. Prod. Rep. 2012, 29, 1074.
- (9) Gocht, M.; Marahiel, M. A. J. Bacteriol. **1994**, 176, 2654.
- (10) Stachelhaus, T.; Mootz, H. D.; Bergendahl, V.; Marahiel, M. A. *J. Biol. Chem.* **1998**, *273*, 22773.
- (11) Stachelhaus, T.: Huser, A.: Marahiel, M. A. Chem. Biol. 1996, 3, 913.
- (12) Stachelhaus, T.; Marahiel, M. A. J. Biol. Chem. 1995, 270, 6163.
- (13) Stachelhaus, T.; Schneider, A.; Marahiel, M. Science 1995, 269, 69.
- (14) Muchiri, R.; Walker, Kevin D. Chem. Biol. 2012, 19, 679.
- (15) Linne, U.; Schäfer, A.; Stubbs, M. T.; Marahiel, M. A. FEBS Lett. **2007**, 581, 905.
- (16) Turgay, K.; Krause, M.; Marahiel, M. A. *Mol. Microbiol.* **1992**, *6*, 529.
- (17) Chang, K.-H.; Xiang, H.; Dunaway-Mariano, D. *Biochemistry* **1997**, *36*, 15650.
- (18) Conti, E.; Franks, N. P.; Brick, P. Structure **1996**, 4, 287.
- (19) Conti, E.; Stachelhaus, T.; Marahiel, M. A.; Brick, P. *Embo J.* **1997**, *16*, 4174.

- (20) May, J. J.; Kessler, N.; Marahiel, M. A.; Stubbs, M. T. *Proc. Natl. Acad. Sci. U. S. A.* **2002**, *99*, 12120.
- (21) Gulick, A. M.; Starai, V. J.; Horswill, A. R.; Homick, K. M.; Escalante-Semerena, J. C. *Biochemistry* **2003**, *42*, 2866.
- (22) Reger, A. S.; Wu, R.; Dunaway-Mariano, D.; Gulick, A. M. *Biochemistry* **2008**, 47, 8016.
- (23) Bains, J.; Boulanger, M. J. J. Mol. Biol. 2007, 373, 965.
- (24) Hughes, Amanda J.; Keatinge-Clay, A. Chem. Biol. 2011, 18, 165.
- (25) Gill, S. C.; Von Hippel, P. H. *Anal. Biochem.* **1989**, *182*, 319.
- (26) Bradford, M. M. Anal. Biochem. 1976, 72, 248.
- (27) Gasteiger, E.; Hoogland, C.; Gattiker, A.; Wilkins, M. R.; Appel, R. D.; Bairoch, A. In *The proteomics protocols handbook*; Springer: 2005, p 571.
- (28) Ehmann, D. E.; Trauger, J. W.; Stachelhaus, T.; Walsh, C. T. *Chem. Biol.* **2000**, *7*, 765.
- (29) Lakowicz, J. R. *Principles of fluorescence spectroscopy*; Springer Science & Business Media, 2007.
- (30) Chen, Y.; Barkley, M. D. *Biochemistry* **1998**, *37*, 9976.
- (31) Lakowicz, J. In *Principles of Fluorescence Spectroscopy*; Lakowicz, J., Ed.; Springer US: 2006, p 529.
- (32) Luo, L. S.; Burkart, M. D.; Stachelhaus, T.; Walsh, C. T. J. Am. Chem. Soc. **2001**, 123, 11208.
- (33) Stevens, B. W.; Lilien, R. H.; Georgiev, I.; Donald, B. R.; Anderson, A. C. *Biochemistry* **2006**, *45*, 15495.
- (34) Ehmann, D. E.; Shaw-Reid, C. A.; Losey, H. C.; Walsh, C. T. *Proc. Natl. Acad. Sci. U. S. A.* **2000**, *97*, 2509.
- (35) Kaneko, M.; Ohnishi, Y.; Horinouchi, S. J. Bacteriol. 2003, 185, 20.
- (36) Bordoli, L.; Kiefer, F.; Arnold, K.; Benkert, P.; Battey, J.; Schwede, T. *Nat. Protocols* **2008**, *4*, 1.
- (37) Villiers, B. R. M.; Hollfelder, F. *Chembiochem* **2009**, *10*, 671.

- (38) Linne, U.; Doekel, S.; Marahiel, M. A. *Biochemistry* **2001**, *40*, 15824.
- (39) Admiraal, S. J.; Walsh, C. T.; Khosla, C. *Biochemistry* **2001**, *40*, 6116.
- (40) Schaffer, M. L.; Otten, L. G. J. Mol. Catal. B-Enzym. 2009, 59, 140.
- (41) Linne, U.; Stein, D. B.; Mootz, H. D.; Marahiel, M. A. *Biochemistry* **2003**, *42*, 5114.
- (42) Hahn, M.; Stachelhaus, T. Proc. Natl. Acad. Sci. U. S. A. 2004, 101, 15585.
- (43) Stein, D. B.; Linne, U.; Hahn, M.; Marahiel, M. A. ChemBioChem 2006, 7, 1807.
- (44) Walker, K.; Fujisaki, S.; Long, R.; Croteau, R. *Proc. Natl. Acad. Sci. U. S. A.* **2002**, *99*, 12715.
- (45) Kingston, D. G.; Chaudhary, A. G.; Chordia, M. D.; Gharpure, M.; Gunatilaka, A. L.; Higgs, P. I.; Rimoldi, J. M.; Samala, L.; Jagtap, P. G.; Giannakakou, P. J. Med. Chem. 1998, 41, 3715.
- (46) Trott, O.; Olson, A. J. J. Comput. Chem. 2010, 31, 455.
- (47) Tintu, I.; Abhilash, J.; Dileep, K. V.; Augustine, A.; Haridas, M.; Sadasivan, C. *Chem. Biol. Drug Des.* **2014**, *84*, 116.
- (48) Keating, T. A.; Walsh, C. T. Curr. Opin. Chem. Biol. **1999**, *3*, 598.
- (49) Stachelhaus, T.; Marahiel, M. A. FEMS Microbiol. Lett. 1995, 125, 3.
- (50) Stachelhaus, T.; Mootz, H. D.; Marahiel, M. A. Chem. Biol. 1999, 6, 493.
- (51) Samel, S. A.; Schoenafinger, G.; Knappe, T. A.; Marahiel, M. A.; Essen, L. O. *Structure* **2007**, *15*, 781.
- (52) Pelludat, C.; Rakin, A.; Jacobi, C. A.; Schubert, S.; Heesemann, J. *J. Bacteriol.* **1998**, *180*, 538.
- (53) Cone, M. C.; Yin, X. H.; Grochowski, L. L.; Parker, M. R.; Zabriskie, T. M. *Chembiochem* **2003**, *4*, 821.
- (54) Schlumbohm, W.; Stein, T.; Ullrich, C.; Vater, J.; Krause, M.; Marahiel, M. A.; Kruft, V.; Wittmannliebold, B. *J. Biol. Chem.* **1991**, *266*, 23135.
- (55) Pfeifer, E.; Pavelavrancic, M.; Vondohren, H.; Kleinkauf, H. *Biochemistry* **1995**, *34*, 7450.

- (56) Mootz, H. D.; Marahiel, M. A. J. Bacteriol. 1997, 179, 6843.
- (57) Luo, L. S.; Kohli, R. M.; Onishi, M.; Linne, U.; Marahiel, M. A.; Walsh, C. T. *Biochemistry* **2002**, *41*, 9184.
- (58) Bergendahl, V.; Linne, U.; Marahiel, M. A. Eur. J. Biochem. 2002, 269, 620.

# 4. SUBSTRATE SPECIFICITY STUDIES OF TYC(PHE-AT) WITH ISOSERINE ANALOGS IN THE BIOSYNTHESIS OF ISOSERINYL COATHIOESTERS

#### 4.1 Introduction

#### 4.1.1. Paclitaxel Analogs and Their Importance

The highly effective antimitotic drug paclitaxel has found wide application in the treatment of various cancers, including cancers of the ovaries, breasts and lungs, and Kaposi's sarcoma. Despite the wide application of paclitaxel and its analog, docetaxel (Taxotere), there have been major concerns regarding their adverse physiological effects and drug resistance. These major drawbacks create a need to develop novel taxoids that have minimal side effects yet maintain superior pharmacological properties. So far, different paclitaxel analogs with improved IC<sub>50</sub> and ED<sub>50</sub> over the parent drug against multidrug resistant ovarian carcinoma, pancreatic cancer, B16 melanoma, human lung cancer, and colon cancer cell lines have been developed. Among them are analogs modified at the C–13 side chain (Figure 4.1).

Figure 4.1. The paclitaxel structure framework showing C-13 (2R,3S)-phenylisoserine side chain

Structure-activity relationship studies have shown that the isoserine side chain at C–13 of paclitaxel is important for its activity<sup>13,14</sup> with maximum activity seen for (2R,3S)– phenylisoserine and lesser activity for the other stereoisomers.<sup>15</sup> Moreover, the 2'–hydroxyl is necessary for activity; when O–acetylated, the drug is inactivated.<sup>14</sup> Replacement of 2'–OH with

fluorine or thiol decreases binding of the paclitaxel analog to the cellular microtubule by twofold. 16,17 Quantitative assessment and computational analysis showed that the 2'-hydroxyl
accounts for 80% of the binding free energy of the side chain. 18 Removal of both 2'-hydroxyl
and 3'-benzoyl groups rendered the resultant *N*-debenzoyl-2'-deoxy-paclitaxel inactive. 18
Following this, various 'second generation' taxanes with modifications at the phenyl ring have
been synthesized and shown to have comparable or improved activity to the parent drug (**Table 4.1**). 3,11,19-22 Most of these analogs have shown promise in treatment of drug-resistant tumor
cells. For example, Ortataxel (Spectrum Pharmaceuticals), 23 currently in phase 2 clinical trials is
active against breast and non-small cell lung cancer resistant to paclitaxel and docetaxel. 23
Tesetaxel, an oral taxane, currently in phase 1 clinical trials is used in combination with the
antineoplastic pharmaceutical Capecitabine in patients with solid tumors 24 (**Figure 4.2**).

**Table 4.1**. Cytotoxic activity of paclitaxel analogs in microtubule assembly and against B16 melanoma cells.

Side C	O NH O 	O O OH O	Side Chain  D-2  D-7	D−3  D−8	N ξ ξ D-4  D-9	D-5  D-10	D−6  D−11	
	Microtubule	Inhibition of B16		Microt	ubule	Inhibiti	on of B16	
	assembly melanoma cells assembly				melanoma cells			
	$ED_{50}/ED_{50}$	proliferation		ED <sub>50</sub> /ED <sub>50</sub> proliferation				
	(Paclitaxel)	ED <sub>50</sub> /ED <sub>50</sub> (Paclitaxel)		(Paclitaxel) ED <sub>50</sub> /ED <sub>50</sub> (Paclitation			(Paclitaxel)	
D-2	1.0	1.0	D-6	0.7		0.8		
D-3	0.5	1.0	D-7	0.9 0.3		0.3		
D-4	0.4	1.3	D-8	0.9			3.3	
D-5	0.4	27	D-9	0.2		-		
D-10	ED <sub>50</sub> /ED <sub>50</sub> (Tax	kol®) cytotoxicity against l	HCTVM4	l6 human c	olon carc	inoma cells	s (0.2)	
D-11	microtubule disassembly ED <sub>50</sub> /ED <sub>50</sub> (Taxol <sup>®</sup> ) (0.8)							

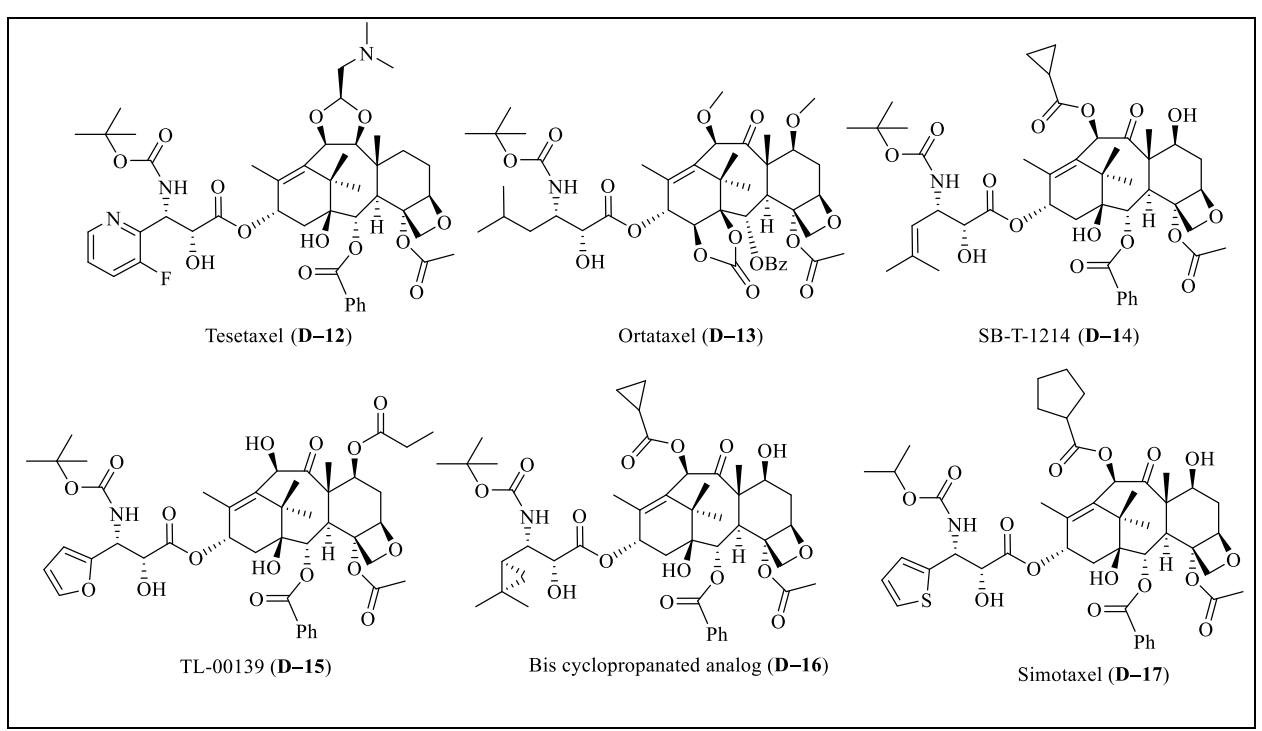


Figure 4.2. Some of the paclitaxel analogs with modification at C-13. D-12, D-13, D-15 and D-17 are currently in clinical trials.

#### 4.1.2. Sources of Paclitaxel: An Historical Time Line

Paclitaxel was isolated initially from the bark of Pacific Yew (*Taxus brevifolia*) at low yield (0.02% w/w).<sup>25</sup> This unsustainable method was succeeded by semisynthesis<sup>26</sup> that supplied paclitaxel for commercial distribution by Bristol – Myers Squibb.<sup>11</sup> The semisynthetic method employed a phenylisoserine precursor (a β–lactam synthesized through six steps), which was coupled to the C–13 hydroxyl of deacetylbaccatin III.<sup>27</sup> This strategy needed large volumes of hazardous solvents and reagents, and implemented redundant protection/deprotection steps.<sup>28</sup> Bristol – Myers Squibb abandoned the semisynthetic method and adopted an environmentally conscience *Taxus* plant cell fermentation process.<sup>29</sup> While this greener biological method of production produces paclitaxel at 500 kg/year by Phyton Pharmaceutical, the plant cells have competing pathways that divert part of the metabolic flux from paclitaxel (**Figure 4.3**).<sup>30</sup> To address these challenges, a sustainable biological method can be envisioned that directs carbon

flux from an abundant pathway intermediate to one desired end product, such as paclitaxel or an analog (**Figure 4.4**).

IPP A-21

OPP

DMAPP

A-22

$$4x$$

FDP, D-19

 $CC_{5}$ ) hemiterpenes

 $CC_{5}$ 

**Figure 4.3.** The biosynthesis of paclitaxel in plants starting from geranylgeranyl diphosphate (GGDP). The different competing pathways are also shown.

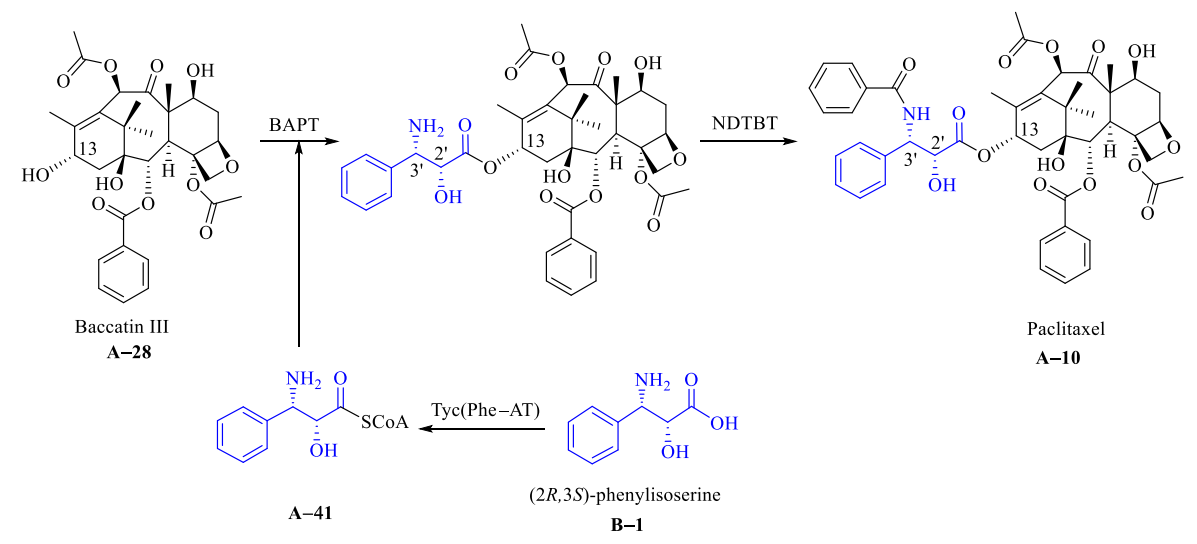


**Figure 4.4.** The proposed biosynthesis of paclitaxel through coupling (2*R*,3*S*)–phenylisoserine to baccatin III by 13–*O*–phenylpropanoyltransferase (BAPT), an acyl CoA dependent enzyme.

### 4.1.3. Catalytic Activity of Baccatin III 13–O–3–Amino–3– Phenylpropanoyltransferase (BAPT) with Aminoacyl CoA Thioesters

To develop a biosynthetic approach, enzymes on the paclitaxel pathway have been identified and characterized.<sup>2</sup> In particular, acyl CoA-dependent 13–*O*–phenylpropanoyltransferase (BAPT) regioselectively phenylpropanoylates the C–13 hydroxyl of baccatin III.<sup>31</sup> An *N*–benzoyltransferase (NDTBT) *N*–benzoylates the phenylisoserinyl side chain using the appropriate acyl CoA substrates (**Figure 4.4**).

In an earlier study, the molecular cloning and heterologous expression of BAPT was described and found to be regioselective.<sup>32</sup> Moreover, the apparent  $K_{\rm M}$  values of BAPT were  $2.4 \pm 0.5~\mu{\rm M}$  and  $4.9 \pm 0.3~\mu{\rm M}$  for baccatin III and  $\beta$ –phenylalanyl CoA, respectively.<sup>32</sup> Also, the catalytic turnover of BAPT with 3–phenylisoserinyl CoA was ~2.5 times slower compared to  $\beta$ –phenylalanyl CoA, and no activity was observed with  $\alpha$ –phenylalanyl CoA or N–benzoylphenylisoserinyl CoA.<sup>32</sup> The synthesis of the aminoacyl CoA thioesters reported in the earlier study involved eight steps requiring protection/deprotection of the amine and hydroxyl

functional groups (see Figure 1.8 in Chapter 1). Additionally, this method was complicated by solvent incompatibility of the hydrophobic acid anhydride intermediate and the hydrophilic CoA reactant.<sup>32</sup>

The broad substrate scope of the acyltransferases has been reported in earlier studies. 33-35 For example, both BAPT and NDTBT showed specificity for various aroyl, heteroaroyl, alkanoyl, and alkenoyl CoA thioesters. BAPT is hypothesized to catalyze the transfer of various isoserinyl analogs to the C–13 hydroxyl of baccatin III. This catalysis provides a direct route to a precursor of a paclitaxel analog. In addition, it replaces the multistep semisynthesis of paclitaxel analogs (**Figure 4.5**) and thus eliminates the use of environmental harmful solvents and reagents. 27

**Figure 4.5**. A representative 11–step semisynthesis of paclitaxel analogs (i) LDA, -78 °C, (ii) a) Bu<sub>4</sub>N<sup>-</sup>F<sup>+</sup>, b) ethyl vinyl ether, H<sup>+</sup>, c) BzCl, Et<sub>3</sub>N, DMAP, (iii) pyridine, DMAP, (iv) 0.5 M HCl, EtOH.

## 4.1.4. Tyrocidine Synthetase A Tyc(Phe–AT) Catalysis in Biosynthesis of Isoserinyl CoA Analogs

Chapter 3 describes the use of the Tyc(Phe–AT) didomain as a CoA ligase that biocatalyzed  $(2S)-\alpha-$ ,  $(3R)-\beta$ -phenylalanyl CoA, and (2R,3S)-phenylisoserinyl CoA from the corresponding amino acids. Thus, Tyc(Phe–AT) could help by-pass lengthy chemical synthesis of arylisoserinyl CoA thioesters for use by acyl CoA dependent acyltransferases (**Figure 4.6**).

**Figure 4.6**. A) Synthesis of (2*R*,3*S*)-phenylisoserinyl CoA via the mixed anhydride intermediate. (i) CH<sub>2</sub>Cl<sub>2</sub>/THF, DMAP in CH<sub>2</sub>Cl<sub>2</sub>, benzyl chloroformate, rt, 1 h, 90% yield; (ii) CH<sub>3</sub>CN, DMAP in CH<sub>3</sub>CN, Boc<sub>2</sub>O, rt, 24 h, 20% yield; (iii) CH<sub>3</sub>OH, 6% Mg(OCH<sub>3</sub>)<sub>2</sub>, rt, 1 h, 80% yield; (iv) step (ii), 80% yield; (v) 2 M NaOH, 12 h; (vi) THF, ethyl chloroformate, rt, 1 h; (vii) CoASH in 0.4 M NaHCO<sub>3</sub>, *t*-BuOH, rt, 0.5 h; (viii) HCOOH, rt, 10% yield. Synthesis of α-, and β-phenylalanyl CoA were carried out similarly except for the 2-hydroxyl protection. **B**) The proposed biosynthesis of isoserinyl CoA thioesters.

An earlier study described the wide range of adenylation domain of Tyc(Phe–ATE) for natural and unnatural amino acid substrates, which differed in their electronic properties and size.<sup>36</sup> The earlier study, however, only evaluated the ability of Tyc(Phe–A) to form an adenylate

anhydride intermediate through an indirect ATP/[<sup>32</sup>P]PPi exchange experiment. This earlier work, showing adenylation of various substrates together with our discovery of the CoA ligase function of Tyc(Phe–AT) prompted us to investigate the didomain catalyst for the production of isoserinyl CoA thioesters<sup>36,37</sup> (**Figure 4.7**).

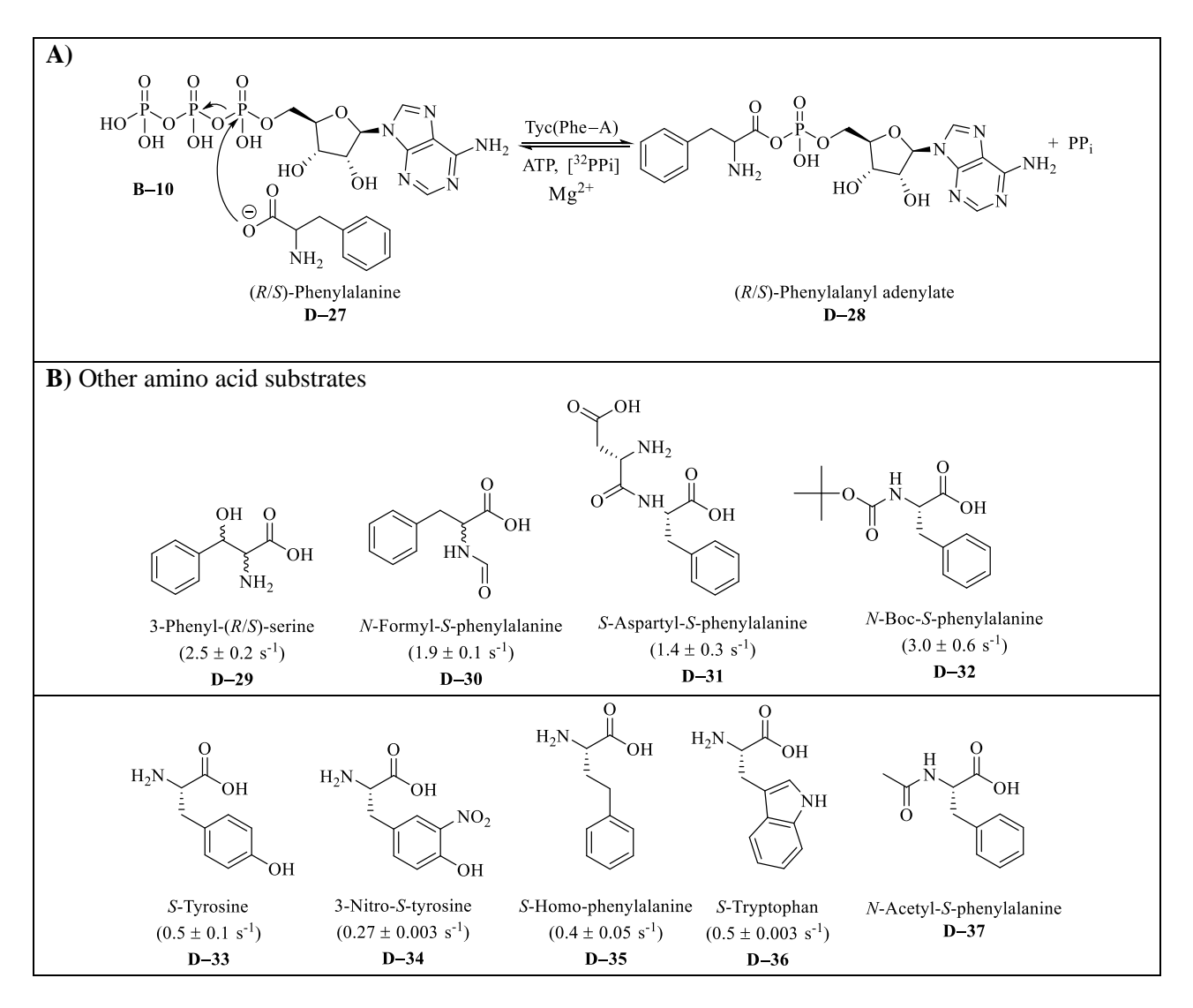


**Figure 4.7**. A) The reversible adenylation of (R/S)—phenylalanine by Tyc(Phe–A) domain through ATP hydrolysis forming the (R/S)—phenylalanyl adenylate. B) Natural and unnatural amino acids that are substrates of TycA. The rates of adenylation  $(k_{cat})$  by Tyc(Phe–A) are shown in parentheses. The substrates whose rates of adenylation are not indicated had less than 20% activity of the (R/S)—phenylalanine substrate.

Figure 4.7. (cont'd)

#### 4.2. Experimental

#### 4.2.1. Substrates, Reagents, and General Instrumentation

The aryl and non-aryl carboxaldehydes, acetoxyacetyl chloride, and *p*-methoxyaniline (also known as *p*-anisidine) were purchased from Sigma-Aldrich and were used without further purification, unless noted otherwise. Triethylamine was obtained from J. T. Baker chemicals, Phillipsburg, NJ.

A Varian Inova-300 or a Varian UnityPlus500 instrument was used to acquire  $^1$ H- and  $^{13}$ C-NMR. A Q-Tof Ultima electrospray ionization tandem mass spectrometer (ESI–MS/MS, Waters, Milford, MA) with a Waters 2795 HPLC was used for mass spectrum analysis. The biosynthetic products were separated and analyzed using Acquity® UPLC system fitted with a C18 Ascentis Express column (2.5  $\times$  50 mm, 2.7  $\mu$ m) on a Quattro–Premier XE Mass

Spectrometer. Thin layer chromatography (TLC) plates and flash column chromatography Silica gel were purchased from EMD Chemicals Inc. (Gibbstown, NJ).

#### 4.2.2. Synthesis of Isoserine Analogs

#### 4.2.2.1. General Procedure 1: Synthesis of N–(p-Methoxyphenyl)benzylimines

Figure 4.8. Synthesis of *N*-protected imines from benzaldehyde analogs and *p*-anisidine.

To an aldehyde solution (1 equiv) dissolved in benzene was added p-methoxyaniline (2.5 equiv). Oven dried molecular sieves ( $\sim$ 1.5 g) were added to remove water formed during the reaction. The reaction was stirred at room temperature for 12 h, then filtered, dried (MgSO<sub>4</sub>), and concentrated under vacuum. The crude mixture was purified by silica gel column

chromatography (1:4 EtOAc/hexane, v/v), and the fractions containing the product were combined and dried under vacuum to obtain the imine. The non-aryl imines (3-trimethyl, 3-cyclohexyl, 3-thiophenyl, and 3-dimethyl-*N*-(*p*-Methoxyphenyl)-imine) were not stable and hence not isolated. The lactams of these imines were synthesized separately in one pot as described in general Procedure 2, Method B (Section 4.2.2.2). *p*-Methoxyphenyl is abbreviated as PMP in the procedures described herein.

*N*-(*p*-Methoxyphenyl)-3-benzylimine (D–49a). Benzaldehyde (0.5 g, 4.72 mmol) and *p*-methoxyaniline (0.87 g, 7.08 mmol, 1.5 equiv) were treated according to Procedure 1 (Section 4.2.2.1) to afford the imine (897 mg, 83% yield, at >99% purity by  $^{1}$ H-NMR analysis).  $^{1}$ H-NMR (500 MHz, CDCl<sub>3</sub>-*d*)  $\delta$ : 3.84 (s, PMP – OCH<sub>3</sub>), 6.91 – 7.93 (aromatic protons), 8.49 (s, imine CH).

*N*-(*p*-Methoxyphenyl)-3-(4-Fluoro)-benzylimine (D–49b). *p*-Fluorobenzaldehyde (0.5 g, 4.06 mmol, 1 equiv) and *p*-methoxyaniline (1.25 g, 10.16 mmol, 2.5 equiv) were treated according to Procedure 1 (Section 4.2.2.1) to afford the imine (464 mg, 50% yield, at >98% purity by <sup>1</sup>H-NMR analysis). <sup>1</sup>H-NMR (500 MHz, CDCl<sub>3</sub>-*d*) δ: 3.84 (s, PMP – OCH<sub>3</sub>), 6.92 – 7.89 (aromatic protons), 8.45 (s, imine CH). <sup>13</sup>C-NMR (126 MHz, CDCl<sub>3</sub>-*d*) δ: 158.33, 156.78, 144.20, 130.53, 130.47, 122.13, 115.94, 115.76, 114.40, 55.48.

*N*-(*p*-Methoxyphenyl)-3-(4-Chloro)-benzylimine (D–49c). *p*-Chlorobenzaldehyde (0.45 g, 3.25 mmol, 1 equiv) and *p*-methoxyaniline (1 g, 8.13 mmol, 2.5 equiv) were treated according to Procedure 1 (Section 4.2.2.1) to afford the imine (670 mg, 84% yield, at >98% purity by  $^{1}$ H-NMR analysis).  $^{1}$ H-NMR (500 MHz, CDCl<sub>3</sub>-*d*)  $\delta$ : 3.84 (s, PMP – OCH<sub>3</sub>), 6.94 – 7.82 (aromatic protons), 8.44 (s, imine CH).

*N*-(*p*-Methoxyphenyl)-3-(4-Bromo)-benzylimine (D–49d). *p*-Bromobenzaldehyde (0.60 g, 3.25 mmol, 1 equiv) and *p*-methoxyaniline (1 g, 8.13 mmol, 2.5 equiv) were treated according to Procedure 1 (Section 4.2.2.1) to afford the imine (500 mg, 53% yield, at >98% purity by <sup>1</sup>H-NMR analysis). <sup>1</sup>H-NMR (500 MHz, CDCl<sub>3</sub>-*d*) δ: 3.85 (s, PMP – OCH<sub>3</sub>), 6.95 – 7.77 (aromatic protons), 8.45 (s, imine CH). <sup>13</sup>C-NMR (126 MHz, CDCl<sub>3</sub>-*d*) δ: 158.52, 156.72, 144.42, 135.39, 131.96, 129.91, 125.41, 122.24, 114.44, 55.50.

*N*-(*p*-Methoxyphenyl)-3-(4-Methyl)-benzylimine (D–49e). *p*-Tolualdehyde (1 g, 8.3 mmol, 1 equiv) and *p*-methoxyaniline (2.6 g, 20.8 mmol, 2.5 equiv) were treated according to Procedure 1 (Section 4.2.2.1) to afford the imine (1.1 g, 57% yield at >98% purity by <sup>1</sup>H-NMR analysis). <sup>1</sup>H-NMR (CDCl<sub>3</sub>-*d*, 500 MHz) δ: 2.41 (s, *p*-CH<sub>3</sub>) 3.83 (s, PMP – OCH<sub>3</sub>), 6.94 – 7.81 (aromatic protons), 8.44 (s, imine CH). <sup>13</sup>C-NMR (126 MHz, CDCl<sub>3</sub>-*d*) δ: 158.48, 158.10, 145.12, 141.47, 133.88, 129.48, 128.58, 122.15, 114.35, 55.50, 21.63.

*N*-(*p*-Methoxyphenyl)-3-(4-Methoxy)-benzylimine (D–49f). *p*-Methoxybenzaldehyde (0.44 g, 3.25 mmol, 1 equiv) and *p*-methoxyaniline (1 g, 8.13 mmol, 2.5 equiv) were treated according to Procedure 1 (Section 4.2.2.1) to afford the imine (310 mg, 40% yield, at >98% purity by  $^{1}$ H-NMR analysis).  $^{1}$ H-NMR (500 MHz, CDCl<sub>3</sub>-*d*) δ: 3.83 (s, *p*-OCH<sub>3</sub>), 3.87 (s, PMP – OCH<sub>3</sub>), 6.90 – 7.84 (aromatic protons), 8.41 (s, imine CH).  $^{13}$ C-NMR (126 MHz, CDCl<sub>3</sub>-*d*) δ: 161.99, 157.93, 152.78, 145.27, 130.26, 129.48, 122.08, 116.41, 114.80, 55.50, 55.42.

*N*-(*p*-Methoxyphenyl)-3-(4-Acetoxy)-benzylimine (D–49g). *p*-Acetoxybenzaldehyde (0.5 g, 3.05 mmol, 1 equiv) and *p*-methoxyaniline (0.93 g, 7.6 mmol, 2.5 equiv) were treated according to Procedure 1 (Section 4.2.2.1) to afford the imine (540 mg, 66% yield, at >98% purity by  $^{1}$ H-NMR analysis).  $^{1}$ H-NMR (500 MHz, CDCl<sub>3</sub>-*d*)  $\delta$ : 2.33 (s, OAc – CH<sub>3</sub>), 3.84 (s, PMP – OCH<sub>3</sub>), 6.94 – 7.92 (aromatic protons), 8.47 (s, imine CH).  $^{13}$ C-NMR (126 MHz, CDCl<sub>3</sub>-

*d*) δ: 169.12, 158.32, 157.05, 152.69, 144.71, 134.16, 129.71, 122.17, 121.96, 114.37, 55.50, 21.18.

*N*-(*p*-Methoxyphenyl)-3-(4-Nitro)-benzylimine (D–49h). *p*-Nitrobenzaldehyde (1 g, 6.62 mmol, 1 equiv) and *p*-methoxyaniline (2.04 g, 16.56 mmol, 2.5 equiv) were treated according to Procedure 1 (Section 4.2.2.1) to afford the imine (930 mg, 55% yield, at >98% purity by <sup>1</sup>H-NMR analysis). <sup>1</sup>H-NMR (500 MHz, CDCl<sub>3</sub>-*d*) δ: 3.87 (s, PMP – OCH<sub>3</sub>), 6.98 – 8.33 (aromatic protons), 8.60 (s, imine CH). <sup>13</sup>C-NMR (126 MHz, CDCl<sub>3</sub>-*d*) δ: 159.24, 154.73, 149.01, 143.60, 141.95, 129.06, 123.97, 122.59, 114.54, 55.52.

*N*-(*p*-Methoxyphenyl)-3-(3-Bromo)-benzylimine (D–49i). *m*-Bromobenzaldehyde (1 g, 7.14 mmol, 1 equiv) and *p*-methoxyaniline (2.2 g, 17.85 mmol, 2.5 equiv) were treated according to Procedure 1 (Section 4.2.2.1) to afford the imine (1.1 g, 54% yield, at >99% purity by <sup>1</sup>H-NMR analysis). <sup>1</sup>H-NMR (500 MHz, CDCl<sub>3</sub>-*d*) δ: 3.84 (s, PMP – OCH<sub>3</sub>), 6.93 – 8.09 (aromatic protons), 8.42 (s, imine CH). <sup>13</sup>C-NMR (126 MHz, CDCl<sub>3</sub>-*d*) δ: 158.60, 156.31, 144.2, 138.44, 133.77, 131.03, 130.22, 127.34, 123.02, 122.30, 114.41, 55.50.

*N*-(*p*-Methoxyphenyl)-3-(3-Acetyl)-benzylimine (D–49j). *m*-Acetoxybenzaldehyde (1 g, 6.10 mmol, 1 equiv) and *p*-methoxyaniline (1.88 g, 15.25 mmol, 2.5 equiv) were treated according to Procedure 1 (Section 4.2.2.1) to afford the imine (965 mg, 59% yield, at >98% purity by <sup>1</sup>H-NMR analysis). <sup>1</sup>H-NMR (500 MHz, CDCl<sub>3</sub>-*d*) δ: 2.34 (s, *p*OAc CH<sub>3</sub>), 3.85 (s, PMP – OCH<sub>3</sub>), 6.93 – 7.73 (aromatic protons), 8.47 (s, imine CH). <sup>13</sup>C-NMR (126 MHz, CDCl<sub>3</sub>-*d*) δ: 169.39, 158.47, 157.02, 151.08, 144.44, 138.06, 129.72, 126.38, 124.19, 122.26, 121.10, 114.40, 55.51, 21.14.

*N*-(*p*-Methoxyphenyl)-3-(2-Methyl)-benzylimine (D–49k). *o*-Methylbenzaldehyde (1 g, 8.3 mmol, 1 equiv) and *p*-methoxyaniline (2.56 g, 20.75 mmol, 2.5 equiv) were treated according

to Procedure 1 (Section 4.2.2.1) to afford the imine (1.3 g, 69% yield, at >99% purity by <sup>1</sup>H-NMR analysis). <sup>1</sup>H-NMR (500 MHz, CDCl<sub>3</sub>-*d*) δ: 2.59 (s, *o*-CH<sub>3</sub>), 3.84 (s, PMP – OCH<sub>3</sub>), 6.92 – 8.08 (aromatic protons), 8.77 (s, imine CH). <sup>13</sup>C-NMR (126 MHz, CDCl<sub>3</sub>-*d*) δ: 158.16, 157.17, 134.31, 130.92, 130.69, 127.49, 126.33, 122.17, 114.35, 55.52, 19.40.

*N*-(*p*-Methoxyphenyl)-3-(2-Methoxy)-benzylimine (D–49l). *o*-Methoxybenzaldehyde (1 g, 7.35 mmol, 1 equiv) and *p*-methoxyaniline (2.71 g, 18.38 mmol, 2.5 equiv) were treated according to Procedure 1 (Section 4.2.2.1) to afford the imine (1.14 g, 64% yield, at >99% purity by <sup>1</sup>H-NMR analysis). <sup>1</sup>H-NMR (500 MHz, CDCl<sub>3</sub>-*d*) δ: 3.83 (s, PMP – OCH<sub>3</sub>), 3.90 (s, *o*-OCH<sub>3</sub>), 6.91 – 8.16 (aromatic protons), 8.94 (s, imine CH). <sup>13</sup>C-NMR (126 MHz, CDCl<sub>3</sub>-*d*) δ: 159.33, 158.09, 154.52, 145.68, 132.37, 127.33, 124.97, 122.39, 120.88, 114.30, 111.08, 55.55, 55.49.

### 4.2.2.2. General Procedure 2: Synthesis of 2-Azetidinones

Figure 4.9. Scheme showing the general synthesis of 2-azetidinones. TEA is triethylamine.

Figure 4.9. (cont'd)

## Method A:

To a solution of imine (1 equiv) dissolved in dichloromethane (18 mL) at 0 °C was added triethylamine (3 equiv). A solution of acetoxyacetyl chloride (2 equiv) in dichloromethane (8 mL) was then added dropwise and the reaction stirred at 0 °C for an additional 5 min. The

mixture was warmed to room temperature and stirred for 2-5 h to complete the reaction. The solution was washed successively with 5% (w/v) NaHCO<sub>3</sub> (15 mL), 5% v/v HCl (15 mL), and water (3 × 15 mL). The organic fraction was dried (MgSO<sub>4</sub>) and concentrated under vacuum. The crude mixture was then purified by silica gel chromatography (1:4 EtOAc/hexane, v/v) to yield the desired 2-azetidinones.

#### Method B:

The aldehyde (1 equiv) was dissolved in dichloromethane and p-methoxyaniline (1.1 equiv) was then added. The reaction was stirred at room temperature until the disappearance of starting material (the reaction progress was followed by TLC (1:4 EtOAc/hexane, v/v). The molecular sieves were removed by filtration and the filtrate transferred to a clean, oven dried round bottomed flask, which was then sealed using a rubber septum. To this crude imine mixture, triethylamine was added (3 equiv) and stirred at 0 °C. Acetoxyacetylchloride (2 equiv) was separately dissolved in dichloromethane and the solution was added slowly to the reaction mixture. The reaction was stirred at 0 °C for additional 5 min, and then warmed up to room temperature. Once the reaction was complete (2 – 3 h), the solution was washed successively with 5% (w/v) NaHCO<sub>3</sub> (15 mL), 5% v/v HCl (15 mL), and water (3 × 15 mL). The organic fraction was dried (MgSO<sub>4</sub>) and concentrated under vacuum. The crude mixture was purified by silica gel chromatography (1:4 EtOAc/hexane, v/v) to yield the respective 2-azetidinone.

*N*-(*p*-Methoxyphenyl)-3-acetoxy-4–phenylazetidin-2-one (**D**–50a). *N*-PMP-3-benzylimine (0.2 g, 0.95 mmol, 1 equiv), triethylamine (2.85 mmol, 3 equiv), and acetoxyacetyl chloride (1.9 mmol, 2 equiv) were treated according to Procedure 2, Method A (Section 4.2.2.2) to afford the lactam (108 mg, 37% yield, at >95% purity by  $^{1}$ H-NMR analysis).  $^{1}$ H-NMR (500 MHz, CDCl<sub>3</sub>-*d*)  $\delta$ : 1.68 (s, acetyl CH<sub>3</sub>), 3.76 (s, PMP – OCH<sub>3</sub>), 5.35 (d, J = 4.89 Hz, H-3), 5.95

(d, J = 4.89 Hz, H-2), 6.80 - 7.37 (aromatic protons). <sup>13</sup>C-NMR (126 MHz, CDCl<sub>3</sub>-*d*)  $\delta$ : 169.22, 161.29, 156.62, 132.27, 130.28, 128.77, 128.46, 127.90, 118.81, 114.41, 76.36, 61.47, 55.43, 19.77.

*N*-(*p*-Methoxyphenyl)-3-acetoxy-4-(4-fluorophenyl)azetidin-2-one (**D**–50b). *N*-PMP-3(4-F)-benzylimine (0.26 g, 1.15 mmol, 1 equiv), triethylamine (3.45 mmol, 3 equiv), and acetoxyacetyl chloride (2.3 mmol, 2 equiv) were treated according to Procedure 2, Method A (Section 4.2.2.2) to afford the lactam (115 mg, 40% yield, at >98% purity by  $^{1}$ H-NMR analysis).  $^{1}$ H-NMR (500 MHz, CDCl<sub>3</sub>-*d*) δ: 1.73 (s, acetyl CH<sub>3</sub>), 3.76 (s, PMP – OCH<sub>3</sub>), 5.33 (d, *J* = 4.89 Hz, H-3), 5.91 (d, *J* = 4.89 Hz, H-2), 6.80 – 7.31 (aromatic protons).  $^{13}$ C-NMR (126 MHz, CDCl<sub>3</sub>-*d*) δ: 169.24, 163.88, 161.14, 156.68, 130.06, 129.91, 128.06, 118.93, 115.84, 114.48, 76.84, 60.90, 55.55, 19.91.

*N*-(*p*-Methoxyphenyl)-3-acetoxy-4-(4-chlorophenyl)azetidin-2-one (D–50c). *N*-PMP-3(4-Cl)-benzylimine (0.5 g, 2.04 mmol, 1 equiv), triethylamine (6.12 mmol, 3 equiv), and acetoxyacetyl chloride (4.08 mmol, 2 equiv) were treated according to Procedure 2, Method A (Section 4.2.2.2) to afford the lactam (629 mg, 84% yield, at >98% purity by  $^{1}$ H-NMR analysis).  $^{1}$ H-NMR (500 MHz, CDCl<sub>3</sub>-*d*) δ: 1.74 (s, acetyl CH<sub>3</sub>), 3.76 (s, PMP – OCH<sub>3</sub>), 5.31 (d, *J* = 4.90 Hz, H-3), 5.92 (d, *J* = 4.89 Hz, H-2), 6.79 – 7.35 (aromatic protons).  $^{13}$ C-NMR (126 MHz, CDCl<sub>3</sub>-*d*) δ: 167.17, 161.02, 156.74, 134.78, 130.95, 130.03, 129.28, 128.77, 118.74, 114.49, 76.32, 60.88, 55.44, 19.88.

*N*-(*p*-Methoxyphenyl)-3-acetoxy-4-(4-bromophenyl)azetidin-2-one (D–50d). *N*-PMP-3(4-Br)-benzylimine (0.59 g, 2.06 mmol, 1 equiv), triethylamine (6.18 mmol, 3 equiv), and acetoxyacetyl chloride (4.12 mmol, 2 equiv) were treated according to Procedure 2, Method A (Section 4.2.2.2) to afford the lactam (640 mg, 95% yield, at >98% purity by <sup>1</sup>H-NMR analysis).

<sup>1</sup>H-NMR (500 MHz, CDCl<sub>3</sub>-d) δ: 1.75 (s, acetyl CH<sub>3</sub>), 3.76 (s, PMP – OCH<sub>3</sub>), 5.31 (d, J = 4.89 Hz, H-3), 5.93 (d, J = 4.89 Hz, H-2), 6.82 – 7.51 (aromatic protons). <sup>13</sup>C-NMR (126 MHz, CDCl<sub>3</sub>-d) δ: 169.18, 160.81, 156.75, 131.73, 131.50, 130.00, 129.57, 122.93, 118.73, 114.49, 76.26, 60.95, 55.44, 19.89.

*N*-(*p*-Methoxyphenyl)-3-acetoxy-4-(4-methylphenyl)azetidin-2-one (D–50e). *N*-PMP-3(4-Me)-benzylimine (0.5 g, 2.2 mmol, 1 equiv), triethylamine (6.6 mmol, 3 equiv), and acetoxyacetyl chloride (4.4 mmol, 2 equiv) were treated according to Procedure 2, Method A (Section 4.2.2.2) to afford the lactam (369 mg, 51% yield, at >98% purity by  $^{1}$ H-NMR analysis).  $^{1}$ H-NMR (500 MHz, CDCl<sub>3</sub>-*d*) δ: 1.71 (s, acetyl CH<sub>3</sub>), 2.35 (s, *p*-CH<sub>3</sub>), 3.76 (s, PMP – OCH<sub>3</sub>), 5.31 (d, J = 4.90 Hz, H-3), 5.92 (d, J = 4.89 Hz, H-2), 6.79 – 7.31 (aromatic protons).  $^{13}$ C-NMR (126 MHz, CDCl<sub>3</sub>-*d*) δ: 169.30, 161.41, 156.54, 138.64, 130.35, 129.19, 129.12, 127.87, 118.83, 114.37, 76.38, 61.38, 55.44, 21.23, 19.92.

*N*-(*p*-Methoxyphenyl)-3-acetoxy-4-(4-methoxyphenyl)azetidin-2-one (**D**–50f). *N*-PMP-3(4-OMe)-benzylimine (0.25 g, 1.04 mmol, 1 equiv), triethylamine (3.12 mmol, 3 equiv) and acetoxyacetyl chloride (2.08 mmol, 2 equiv) were treated according to Procedure 2, Method A (Section 4.2.2.2) to afford the lactam (279 mg, 79% yield, at >98% purity by  $^{1}$ H-NMR analysis).  $^{1}$ H-NMR (500 MHz, CDCl<sub>3</sub>-*d*) δ: 1.73 (s, acetyl CH<sub>3</sub>), 3.75 (s, PMP – OCH<sub>3</sub>), 3.80 (s, *p*-OCH<sub>3</sub>), 5.29 (d, *J* = 4.90 Hz, H-3), 5.89 (d, *J* = 4.89 Hz, H-2), 6.78 – 7.30 (aromatic protons).  $^{13}$ C-NMR (126 MHz, CDCl<sub>3</sub>-*d*) δ: 169.33, 161.41, 159.91, 156.54, 130.32, 129.25, 123.99, 118.85, 114.37, 113.90, 76.50, 61.15, 55.44, 55.27, 19.94.

*N*-(*p*-Methoxyphenyl)-3-acetoxy-4-(4-acetoxyphenyl)azetidin-2-one (**D**–50g). *N*-PMP-3(4-OAc)-benzylimine (0.54 g, 2.0 mmol, 1 equiv), triethylamine (5.96 mmol, 3 equiv), and acetoxyacetyl chloride (3.98 mmol, 2 equiv) were treated according to Procedure 2, Method A

(Section 4.2.2.2) to afford the lactam (692 mg, 94% yield, at >95% purity by  ${}^{1}$ H-NMR analysis).  ${}^{1}$ H-NMR (500 MHz, CDCl<sub>3</sub>-d)  $\delta$ : 1.71 (s, acetyl CH<sub>3</sub>) 2.29 (s, p-OAC–CH<sub>3</sub>), 3.76 (s, PMP – OCH<sub>3</sub>), 5.35 (d, J = 4.89 Hz, H-3), 5.93 (d, J = 4.89 Hz, H-2), 6.82 – 7.33 (aromatic protons).  ${}^{13}$ C-NMR (126 MHz, CDCl<sub>3</sub>-d)  $\delta$ : 169.33, 169.16, 161.15, 156.89, 150.98, 130.09, 129.78, 128.94, 121.77, 118.81, 114.47, 76.36, 60.98, 55.45, 21.11, 19.80.

*N*-(*p*-Methoxyphenyl)-3-acetoxy-4-(4-nitrophenyl)azetidin-2-one (**D**–50h). *N*-PMP-3(4-nitro)-benzylimine (0.93 g, 3.63 mmol, 1 equiv), triethylamine (10.89 mmol, 3 equiv) and acetoxyacetyl chloride (7.29 mmol, 2 equiv) were treated according to Procedure 2, Method A (Section 4.2.2.2) to afford the lactam (1.1 g, 82% yield, at >99% purity by  $^{1}$ H-NMR analysis).  $^{1}$ H-NMR (500 MHz, CDCl<sub>3</sub>-*d*) δ: 1.74 (s, acetyl CH<sub>3</sub>), 3.76 (s, PMP – OCH<sub>3</sub>), 5.45 (d, *J* = 4.89 Hz, H-3), 6.00 (d, *J* = 4.89 Hz, H-2), 6.81 – 8.25 (aromatic protons).  $^{13}$ C-NMR (126 MHz, CDCl<sub>3</sub>-*d*) δ: 169.33, 161.41, 156.94, 148.19, 140.01, 129.66, 128.88, 123.72, 118.62, 114.61, 76.41, 60.66, 55.47, 19.90.

*N*-(*p*-Methoxyphenyl)-3-acetoxy-4-(3-fluorophenyl)azetidin-2-one (**D**–50i). 3-Fluorobenzaldehyde (1 g, 8.07 mmol, 1 equiv), *p*-methoxyaniline (1.49 g, 12.10 mmol, 1.5 equiv), triethylamine (24.2 mmol, 3 equiv) and acetoxyacetyl chloride (16.13 mmol, 2 equiv) were treated according to Procedure 2, Method B (Section 4.2.2.2) to afford the lactam (1.3 g, 51% yield, at >99% purity by  $^{1}$ H-NMR analysis).  $^{1}$ H-NMR (500 MHz, CDCl<sub>3</sub>-*d*) δ: 1.74 (s, acetyl CH<sub>3</sub>), 3.76 (s, PMP – OCH<sub>3</sub>), 5.33 (d, J = 4.89 Hz, H-3), 5.95 (d, J = 4.89 Hz, H-2), 6.80 – 7.33 (aromatic protons).  $^{13}$ C-NMR (126 MHz, CDCl<sub>3</sub>-*d*) δ: 169.41, 164.95, 161.71, 156.73, 135.12, 130.24, 130.00, 123.67, 118.72, 115.96, 114.95, 114.48, 76.26, 60.84, 55.44, 19.85.

*N*-(*p*-Methoxyphenyl)-3-acetoxy-4-(3-chlorophenyl)azetidin-2-one (**D**–50j). 3-Chlorobenzaldehyde (1 g, 7.1 mmol, 1 equiv), *p*-methoxyaniline (1.31 g, 10.67 mmol, 1.5 equiv),

triethylamine (21.34 mmol, 3 equiv) and acetoxyacetyl chloride (14.23 mmol, 2 equiv) were treated according to Procedure 2, Method B (Section 4.2.2.2) to afford the lactam (1.1 g, 47% yield, at >99% purity by  $^{1}$ H-NMR analysis).  $^{1}$ H-NMR (500 MHz, CDCl<sub>3</sub>-d)  $\delta$ : 1.74 (s, acetyl CH<sub>3</sub>), 3.76 (s, PMP – OCH<sub>3</sub>), 5.30 (d, J = 4.89 Hz, H-3), 5.94 (d, J = 4.89 Hz, H-2), 6.80 – 7.34 (aromatic protons).  $^{13}$ C-NMR (126 MHz, CDCl<sub>3</sub>-d)  $\delta$ : 169.16, 160.99, 156.74, 134.62, 134.57, 129.83, 129.10, 127.93, 126.12, 118.72, 114.50, 76.25, 60.85, 55.45, 19.87.

*N*-(*p*-Methoxyphenyl)-3-acetoxy-4-(3-bromophenyl)azetidin-2-one (D–50k). *N*-PMP-3(3-bromo)-benzylimine (1.11 g, 3.85 mmol, 1 equiv), triethylamine (11.54 mmol, 3 equiv), and acetoxyacetyl chloride (7.7 mmol, 2 equiv) were treated according to Procedure 2, Method A (Section 4.2.2.2) to afford the lactam (500 mg, 33% yield, at >97% purity by  $^{1}$ H-NMR analysis).  $^{1}$ H-NMR (500 MHz, CDCl<sub>3</sub>-*d*) δ: 1.76 (s, acetyl CH<sub>3</sub>), 3.77 (s, PMP – OCH<sub>3</sub>), 5.30 (d, *J* = 4.89 Hz, H-3), 5.95 (d, *J* = 4.89 Hz, H-2), 6.82 – 7.51 (aromatic protons).  $^{13}$ C-NMR (126 MHz, CDCl<sub>3</sub>-*d*) δ: 169.17, 160.99, 156.95, 134.86, 132.06, 130.85, 130.10, 129.98, 126.61, 122.61, 118.73, 114.52, 76.27, 60.81, 55.47, 19.88.

*N*-(*p*-Methoxyphenyl)-3-acetoxy-4-(3-methylphenyl)azetidin-2-one (D–50l). 3-Methylbenzaldehyde (0.5 g, 4.17 mmol, 1 equiv), *p*-methoxyaniline (0.77 g, 6.26 mmol, 1.5 equiv), triethylamine (12.51 mmol, 3 equiv) and acetoxyacetyl chloride (8.34 mmol, 2 equiv) were treated according to Procedure 2, Method B (Section 4.2.2.2) to afford the lactam (760 mg, 81% yield, at >99% purity by  $^{1}$ H-NMR analysis).  $^{1}$ H-NMR (500 MHz, CDCl<sub>3</sub>-*d*)  $\delta$ : 1.70 (s, acetyl CH<sub>3</sub>), 2.34 (s, *m*-CH<sub>3</sub>), 3.77 (s, PMP – OCH<sub>3</sub>), 5.30 (d, *J* = 4.89 Hz, H-3), 5.94 (d, *J* = 4.89 Hz, H-2), 6.80 – 7.32 (aromatic protons).

*N*-(*p*-Methoxyphenyl)-3-acetoxy-4-(3-methoxyphenyl)azetidin-2-one (D–50m). 3-Methoxybenzaldehyde (1 g, 7.35 mmol, 1 equiv), *p*-methoxyaniline (1.36 g, 11.03 mmol, 1.5

equiv), triethylamine (22.05 mmol, 3 equiv) and acetoxyacetyl chloride (14.7 mmol, 2 equiv) were treated according to Procedure 2, Method B (Section 4.2.2.2) to afford the lactam (1.6 g, 66% yield, at >95% purity by  $^{1}$ H-NMR analysis).  $^{1}$ H-NMR (500 MHz, CDCl<sub>3</sub>-d)  $\delta$ : 1.73 (s, acetyl CH<sub>3</sub>), 3.76 (s, m-OCH<sub>3</sub>), 3.77 (s, PMP – OCH<sub>3</sub>), 5.30 (d, J = 4.89 Hz, H-3), 5.95 (d, J = 4.89 Hz, H-2), 6.79 – 7.30 (aromatic protons).

*N*-(*p*-Methoxyphenyl)-3-acetoxy-4-(3-acetoxyphenyl)azetidin-2-one (D–50n). *N*-PMP-3-(3-OAc)-benzylimine (0.97 g, 3.59 mmol, 1 equiv), triethylamine (10.77 mmol, 3 equiv), and acetoxyacetyl chloride (7.18 mmol, 2 equiv) were treated according to Procedure 2, Method A (Section 4.2.2.2) to afford the lactam (1.05 g, 79% yield, at >99% purity by  $^{1}$ H-NMR analysis).  $^{1}$ H-NMR (500 MHz, CDCl<sub>3</sub>-*d*) δ: 1.74 (s, acetyl CH<sub>3</sub>), 2.27 (s, *m*-OAc CH<sub>3</sub>), 3.76 (s, PMP – OCH<sub>3</sub>), 5.33 (d, J = 4.89 Hz, H-3), 5.94 (d, J = 4.89 Hz, H-2), 6.80 – 7.38 (aromatic protons).  $^{13}$ C-NMR (126 MHz, CDCl<sub>3</sub>-*d*) δ: 169.43, 169.22, 161.14, 156.69, 150.77, 134.19, 130.09, 129.56, 125.41, 122.29, 121.09, 118.77, 114.45, 76.27, 61.00, 55.44, 21.07, 19.78.

*N*-(*p*-Methoxyphenyl)-3-acetoxy-4-(3-nitrophenyl)azetidin-2-one (**D**–50o). 3-Nitrobenzaldehyde (1 g, 6.62 mmol, 1 equiv), *p*-methoxyaniline (1.22 g, 9.93 mmol, 1.5 equiv), triethylamine (19.86 mmol, 3 equiv) and acetoxyacetyl chloride (13.24 mmol, 2 equiv) were treated according to Procedure 2, Method B (Section 4.2.2.2) to afford the lactam (588 mg, 25% yield, at >95% purity by  $^{1}$ H-NMR analysis).  $^{1}$ H-NMR (500 MHz, CDCl<sub>3</sub>-*d*) δ: 1.73 (s, acetyl CH<sub>3</sub>), 3.76 (s, PMP – OCH<sub>3</sub>), 5.45 (d, J = 4.89 Hz, H-3), 5.99 (d, J = 4.89 Hz, H-2), 6.80 – 8.25 (aromatic protons).  $^{13}$ C-NMR (126 MHz, CDCl<sub>3</sub>-*d*) δ: 169.03, 160.65, 156.95, 148.39, 135.06, 133.84, 129.67, 129.64, 123.96, 123.01, 118.68, 114.64, 76.37, 60.62, 55.49 19.87.

*N*-(*p*-Methoxyphenyl)-3-acetoxy-4-(2-fluorophenyl)azetidin-2-one (D–50p). 2-Fluorobenzaldehyde (1 g, 8.07 mmol, 1 equiv), *p*-methoxyaniline (1.49 g, 12.1 mmol, 1.5 equiv),

triethylamine (24.2 mmol, 3 equiv), and acetoxyacetyl chloride (16.13 mmol, 2 equiv) were treated according to Procedure 2, Method B (Section 4.2.2.2) to afford the lactam (1.1 g, 41% yield, at >99% purity by  $^{1}$ H-NMR analysis).  $^{1}$ H-NMR (500 MHz, CDCl<sub>3</sub>-d)  $\delta$ : 1.76 (s, acetyl CH<sub>3</sub>), 3.76 (s, PMP – OCH<sub>3</sub>), 5.67 (d, J = 4.89 Hz, H-3), 6.02 (d, J = 4.89 Hz, H-2), 6.80 – 7.36 (aromatic protons).  $^{13}$ C-NMR (126 MHz, CDCl<sub>3</sub>-d)  $\delta$ : 168.81, 161.99, 161.20, 156.62, 130.57, 130.06, 129.05, 124.09, 119.80, 118.54, 115.77, 114.41, 75.98, 63.00, 55.32, 19.72.

*N*-(*p*-Methoxyphenyl)-3-acetoxy-4-(2-chlorophenyl)azetidin-2-one (D–50q). 2-Chlorobenzaldehyde (1 g, 7.11 mmol, 1 equiv), *p*-methoxyaniline (1.31 g, 10.67 mmol, 1.5 equiv), triethylamine (21.34 mmol, 3 equiv), and acetoxyacetyl chloride (14.23 mmol, 2 equiv) were treated according to Procedure 2, Method B (Section 4.2.2.2) to afford the lactam (2.0 g, 80% yield, at >98% purity by  $^{1}$ H-NMR analysis).  $^{1}$ H-NMR (500 MHz, CDCl<sub>3</sub>-*d*) δ: 1.76 (s, acetyl CH<sub>3</sub>), 3.77 (s, PMP – OCH<sub>3</sub>), 5.79 (d, J = 4.89 Hz, H-3), 6.17 (d, J = 4.89 Hz, H-2), 6.81 – 7.45 (aromatic protons).  $^{13}$ C-NMR (126 MHz, CDCl<sub>3</sub>-*d*) δ: 168.74, 161.45, 156.68, 133.87, 130.16, 130.04, 129.84, 128.72, 126.77, 118.66, 114.49, 75.45, 58.22, 55.45, 19.94.

*N*-(*p*-Methoxyphenyl)-3-acetoxy-4-(2-bromophenyl)azetidin-2-one (D–50r). 2-Bromobenzaldehyde (1 g, 5.41 mmol, 1 equiv), *p*-methoxyaniline (1.0 g, mmol, 1.5 equiv), triethylamine (16.22 mmol, 3 equiv) and acetoxyacetyl chloride (10.81 mmol, 2 equiv) were treated according to Procedure 2, Method B (Section 4.2.2.2) to afford the lactam (1.2 g, 59% yield, at >98% purity by  $^{1}$ H-NMR analysis).  $^{1}$ H-NMR (500 MHz, CDCl<sub>3</sub>-*d*) δ: 1.77 (s, acetyl CH<sub>3</sub>), 3.76 (s, PMP – OCH<sub>3</sub>), 5.76 (d, *J* = 4.89 Hz, H-3), 6.19 (d, *J* = 4.89 Hz, H-2), 6.81 – 7.64 (aromatic protons).  $^{13}$ C-NMR (126 MHz, CDCl<sub>3</sub>-*d*) δ: 168.69, 161.44, 156.68, 144.45, 133.10, 130.11, 128.88, 127.37, 122.55, 118.67, 114.50, 75.35, 60.64, 55.45 19.98.

*N*-(*p*-Methoxyphenyl)-3-acetoxy-4-(2-methylphenyl)azetidin-2-one (D–50s). *N*-PMP-3(2-Me)-benzylimine (1.28 g, 5.69 mmol, 1 equiv), triethylamine (17.08 mmol, 3 equiv) and acetoxyacetyl chloride (11.39 mmol, 2 equiv) were treated according to Procedure 2, Method A (Section 4.2.2.2) to afford the lactam (1.4 g, 75% yield, at >99% purity by  $^{1}$ H-NMR analysis).  $^{1}$ H-NMR (500 MHz, CDCl<sub>3</sub>-*d*) δ: 1.68 (s, acetyl CH<sub>3</sub>), 2.43 (s, *o*-CH<sub>3</sub>), 3.77 (s, PMP – OCH<sub>3</sub>), 5.55 (d, J = 4.89 Hz, H-3), 6.01 (d, J = 4.89 Hz, H-2), 6.81 – 7.27 (aromatic protons).  $^{13}$ C-NMR (126 MHz, CDCl<sub>3</sub>-*d*) δ: 169.39, 161.17, 156.54, 136.74, 130.71, 130.29, 129.97, 128.46, 126.98, 125.87, 118.76, 114.39, 76.05, 58.26, 55.38, 19.74, 19.06.

*N*-(*p*-Methoxyphenyl)-3-acetoxy-4-(2-methoxyphenyl)azetidin-2-one (D–50t). *N*-PMP-3-(2-OMe)-benzylimine (1.14 g, 4.72 mmol, 1 equiv), triethylamine (14.16 mmol, 3 equiv) and acetoxyacetyl chloride (9.44 mmol, 2 equiv) were treated according to Procedure 2, Method A (Section 4.2.2.2) to afford the lactam (1.3 g, 84% yield, at >99% purity by  $^{1}$ H-NMR analysis).  $^{1}$ H-NMR (500 MHz, CDCl<sub>3</sub>-*d*)  $\delta$ : 1.71 (s, acetyl CH<sub>3</sub>), 3.75 (s, PMP – OCH<sub>3</sub>), 3.85 (s, *o*-OCH<sub>3</sub>), 5.73 (d, J = 4.89 Hz, H-3), 6.06 (d, J = 4.89 Hz, H-2), 6.79 – 7.32 (aromatic protons).

*N*-(*p*-Methoxyphenyl)-3-acetoxy-4-(2-nitrophenyl)azetidin-2-one (D–50u). 2-Nitrobenzaldehyde (1 g, 6.62 mmol, 1 equiv), *p*-methoxyaniline (0.82 g, 6.62 mmol, 1.5 equiv), triethylamine (19.87 mmol, 3 equiv) and acetoxyacetyl chloride (13.25 mmol, 2 equiv) were treated according to Procedure 2, Method B (Section 4.2.2.2) to afford the lactam (1.1 g, 47% yield, at >95% purity by  $^{1}$ H-NMR analysis).  $^{1}$ H-NMR (500 MHz, CDCl<sub>3</sub>-*d*) δ: 1.77 (s, acetyl CH<sub>3</sub>), 3.78 (s, PMP – OCH<sub>3</sub>), 6.06 (d, J = 5.38 Hz, H-3), 6.36 (d, J = 5.38 Hz, H-2), 6.84 – 8.22 (aromatic protons).  $^{13}$ C-NMR (126 MHz, CDCl<sub>3</sub>-*d*) δ: 168.37, 161.80, 156.86, 148.20, 133.88, 130.04, 129.50, 129.32, 129.25, 125.44, 118.58, 114.64, 75.89, 60.18, 55.51, 19.97.

*N*-(*p*-Methoxyphenyl)-3-acetoxy-4-trimethylazetidin-2-one (D–50v). Trimethylacetaldehyde (1 g, 11.61 mmol, 1 equiv), *p*-methoxyaniline (1.43 g, 11.61 mmol, 1.0 equiv), triethylamine (26.13 mmol, 3 equiv), and acetoxyacetyl chloride (17.42 mmol, 2 equiv) were treated according to Procedure 2, Method B (Section 4.2.2.2) to afford the lactam (0.9 g, 35% yield, at >99% purity by  $^{1}$ H-NMR analysis).  $^{1}$ H-NMR (500 MHz, CDCl<sub>3</sub>-*d*) δ: 1.00 (s, *t*-butyl (CH<sub>3</sub>)<sub>3</sub>), 2.18 (s, acetyl CH<sub>3</sub>), 3.79 (s, PMP – OCH<sub>3</sub>), 4.23 (d, *J* = 5.38 Hz, H-3), 6.15 (d, *J* = 5.38 Hz, H-2), 6.88 – 7.29 (aromatic protons).  $^{13}$ C-NMR (126 MHz, CDCl<sub>3</sub>-*d*) δ: 169.38, 164.03, 157.15, 129.94, 121.99, 114.24, 73.46, 66.89, 55.47, 34.77, 27.02, 20.92.

*N*-(*p*-Methoxyphenyl)-3-acetoxy-4-cyclohexylazetidin-2-one (D–50w). Cyclohexylacetaldehyde (1 g, 8.92 mmol, 1 equiv), *p*-methoxyaniline (2.74 g, 22.29 mmol, 1.5 equiv), triethylamine (13.8 mmol, 3 equiv) and acetoxyacetyl chloride (9.2 mmol, 2 equiv) were treated according to Procedure 2, Method B (Section 4.2.2.2) to afford the lactam (223 mg, 70% yield, at >99% purity by  $^{1}$ H-NMR analysis).  $^{1}$ H-NMR (500 MHz, CDCl<sub>3</sub>-*d*) δ: 0.96 – 1.78 (cyclohexyl protons), 1.85 (dd, J = 6.36, 2.93 Hz, cyclohexyl CH), 2.20 (s, acetyl CH<sub>3</sub>), 3.81 (s, PMP – OCH<sub>3</sub>), 4.20 (t, J = 5.87 Hz, H-3), 6.05 (d, J = 5.38 Hz, H-2), 6.87 – 7.37 (aromatic protons).  $^{13}$ C-NMR (126 MHz, CDCl<sub>3</sub>-*d*) δ: 169.60, 162.95, 156.68, 130.82, 119.73, 114.26, 73.77, 61.97, 55.47, 38.59, 29.78, 29.64, 26.13, 20.72.

*N*-(*p*-Methoxyphenyl)-3-acetoxy-4-thiophenylazetidin-2-one (**D**–50x). Thiophene-carboxaldehyde (1 g, 8.93 mmol, 1 equiv), *p*-methoxyaniline (1.1 g, 8.93 mmol, 1.5 equiv), triethylamine (26.78 mmol, 3 equiv) and acetoxyacetyl chloride (17.86 mmol, 2 equiv) were treated according to Procedure 2, Method B (Section 4.2.2.2) to afford the lactam (322 mg, 8% yield, at >99% purity by  $^{1}$ H-NMR analysis).  $^{1}$ H-NMR (500 MHz, CDCl<sub>3</sub>-*d*)  $\delta$ : 1.86 (s, acetyl CH<sub>3</sub>), 3.76 (s, PMP – OCH<sub>3</sub>), 5.61 (d, J = 4.89 Hz, H-3), 5.95 (d, J = 4.89 Hz, H-2), 6.80 – 7.34

(aromatic protons). <sup>13</sup>C-NMR (126 MHz, CDCl<sub>3</sub>-*d*) δ: 169.37, 161.05, 156.72, 135.58, 130.08, 128.16, 127.08, 126.87, 118.85, 114.40, 76.52, 57.66, 55.45, 20.05.

*N*-(*p*-Methoxyphenyl)-3-acetoxy-4-dimethylazetidin-2-one (D–50y). Isopropylaldehyde (1 g, 13.89 mmol, 1 equiv), *p*-methoxyaniline (2.56 g, 20.84 mmol, 1.5 equiv), triethylamine (41.67 mmol, 3 equiv) and acetoxyacetyl chloride (27.78 mmol, 2 equiv) were treated according to Procedure 2, Method B (Section 4.2.2.2) to afford the lactam (327 mg, 9% yield, at >99% purity by  $^{1}$ H-NMR analysis).  $^{1}$ H-NMR (500 MHz, CDCl<sub>3</sub>-*d*) δ: 0.96 – 1.01 (m, (CH<sub>3</sub>)<sub>2</sub>) 2.18 (s, acetyl CH<sub>3</sub>), 2.23 (dd, J = 12.72, 6.85 Hz, H-1), 3.79 (s, PMP – OCH<sub>3</sub>), 4.22 (t, J = 5.38 Hz, H-3), 6.04 (d, J = 5.38 Hz, H-2), 6.86 – 7.37 (aromatic protons).  $^{13}$ C-NMR (126 MHz, CDCl<sub>3</sub>-*d*) δ: 169.58, 162.87, 156.71, 130.56, 119.78, 114.32, 73.82, 62.64, 55.48, 28.43, 20.74, 18.84.

#### 4.2.2.3. General Procedure 3: Deprotection of Azetidinones

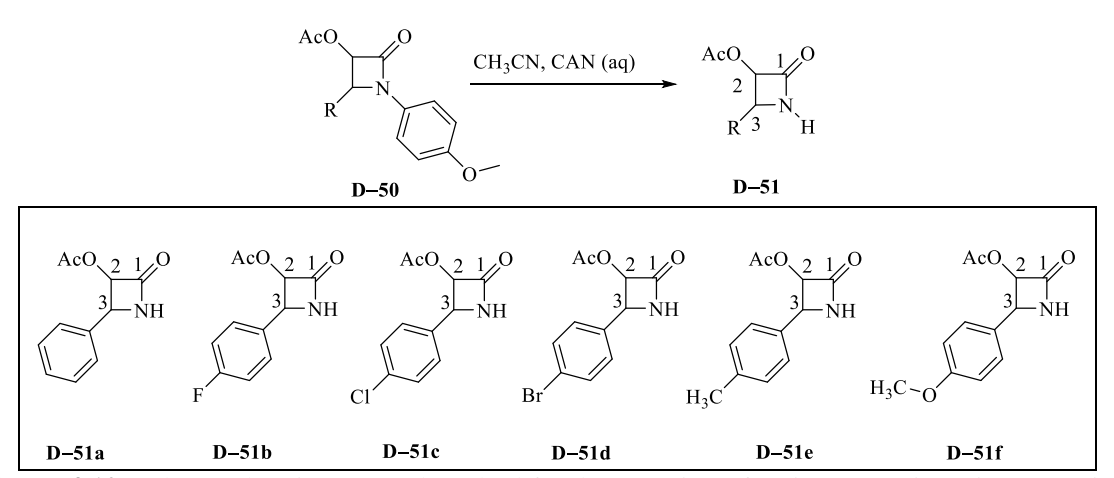


**Figure 4.10.** Scheme showing general method for deprotection of amine. CAN is ceric ammonium nitrate.

**Figure 4.10.** (cont'd)

The deprotection of azetidinones was carried out similarly to a reported procedure. <sup>38</sup> Briefly, to the solution of 2-azetidinone (1 equiv) in CH<sub>3</sub>CN was added dropwise a solution of ceric ammonium nitrate ( $(NH_4)_2Ce(NO_3)_6$ ) (3 equiv) in water at 0 °C. The mixture was stirred at 0 °C until the disappearance of starting material and then diluted with water (20 mL). The mixture was then extracted with EtOAc (3 × 20 mL). The organic layer was washed with 5% (w/v) NaHCO<sub>3</sub> (15 mL) and the aqueous extracts were washed with EtOAc (20 mL). The combined organic extracts were washed with 10% (w/v) Na<sub>2</sub>SO<sub>3</sub> (15 mL), 5% (w/v) NaHCO<sub>3</sub> (15 mL), and brine (15 mL) successively. The combined extracts were dried over MgSO<sub>4</sub> and

concentrated under vacuum. The crude mixture was purified by silica gel chromatography (1:3 EtOAc/hexane, v/v) to yield the desired 2-azetidinones.

**3-Acetoxy-4-phenylazetidin-2-one** (**D**–**51a**). *N*-(*p*-methoxyphenyl)-3-acetoxy-4-phenylazetidin-2-one (0.14 g, 0.43 mmol) in CH<sub>3</sub>CN (8.5 mL), and (NH<sub>4</sub>)<sub>2</sub>Ce(NO<sub>3</sub>)<sub>6</sub> (0.71 g, 1.3 mmol, 3 equiv) in water (9 mL) were treated according to Procedure 3 (Section 4.2.2.3) to afford the azetidinone (59.6 mg, 80% yield, at >95% purity by  $^{1}$ H-NMR analysis).  $^{1}$ H-NMR (500 MHz, CDCl<sub>3</sub>-*d*)  $\delta$ : 1.68 (s, acetyl CH<sub>3</sub>), 5.04 (d, J = 4.89 Hz, H-3), 5.89 (dd, J = 4.89, 2.70 Hz, H-2), 6.16 – 6.21 (m, amide NH), 7.30 – 7.39 (aromatic protons).

**3-Acetoxy-4-(4-fluorophenyl)azetidin-2-one** (**D–51b**). *N*-(*p*-methoxyphenyl)-3-acetoxy-4-(4-fluorophenyl)azetidin-2-one (0.23 g, 0.7 mmol) in CH<sub>3</sub>CN (9 mL), and (NH<sub>4</sub>)<sub>2</sub>Ce(NO<sub>3</sub>)<sub>6</sub> (1.15 g, 2.1 mmol, 3 equiv) in water (10 mL) were treated according to Procedure 3 (Section 4.2.2.3) to afford the azetidinone (63.1 mg, 78% yield, at >98% purity by  $^{1}$ H-NMR analysis).  $^{1}$ H-NMR (500 MHz, CDCl<sub>3</sub>-*d*)  $\delta$ : 1.73 (s, acetyl CH<sub>3</sub>), 5.03 (d, J = 4.89 Hz, H-3), 5.86 (dd, J = 4.89, 2.69 Hz, H-2), 6.18 (br. s, amide NH), 7.04 – 7.32 (aromatic protons).  $^{13}$ C-NMR (126 MHz, CDCl<sub>3</sub>-*d*)  $\delta$ : 169.09, 165.58, 161.82, 130.22, 129.34, 115.43, 78.24, 57.37, 19.89.

**3-Acetoxy-4-(4-chlorophenyl)azetidin-2-one** (**D–51c**). *N*-(*p*-methoxyphenyl)-3-acetoxy-4-(4-chlorophenyl)azetidin-2-one (0.40 g, 1.2 mmol) in CH<sub>3</sub>CN (14 mL) and (NH<sub>4</sub>)<sub>2</sub>Ce(NO<sub>3</sub>)<sub>6</sub> (1.91 g, 3.48 mmol, 3 equiv) in water (16 mL) were treated according to Procedure 3 (Section 4.2.2.3) to afford the azetidinone (177 mg, 69% yield, at >98% purity by  $^{1}$ H-NMR analysis).  $^{1}$ H-NMR (500 MHz, CDCl<sub>3</sub>-*d*)  $\delta$ : 1.74 (s, acetyl CH<sub>3</sub>), 5.02 (d, J = 4.89 Hz, H-3), 5.87 (dd, J = 4.89, 2.93 Hz, H-2), 6.34 (br. s., amide NH), 7.26 – 7.36 (aromatic protons).

<sup>13</sup>C-NMR (126 MHz, CDCl<sub>3</sub>-*d*) δ: 169.01, 165.16, 134.60, 133.06, 128.90, 128.55, 78.28, 57.39, 19.91.

**3-Acetoxy-4-(4-bromophenyl)azetidin-2-one** (D–51d). N-(p-methoxyphenyl)-3-acetoxy-4-(4-bromophenyl)azetidin-2-one (0.25 g, 0.64 mmol) in CH<sub>3</sub>CN (9 mL), and (NH<sub>4</sub>)<sub>2</sub>Ce(NO<sub>3</sub>)<sub>6</sub> (1.04 g, 4.94 mmol, 3 equiv) in water (9 mL) were treated according to Procedure 3 (Section 4.2.2.3) to afford the azetidinone (440 mg, 95% yield, at >95% purity by  $^{1}$ H-NMR analysis).  $^{1}$ H-NMR (500 MHz, CDCl<sub>3</sub>-d)  $\delta$ : 1.74 (s, acetyl CH<sub>3</sub>), 5.00 (d, J = 4.89 Hz, H-3), 5.86 (dd, J = 4.89, 2.93 Hz, H-2), 6.40 (br. s., amide NH), 7.19 – 7.50 (aromatic protons).  $^{13}$ C-NMR (126 MHz, CDCl<sub>3</sub>-d)  $\delta$ : 169.03, 165.28, 136.52, 133.58, 131.51, 129.19, 78.18, 57.47, 19.93.

**3-Acetoxy-4-(4-methylphenyl)azetidin-2-one** (**D–51e**). *N*-(*p*-methoxyphenyl)-3-acetoxy-4-(4-methylphenyl)azetidin-2-one (0.25 g, 0.8 mmol) in CH<sub>3</sub>CN (10 mL), and (NH<sub>4</sub>)<sub>2</sub>Ce(NO<sub>3</sub>)<sub>6</sub> (1.27 g, 2.31 mmol 3 equiv) in water (10 mL) were treated according to Procedure 3 (Section 4.2.2.3) to afford the azetidinone (146 mg, 87% yield, at >98% purity by  $^{1}$ H-NMR analysis).  $^{1}$ H-NMR (500 MHz, CDCl<sub>3</sub>-*d*)  $\delta$ : 1.70 (s, acetyl CH<sub>3</sub>), 2.33 (s, *p*-CH<sub>3</sub>), 4.99 (d, J = 4.89 Hz, H-3), 5.85 (dd, J = 4.89, 2.69 Hz, H-2), 6.33 (br. s., amide NH), 7.13 – 7.21 (aromatic protons).  $^{13}$ C-NMR (126 MHz, CDCl<sub>3</sub>-*d*)  $\delta$ : 169.15, 165.43, 138.50, 131.31, 129.01, 127.52, 78.26, 57.79, 31.19, 19.97.

**3-Acetoxy-4-(4-methoxyphenyl)azetidin-2-one** (**D–51f).** N-(p-methoxyphenyl)-3-acetoxy-4-(4-methoxyphenyl)azetidin-2-one (0.20 g, 0.59 mmol) in CH<sub>3</sub>CN (7 mL), and (NH<sub>4</sub>)<sub>2</sub>Ce(NO<sub>3</sub>)<sub>6</sub> (0.96 g, 1.76 mmol, 3 equiv) in water (8 mL) were treated according to Procedure 3 (Section 4.2.2.3) to afford the azetidinone (130.4 mg, 95% yield, at >98% purity by  $^{1}$ H-NMR analysis).  $^{1}$ H-NMR (500 MHz, CDCl<sub>3</sub>-d)  $\delta$ : 1.72 (s, acetyl CH<sub>3</sub>), 3.81 (s, p-OCH<sub>3</sub>),

4.98 (d, J = 4.40 Hz, H-3), 5.83 (dd, J = 4.40, 2.69 Hz, H-2), 6.31 (br. s., amide NH), 6.87 – 7.25 (aromatic protons). <sup>13</sup>C-NMR (126 MHz, CDCl<sub>3</sub>-d)  $\delta$ : 169.12, 165.56, 159.85, 136.52, 128.87, 126.29, 78.33, 57.56, 55.28, 19.93.

**3-Acetoxy-4-(4-acetoxyphenyl)azetidin-2-one** (**D**–**51g**). *N*-(*p*-methoxyphenyl)-3-acetoxy-4-(4-acetoxyphenyl)azetidin-2-one (690 mg, 1.87 mmol) in CH<sub>3</sub>CN (30 mL), and (NH<sub>4</sub>)<sub>2</sub>Ce(NO<sub>3</sub>)<sub>6</sub> (3.08 g, 5.61 mmol, 3 equiv) in water (32 mL) were treated according to Procedure 3 (Section 4.2.2.3) to afford the azetidinone (0.26 g, 54% yield, at >95% purity by  $^{1}$ H-NMR analysis).  $^{1}$ H-NMR (500 MHz, CDCl<sub>3</sub>-*d*)  $\delta$ : 1.68 (s, acetyl CH<sub>3</sub>), 2.29 (s, *p*-OAC – CH<sub>3</sub>), 5.02 (d, J = 4.89 Hz, H-3), 5.84 (dd, J = 4.89, 2.69 Hz, H-2), 6.56 (br. s., amide NH), 7.08 – 7.31 (aromatic protons).  $^{13}$ C-NMR (126 MHz, CDCl<sub>3</sub>-*d*)  $\delta$ : 169.34, 169.17, 165.42, 150.81, 132.09, 128.65, 121.61, 78.28, 57.40, 21.09, 19.87.

**3-Acetoxy-4-(4-nitrophenyl)azetidin-2-one** (**D–51h**). *N*-(*p*-methoxyphenyl)-3-acetoxy-4-(4-nitrophenyl)azetidin-2-one (0.72 g, 2.01 mmol) in CH<sub>3</sub>CN (25 mL), and (NH<sub>4</sub>)<sub>2</sub>Ce(NO<sub>3</sub>)<sub>6</sub> (3.31 g, 6.04 mmol, 3 equiv) in water (28 mL) were treated according to Procedure 3 (Section 4.2.2.3) to afford the azetidinone (412 mg, 55% yield, at >98% purity by  $^{1}$ H-NMR analysis).  $^{1}$ H-NMR (500 MHz, CDCl<sub>3</sub>-*d*)  $\delta$ : 1.75 (s, acetyl CH<sub>3</sub>), 5.18 (d, J = 4.89 Hz, H-3), 5.97 (dd, J = 4.89, 2.93 Hz, H-2), 6.47 (br. s., amide NH), 7.51 – 8.28 (aromatic protons).  $^{13}$ C-NMR (126 MHz, CDCl<sub>3</sub>-*d*)  $\delta$ : 168.95, 164.71, 141.97, 135.56, 128.47, 123.56, 78.51, 57.38, 19.94.

**3-Acetoxy-4-(3-fluorophenyl)azetidin-2-one (D–51i).** *N*-(*p*-methoxyphenyl)-3-acetoxy-4-(3-fluorophenyl)azetidin-2-one (1.35 g, 4.1 mmol) in CH<sub>3</sub>CN (54 mL), and (NH<sub>4</sub>)<sub>2</sub>Ce(NO<sub>3</sub>)<sub>6</sub> (6.74 g, 12.3 mmol, 3 equiv) in water (56 mL) were treated according to Procedure 3 (Section 4.2.2.3) to afford the azetidinone (610 mg, 67% yield, at >99% purity by  $^{1}$ H-NMR analysis).  $^{1}$ H-NMR (500 MHz, CDCl<sub>3</sub>-*d*)  $\delta$ : 1.75 (s, acetyl CH<sub>3</sub>), 5.06 (d, J = 4.90 Hz, H-3), 5.91 (dd, J = 4.89,

2.93 Hz, H-2), 6.33 (br. s., amide NH), 7.03 – 7.40 (aromatic protons). <sup>13</sup>C-NMR (126 MHz, CDCl<sub>3</sub>-*d*) δ: 169.08, 165.23, 161.69, 137.21, 130.04, 123.25, 115.73, 114.55, 78.24, 57.47, 19.91.

**3-Acetoxy-4-(3-chlorophenyl)azetidin-2-one** (**D**–**51j**). *N*-(*p*-methoxyphenyl)-3-acetoxy-4-(3-chlorophenyl)azetidin-2-one (1.15 g, 3.34 mmol) in CH<sub>3</sub>CN (47 mL), and (NH<sub>4</sub>)<sub>2</sub>Ce(NO<sub>3</sub>)<sub>6</sub> (5.49 g, 10.02 mmol, 3 equiv) in water (44 mL) were treated according to Procedure 3 (Section 4.2.2.3) to afford the azetidinone (647 mg, 81% yield, at >98% purity by  $^{1}$ H-NMR analysis).  $^{1}$ H-NMR (500 MHz, CDCl<sub>3</sub>-*d*)  $\delta$ : 1.76 (s, acetyl CH<sub>3</sub>), 5.03 (d, J = 4.40 Hz, H-3), 5.91 (dd, J = 4.89, 2.93 Hz, H-2), 6.28 (br. s., amide NH), 7.19 – 7.36 (aromatic protons).  $^{13}$ C-NMR (126 MHz, CDCl<sub>3</sub>-*d*)  $\delta$ : 169.04, 165.04, 136.68, 134.47, 129.66, 128.86, 127.56, 125.82, 78.27, 57.41, 19.93.

**3-Acetoxy-4-(3-bromophenyl)azetidin-2-one** (**D–51k**). *N*-(*p*-methoxyphenyl)-3-acetoxy-4-(3-bromophenyl)azetidin-2-one (0.5 g, 1.29 mmol) in CH<sub>3</sub>CN (17 mL), and (NH<sub>4</sub>)<sub>2</sub>Ce(NO<sub>3</sub>)<sub>6</sub> (2.11 g, 3.86 mmol, 3 equiv) in water (20 mL) were treated according to Procedure 3 (Section 4.2.2.3) to afford the azetidinone (255 mg, 70% yield, at >90% purity by  $^{1}$ H-NMR analysis).  $^{1}$ H-NMR (500 MHz, CDCl<sub>3</sub>-*d*)  $\delta$ : 1.75 (s, acetyl CH<sub>3</sub>), 5.01 (d, J = 4.89 Hz, H-3), 5.90 (dd, J = 4.90, 2.90 Hz, H-2), 6.24 (br. s., amide NH), 7.22 – 7.51 (aromatic protons).  $^{13}$ C-NMR (126 MHz, CDCl<sub>3</sub>-*d*)  $\delta$ : 169.05, 165.17, 136.90, 131.78, 130.44, 129.91, 126.29, 122.49, 78.25, 57.34, 19.92.

**3-Acetoxy-4-(3-methylphenyl)azetidin-2-one** (**D**–**51l).** N-(p-methoxyphenyl)-3-acetoxy-4-(3-methylphenyl)azetidin-2-one (0.76 g, 2.34 mmol) in CH<sub>3</sub>CN (30 mL), and (NH<sub>4</sub>)<sub>2</sub>Ce(NO<sub>3</sub>)<sub>6</sub> (3.85 g, 7.02 mmol, 3 equiv) in water (33 mL) were treated according to Procedure 3 (Section 4.2.2.3) to afford the azetidinone (210 mg, 41% yield, at >99% purity by

<sup>1</sup>H-NMR analysis). <sup>1</sup>H-NMR (500 MHz, CDCl<sub>3</sub>-*d*) δ: 1.70 (s, acetyl CH<sub>3</sub>), 2.35 (s, *m*-CH<sub>3</sub>), 5.00 (d, J = 4.89 Hz, H-3), 5.88 (dd, J = 4.65, 2.69 Hz, H-2), 6.27 (br. s., amide NH), 7.07 – 7.25 (aromatic protons). <sup>13</sup>C-NMR (126 MHz, CDCl<sub>3</sub>-*d*) δ: 169.12, 165.48, 138.03, 134.34, 129.35, 128.22, 128.09, 124.66, 78.19, 57.89, 21.36, 19.93.

**3-Acetoxy-4-(3-methoxyphenyl)azetidin-2-one** (**D**–**51m**). *N*-(*p*-methoxyphenyl)-3-acetoxy-4-(3-methoxyphenyl)azetidin-2-one (1.05 g, 2.84 mmol) in CH<sub>3</sub>CN (35 mL), and (NH<sub>4</sub>)<sub>2</sub>Ce(NO<sub>3</sub>)<sub>6</sub> (4.67 g, 8.52 mmol, 3 equiv) in water (37 mL) were treated according to Procedure 3 (Section 4.2.2.3) to afford the azetidinone (900 mg, 81% yield, at >85% purity by  $^{1}$ H-NMR analysis).  $^{1}$ H-NMR (500 MHz, CDCl<sub>3</sub>-*d*)  $\delta$ : 1.72 (s, acetyl CH<sub>3</sub>), 3.80 (s, *m*-OCH<sub>3</sub>), 5.01 (d, *J* = 4.89 Hz, H-3), 5.89 (dd, *J* = 4.89, 2.93 Hz, H-2), 6.44 (br. s., amide NH), 6.82 – 7.29 (aromatic protons).

**3-Acetoxy-4-(3-acetoxyphenyl)azetidin-2-one** (**D**–**51n**). *N*-(*p*-methoxyphenyl)-3-acetoxy-4-(3-acetoxyphenyl)azetidin-2-one (1.6 g, 4.83 mmol) in CH<sub>3</sub>CN (60 mL), and (NH<sub>4</sub>)<sub>2</sub>Ce(NO<sub>3</sub>)<sub>6</sub> (7.95 g, 17.5 mmol, 3 equiv) in water (62 mL) were treated according to Procedure 3 (Section 4.2.2.3) to afford the azetidinone (570.7 mg, 50% yield, at >99% purity by  $^{1}$ H-NMR analysis).  $^{1}$ H-NMR (500 MHz, CDCl<sub>3</sub>-*d*)  $\delta$ : 1.74 (s, acetyl CH<sub>3</sub>), 2.30 (s, *m*-OAc CH<sub>3</sub>), 5.04 (d, J = 4.89 Hz, H-3), 5.88 (dd, J = 4.89, 2.93 Hz, H-2), 6.29 (br. s., amide NH), 7.03 – 7.40 (aromatic protons).  $^{13}$ C-NMR (126 MHz, CDCl<sub>3</sub>-*d*)  $\delta$ : 169.51, 169.28, 165.47, 150.64, 136.51, 129.40, 125.13, 121.92, 120.86, 78.19, 57.45, 21.08, 19.86.

**3-Acetoxy-4-(3-nitrophenyl)azetidin-2-one (D–51o).** *N*-(*p*-methoxyphenyl)-3-acetoxy-4-(3-nitrophenyl)azetidin-2-one (0.59 g, 1.65 mmol) in CH<sub>3</sub>CN (20 mL), and (NH<sub>4</sub>)<sub>2</sub>Ce(NO<sub>3</sub>)<sub>6</sub> (2.72 g, 4.96 mmol, 3 equiv) in water (20 mL) were treated according to Procedure 3 (Section 4.2.2.3) to afford the azetidinone (231 mg, 56% yield, at >95% purity by <sup>1</sup>H-NMR analysis). <sup>1</sup>H-

NMR (500 MHz, CDCl<sub>3</sub>-d)  $\delta$ : 1.73 (s, acetyl CH<sub>3</sub>), 5.18 (d, J = 4.89 Hz, H-3), 5.95 (dd, J = 4.40, 2.93 Hz, H-2), 6.63 (br. s., amide NH), 7.55 – 8.26 (aromatic protons). <sup>13</sup>C-NMR (126 MHz, CDCl<sub>3</sub>-d)  $\delta$ : 168.93, 164.82, 148.28, 137.09, 133.65, 129.46, 123.71, 122.44, 78.42, 57.25, 19.91.

**3-Acetoxy-4-(2-fluorophenyl)azetidin-2-one** (**D**–**51p**). *N*-(*p*-methoxyphenyl)-3-acetoxy-4-(2-fluorophenyl)azetidin-2-one (1.08 g, 3.28 mmol) in CH<sub>3</sub>CN (43 mL), and (NH<sub>4</sub>)<sub>2</sub>Ce(NO<sub>3</sub>)<sub>6</sub> (5.4 g, 9.85 mmol, 3 equiv) in water (48 mL) were treated according to Procedure 3 (Section 4.2.2.3) to afford the azetidinone (592 mg, 81% yield, at >95% purity by  $^{1}$ H-NMR analysis).  $^{1}$ H-NMR (500 MHz, CDCl<sub>3</sub>-*d*)  $\delta$ : 1.75 (s, acetyl CH<sub>3</sub>), 5.34 (d, J = 4.90 Hz, H-3), 5.99 (dd, J = 4.90, 2.69 Hz, H-2), 6.53 (br. s., amide NH), 7.02 – 7.45 (aromatic protons).  $^{13}$ C-NMR (126 MHz, CDCl<sub>3</sub>-*d*)  $\delta$ : 168.84, 165.68, 161.68, 130.31, 128.52, 123.97, 121.98, 115.35, 77.81, 51.99, 19.89.

**3-Acetoxy-4-(2-chlorophenyl)azetidin-2-one** (**D–51q**). *N*-(*p*-methoxyphenyl)-3-acetoxy-4-(2-chlorophenyl)azetidin-2-one (1.97 g, 5.71 mmol) in CH<sub>3</sub>CN (75 mL), and (NH<sub>4</sub>)<sub>2</sub>Ce(NO<sub>3</sub>)<sub>6</sub> (9.39 g, 17.13 mmol, 3 equiv) in water (80 mL) were treated according to Procedure 3 (Section 4.2.2.3) to afford the azetidinone (853 mg, 63% yield, at >95% purity by  $^{1}$ H-NMR analysis).  $^{1}$ H-NMR (500 MHz, CDCl<sub>3</sub>-*d*)  $\delta$ : 1.76 (s, acetyl CH<sub>3</sub>), 5.41 (d, J = 4.89 Hz, H-3), 6.16 (dd, J = 4.89, 2.93 Hz, H-2), 6.76 (br. s., amide NH), 7.27 – 7.48 (aromatic protons).  $^{13}$ C-NMR (126 MHz, CDCl<sub>3</sub>-*d*)  $\delta$ : 168.76, 166.11, 133.35, 132.59, 129.59, 128.07, 126.79, 116.13, 76.80, 55.29, 20.02.

**3-Acetoxy-4-(2-bromophenyl)azetidin-2-one** (**D–51r**). N-(p-methoxyphenyl)-3-acetoxy-4-(2-bromophenyl)azetidin-2-one (1.24 g, 3.17 mmol) in CH<sub>3</sub>CN (42 mL), and (NH<sub>4</sub>)<sub>2</sub>Ce(NO<sub>3</sub>)<sub>6</sub> (5.22 g, 9.52 mmol, 3 equiv) in water (44 mL) were treated according to

Procedure 3 (Section 4.2.2.3) to afford the azetidinone (381 mg, 42% yield, at >99% purity by  $^{1}$ H-NMR analysis).  $^{1}$ H-NMR (500 MHz, CDCl<sub>3</sub>-d)  $\delta$ : 1.77 (s, acetyl CH<sub>3</sub>), 5.37 (d, J = 4.89 Hz, H-3), 6.19 (dd, J = 4.89, 2.93 Hz, H-2), 6.58 (br. s., amide NH), 7.20 – 7.58 (aromatic protons).  $^{13}$ C-NMR (126 MHz, CDCl<sub>3</sub>-d)  $\delta$ : 168.67, 165.77, 134.17, 132.81, 129.87, 128.27, 127.36, 123.20, 77.19 57.50 20.06.

**3-Acetoxy-4-(2-methylphenyl)azetidin-2-one** (**D–51s**). *N*-(*p*-methoxyphenyl)-3-acetoxy-4-(2-methylphenyl)azetidin-2-one (1.39 g, 4.29 mmol) in CH<sub>3</sub>CN (50 mL), and (NH<sub>4</sub>)<sub>2</sub>Ce(NO<sub>3</sub>)<sub>6</sub> (7.05 g, 12.86 mmol, 3 equiv) in water (55 mL) were treated according to Procedure 3 (Section 4.2.2.3) to afford the azetidinone (487 mg, 52% yield, at >95% purity by  $^{1}$ H-NMR analysis).  $^{1}$ H-NMR (500 MHz, CDCl<sub>3</sub>-*d*)  $\delta$ : 1.67 (s, acetyl CH<sub>3</sub>), 2.29 (s, *o*-CH<sub>3</sub>), 5.24 (d, J = 4.60 Hz, H-3), 5.96 (dd, J = 4.60, 3.18 Hz, H-2), 6.19 (br. s, amide NH), 7.13 – 7.43 (aromatic protons).  $^{13}$ C-NMR (126 MHz, CDCl<sub>3</sub>-*d*)  $\delta$ : 169.11, 165.45, 136.47, 132.30, 130.30, 128.36, 126.44, 125.80, 77.95, 54.92, 19.84, 18.88.

**3-Acetoxy-4-(2-methoxyphenyl)azetidin-2-one** (**D–51t**). *N*-(*p*-methoxyphenyl)-3-acetoxy-4-(2-methoxyphenyl)azetidin-2-one (1.35 g, 3.96 mmol) in CH<sub>3</sub>CN (47 mL), and (NH<sub>4</sub>)<sub>2</sub>Ce(NO<sub>3</sub>)<sub>6</sub> (6.51 g, 11.88 mmol, 3 equiv) in water (52 mL) were treated according to Procedure 3 (Section 4.2.2.3) to afford the azetidinone (815 mg, 88% yield, at >94% purity by  $^{1}$ H-NMR analysis).  $^{1}$ H-NMR (500 MHz, CDCl<sub>3</sub>-*d*)  $\delta$ : 1.73 (s, acetyl CH<sub>3</sub>), 3.78 (s, *o*-OCH<sub>3</sub>), 5.37 (d, J = 4.89 Hz, H-3), 6.06 (dd, J = 4.89, 2.93 Hz, H-2), 6.26 (br. s., amide NH), 6.84 – 7.37 (aromatic protons).  $^{13}$ C-NMR (126 MHz, CDCl<sub>3</sub>-*d*)  $\delta$ : 168.78, 166.20, 157.15, 129.53, 127.39, 123.03, 120.29, 110.08, 77.38, 55.35, 53.07, 20.06.

**3-Acetoxy-4-(2-nitrophenyl)azetidin-2-one (D–51u).** *N*-(*p*-methoxyphenyl)-3-acetoxy-4-(2-nitrophenyl)azetidin-2-one (0.21 g, 0.59 mmol) in CH<sub>3</sub>CN (7 mL), and (NH<sub>4</sub>)<sub>2</sub>Ce(NO<sub>3</sub>)<sub>6</sub>

(0.97 g, 1.77 mmol, 3 equiv) in water (8 mL) were treated according to Procedure 3 (Section 4.2.2.3) to afford the azetidinone (90 mg, 61% yield, at >99% purity by  $^{1}$ H-NMR analysis).  $^{1}$ H-NMR (500 MHz, CDCl<sub>3</sub>-d)  $\delta$ : 1.79 (s, acetyl CH<sub>3</sub>), 5.71 (d, J = 5.38 Hz, H-3), 6.33 (dd, J = 5.38, 3.42 Hz, H-2), 6.54 (br. s., amide NH), 7.55 – 8.20 (aromatic protons).

**3-Acetoxy-4-trimethylazetidin-2-one** (**D**–**51v**). *N*-(*p*-methoxyphenyl)-3-acetoxy-4-trimethylazetidin-2-one (0.36 g, 1.25 mmol) in CH<sub>3</sub>CN (17 mL), and (NH<sub>4</sub>)<sub>2</sub>Ce(NO<sub>3</sub>)<sub>6</sub> (2.05 g, 3.75 mmol, 3 equiv) in water (17 mL) were treated according to Procedure 3 (Section 4.2.2.3) to afford the azetidinone (167 mg, 72% yield, at >95% purity by  $^{1}$ H-NMR analysis).  $^{1}$ H-NMR (500 MHz, CDCl<sub>3</sub>-*d*)  $\delta$ : 0.96 – 1.00 (m, *t*-butyl CH<sub>3</sub>), 2.16 (s, acetyl CH<sub>3</sub>), 3.62 (d, *J* = 4.89 Hz, H-3), 6.00 (d, *J* = 4.89 Hz, H-2), 6.30 (br. s, amide NH).  $^{13}$ C-NMR (126 MHz, CDCl<sub>3</sub>-*d*)  $\delta$ : 169.33, 166.85, 74.76, 63.17, 32.82, 26.00, 20.82.

**3-Acetoxy-4-cyclohexylazetidin-2-one** (**D–51w**). *N*-(*p*-methoxyphenyl)-3-acetoxy-4-cyclohexylazetidin-2-one (0.22 g, 0.7 mmol) in CH<sub>3</sub>CN (10 mL), and (NH<sub>4</sub>)<sub>2</sub>Ce(NO<sub>3</sub>)<sub>6</sub> (1.16 g, 2.11 mmol, 3 equiv) in water (11 mL) were treated according to Procedure 3 (Section 4.2.2.3) to afford the azetidinone (127 mg, 85% yield, at >95% purity by  $^{1}$ H-NMR analysis).  $^{1}$ H-NMR (500 MHz, CDCl<sub>3</sub>-*d*)  $\delta$ : 0.84 – 1.81 (cyclohexyl protons), 2.15 (s, acetyl CH<sub>3</sub>), 3.52 (dd, J = 9.29, 4.89 Hz, H-3), 5.95 (dd, J = 4.89, 2.45 Hz, H-2), 6.24 (br. s., amide NH).

3-Acetoxy-4-thiophenylazetidin-2-one (D–51x). N-(p-methoxyphenyl)-3-acetoxy-4-thiopheneazetidin-2-one (0.22 g, 0.7 mmol) in CH<sub>3</sub>CN (10 mL), and (NH<sub>4</sub>)<sub>2</sub>Ce(NO<sub>3</sub>)<sub>6</sub> (1.15 g, 2.09 mmol, 3 equiv) in water (12 mL) were treated according to Procedure 3 (Section 4.2.2.3) to afford the azetidinone (210 mg, 98% yield, at >98% purity by  $^{1}$ H-NMR analysis).  $^{1}$ H-NMR (500 MHz, CDCl<sub>3</sub>-d)  $\delta$ : 1.81 (s, acetyl CH<sub>3</sub>), 5.25 (d, J = 4.89 Hz, H-3), 5.83 (dd, J = 4.89, 2.69 Hz,

H-2), 6.30 (br. s., amide NH), 6.95 – 7.35 (aromatic protons).  $^{13}$ C-NMR (126 MHz, CDCl<sub>3</sub>-d) δ: 169.30, 165.48, 138.30, 127.16, 127.08, 126.28, 78.27, 54.07, 20.03.

**3-Acetoxy-4-dimethylazetidin-2-one (D–51y).** *N*-(*p*-methoxyphenyl)-3-acetoxy-4-dimethylazetidin-2-one (0.33 g, 1.18 mmol) in CH<sub>3</sub>CN (17 mL), and (NH<sub>4</sub>)<sub>2</sub>Ce(NO<sub>3</sub>)<sub>6</sub> (1.94 g, 3.54 mmol, 3 equiv) in water (18 mL) were treated according to Procedure 3 (Section 4.2.2.3) to afford the azetidinone (133 mg, 66% yield, at >99% purity by  $^{1}$ H-NMR analysis).  $^{1}$ H-NMR (500 MHz, CDCl<sub>3</sub>-*d*)  $\delta$ : 0.84 (d, J = 6.85 Hz, CH<sub>3</sub>), 0.97 (d, J = 6.85 Hz, CH<sub>3</sub>), 1.83 – 1.93 (m, H-1), 2.15 (s, acetyl CH<sub>3</sub>), 3.50 (dd, J = 9.29, 4.89 Hz, H-3), 5.94 (dd, J = 4.89, 2.45 Hz, H-2), 6.28 (br. s., amide NH).  $^{13}$ C-NMR (126 MHz, CDCl<sub>3</sub>-*d*)  $\delta$ : 169.51, 166.16, 75.23, 60.67, 28.42, 20.61, 18.96, 18.74.

#### 4.2.2.4. General Procedure 4: Hydroxyl Deprotection of the 2-Azetidinones

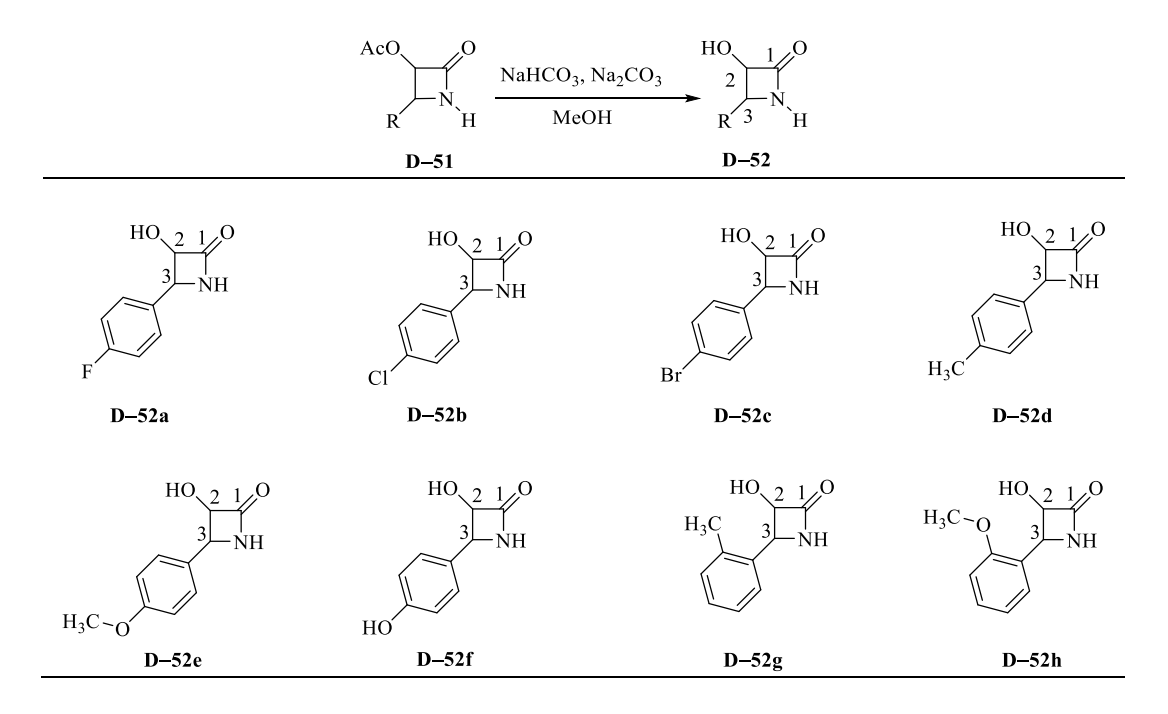


Figure 4.11. Scheme showing the general method for hydroxyl deprotection.

To a solution of 2-azetidinone (1 equiv) in MeOH, saturated NaHCO<sub>3</sub>, and Na<sub>2</sub>CO<sub>3</sub> (0.1 equiv) were added at room temperature. After the disappearance of the starting material, the reaction mixture was filtered and the filtrate was concentrated under vacuum. The residue was purified by column chromatography (EtOAc:hexane 2:1, v/v) to yield the desired 2-azetidinones.

3-Hydroxy-4-(4-fluorophenyl)azetidin-2-one (D–52a). 3-Acetoxy-4-(4-fluorophenyl)azetidin-2-one (108 mg, 0.48 mmol, 1 equiv) in MeOH (0.7 mL), saturated NaHCO<sub>3</sub> (1 mL) and Na<sub>2</sub>CO<sub>3</sub> (5 mg, 0.048 mmol, 0.1 equiv) were treated according to Procedure 4 (Section 4.2.2.4) to afford the deprotected 2-azetidinone (55.2 mg, 98% yield, at >99% purity by  $^{1}$ H-NMR analysis).  $^{1}$ H-NMR (500 MHz, DMSO- $d_6$ )  $\delta$ : 4.70 (d, J = 4.89 Hz, H-3), 4.92 (ddd, J = 7.34, 4.89, 2.45 Hz, H-2), 5.83 (d, J = 7.34 Hz, OH), 7.13 – 7.30 (aromatic protons), 8.46 (br. s., amide NH) (see **Figure III–10** for a sample spectrum).  $^{13}$ C-NMR (126 MHz, DMSO- $d_6$ )  $\delta$ : 170.44, 162.94, 134.56, 129.88, 115.17, 78.93, 57.22.

3-Hydroxy-4-(4-chlorophenyl)azetidin-2-one (D–52b). 3-Acetoxy-4-(4-chlorophenyl)azetidin-2-one (130 mg, 0.54 mmol, 1 equiv) in MeOH (0.8 mL), saturated NaHCO<sub>3</sub> (1.2 mL) and Na<sub>2</sub>CO<sub>3</sub> (5.7 mg, 0.05 mmol, 0.1 equiv) were treated according to Procedure 4 (Section 4.2.2.4) to afford the deprotected 2-azetidinone (100 mg, 93% yield, at >99% purity by  $^{1}$ H-NMR analysis).  $^{1}$ H-NMR (500 MHz, DMSO- $d_6$ )  $\delta$ : 4.71 (d, J = 4.90 Hz, H-3), 4.92 – 4.95 (m, H-2), 5.87 (br. s, OH), 7.23 – 7.43 (aromatic protons), 8.48 (br. s, amide NH).

3-Hydroxy-4-(4-bromophenyl)azetidin-2-one (D–52c). 3-Acetoxy-4-(4-bromophenyl)azetidin-2-one (440 mg, 1.6 mmol, 1 equiv) in MeOH (2.4 mL), saturated NaHCO<sub>3</sub> (3.45 mL) and Na<sub>2</sub>CO<sub>3</sub> (16.3 mg, 0.16 mmol, 0.1 equiv) were treated according to Procedure 4 (Section 4.2.2.4) to afford the deprotected 2-azetidinone (210 mg, 56% yield, at >99% purity by  $^{1}$ H-NMR analysis).  $^{1}$ H-NMR (500 MHz, DMSO- $d_{6}$ )  $\delta$ : 4.70 (d, J = 4.89 Hz, H-3), 4.94 (ddd, J =

6.85, 4.89, 2.45 Hz, H-2), 5.89 (d, J = 6.85 Hz, OH), 7.17 – 7.56 (aromatic protons), 8.51 (s, amide NH). <sup>13</sup>C-NMR (126 MHz, DMSO- $d_6$ )  $\delta$ : 170.38, 138.00, 131.20, 130.16, 120.75, 79.04, 57.35.

**3-Hydroxy-4-(4-methylphenyl)azetidin-2-one** (**D**–**52d**). 3-Acetoxy-4-(4-methylphenyl)azetidin-2-one (146 mg, 0.7 mmol) in MeOH (1 mL), saturated NaHCO<sub>3</sub> (1.2 mL) and Na<sub>2</sub>CO<sub>3</sub> (7 mg, 0.07 mmol) were treated according to Procedure 4 (Section 4.2.2.4) to afford the deprotected 2-azetidinone (64.8 mg, 55% yield, at >95% purity by  $^{1}$ H-NMR analysis).  $^{1}$ H-NMR (500 MHz, DMSO- $d_6$ )  $\delta$ : 2.29 (s, p-CH<sub>3</sub>), 4.65 (d, J = 4.89 Hz, H-3), 4.90 (ddd, J = 6.85, 4.89, 2.20 Hz, H-2), 5.75 (d, J = 6.85 Hz, OH), 7.09 – 7.17 (aromatic protons), 8.40 (br. s., amide NH).  $^{13}$ C-NMR (126 MHz, DMSO- $d_6$ )  $\delta$ : 170.55, 136.67, 135.38, 128.86, 127.94, 78.97, 57.76, 21.71.

**3-Hydroxy-4-(4-methoxyphenyl)azetidin-2-one** (**D**–**52e**). 3-Acetoxy-4-(4-methoxyphenyl)azetidin-2-one (120 mg, 0.51 mmol, 1 equiv) in MeOH (0.74 mL), saturated NaHCO<sub>3</sub> (1.1 mL) and Na<sub>2</sub>CO<sub>3</sub> (5.36 mg, 0.05 mmol, 0.1 equiv) were treated according to Procedure 4 (Section 4.2.2.4) to afford the deprotected 2-azetidinone (77.4 mg, 79% yield, at >99% purity by  $^{1}$ H-NMR analysis).  $^{1}$ H-NMR (500 MHz, DMSO- $d_{6}$ )  $\delta$ : 3.74 (s, p-OCH<sub>3</sub>), 4.63 (d, J = 4.89 Hz, H-3), 4.85 – 4.91 (m, H-2), 5.74 (d, J = 6.85 Hz, OH), 6.88 – 7.19 (aromatic protons), 8.38 (s, amide NH).  $^{13}$ C-NMR (126 MHz, DMSO- $d_{6}$ )  $\delta$ : 170.58, 159.06, 130.25, 129.20, 113.78, 78.88, 57.47 55.52.

**3-Hydroxy-4-(4-hydroxyphenyl)azetidin-2-one** (**D–52f**). 3-Acetoxy-4-(4-acetoxyphenyl)azetidin-2-one (262 mg, 1.0 mmol, 1 equiv) in MeOH (3.2 mL), saturated NaHCO<sub>3</sub> (4.7 mL) and Na<sub>2</sub>CO<sub>3</sub> (10.45 mg, 0.1 mmol, 0.1 equiv) were treated according to Procedure 4 (Section 4.2.2.4) to afford the deprotected 2-azetidinone (112 mg, 63% yield, at >99% purity by

<sup>1</sup>H-NMR analysis). <sup>1</sup>H-NMR (500 MHz, DMSO- $d_6$ ) δ: 4.56 (d, J = 4.89 Hz, H-3), 4.84 (ddd, J = 7.30, 4.89, 2.45 Hz, H-2), 5.71 (d, J = 7.30 Hz, OH), 6.70 – 7.03 (aromatic protons), 8.33 (br. s, amide NH), 9.29 (s, p-OH). <sup>13</sup>C-NMR (126 MHz, DMSO- $d_6$ ) δ: 170.61, 157.11, 129.22, 128.37, 115.10, 78.77, 57.59.

3-Hydroxy-4-(2-methylphenyl)azetidin-2-one (D–52g). 3-Acetoxy-4-(2-methylphenyl)azetidin-2-one (487 mg, 2.2 mmol, 1 equiv) in MeOH (3.0 mL), saturated NaHCO<sub>3</sub> (4.0 mL) and Na<sub>2</sub>CO<sub>3</sub> (23.35 mg, 0.22 mmol, 0.1 equiv) were treated according to Procedure 4 (Section 4.2.2.4) to afford the deprotected 2-azetidinone (60 mg, 15% yield, at >99% purity by  $^{1}$ H-NMR analysis).  $^{1}$ H-NMR (500 MHz, DMSO- $d_{6}$ )  $\delta$ : 2.19 (s, o-CH<sub>3</sub>), 4.82 (d, J = 5.00 Hz, H-3), 5.00 (ddd, J = 7.73, 5.00, 2.45 Hz, H-2), 5.78 (d, J = 7.30 Hz, OH), 7.10 – 7.22 (aromatic protons), 8.47 (br. s., amide NH).  $^{13}$ C-NMR (126 MHz, DMSO- $d_{6}$ )  $\delta$ : 170.20, 136.68, 136.16, 129.94, 127.12, 126.35, 125.84, 78.81, 56.47, 19.16.

3-Hydroxy-4-(2-methoxyphenyl)azetidin-2-one (D–52h). 3-Acetoxy-4-(2-methoxyphenyl)azetidin-2-one (815 mg, 3.46 mmol, 1 equiv) in MeOH (5.0 mL), saturated NaHCO<sub>3</sub> (7.4 mL) and Na<sub>2</sub>CO<sub>3</sub> (36.4 mg, 0.35 mmol, 0.1 equiv) were treated according to Procedure 4 (Section 4.2.2.4) to afford the deprotected 2-azetidinone (214 mg, 32% yield, at >96% purity by  $^{1}$ H-NMR analysis).  $^{1}$ H-NMR (500 MHz, DMSO- $d_{6}$ )  $\delta$ : 3.74 (s, o-CH<sub>3</sub>), 4.88 (d, J = 4.90 Hz, 1H), 4.89 – 4.93 (m, 1H), 5.68 (d, J = 7.34 Hz, OH), 6.91 – 7.26 (aromatic protons), 8.33 (br. s., amide NH).

# 4.2.2.5. General Procedure 5: Hydrolysis of Azetidinone Ring

Figure 4.12. Scheme showing the general method for the lactam ring hydrolysis.

### Figure 4.12. (cont'd)

#### Method A:

Hydrolysis of azetidinone ring to unveil the isoserine was carried out by addition of 7 N HCl. The reaction mixture was stirred at reflux conditions (85 °C) for 24 h. The reaction was lyophilized yielding the hydrochloride salt of the isoserine products as racemic mixtures.

#### Method B:

The hydroxyl group deprotection and lactam ring hydrolysis were done in one pot reaction. Briefly, 7 N HCl was added to the 3-acetoxy-azetidinones and the reaction was stirred at reflux conditions for 24 h. The reaction mixture was lyophilized to dryness to afford the isoserine products as racemic mixtures. (Refer to the Appendix for the <sup>1</sup>H-NMR spectrum assignment and numbering for the isoserine analogs).

**Phenylisoserine** (**D**–**53a**). 7 N HCl (1 mL) and 3-hydroxy-4–phenylazetidin-2-one (29 mg) were treated according to Procedure 5, Method A (Section 4.2.2.5) to afford the desired isoserine (30 mg, 78% yield, at >99% purity by  $^{1}$ H-NMR analysis).  $^{1}$ H-NMR (500 MHz, D<sub>2</sub>O) δ: 4.36 (d, J = 6.40 Hz, 1H), 4.55 (d, J = 6.40 Hz, 1H), 7.35 – 7.42 (aromatic protons).  $^{13}$ C-NMR (126 MHz, D<sub>2</sub>O) δ: 176.30, 133.44, 129.27, 128.98, 127.17, 73.35, 57.42. HRMS (ESI-TOF) m/z 182.0855 [M + H] $^{+}$ ; calculated for C<sub>9</sub>H<sub>12</sub>NO<sub>3</sub>: 182.0817.

**4-Fluorophenylisoserine** (**D–53b**). 7 N HCl (1 mL) and 3-hydroxy-4-(4-fluoro)phenylazetidin-2-one (13.3 mg, 0.07 mmol) were treated according to Procedure 5,

Method A (Section 4.2.2.5) to afford the desired isoserine (12.2 mg, 81% yield, at >99% purity by  $^{1}$ H-NMR analysis).  $^{1}$ H-NMR (500 MHz, D<sub>2</sub>O)  $\delta$ : 4.51 (d, J = 6.36 Hz, 1H), 4.61 (d, J = 6.36 Hz, 1H), 7.16 – 7.43 (aromatic protons).  $^{13}$ C-NMR (126 MHz, D<sub>2</sub>O)  $\delta$ : 173.84, 163.96, 129.50, 128.71, 116.08, 71.70, 56.21. HRMS (ESI-TOF) m/z HRMS (ESI-TOF) m/z 200.0760 [M + H] $^{+}$ ; calculated for C<sub>9</sub>H<sub>11</sub>NO<sub>3</sub>F: 200.0723.

**4-Chlorophenylisoserine** (**D**–**53c**). 7 N HCl (2.0 mL) and 3-hydroxy-4-(4-chloro)phenylazetidin-2-one (40 mg, 0.20 mmol) were treated according to Procedure 5, Method A (Section 4.2.2.5) to afford the desired isoserine (42.6 mg, 84% yield, at >99% purity by  $^{1}$ H-NMR analysis).  $^{1}$ H-NMR (500 MHz, D<sub>2</sub>O)  $\delta$ : 4.53 (d, J = 6.40 Hz, 1H), 4.65 (d, J = 6.40 Hz, 1H), 7.44 – 7.51 (aromatic protons).  $^{13}$ C-NMR (126 MHz, D<sub>2</sub>O)  $\delta$ : 174.02, 133.99, 131.53, 129.13, 128.87, 71.77, 56.29. HRMS (ESI-TOF) m/z 216.0464 [M + H] $^{+}$ ; calculated for C<sub>9</sub>H<sub>11</sub>NO<sub>3</sub>Cl: 216.0427.

**4-Bromophenylisoserine** (**D**–**53d**). 7 N HCl (12 mL) and 3-hydroxy-4-(4-bromo)phenylazetidin-2-one (186 mg, 0.77 mmol) were treated according to Procedure 5, Method A (Section 4.2.2.5) to afford the desired isoserine (220 mg, 100% yield, at >99% purity by  $^{1}$ H-NMR analysis).  $^{1}$ H-NMR (500 MHz, D<sub>2</sub>O) δ: 4.58 (d, J = 6.40 Hz, 1H), 4.66 (d, J = 6.40 Hz, 1H), 7.38 – 7.65 (aromatic protons).  $^{13}$ C-NMR (126 MHz, D<sub>2</sub>O) δ: 173.43, 132.14, 131.86, 129.10, 123.26, 71.70, 56.21. HRMS (ESI-TOF) m/z 259.9960 [M + H]<sup>+</sup>; calculated for  $C_{9}$ H<sub>12</sub>NO<sub>3</sub>Br: 259.9922.

**4-Methylphenylisoserine** (**D**–**53e**). 7 N HCl (2 mL) and 3-hydroxy-4-(4-methyl)phenylazetidin-2-one (20 mg, 0.1 mmol) were treated according to Procedure 5, Method A (Section 4.2.2.5) to afford the desired isoserine (25.9 mg, 95% yield, at >98% purity by  $^{1}$ H-NMR analysis).  $^{1}$ H-NMR (500 MHz, D<sub>2</sub>O)  $\delta$ : 2.35 (s, *p*-CH<sub>3</sub>), 4.49 (d, J = 6.40 Hz, 1H), 4.57 (d,

J = 6.40 Hz, 1H), 7.29 – 7.37 (benzylic protons). <sup>13</sup>C-NMR (126 MHz, D<sub>2</sub>O)  $\delta$ : 173.87, 140.24, 129.74, 129.62, 127.34, 71.87, 56.76, 20.19. HRMS (ESI-TOF) m/z 196.1008 [M + H]<sup>+</sup>; calculated for C<sub>10</sub>H<sub>14</sub>NO<sub>3</sub>: 196.0974.

**4-Methoxyphenylisoserine** (**D**–**53f**). 7 N HCl (2 mL) and 3-hydroxy-4-(4-methoxyl)phenylazetidin-2-one (25 mg, 0.13 mmol) were treated according to Procedure 5, Method A (Section 4.2.2.5) to afford the desired isoserine (27 mg, 99% yield, at >98% purity by  $^{1}$ H-NMR analysis).  $^{1}$ H-NMR (500 MHz, D<sub>2</sub>O)  $\delta$ : 3.84 (s, p-OCH<sub>3</sub>), 4.57 – 4.62 (m, 2H), 7.06 – 7.42 (aromatic protons).  $^{13}$ C-NMR (126 MHz, D<sub>2</sub>O)  $\delta$ : 174.05, 159.65, 129.06, 128.89, 114.48, 71.91, 56.46, 55.24. HRMS (ESI-TOF) m/z 212.0956 [M + H]<sup>+</sup>; calculated for C<sub>10</sub>H<sub>14</sub>NO<sub>4</sub>: 212.0923.

**4-Hydroxyphenylisoserine** (**D**–**53g**). 7 N HCl (7 mL) and 3-hydroxy-4-(4-hydroxy)phenylazetidin-2-one (110 mg, 0.62 mmol) were treated according to Procedure 5, Method A (Section 4.2.2.5) to afford the desired isoserine (119 mg, 98% yield, at >99% purity by  $^{1}$ H-NMR analysis).  $^{1}$ H-NMR (500 MHz, D<sub>2</sub>O) δ: 4.42 (d, J = 6.40 Hz, 1H), 4.47 (d, J = 6.40 Hz, 1H), 6.88 – 7.27 (aromatic protons).  $^{13}$ C-NMR (126 MHz, D<sub>2</sub>O) δ: 173.95, 156.54, 129.10, 124.37, 115.84, 71.86, 56.50. HRMS (ESI-TOF) m/z 198.0798 [M + H]<sup>+</sup>; calculated for C<sub>9</sub>H<sub>12</sub>NO<sub>4</sub>: 198.0766.

**4-Nitrophenylisoserine** (**D**–**53h**). 7 N HCl (3 mL) and 3-acetoxy-4-(4-nitro)-phenylazetidin-2-one (20 mg, 0.08 mmol) were treated according to Procedure 5, Method B (Section 4.2.2.5) to afford the desired isoserine (20 mg, 95% yield, at >99% purity by  $^{1}$ H-NMR analysis).  $^{1}$ H-NMR (500 MHz, D<sub>2</sub>O)  $\delta$ : 4.49 (d, J = 5.40 Hz, 1H), 4.78 (d, J = 5.40 Hz, 1H), 7.64 – 8.27 (aromatic protons).  $^{13}$ C-NMR (126 MHz, D<sub>2</sub>O)  $\delta$ : 173.95, 148.14, 140.29, 128.62, 124.19, 71.54, 56.20. HRMS (ESI-TOF) m/z 227.0711 [M + H] $^{+}$ ; calculated for C<sub>9</sub>H<sub>11</sub>N<sub>2</sub>O<sub>5</sub>: 227.0668.

**3-Fluorophenylisoserine** (**D–53i**). 7 N HCl (20 mL) and 3-acetoxy-4-(3-fluoro)-phenylazetidin-2-one (600 mg, 2.69 mmol) were treated according to Procedure 5, Method B (Section 4.2.2.5) to afford the desired isoserine (507 mg, 98% yield, at >98% purity by  $^{1}$ H-NMR analysis).  $^{1}$ H-NMR (500 MHz, D<sub>2</sub>O)  $\delta$ : 4.52 (d, J = 5.87 Hz, 1H), 4.63 (d, J = 5.87 Hz, 1H), 7.12 -7.50 (aromatic protons).  $^{13}$ C-NMR (126 MHz, D<sub>2</sub>O)  $\delta$ : 173.78, 163.43, 135.15, 131.07, 123.15, 116.55, 114.41, 71.59, 56.28. HRMS (ESI-TOF) m/z 200.0765 [M + H]<sup>+</sup>; calculated for  $C_{9}$ H<sub>11</sub>NO<sub>3</sub>F: 200.0723.

**3-Chlorophenylisoserine** (**D–53j**). 7 N HCl (20 mL) and 3-acetoxy-4-(3-chloro)-phenylazetidin-2-one (645 mg, 2.7 mmol) were treated according to Procedure 5, Method B (Section 4.2.2.5) to afford the desired isoserine (643 mg, 95% yield, at >98% purity by  $^{1}$ H-NMR analysis).  $^{1}$ H-NMR (500 MHz, D<sub>2</sub>O)  $\delta$ : 4.53 (d, J = 6.40 Hz, 1H), 4.62 (d, J = 6.40 Hz, 1H), 7.30 – 7.46 (aromatic protons).  $^{13}$ C-NMR (126 MHz, D<sub>2</sub>O)  $\delta$ : 173.32, 134.69, 134.25, 130.65, 129.70, 127.40, 125.66, 71.29, 56.15. HRMS (ESI-TOF) m/z 216.0467 [M + H]<sup>+</sup>; calculated for C<sub>9</sub>H<sub>11</sub>NO<sub>3</sub>Cl: 216.0427.

**3-Bromophenylisoserine** (**D**–**53k**). 7 N HCl (5 mL) and 3-hydroxy-4-(3-bromo)-phenylazetidin-2-one (112 mg, 0.47 mmol) were treated according to Procedure 5, Method A (Section 4.2.2.5) to afford the desired isoserine (134 mg, 98% yield, at >99% purity by  $^{1}$ H-NMR analysis).  $^{1}$ H-NMR (500 MHz, D<sub>2</sub>O)  $\delta$ : 4.50 (d, J = 5.87 Hz, 1H), 4.60 (d, J = 5.87 Hz, 1H), 7.31 – 7.60 (aromatic protons).  $^{13}$ C-NMR (126 MHz, D<sub>2</sub>O)  $\delta$ : 173.32, 134.97, 132.67, 130.86, 130.33, 126.10, 122.32, 71.30, 56.09. HRMS (ESI-TOF) m/z 259.9964 [M + H]<sup>+</sup>; calculated for  $C_{9}$ H<sub>11</sub>NO<sub>3</sub>Br: 259.9922.

**3-Methylphenylisoserine** (**D**–**53l**). 7 N HCl (15 mL) and 3-acetoxy-4-(3-methyl)-phenylazetidin-2-one (405 mg, 1.8 mmol) were treated according to Procedure 5, Method A

(Section 4.2.2.5) to afford the desired isoserine (406 mg, 95% yield, at >99% purity by  $^{1}$ H-NMR analysis).  $^{1}$ H-NMR (500 MHz, D<sub>2</sub>O)  $\delta$ : 2.29 (s, m-CH<sub>3</sub>), 4.49 (d, J = 6.80 Hz, 1H), 4.53 (d, J = 6.80 Hz, 1H), 7.16 – 7.31 (aromatic protons).  $^{13}$ C-NMR (126 MHz, D<sub>2</sub>O)  $\delta$ : 173.94, 139.42, 132.67, 130.21, 129.03, 127.81, 124.12, 71.90, 56.87, 20.29. HRMS (ESI-TOF) m/z 196.1010 [M + H] $^{+}$ ; calculated for C<sub>10</sub>H<sub>14</sub>NO<sub>3</sub>: 196.0974.

**3-Methoxyphenylisoserine (D–53m).** 7 N HCl (25 mL) and 3-acetoxy-4-(3-methoxy)-phenylazetidin-2-one (774 mg, 3.3 mmol) were treated according to Procedure 5, Method B (Section 4.2.2.5) to afford the desired isoserine (798 mg, 98% yield, at >96% purity by  $^{1}$ H-NMR analysis).  $^{1}$ H-NMR (500 MHz, D<sub>2</sub>O)  $\delta$ : 3.78 (s, m-OCH<sub>3</sub>), 4.50 (d, J = 6.40 Hz, 1H), 4.56 (d, J = 6.40 Hz, 1H), 6.96 – 7.40 (aromatic protons).  $^{13}$ C-NMR (126 MHz, D<sub>2</sub>O)  $\delta$ : 173.56, 159.16, 134.26, 130.50, 119.81, 115.16, 112.99, 71.62, 56.69, 55.30. HRMS (ESI-TOF) m/z 212.0959 [M + H] $^{+}$ ; calculated for C<sub>10</sub>H<sub>14</sub>NO<sub>4</sub>: 212.0923.

**3-Hydroxyphenylisoserine** (**D**–**53n**). 7 N HCl (4 mL) and 3-acetoxy-4-(3-acetoxy)-phenylazetidin-2-one (50 mg, 0.19 mmol) were treated according to Procedure 5, Method B (Section 4.2.2.5) to afford the desired isoserine (18 mg, 41% yield, at >99% purity by  $^{1}$ H-NMR analysis).  $^{1}$ H-NMR (500 MHz, D<sub>2</sub>O)  $\delta$ : 4.48 (d, J = 6.40 Hz, 1H), 4.52 (d, J = 6.40 Hz, 1H), 6.86 – 7.32 (aromatic protons).  $^{13}$ C-NMR (126 MHz, D<sub>2</sub>O)  $\delta$ : 173.96, 155.86, 134.49, 130.59, 119.13, 116.47, 114.20, 71.83, 56.68. HRMS (ESI-TOF) m/z 198.0806 [M + H] $^{+}$ ; calculated for C<sub>9</sub>H<sub>12</sub>NO<sub>4</sub>: 198.0766.

**3-Nitrophenylisoserine** (**D–530**). 7 N HCl (8 mL) and 3-acetoxy-4-(3-nitro)-phenylazetidin-2-one (229 mg, 0.91 mmol) were treated according to Procedure 5, Method B (Section 4.2.2.5) to afford the desired isoserine (230 mg, 96% yield, at >98% purity by  $^{1}$ H-NMR analysis).  $^{1}$ H-NMR (500 MHz, D<sub>2</sub>O)  $\delta$ : 4.53 (d, J = 5.90 Hz, 1H), 4.80 (d, J = 5.90 Hz, 1H), 7.64

-8.35 (aromatic protons). <sup>13</sup>C-NMR (126 MHz, D<sub>2</sub>O)  $\delta$ : 173.29, 147.99, 134.83, 134.02, 130.47, 124.54, 122.52, 71.09, 55.89. HRMS (ESI-TOF) m/z 227.0708 [M + H]<sup>+</sup>; calculated for C<sub>9</sub>H<sub>11</sub>N<sub>2</sub>O<sub>5</sub>: 227.0668.

**2-Fluorophenylisoserine** (**D**–**53p**). 7 N HCl (18 mL) and 3-acetoxy-4-(2-fluoro)-phenylazetidin-2-one (502 mg, 2.24 mmol) were treated according to Procedure 5, Method B (Section 4.2.2.5) to afford the desired isoserine (518 mg, 98% yield, at >98% purity by  $^{1}$ H-NMR analysis).  $^{1}$ H-NMR (500 MHz, D<sub>2</sub>O)  $\delta$ : 4.57 (d, J = 6.80 Hz, 1H) 4.82 (d, J = 6.80 Hz, 1H) 7.15 – 7.48 (aromatic protons).  $^{13}$ C-NMR (126 MHz, D<sub>2</sub>O)  $\delta$ : 173.50, 161.02, 131.91, 128.76, 125.00, 119.61, 116.08, 70.81, 51.61. HRMS (ESI-TOF) m/z 200.0762 [M + H] $^{+}$ ; calculated for C<sub>9</sub>H<sub>11</sub>NO<sub>3</sub>F: 200.0723.

**2-Chlorophenylisoserine** (**D–53q**). 7 N HCl (28 mL) and 3-acetoxy-4-(2-chloro)-phenylazetidin-2-one (870 mg, 3.64 mmol) were treated according to Procedure 5, Method B (Section 4.2.2.5) to afford the desired isoserine (896 mg, 98% yield, at >99% purity by  $^{1}$ H-NMR analysis).  $^{1}$ H-NMR (500 MHz, D<sub>2</sub>O)  $\delta$ : 4.57 (d, J = 5.87 Hz, 1H), 5.15 (d, J = 5.87 Hz, 1H), 7.37 – 7.52 (aromatic protons).  $^{13}$ C-NMR (126 MHz, D<sub>2</sub>O)  $\delta$ : 173.59, 132.93, 130.90, 130.49, 130.14, 127.75, 127.72, 70.52, 53.18. HRMS (ESI-TOF) m/z 216.0467 [M + H] $^{+}$ ; calculated for C<sub>9</sub>H<sub>11</sub>NO<sub>3</sub>Cl: 216.0427.

**2-Bromophenylisoserine** (**D**–**53r**). 7 N HCl (10 mL) and 3-acetoxy-4-(2-bromo)-phenylazetidin-2-one (395 mg, 1.4 mmol) were treated according to Procedure 5, Method B (Section 4.2.2.5) to afford the desired isoserine (396 mg, 96% yield, at >99% purity by  $^{1}$ H-NMR analysis).  $^{1}$ H-NMR (500 MHz, D<sub>2</sub>O)  $\delta$ : 4.55 (d, J = 5.87 Hz, 1H), 5.15 (d, J = 5.87 Hz, 1H), 7.28 – 7.73 (aromatic protons).  $^{13}$ C-NMR (126 MHz, D<sub>2</sub>O)  $\delta$ : 173.38, 133.53, 132.11, 131.12, 128.34,

127.78, 123.20, 70.46, 55.47. HRMS (ESI-TOF) m/z 259.9962 [M + H]<sup>+</sup>; calculated for  $C_9H_{11}NO_3Br$ : 259.9922.

**2-Methylphenylisoserine** (**D**–**53s**). 7 N HCl (6 mL) and 3-hydroxy-4-(2-methyl)phenylazetidin-2-one (54 mg, 0.31 mmol) were treated according to Procedure 5, Method A (Section 4.2.2.5) to afford the desired isoserine (71 mg, 95% yield, at >99% purity by  $^{1}$ H-NMR analysis).  $^{1}$ H-NMR (500 MHz, D<sub>2</sub>O)  $\delta$ : 2.32 (s, o-CH<sub>3</sub>), 4.45 (d, J = 6.80 Hz, 1H), 4.86 (d, J = 6.80 Hz, 1H), 7.26 – 7.39 (aromatic protons).  $^{13}$ C-NMR (126 MHz, D<sub>2</sub>O)  $\delta$ : 173.92, 136.72, 131.25, 131.06, 129.39, 126.67, 125.77, 71.42, 52.62, 18.28. HRMS (ESI-TOF) m/z 196.1011 [M + H] $^{+}$ : calculated for C<sub>10</sub>H<sub>14</sub>NO<sub>3</sub>: 196.0974.

**2-Methoxyphenylisoserine** (**D**–**53t**). 7 N HCl (18 mL) and 3-hydroxy-4-(2-methoxy)-phenylazetidin-2-one (214 mg, 1.1 mmol) were treated according to Procedure 5, Method A (Section 4.2.2.5) to afford the desired isoserine (229 mg, 98% yield, at >99% purity by  $^{1}$ H-NMR analysis).  $^{1}$ H-NMR (500 MHz, D<sub>2</sub>O)  $\delta$ : 3.83 (s, o-OCH<sub>3</sub>), 4.60 (d, J = 8.30 Hz, 1H), 4.66 (d, J = 8.30 Hz, 1H), 6.99 – 7.44 (aromatic protons).  $^{13}$ C-NMR (126 MHz, D<sub>2</sub>O)  $\delta$ : 174.04, 157.06, 131.45, 129.64, 120.94, 119.54, 111.61, 70.53, 55.23, 55.15. HRMS (ESI-TOF) m/z 212.0961 [M + H] $^{+}$ ; calculated for C<sub>10</sub>H<sub>14</sub>NO<sub>4</sub>: 212.0923.

**2-Nitrophenylisoserine** (**D**–**53u**). 7 N HCl (5 mL) and 3-acetoxy-4-(2-nitro)-phenylazetidin-2-one (92.6 mg, 0.37 mmol) were treated according to Procedure 5, Method B (Section 4.2.2.5) to afford the desired isoserine (94 mg, 97% yield, at >99% purity by  $^{1}$ H-NMR analysis).  $^{1}$ H-NMR (500 MHz, D<sub>2</sub>O)  $\delta$ : 4.64 (d, J = 5.40 Hz, 1H), 5.32 (d, J = 5.40 Hz, 1H), 7.62 – 8.10 (aromatic protons).  $^{13}$ C-NMR (126 MHz, D<sub>2</sub>O)  $\delta$ : 173.40, 148.10, 134.45, 130.67, 128.38, 128.01, 125.71, 70.59, 51.63. HRMS (ESI-TOF) m/z 227.0706 [M + H]<sup>+</sup>; calculated for C<sub>9</sub>H<sub>11</sub>N<sub>2</sub>O<sub>5</sub>: 227.0668.

**Trimethylisoserine (D–53v).** 7 N HCl (5 mL) and 3-acetoxy-4-trimethylazetidin-2-one (210 mg, 1.13 mmol) were treated according to Procedure 5, Method B (Section 4.2.2.5) to afford the desired isoserine (145 mg, 65% yield, at >99% purity by  $^{1}$ H-NMR analysis).  $^{1}$ H-NMR (500 MHz, D<sub>2</sub>O) δ: 1.01 (s, *t*-butyl CH<sub>3</sub>), 3.43 (d, J = 1.50 Hz, H-3), 4.55 (d, J = 1.50 Hz, H-2).  $^{13}$ C-NMR (126 MHz, D<sub>2</sub>O) δ: 175.92, 66.74, 60.51, 32.62, 25.47. HRMS (ESI-TOF) m/z 162.1168 [M + H] $^{+}$ ; calculated for C<sub>7</sub>H<sub>16</sub>NO<sub>3</sub>: 162.1130.

**Cyclohexylisoserine (D–53w).** 7 N HCl (7 mL) and 3-acetoxy-4-cyclohexylazetidin-2-one (211 mg, 1.0 mmol) were treated according to Procedure 5, Method B (Section 4.2.2.5) to afford the desired isoserine (219 mg, 98% yield, at >98% purity by  $^{1}$ H-NMR analysis).  $^{1}$ H-NMR (500 MHz, D<sub>2</sub>O)  $\delta$ : 1.00 – 1.15 (m, 2H), 1.16 – 1.26 (m, 4H), 1.57 – 1.64 (m, 1H), 1.66 – 1.77 (m, 4H), 3.34 – 3.38 (m, H-3), 4.49 (d, J = 2.93 Hz, H-2).  $^{13}$ C-NMR (126 MHz, D<sub>2</sub>O)  $\delta$ : 175.27, 67.64, 57.70, 37.05, 28.56, 28.03, 25.23, 25.11. HRMS (ESI-TOF) m/z 188.1324 [M + H] $^{+}$ ; calculated for C<sub>9</sub>H<sub>18</sub>NO<sub>3</sub>: 188.1287.

Thiophenylisoserine (D–53x). 7 N HCl (5 mL) and 3-hydroxy-4-thiopheneazetidin-2-one (144 mg, 0.68 mmol) were treated according to Procedure 5, Method B (Section 4.2.2.5) to afford the desired isoserine (145 mg, 65% yield, at >99% purity by  $^{1}$ H-NMR analysis).  $^{1}$ H-NMR (500 MHz, D<sub>2</sub>O) δ: 4.54 (d, J = 5.90 Hz, H-2), 4.98 (d, J = 5.90 Hz, H-3), 7.04 – 7.50 (aromatic protons).  $^{13}$ C-NMR (126 MHz, D<sub>2</sub>O) δ: 173.94, 134.05, 128.60, 127.89, 127.31, 71.66, 52.41. HRMS (ESI-TOF) m/z 188.0414 [M + H]<sup>+</sup>; calculated for C<sub>7</sub>H<sub>10</sub>NO<sub>3</sub>S: 188.0381.

**Isopropylisoserine** (**D–53y**). 7 N HCl (4 mL) and 3-acetoxy-4-dimethylazetidin-2-one (139 mg, 0.81 mmol) were treated according to Procedure 5, Method B (Section 4.2.2.5) to afford the desired isoserine (142 mg, 95% yield, at >99% purity by  $^{1}$ H-NMR analysis).  $^{1}$ H-NMR (500 MHz, D<sub>2</sub>O)  $\delta$ : 0.99 (d, J = 6.85 Hz, CH<sub>3</sub>), 1.97 – 2.07 (m, CH), 3.35 (dd, J = 3.42, 2.90 Hz,

H-3), 4.46 (d, J = 3.42 Hz, H-2). <sup>13</sup>C-NMR (126 MHz, D<sub>2</sub>O)  $\delta$ : 175.16, 67.91, 58.47, 27.83, 18.09, 17.38. HRMS (ESI-TOF) m/z 148.1015 [M + H]<sup>+</sup>; calculated for C<sub>6</sub>H<sub>14</sub>NO<sub>3</sub>: 148.0974.

#### 4.2.3. Synthesis of Pyridinylisoserine Analogs

The method described for the isoserine analogs above was not successful with the synthesis of pyridinylisoserine. The oxidative removal of *p*-methoxyphenol group using cerium ammonium nitrate did not yield the expected product. This prompted a search for an alternative amine protecting group. Benzhydryl amine was chosen which could be easily cleaved off through hydrogenolysis.

#### 4.2.3.1. General Procedure 6: Synthesis of Pyridinyl-N-benzhydryl Imine

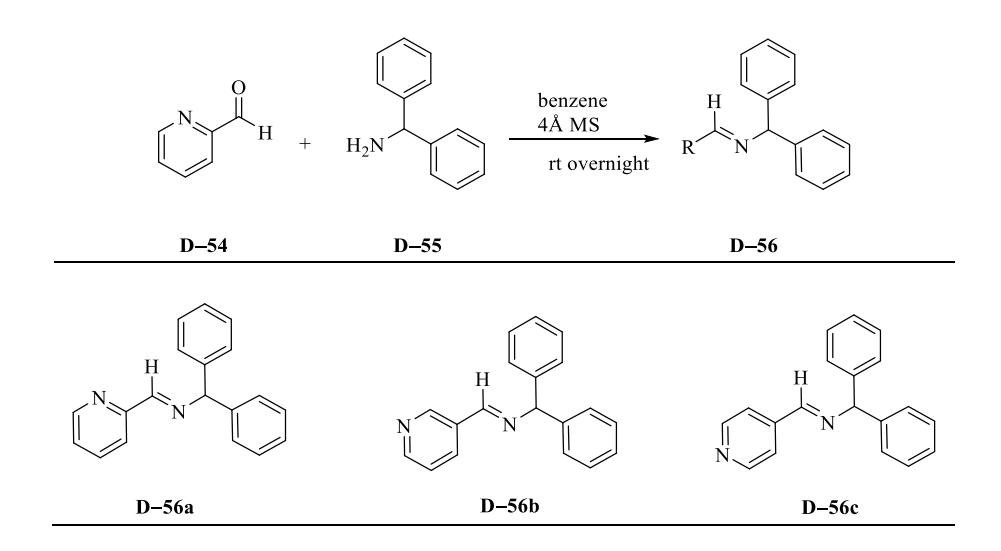


Figure 4.13. Scheme showing synthesis of 2-pyridinylimines.

To a solution of pyridinylcarboxaldehyde (1 equiv) dissolved in benzene was added benzhydrylamine (1.1 equiv) and oven dried molecular sieves (~1.5 g). The reaction was stirred

at room temperature for 12 h, then filtered, dried (MgSO<sub>4</sub>), and concentrated under vacuum. The crude mixture was purified by silica gel column chromatography (1:4 EtOAc/hexane v/v), and the fractions containing the product were combined and dried under vacuum to obtain the imine.

**2-pyridinyl-***N***-benzhydryl imine** (**D**–**56a**) was synthesized according to the General Procedure 6 (Section 4.2.3.1) by addition of 2-pyridinylcarboxaldehyde (21 mmol, 2 mL, 1 equiv) to benzhydrylamine (23.4 mmol, 1.1 equiv) dissolved in benzene (20 mL) to yield the imine (5.7 g, 99.6% yield, at >99% purity by  $^{1}$ H-NMR analysis).  $^{1}$ H-NMR (500 MHz, CDCl<sub>3</sub>-*d*)  $\delta$ : 5.72 (s, benzhydryl CH), 7.24 – 8.66 (aromatic protons).  $^{13}$ C-NMR (126 MHz, CDCl<sub>3</sub>-*d*)  $\delta$ : 162.02, 154.75, 149.40, 143.37, 136.54, 128.58, 127.81, 127.22, 124.91, 121.57, 77.74.

**3-pyridinyl-***N***-benzhydryl imine** (**D**–**56b**) was synthesized according to the General Procedure 6 (Section 4.2.3.1) by addition of 3-pyridinylcarboxaldehyde (9.35 mmol, 0.9 mL, 1 equiv) to benzhydrylamine (10.3 mmol, 1.1 equiv) dissolved in benzene (10 mL) to yield the imine (2.5 g, 100% yield, at >99% purity by <sup>1</sup>H-NMR analysis). <sup>1</sup>H-NMR (500 MHz, CDCl<sub>3</sub>-*d*) δ: 5.64 (s, benzhydryl CH), 7.23 – 8.25 (aromatic protons), 8.47 (s, imine CH), 8.66 – 8.93 (aromatic protons). <sup>13</sup>C-NMR (126 MHz, CDCl<sub>3</sub>-*d*) δ: 157.97, 151.65, 150.50, 143.43, 134.84, 131.78, 128.54, 127.58, 127.18, 123.63, 78.14.

**4-pyridinyl-***N***-benzhydryl imine (D–56c)** was synthesized according to the General Procedure 6 (Section 4.2.3.1) by addition of 4-pyridinylcarboxaldehyde (9.35 mmol, 0.9 mL, 1 equiv) to benzhydrylamine (10.3 mmol, 1.1 equiv) dissolved in benzene (10 mL) to yield the imine (2.49 g, 98% yield, at >99% purity by <sup>1</sup>H-NMR analysis). <sup>1</sup>H-NMR (500 MHz, CDCl<sub>3</sub>-*d*) δ: 5.68 (s, benzhydryl CH), 7.26 – 7.73 (aromatic protons), 8.43 (s, imine CH), 8.71 – 8.74 (aromatic protons). <sup>13</sup>C-NMR (126 MHz, CDCl<sub>3</sub>-*d*) δ: 158.98, 150.42, 143.18, 142.94, 128.61, 128.36, 127.59, 127.31, 122.22, 78.14.

# 4.2.3.2. General Procedure 7: Synthesis of N-benzhydryl-3-acetoxy-4(pyridinyl)azetidin-2-one

Figure 4.14. Scheme showing the synthesis of pyridinyl-2-azetidinones.

To a solution of imine (**D–56**, 1 equiv) dissolved in dichloromethane (38 mL) at 0 °C was added triethylamine (11.04 mmol, 3 equiv). A solution of acetoxyacetyl chloride (7.36 mmol, 2 equiv) in dichloromethane (20 mL) was then added dropwise and the reaction stirred at 0 °C for 2 h. The mixture was then warmed to room temperature and stirred for 1.5 h to complete the reaction. The solution was washed with water (3 × 15 mL) and the organic fraction dried (MgSO<sub>4</sub>) and concentrated under vacuum. The crude mixture was then purified by silica gel chromatography (1:4 EtOAc/hexane, v/v) and the fractions containing product concentrated under vacuum to obtain the pure product.

**Synthesis of N-benzhydryl-3-acetoxy-4-(2-pyridinyl)azetidin-2-one (D–57a).** 2-Pyridinyl-*N*-benzhydryl imine (1 g, 3.68 mmol, 1 equiv), triethylamine (11.04 mmol, 3 equiv) dissolved in dichloromethane (20 mL) at 0 °C and acetoxyacetyl chloride (7.36 mmol, 2 equiv)

were treated according to Procedure 7 (Section 4.2.3.2) to afford the *N*-benzhydryl-3-acetoxy-4-(2-pyridinyl)azetidin-2-one (243 mg, 17.8% yield, at >99% purity by  $^{1}$ H-NMR analysis).  $^{1}$ H-NMR (500 MHz, CDCl<sub>3</sub>-d)  $\delta$ : 1.71 (s, acetyl CH<sub>3</sub>), 5.11 (d, J = 4.89 Hz, H-3), 5.96 (s, benzhydryl CH), 5.98 (d, J = 4.89 Hz, H-2), 6.97 – 8.51 (aromatic protons).  $^{13}$ C-NMR (126 MHz, CDCl<sub>3</sub>-d)  $\delta$ : 169.06, 164.94, 153.79, 149.18, 138.00, 137.78, 135.64, 128.97, 128.41, 127.96, 127.80, 123.36, 122.82, 75.79, 63.11, 61.75, 19.94.

Synthesis of *N*-benzhydryl-3-acetoxy-4-(3-pyridinyl)azetidin-2-one (D–57b). 3-Pyridinyl-*N*-benzhydrylimine (1 g, 3.68 mmol, 1 equiv), triethylamine (11.04 mmol, 3 equiv) dissolved in dichloromethane (20 mL) at 0 °C and acetoxyacetyl chloride (7.36 mmol, 2 equiv) were treated according to Procedure 7 (Section 4.2.3.2) to afford the *N*-benzhydryl-3-acetoxy-4-(3-pyridinyl)azetidin-2-one (356 mg, 26% yield, at >99% purity by  $^{1}$ H-NMR analysis).  $^{1}$ H-NMR (500 MHz, CDCl<sub>3</sub>-*d*)  $\delta$ : 1.73 (s, acetyl CH<sub>3</sub>), 4.98 (d, J = 4.89 Hz, H-3), 5.92 (s, benzhydryl CH), 5.93 (d, J = 4.90 Hz, H-2), 7.08 – 8.46 (aromatic protons).  $^{13}$ C-NMR (126 MHz, CDCl<sub>3</sub>-*d*)  $\delta$ : 168.93, 164.72, 150.00, 149.69, 137.47, 137.32, 136.02, 128.78, 128.61, 128.54, 76.06, 61.75, 60.29, 19.90.

Synthesis of *N*-benzhydryl-3-acetoxy-4-(4-pyridinyl)azetidin-2-one (D–57c). 4-Pyridinyl-*N*-benzhydrylimine (1 g, 3.68 mmol, 1 equiv), triethylamine (11.04 mmol, 3 equiv) dissolved in dichloromethane (20 mL) at 0 °C and acetoxyacetyl chloride (7.36 mmol, 2 equiv) were treated according to Procedure 7 (Section 4.2.3.2) to afford the *N*-benzhydryl-3-acetoxy-4-(4-pyridinyl)azetidin-2-one (164 mg, 12% yield, at >99% purity by  $^{1}$ H-NMR analysis).  $^{1}$ H-NMR (500 MHz, CDCl<sub>3</sub>-*d*)  $\delta$ : 1.70 (s, acetyl CH<sub>3</sub>), 4.93 (d, J = 4.89 Hz, H-3), 5.90 (s, benzhydryl C–H), 5.91 (d, J = 4.89 Hz, H-2), 6.96 – 8.43 (aromatic protons).  $^{13}$ C-NMR (126 MHz, CDCl<sub>3</sub>-*d*)  $\delta$ :

169.01, 164.54, 149.40, 142.56, 137.42, 128.78, 128.63, 127.93, 123.23, 75.90, 61.95, 61.42, 19.90.

# 4.2.3.3. General Procedure 8: Lactam Ring Opening Along with Amine and Hydroxyl Deprotection of N-benzhydryl-3-acetoxypyridinylazetidin-2-one

Briefly, to the starting material, N-benzhydryl-3-acetoxy-4-(2-pyridinyl)azetidin-2-one (100 mg, 0.27 mmol, 1 equiv) dissolved in acetonitrile (2 mL), was added 6 N HCl (2 mL). The reaction mixture was stirred under reflux, monitored by TLC (4:1:1 butanol/AcOH/H<sub>2</sub>O v/v) and stopped after 12 h. The acetonitrile was removed by evaporation under a stream of dry nitrogen and the resultant crude residue was dissolved in water (3 mL) and adjusted to pH 3 (3 N HCl). The solution was extracted with ethyl acetate (3 × 3 mL), the organic layer was washed with dH<sub>2</sub>O (2 × 3 mL), and the aqueous fractions were combined and lyophilized. The resultant crude residue was loaded onto a C18 reverse phase silica gel (SiliCycle, Quebec City, Canada) column (diameter: 1.2 mm, height: 32 cm) and eluted with 2.5% acetonitrile in water.

The fractions containing the product were pooled and dried under vacuum to obtain 2-pyridinylisoserine as a white powder (41.1 mg, 84% converted yield from the lactam, at >90% purity by  $^{1}$ H-NMR analysis).  $^{1}$ H-NMR (500 MHz, D<sub>2</sub>O)  $\delta$ : 4.37 (d, J = 5.40 Hz, 1H), 4.69 (d, J = 5.40 Hz, 1H), 7.41 – 8.56 (aromatic protons).  $^{13}$ C-NMR (126 MHz, D<sub>2</sub>O)  $\delta$ : 175.85, 152.11, 149.06, 138.14, 124.37, 122.94, 72.77, 57.20. HRMS (ESI-TOF) m/z 183.0777 [M + H] $^{+}$ ; calculated for C<sub>8</sub>H<sub>11</sub>N<sub>2</sub>O<sub>3</sub>: 183.0770.

Removal of ethyl acetate from the organic layer under vacuum yielded benzhydrylacetamide as a white solid (45.6 mg, 75% yield).  $^{1}$ H-NMR (500 MHz, CDCl<sub>3</sub>-d)  $\delta$ : 2.04 (s, 3 H), 6.18 (d, J = 7.34 Hz, 1 H), 6.24 (d, J = 7.30 Hz, 1 H), 7.21 – 7.24 (m, 4 H), 7.26 (t,

J = 2.20 Hz, 1 H), 7.28 (d, J = 0.98 Hz, 1 H), 7.30 – 7.35 (m, 4 H). <sup>13</sup>C-NMR (126 MHz, CDCl<sub>3</sub>-d)  $\delta$ : 169.16, 141.49, 128.67, 127.49, 127.42, 57.01, 23.36 (see Appendix **Figure III–38** for numbering).

Synthesis of 3-pyridinylisoserine. 3-pyridinylisoserine was synthesized according to Procedure 8 (Section 4.2.3.3) except *N*-benzhydryl-3-acetoxy-4-(3-pyridinyl)azetidin-2-one (350 mg, 0.94 mmol, 1 equiv) was used as the azetidine precursor to make 3-pyridinylisoserine as the HCl salt (161.5 mg, 94% converted yield from the lactam, at >95% purity by  $^{1}$ H-NMR analysis).  $^{1}$ H-NMR (500 MHz, D<sub>2</sub>O)  $\delta$ : 4.59 (d, J = 4.40 Hz, 1H), 5.07 (d, J = 4.40 Hz, 1H), 8.14 – 8.96 (aromatic protons).  $^{13}$ C-NMR (126 MHz, D<sub>2</sub>O)  $\delta$ : 173.31, 145.87, 142.27, 140.90, 134.19, 127.80, 70.35, 53.49. HRMS (ESI-TOF) m/z 183.0810 [M + H] $^{+}$ ; calculated for C<sub>8</sub>H<sub>11</sub>N<sub>2</sub>O<sub>3</sub>: 183.0770.

Synthesis of 4-pyridinylisoserine. 4-pyridinylisoserine was synthesized according to Procedure 8 (Section 4.2.3.3) except *N*-benzhydryl-3-acetoxy-4-(4-pyridinyl)azetidin-2-one (164 mg, 0.44 mmol, 1 equiv) was used as the azetidine precursor to make the HCl salt of 4-pyridinylisoserine (57.9 mg, 72% yield, at 80% purity by  $^{1}$ H-NMR analysis).  $^{1}$ H-NMR (500 MHz, D<sub>2</sub>O)  $\delta$ : 4.38 (d, J = 4.40 Hz, 1H), 4.93 (d, J = 4.40 Hz, 1H), 7.99 – 8.82 (aromatic protons).  $^{13}$ C-NMR (126 MHz, D<sub>2</sub>O)  $\delta$ : 173.45, 153.88, 141.98, 126.21, 70.80, 55.68. HRMS (ESI-TOF) m/z 183.0809 [M + H] $^{+}$ ; calculated for C<sub>8</sub>H<sub>11</sub>N<sub>2</sub>O<sub>3</sub>: 183.0770.

# 4.2.4. Activity Assay for the Determination of the Substrate Specificity of Tyc(Phe–AT)

To identify productive isoserine substrates, each isoserine (2 mM) was incubated separately with CoA (1 mM), ATP (1 mM), MgCl<sub>2</sub> (3 mM) and purified Tyc(Phe–AT) enzyme (1 mg) in

100 mM HEPES (pH 8.0) in a total volume of 1 mL. The reactions were incubated at 31 °C. Aliquots (100  $\mu$ L) were withdrawn at 10 min, 20 min, 40 min, 1 h, 2 h, 4 h, 6 h and 8 h, and transferred to 96 well plates, quenched immediately with 10% formic acid (20  $\mu$ L), and analyzed by LC-MS (Quattro–Premier XE Mass Spectrometer coupled with Acquity® UPLC system fitted with a C18 Ascentis Express column (2.5 × 50 mm, 2.7  $\mu$ m) at 30 °C). An aliquot (5  $\mu$ L) of each sample was loaded onto the column, and the analytes were eluted with a solvent gradient of acetonitrile (Solvent A) and 0.05% triethylamine in distilled water (Solvent B) (held at 2.5% Solvent A for 3.17 min, increased to 100% Solvent A over 5 sec with a 2–min hold, and then returned to 2.5% Solvent A over 5 sec with a 50-sec hold) at a flow rate of 0.3 mL/min.

#### 4.2.5. Apparent Rates of Tyc(Phe–AT) with the Isoserine Substrates

The conversion rate of Tyc(Phe–AT) for thioesterification of the isoserine analogs to their isoserinyl CoA thioesters was determined by incubating each isoserine (2 mM) separately with ATP (1 mM), CoA (1 mM), MgCl<sub>2</sub> (3 mM) and purified Tyc(Phe–AT) enzyme (1 mg) in 100 mM HEPES (pH 8.0) at 31 °C for 2 h in triplicate. Time course assays done using 1 mg Tyc(Phe–AT) with the isoserine substrates provided a justification for the estimation of the relative rates to be at steady state at 2 h. At the end of each reaction, acetyl CoA (1 μM) was added as the internal standard to each sample to correct for losses during work-up. The biosynthetic thioester products were quantified by a liquid chromatography multiple reaction monitoring (MRM) mass spectrometry technique<sup>39</sup> on the Quattro–Premier XE Mass Spectrometer with an elution gradient described in Section 4.2.4.

The effluent from the chromatography column was directed to a mass spectrometer where the first quadruple mass analyzer (in negative ion mode) was set to select for the molecular ion of a biosynthesized acyl CoA. The selected ion was then directed to a collision gas chamber where the collision energy was optimized to maximize the abundance of a single signature fragment ion (m/z 408.31) monitored in the second quadruple mass analyzer (in negative ion mode). The monitored ion was derived by a fragmentation reaction in the CoA moiety that is characteristic of acyl CoA thioesters analyzed by this MRM method. The peak area of the monitored fragment ion m/z 408.31 corresponding to each biosynthetic isoserinyl CoA thioester was converted to concentration by comparing the peak area of the same ion generated by authentic CoA using linear regression analysis.

# 4.2.6. Kinetic Evaluation of Tyc(Phe–AT), CoA, and Racemic (2R,3S)Phenylisoserine

Racemic (2R,3S)-phenylisoserine at  $5-2000~\mu\text{M}$  was incubated with ATP (1 mM), MgCl<sub>2</sub> (3 mM), CoA (1 mM), 100 mM HEPES (pH 8.0), and Tyc(Phe–AT) (100  $\mu\text{g·mL}$ ) for 15 min. At the end of each reaction and prior to mass spectrometry analysis, acetyl CoA (1  $\mu\text{M}$ ) was added as the internal standard to each sample to correct for losses during workup. The biosynthetic products were quantified by a LC–ESI–MRM as described is Section 4.2.4.

#### 4.3. Results and Discussion

#### 4.3.1. Synthesis of Isoserine Analogs via Staudinger Cycloaddition Reaction

The substituents on phenyl ring of the isoserines used as substrates herein varied in their electronic properties and the size. The reported improved potency in paclitaxel analogs

containing modified isoserinyl moieties (see **Table 4.1, Section 4.1.1**)<sup>11,19,40</sup> guided the choice of some isoserines synthesized herein.

Several methods for the synthesis of phenylisoserine analogs proceed through intermediary asymmetric epoxidation,  $^{41}$  dihydroxylation,  $^{42}$  chemoenzymology,  $^{43}$  aminohydroxylation, and Staudinger cycloaddition reactions. Readily available starting materials make the latter method widely popular for the synthesis of  $\beta$ -lactams. Also, unlike other methods, the Staudinger [2 + 2] cycloaddition reaction between an imine and ketene is direct and facile for the synthesis of racemic isoserine analogs (**Figure 4.15**).

**Figure 4.15**. A scheme showing the synthesis of isoserine analogs. (i) (a) DCM, 4 Å molecular sieves, rt, 12 h, (b) TEA, acetoxyacetyl chloride, DCM, 0 °C, then rt, 2-5 h, (ii) ceric ammonium nitrate in H<sub>2</sub>O, CH<sub>3</sub>CN, 0 °C, 1-3 h, (iii) 7 N HCl, reflux, 24 h.

The first step involved the formation of a Schiff base between benzaldehyde analogs (**D**–47) and p-anisidine (**D**–48). This base was then reacted with acetoxyacetyl chloride in the presence of triethylamine to form the cis– $\beta$ –lactam racemate via electrocyclic conrotatory ring closure to afford the  $\beta$ –lactam. Oxidation by ceric ammonium nitrate removed the p-methoxyphenol group to afford the free amide. Ordinarily, treatment with base followed by acidic work up deprotected the hydroxyl group at  $C_{\alpha}$  and hydrolyzed the  $\beta$ -lactam. However, reflux in 7 N HCl hydrolyzed **D**–51 to isoserine **D**–53 in a single step, shortening the route to isoserine racemates to three steps (**Figure 4.15**).

The pyridinylisoserines were synthesized with some modifications to the general method (**Figure 4.16**). A benzhydrylamine intermediate was used as the amine source instead of *p*-anisidine. The synthesis of pyridinylisoserine employed the [2 + 2] cycloaddition reaction step to form the lactam ring. A proposed deprotection sequence included acid-catalyzed hydrolysis of the lactam and *O*-acetyl group followed by hydrogenolysis to remove the benzhydryl moiety. Surprisingly, the acidic reflux removed all of the protecting groups, and the hydrogenolysis step was unnecessary (**Figure 4.16**).

AcO 
$$(ii)$$
  $(ii)$   $(ii$ 

**Figure 4.16**. Synthesis of pyridinylisoserine isomers. (i) (a) DCM, 4 Å molecular sieves, rt, 12 h, (b) TEA, acetoxyacetyl chloride, DCM, 0 °C, 3 h, (ii) Acetonitrile, 7 N HCl, reflux, 24 h.

The hydrolysis of the benzhydryl-protected pyridinyl- $\beta$ -lactams formed two products: the expected aqueous soluble pyridinylisoserine hydrochlorides and the benzhydrylacetamide whose identity was confirmed by  ${}^{1}$ H-NMR. The H/D-exchange NMR showed disappearance of the doublet at 6.18 ppm, and loss of coupling to the proton resonance at 6.24 ppm upon addition of D<sub>2</sub>O (Appendix, **Figure III-39**). The gHSQC-NMR did not show evidence of a carbon correlating to the proton at 6.18 ppm. Using this information, the compound was identified as benzhydrylacetamide. This side product was formed through the amidation of benzhydryl carbocation intermediate by acetonitrile used to dissolve the starting material according to the

scheme below (**Figure 4.17**). The reaction intermediate (**D–59**) was identified by LC–ESI–MS analysis (see Appendix, **Figure III–42**).

Figure 4.17. Reaction mechanism for the formation of benzhydrylacetamide.

### 4.3.2. Relative Rates of Tyc(Phe–AT) for Isoserine Substrate Analogs

Racemic isoserine substrates synthesized by the Staudinger reaction (see Section 4.3.1) informed on the substrate scope of Tyc(Phe–AT). All substrates in which the phenyl ring had a substituent at *ortho*- (F, Cl, NO<sub>2</sub>), *para*- (F, Cl, Br, Me, OH, and NO<sub>2</sub>), or *meta*- (F, Cl, Br, Me, OH, CH<sub>3</sub>O and NO<sub>2</sub>) position were converted to their acyl CoA by Tyc(Phe–AT). The enzyme activity was

also observed with the non-aromatic  $\beta$ -(cyclohexyl)isoserine and heteroaromatic  $\beta$ -(thiophenyl)isoserine analogs, but not with the aliphatic groups (isopropyl- and *tert*-butyl isoserine) and pyridine analogs.

The kinetic evaluation of racemic (2R,3S)-phenylisoserine showed a 12-fold reduction in turnover rates of Tyc(Phe–AT)  $(0.12 \pm 0.010 \text{ min}^{-1})$  compared to that of the single isomer (2R,3S)-phenylisoserine  $(1.51 \pm 0.17 \text{ min}^{-1})$ . Also, the data from initial analysis showed that the non-natural (2S,3R)-phenylisoserine inhibited Tyc(Phe–AT)  $(K_I = 92.0 \mu\text{M})$  in a (2R,3S)-phenylisoserine assay (see Chapter 3, Section 3.3.7.1), thus confounding efforts to obtain accurate apparent Michaelis parameters for each racemic isoserine substrate tested herein. Therefore, the relative steady-state rate of Tyc(Phe–AT) for each racemic isoserine substrate was determined through analysis of the biosynthesized isoserinyl CoA by ESI–MS–MRM method. These assays, run at apparent steady-state gave an approximation of relative steady-state velocity of Tyc(Phe–AT) for various isoserine analogs.

The rate (7 nmol·h<sup>-1</sup>) at which Tyc(Phe–AT) converted (2R,3S)–phenylisoserine to (2R,3S)–phenylisoserinyl CoA was set at 100% and used for comparison against the apparent rates of Tyc(Phe–AT) for the other isoserine substrates at apparent saturation (also incubated at 2 mM) (**Table 4.2**). In general, the  $v_{app}$  values of Tyc(Phe–AT) for substrates with *meta*-substituents on the aryl ring were higher than for the *para*- and *ortho*-isomers. For example, the  $v_{app}$  was ~1.5- and 6-fold lower for p- and o-fluoro isomers respectively compared to the m-fluoro isomer. Similarly, the  $v_{app}$  for the methyl-substituent on phenyl ring decreased for *ortho*-methyl ( $v_{app}$  = below detection limit) and *para*-methyl ( $v_{app}$  = 1.13 nmol·h<sup>-1</sup>) compared to *meta*-methyl-substituent ( $v_{app}$  = 2.61 nmol·h<sup>-1</sup>) (**Table 4.2**).

Table 4.2. Relative rates of Tyc(Phe-AT) with aryl- and non-aryl isoserine and CoA

$ \begin{array}{c ccccc} & & & & & & & & & & & & & & & & & & & $									
R		(nmol·h <sup>-1</sup> )	$v_{ m app}$	R		$v_{app}$ (nmol·h <sup>-1</sup> )	$v_{ m app}$		
	a	$7.3 \pm 0.91$	100%	Br	l	$0.22 \pm 0.05$	3.0%		
F	b	$6.1 \pm 0.41$	84%	Me ZZ	m	1.1 ± 0.019	15%		
Cl	c	$1.7 \pm 0.27$	24%	HO	n	$0.04 \pm 0.01$	<1%		
Br	d	$1.4 \pm 0.15$	19%	O <sub>2</sub> N	0	$0.05 \pm 0.01$	<1%		
Me	e	$2.6 \pm 0.15$	36%	MeO Zź	p				
O <sub>2</sub> N Zz	f	$5.2 \pm 0.10$	72%	F	q	$0.98 \pm 0.12$	14%		
MeO	g	$0.6 \pm 0.07$	8.2%	Cl	r	$0.11 \pm 0.02$	1.5%		
HO	h	$0.3 \pm 0.03$	3.9%	Br	s				
S	i	$0.9 \pm 0.09$	12%	Me Ne	t				
F	j	4.0 ± 1.0	55%	NO <sub>2</sub>	u	$0.18 \pm 0.02$	2.5%		
CI	k	$0.45 \pm 0.12$	6.2%	OMe	v				

The dashed line (---) indicates that the corresponding biosynthetic product was below the detection limit of the mass spectrometer.

Table 4.2. (cont'd)

R		(nmol·h <sup>-1</sup> )	$v_{ m app}$	R		(nmol·h <sup>-1</sup> )	$v_{ m app}$
75	w	$0.09 \pm 0.005$	1.2%	N Ze	z		
Nyz	X			, con	ab		
N ZZ	y			× cr	ac		

The  $v_{app}$  values of Tyc(Phe–AT) also decreased with size for the halogen substituents regardless of the position on the phenyl ring. For example, the fluoro substituent was converted to the CoA thioester the fastest in each category; o-F > o-Cl > o-Br ( $v_{app} = 0.98$ , 0.11, and 0.0 nmol·h<sup>-1</sup> respectively), p-F > p-Cl > p-Br ( $v_{app} = 4.0$ , 0.45, and 0.22 nmol·h<sup>-1</sup> respectively), and m-F > m-Cl > m-Br ( $v_{app} = 6.1$ , 1.7, and 1.4 nmol·h<sup>-1</sup> respectively). The  $v_{app}$  for the production of the acyl CoA analogs decreased also with the size of the para—substituent (H > F > Cl > Br > OH ~ NO<sub>2</sub> > OMe), ranging from a  $v_{app} = 3.98$  nmol·h<sup>-1</sup> for p-fluoro to  $v_{app}$  below detection limit for p-methoxy. Among the heteroaromatic analogs, only thiofuranylisoserine was converted to the CoA thioester by Tyc(Phe–AT) at  $v_{app} = 0.89$  nmol·h<sup>-1</sup>. There was no Tyc(Phe–AT) activity observed for the pyridinylisoserine isomers. Similarly, the isopropyl- and trimethylisoserine analogs were not converted to their respective CoA thioesters in this study.

#### 4.3.3. Docking (2R,3S)-Phenylisoserine into Grs1(Phe-A) Domain

To gain further information about the binding interactions between the isoserine substrates and Tyc(Phe-AT), (2R,3S)-phenylisoserine was docked into the active site of Grs1(Phe-A) which is

highly homologous to Tyc(Phe–AT) (**Figure 4.18**). In this model, the aryl ring of (2R,3S)– phenylisoserine is docked according to that of the (2S)-phenylalanine substrate in complex with Grs1(Phe-A). The phenyl ring binding pocket is highly hydrophobic and consists of A236, W239, T278, I299, A322, I330, and C331 residues. The *ortho-*, *meta-*, and *para-* ring carbons point towards A236, T278, and W239, respectively (this is the residue numbering in Grs1(Phe-A). These steric interactions may explain why the turnover of Tyc(Phe-AT) for aromatic substrates with small substituents on phenyl ring is higher compared to the bulky substituents at similar positions on the phenyl ring. For instance, the  $v_{app}$  for m-fluoro was ~2.5-fold higher compared to that for m-methylisoserine analog (**Table 4.2**). It is also not surprising that the isoserine substrates with aliphatic side chains (namely isopropyl-, and trimethylisoserine analogs) were not converted to their CoA thioesters (Table 4.2). This is possibly due to bulky methyl groups, which would not bind to the Tyc(Phe-AT) active site in a conformation that would enable a catalytic reaction to occur. Additionally, since the residues lining the active site are mainly hydrophobic, the substrates containing hydrophilic substituents (for example hydroxyphenylisoserine isomers) would not be favored during catalysis as evident from their lower  $v_{app}$  compared to the hydrophobic ones (for example  $v_{app}$  for m-methyl was ~9-fold higher  $(2.6 \text{ nmol}\cdot\text{h}^{-1})$  compared to the *m*-hydroxy  $(0.29 \text{ nmol}\cdot\text{h}^{-1})$ ). It can also be argued that before binding, the hydrophilic substituents would require desolvation to break the hydrogen bonding network with water in the medium, which would require an additional step and hence kinetically unfavorable.

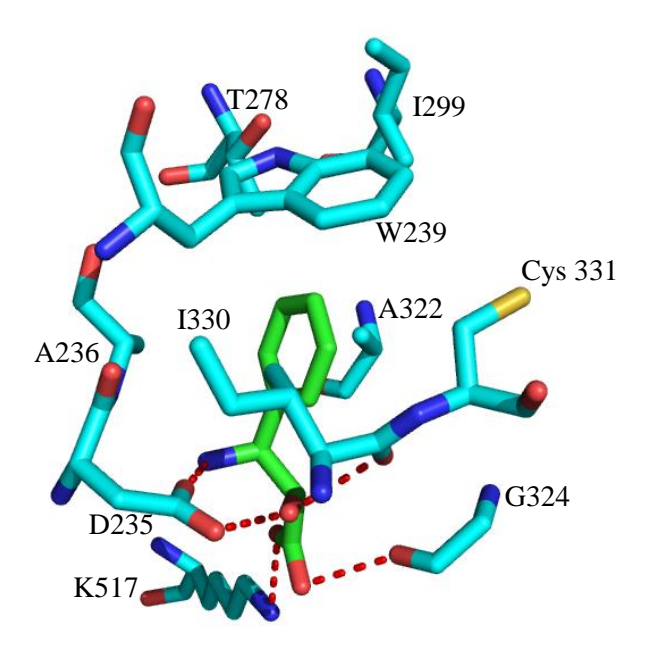


**Figure 4.18.** (2R,3S)—phenylisoserine (green) docked into Grs1(Phe-A) active site, a close homolog of Tyc(Phe–AT).

Chapter 3 describes the enantiospecificity of Tyc(Phe–AT) for (2R,3S)–phenylisoserine over (2S,3R)–phenylisoserine in aminoacyl CoA biosynthesis. Further inhibition studies showed the non-productive enantiomer inhibited Tyc(Phe–AT)  $(K_I = 92.0 \, \mu\text{M})$ . The isoserine substrates described here were synthesized as racemates. Considering that the (2S,3R)–isomer is an inhibitor, the intrinsic  $K_M$  and  $k_{cat}$  of Tyc(Phe–AT) for the isoserines could not be calculated. To overcome this challenge, there is need to develop a method to separate the isoserine racemates prior to their conversion to thioesters. A lipase-catalyzed enantioselective method is proposed based on previously reported studies. A lipase-catalyzed enantioselective method is proposed amino acids mainly employ enzymatic reactions such as N–phenylacetylation by penicillin acylase from E. coli, amide bond cleavage of L-amino acids by an aminoacylase from pig kidneys, formation of L-anilide using papain as a chemoselective catalyst, A7,48,51 and separation of amino acids using lipases. Of all the chiral catalysts investigated in resolution of racemates, lipases are the most extensively studied.

antarctica to resolve alicyclic  $\beta$ -amino esters through hydrolysis was investigated. A 100% enantioselectivity was reported in good yields (42 – 48%). Additionally, a lipase PS (*Pseudomonal cepacia*) showed superior enantioselective separation of  $\beta$ -aryl- $\beta$ -amino acids with upto 100% enantioselectivity and 50% yields. Even more encouraging, an enzymatic strategy for separation of (2*R*,3*S*)—phenylisoserine from the enantiomer using a lipase PS (from *Burkholderia cepacia*) was also reported in high yields and enantioselectivity. From these initial studies, lipase PS from two different organisms (*Pseudomonal cepacia* and *Burkholderia cepacia*) is the most ideal in the separation of the isoserine racemates described here. The high enantioselectivity, yields, wide substrate scope, and application in gram scale separation of racemic  $\beta$ -aryl- $\beta$ -amino acids make this lipase a promising choice in the future investigations with the isoserine analogs.

#### 4.4. Conclusion

Earlier substrate specificity studies showed that compared to other NRPS adenylation enzymes, TycA could adenylate an array of  $\alpha$ -amino acids and a few  $\beta$ -amino acids such as (*S*)- $\beta$ -homophenylalanine. <sup>36,37</sup> These data suggested indirectly that these amino acids could continue along the polyketide pathway to tyrocidine analogs. No isoserine analogs were tested except the bifunctional phenylserine isomer that was nearly as active ( $k_{cat} = 2.5 \pm 0.2 \text{ s}^{-1}$ ) as the natural substrate  $\alpha$ -phenylalanine ( $k_{cat} = 3.6 \pm 0.1 \text{ s}^{-1}$ ). <sup>36</sup> Tyc(Phe–AT) is involved in transient thioesterification of variously acylated AMP intermediates on its native pathway, and this guided the study herein to test the activity of Tyc(Phe–AT) with an isoserine and CoA substrates. In addition, the crystal structure of the orthologous gramicidin synthetase 1 (Grs1(Phe–A)) helped to select potentially productive isoserine analogs based on the modeled docking conformation of

(2R,3S)-phenylisoserine. It was interesting that Tyc(Phe–AT) could catalyze the thioesterification of isoserines since the active site shown previously has high structural complementarity to the natural substrate (S)- $\alpha$ -phenylalanine.<sup>37</sup> The hydrophobicity of the binding pocket residues that bind the aryl ring of the isoserines likely caused arylisoserines with small hydrophobic substituents to bind in a catalytically favorable orientation in the active site, thus speeding their turnover to the thioester products better than substrates with more hydrophilic substituents.

Tyc(Phe–AT) has similar relaxed substrate specificity as observed for other biocatalysts on the biosynthetic pathway of specialized metabolites. This is a desirable feature in synthetic biology when selecting biocatalysts to engineer a biosynthetic pathway that can recognize surrogate substrates. Thus Tyc(Phe–AT) catalyst has significant potential to biosynthesize an array of aminoacyl CoAs that can be used by different acyl CoA dependent acyltransferases to construct rare bioactive natural product analogs. For example, Tyc(Phe–AT) has direct application towards designing a biosynthetic route to produce paclitaxel analogs that contain modified arylisoserine side chains. To the best of my knowledge, there is currently no isoserine CoA ligase reported besides Tyc(Phe–AT).

#### 4.5. Future Direction

The synthesis of prostate cancer drug, cabazetaxel (Jevtana<sup>®</sup>) proceeds through an intermediate similar to that to paclitaxel (**Figure 4.19**). Foreseeably, Tyc(Phe–AT) can be used in the semi-biosynthetic process by providing biosynthetically derived precursors that can be further elaborated chemically to make the final product (**Figure 4.19**) without the need for protection groups.

**Figure 4.19**. Synthesis of cabazetaxel (Jevtana<sup>®</sup>). The broken arrow shows processes yet to be demonstrated in the proposed biosynthesis.

Some of the paclitaxel analogs that have shown promise in clinical trials contain pyridinyl in place of the phenyl ring at C-3' (see **Table 4.1** and **Figure 4.2**). Therefore, to support

the proposed paclitaxel analogs' biosynthesis pathway (see Figure 4.4), engineering Tyc(Phe-AT) to turnover pyridinyl substrates (such as in Tesetaxel) is proposed. In the literature, various crystal structures of enzymes that bind pyridinyl containing substrates contain residues capable of forming H bonding interaction with the nitrogen of the pyridinyl moiety in the binding pocket. 63-67 For example, the nitrogen of pyrimidinedione forms H-bonding interaction with the side chain hydroxyl of S367 in hepatitis CV NS5B polymerase inhibitor.<sup>68</sup> Additionally, a pyridylacetic acid derivative in complex with human dipeptidyl peptidase-4 binds close to Y547.<sup>69</sup> Also, the pyridinyl nitrogen at position 6 of naphthyridine forms a hydrogen bond with K384 of a protein kinase C protein. 70 In a different study, the nitrogen of pyridyldiaminothiazole (an inhibitor of cyclin-dependent kinase 2) forms H-bonding interaction with K33,71 whereas a Q726 side chain amine binds next to the nitrogen of pyrazologuinoline derivative in the phosphodiesterase 10A active site.<sup>72</sup> This trend in H-bonding interaction was also observed with N-arylamidopyridinylacetamide and H163 in SARS coronavirus 3Cl protease. 73 Thus, mutation of the aryl binding site in Tyc(Phe-AT) to parallel the residues capable of H-bonding in the highlighted examples may enhance the binding of pyridinylisoserine analogs in a conformation favorable for catalysis. At a starting point, the proposed mutations would involve the residues that interact with the phenyl ring carbons at the *ortho-*, *meta-*, and *para-* positions, namely A224, T266, and W227, respectively (this is the residue numbering in Tyc(Phe–AT)).

## **APPENDIX**

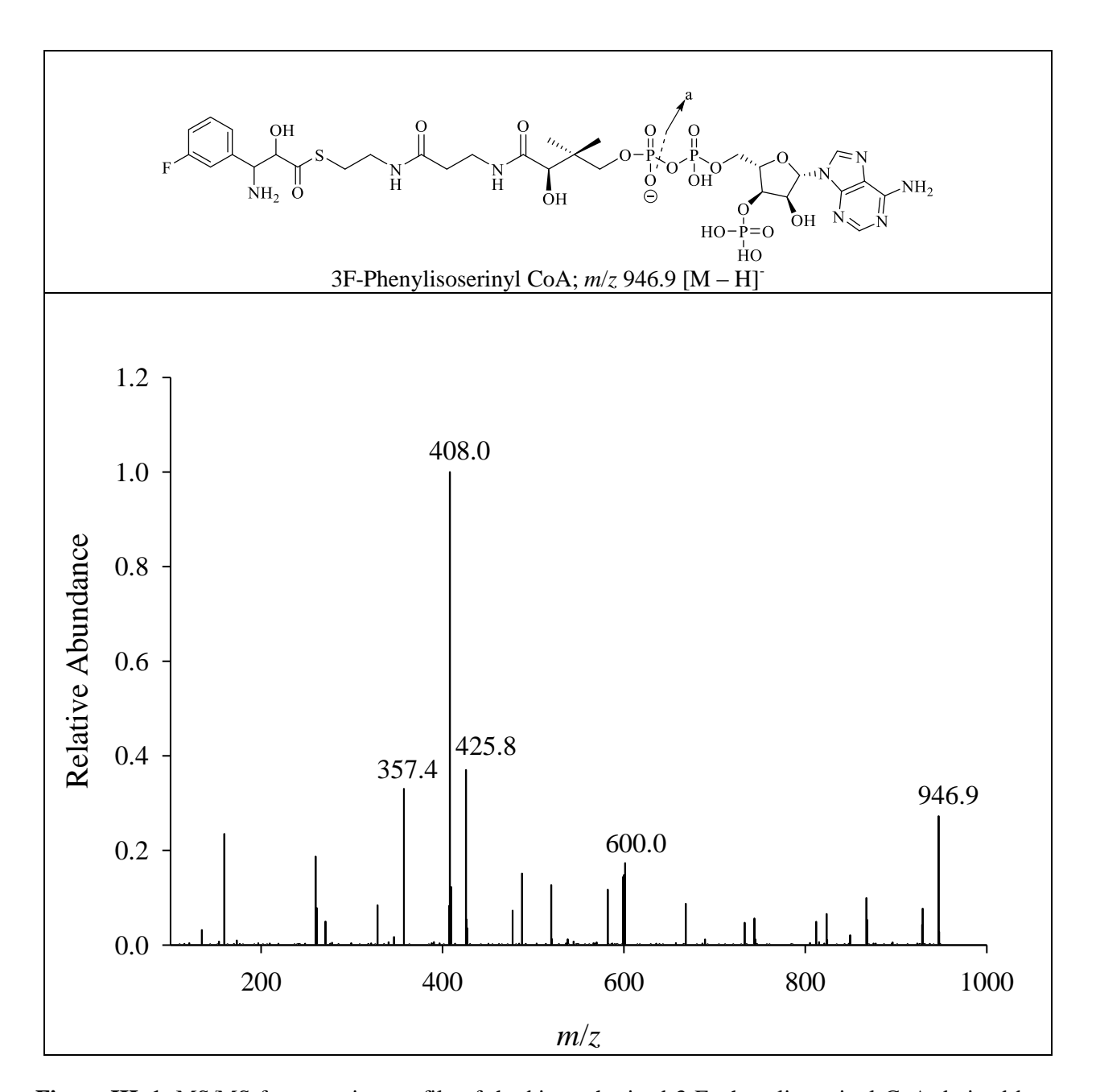


**Figure III–1**. MS/MS fragment ion profile of the biosynthesized 3-F–phenylisoserinyl CoA derived by Tyc(Phe–AT) catalysis is shown. The diagnostic fragment ions were identified as m/z: 946.9 [M – H]<sup>-</sup>, 600.0 [m/z 946.9 – AMP]<sup>-</sup>, 425.8 (fragment a), 408.0 [m/z 425.8 – H<sub>2</sub>O]<sup>-</sup>.

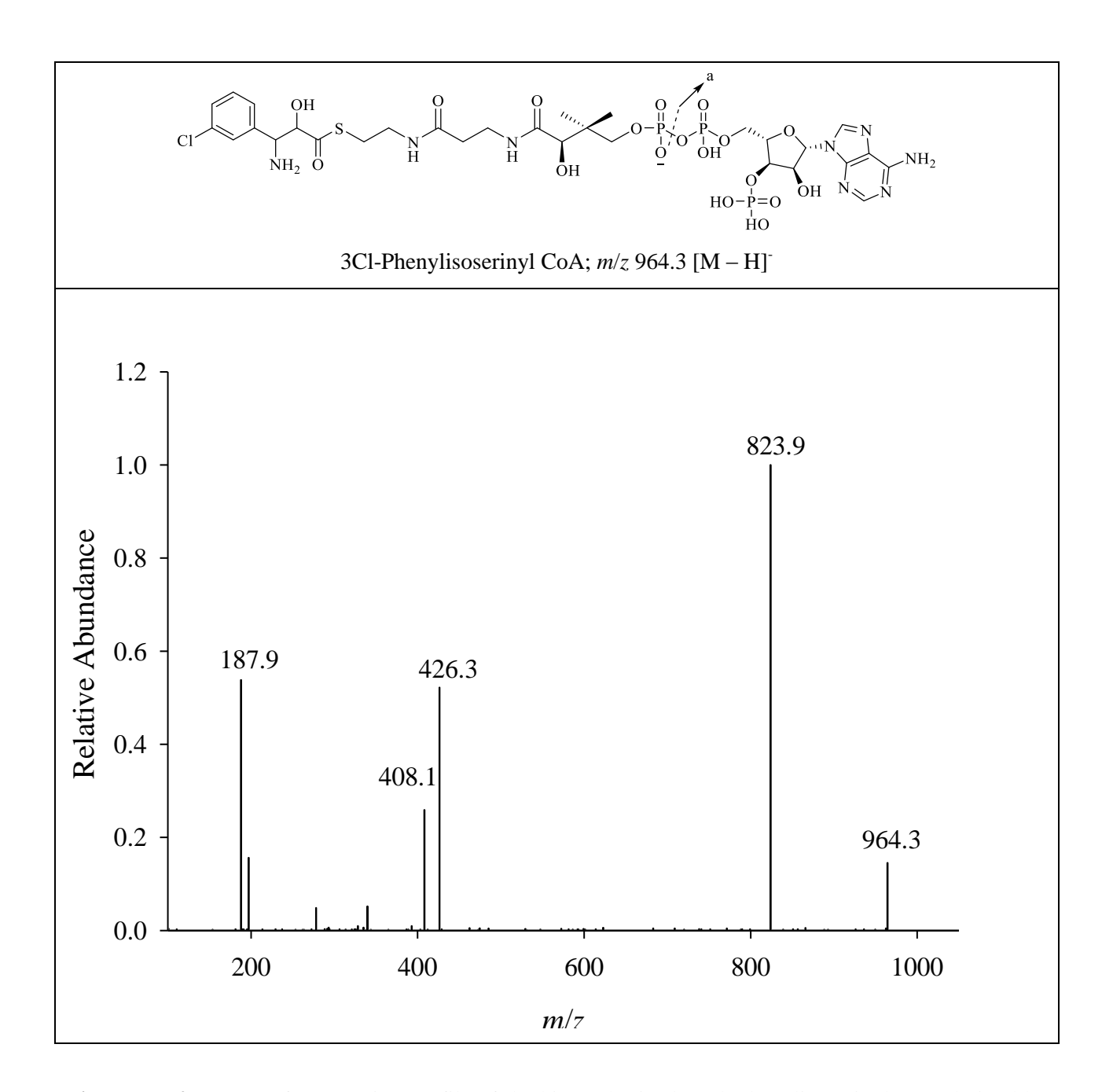


**Figure III–2.** MS/MS fragment ion profile of the biosynthesized 3-Cl–phenylisoserinyl CoA derived by Tyc(Phe–AT) catalysis is shown. The diagnostic fragment ions were identified as m/z: 964.3 [M – H]<sup>-</sup>, 823.9 [m/z 964.3 – 3Cl-benzylamine]<sup>-</sup>, 426.3 (fragment a), 408.1 [m/z 426.3 – H<sub>2</sub>O]<sup>-</sup>.

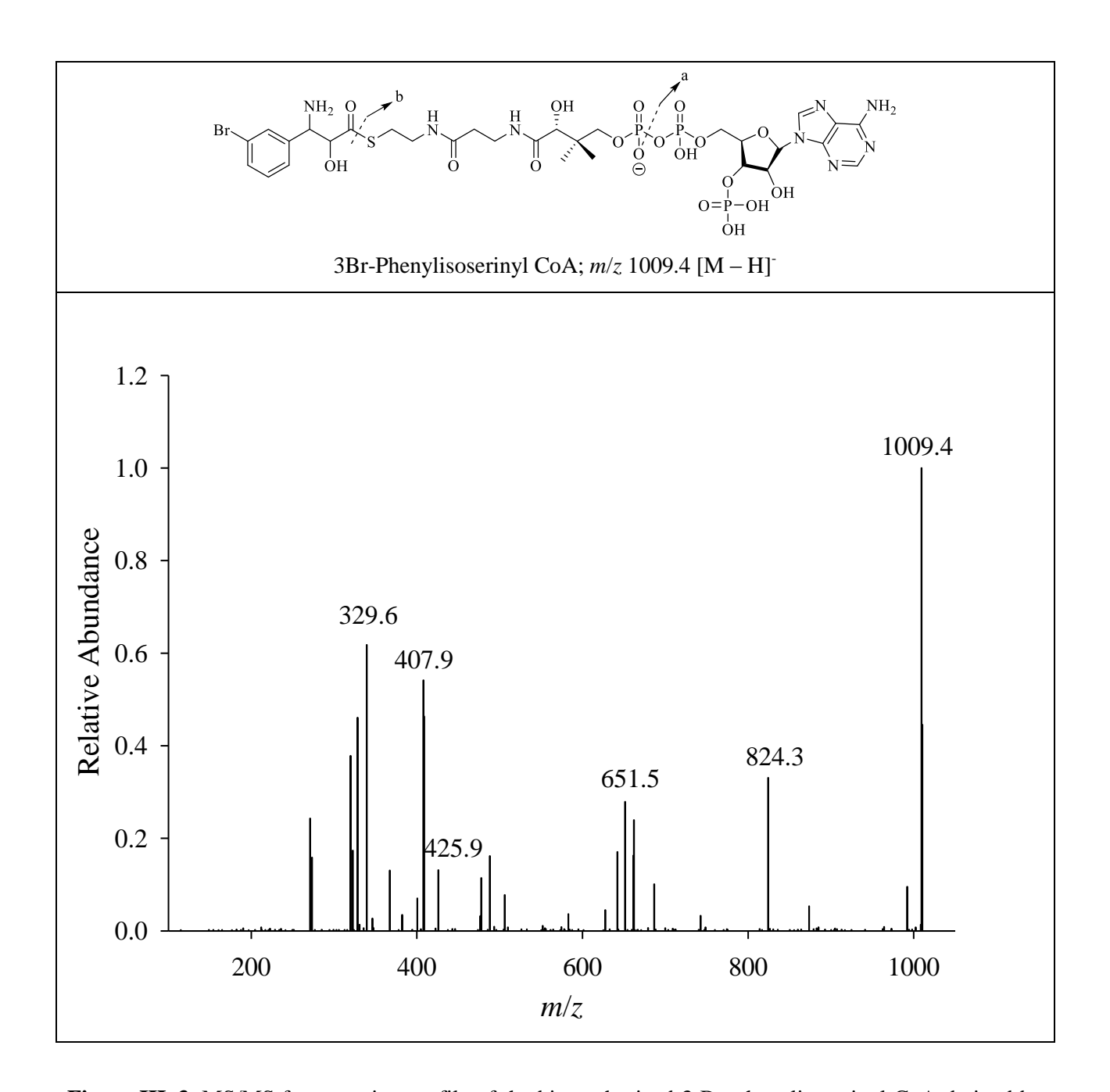


**Figure III–3.** MS/MS fragment ion profile of the biosynthesized 3-Br–phenylisoserinyl CoA derived by Tyc(Phe–AT) catalysis is shown. The diagnostic fragment ions were identified as m/z: 1009.4 [M – H]<sup>-</sup>, 824.3 [m/z 1009.4 – 3-Br-benzylamine]<sup>-</sup>, 651.5 [b – H<sub>2</sub>PO4 – H<sub>2</sub>O]<sup>-</sup>, 425.9 (fragment a), 407.9 [m/z 425.9 – H<sub>2</sub>O]<sup>-</sup>, 329.6 [m/z 407.9 – H<sub>2</sub>PO<sub>3</sub>]<sup>-</sup>.

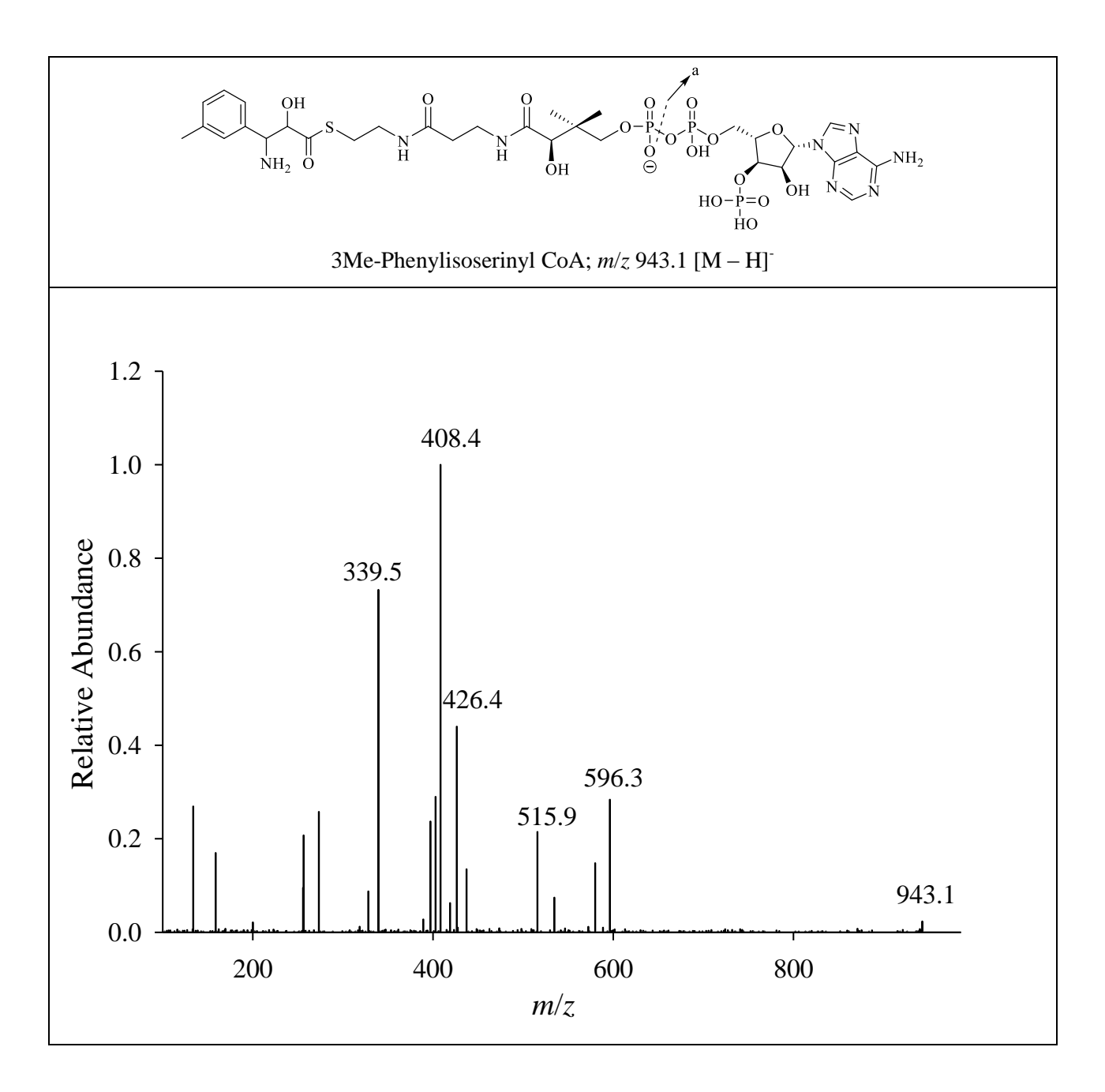


**Figure III–4.** MS/MS fragment ion profile of the biosynthesized 3-Me–phenylisoserinyl CoA derived by Tyc(Phe–AT) catalysis is shown. The diagnostic fragment ions were identified as m/z: 943.1 [M – H]<sup>-</sup>, 596.3 [m/z 943.1 – AMP]<sup>-</sup>, 515.9 [m/z 596.3 – HPO<sub>3</sub>]<sup>-</sup>, 426.4 (fragment a), 408.4 [m/z 426.4 – H<sub>2</sub>O]<sup>-</sup>.

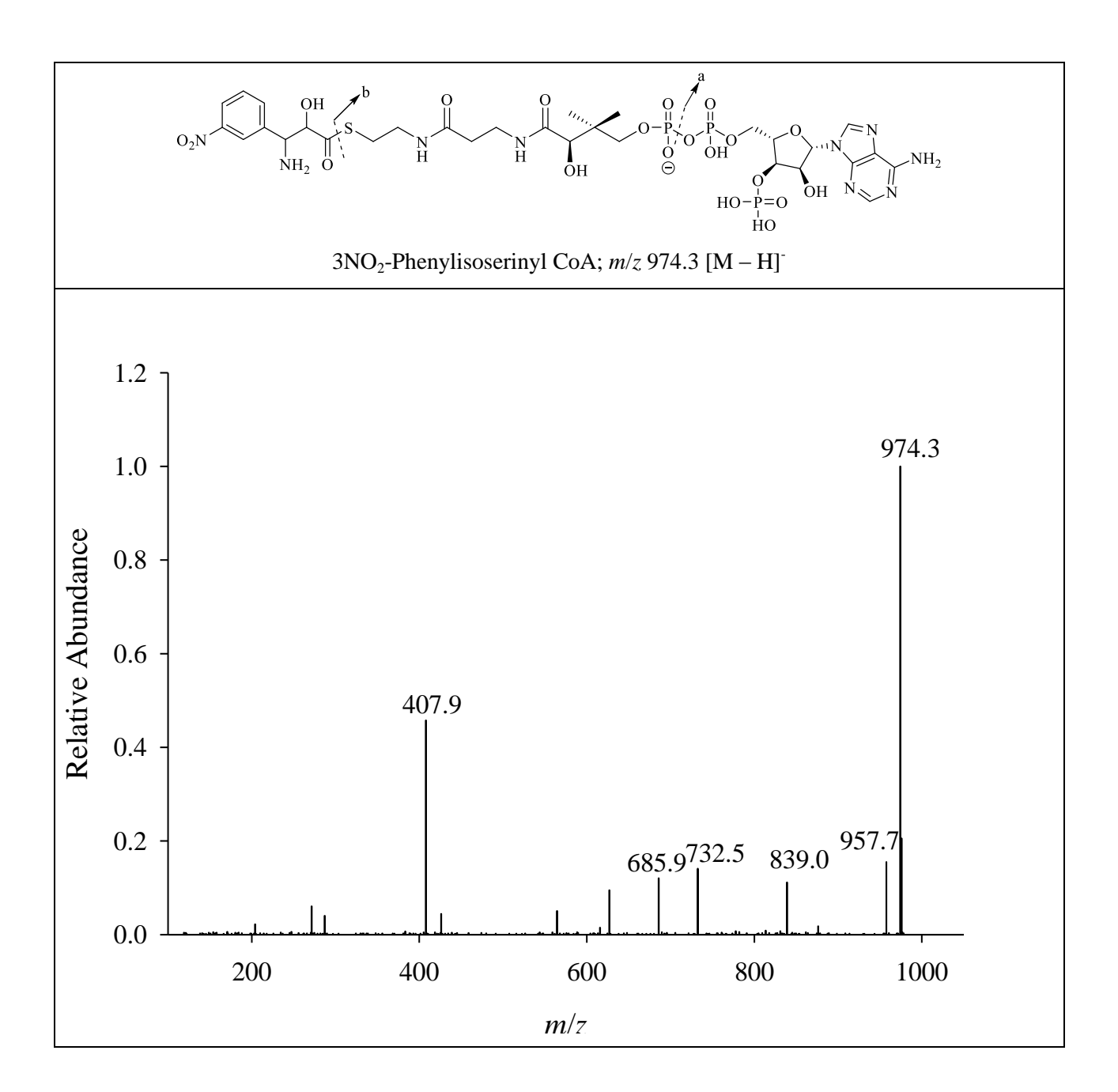


**Figure III–5**. MS/MS fragment ion profile of the biosynthesized 3-NO<sub>2</sub>—phenylisoserinyl CoA derived by Tyc(Phe–AT) catalysis is shown. The diagnostic fragment ions were identified as m/z: 974.3 [M – H]<sup>-</sup>, 957.7 [m/z 974.3 – OH]<sup>-</sup>, 839.0 [m/z 974.3 – adenine]<sup>-</sup>, 732.5 [m/z 974.3 – 3-NO<sub>2</sub>—phenylisoserinyl – H<sub>2</sub>O]<sup>-</sup>, 685.9 [b – H<sub>2</sub>PO<sub>3</sub>]<sup>-</sup>. 407.9 [a – H<sub>2</sub>O]<sup>-</sup>.

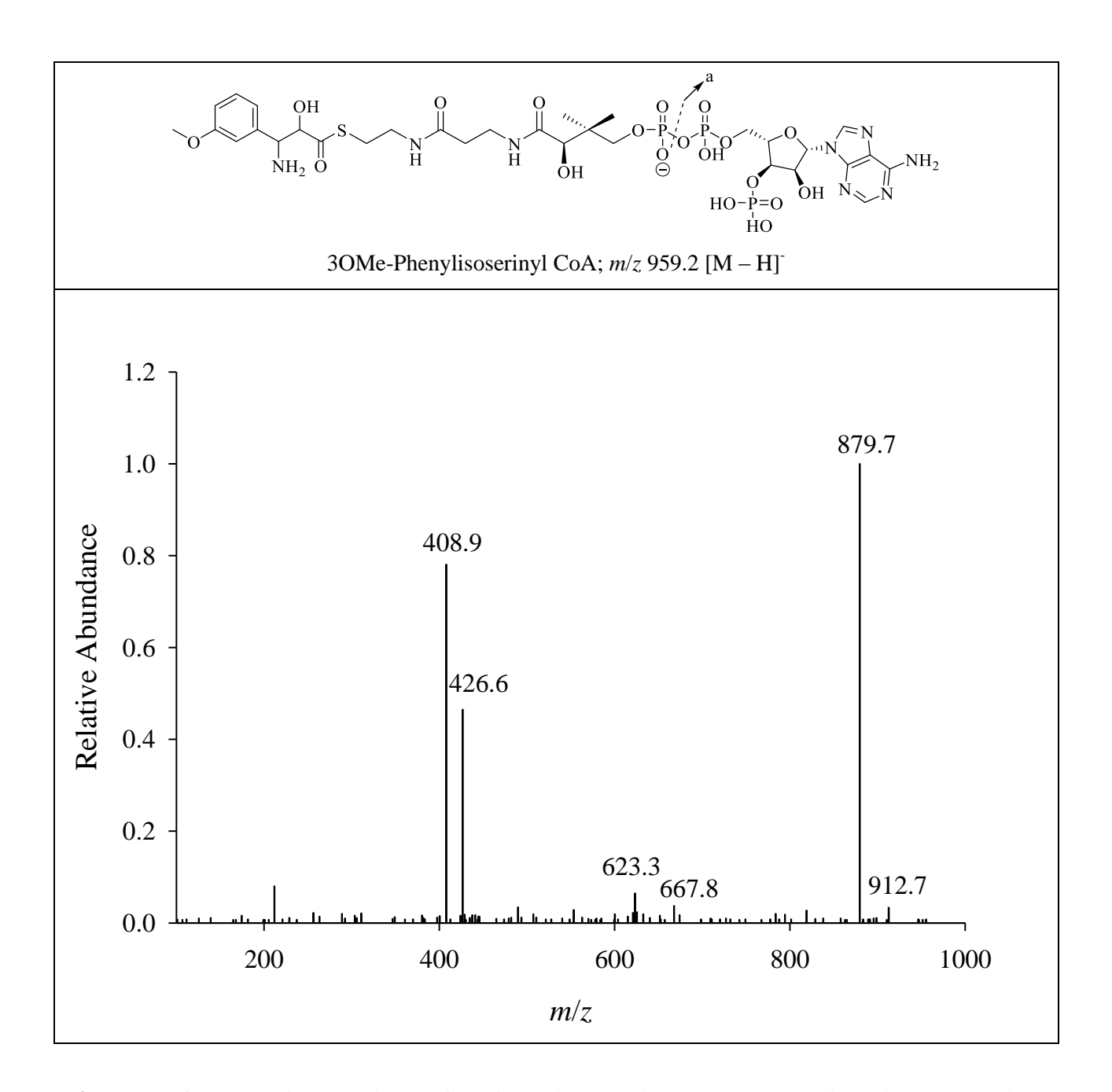


**Figure III–6**. MS/MS fragment ion profile of the biosynthesized 4-OMe–phenylisoserinyl CoA derived by Tyc(Phe–AT) catalysis is shown. The diagnostic fragment ions were identified as m/z: 879.7 [m/z 959.2 – HPO<sub>3</sub>], 667.8 [m/z 879.7 – 4-OMe–phenylisoserinyl – H<sub>2</sub>O], 426.6 (fragment a), 407.9 [m/z 426.6 – H<sub>2</sub>O].

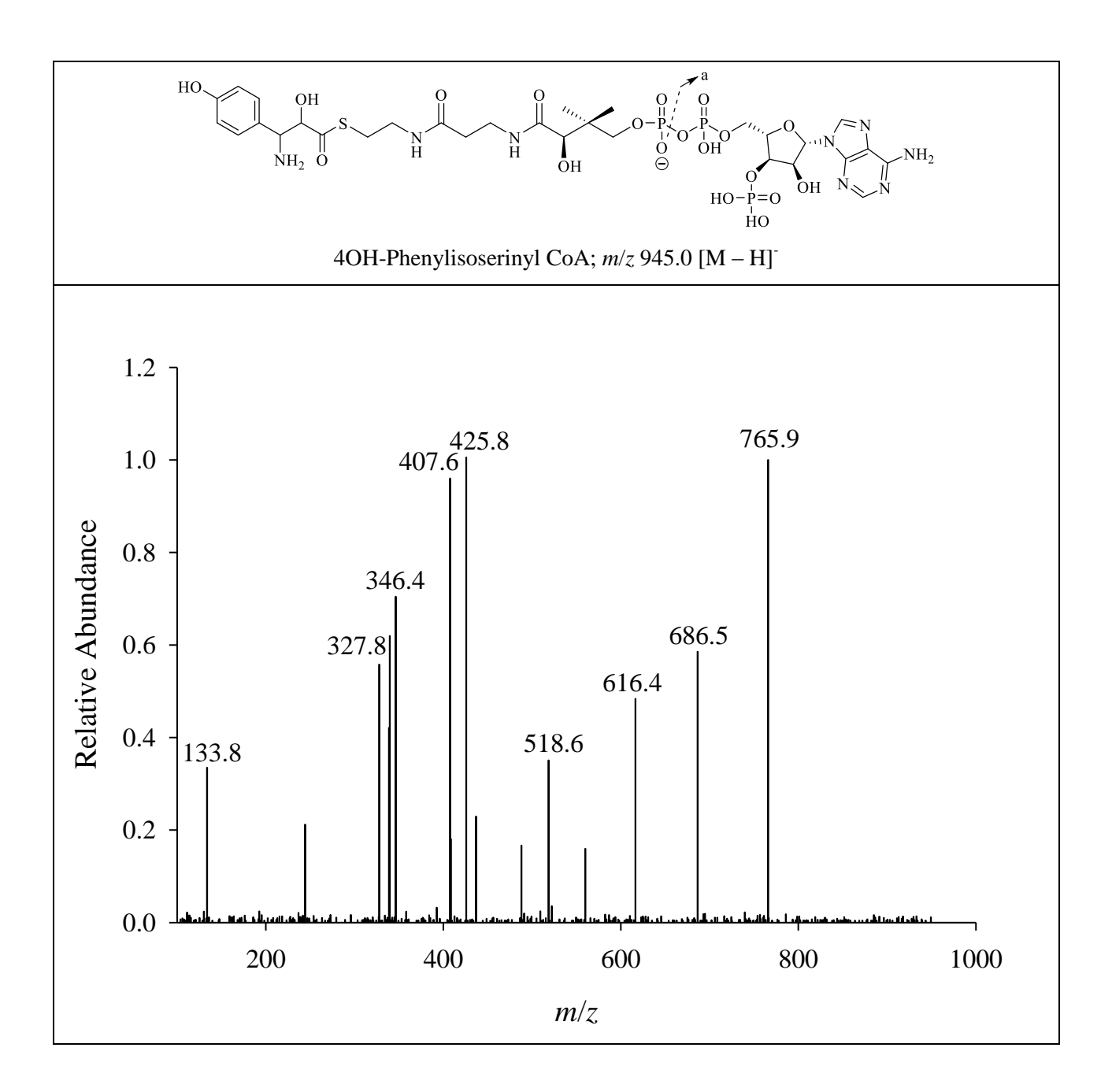


**Figure III–7**. MS/MS fragment ion profile of the biosynthesized 4-OH–Phenylisoserinyl CoA derived by Tyc(Phe–AT) catalysis is shown. The diagnostic fragment ions were identified as m/z: 765.9 [m/z 945.0 – 4-OH–phenylisoserinyl], 686.5 [m/z 765.9 – H<sub>2</sub>PO<sub>3</sub>], 616.4 [m/z 945.0 – adenosine], 518.6 [m/z 616.4 – HPO<sub>4</sub>], 425.8 (fragment a), 407.8 [m/z 425.8 – H<sub>2</sub>O], 346.4 [m/z 425.8 – HPO<sub>3</sub>], 133.8 [adenine].

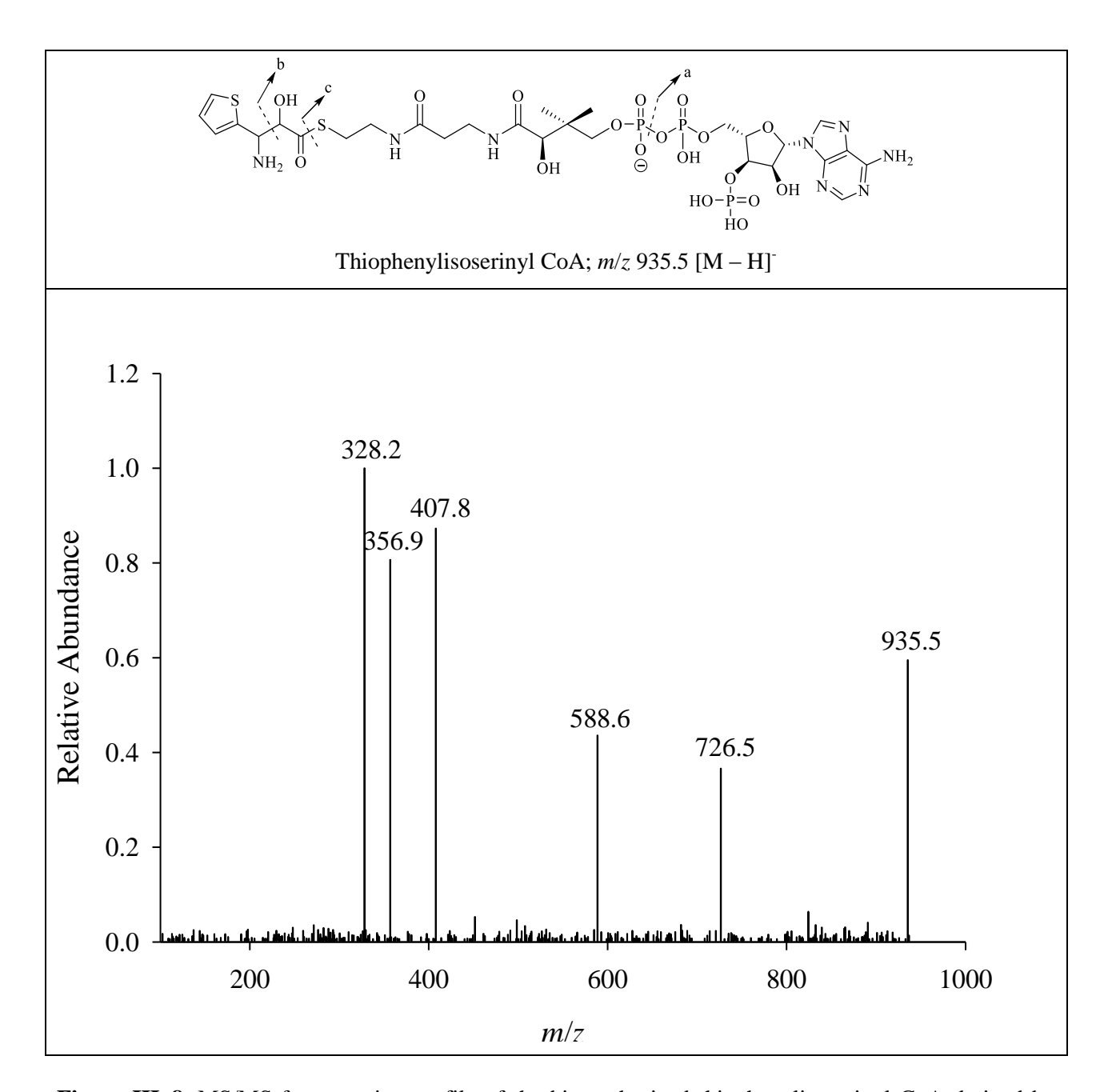


**Figure III–8**. MS/MS fragment ion profile of the biosynthesized thiophenylisoserinyl CoA derived by Tyc(Phe–AT) catalysis is shown. The diagnostic fragment ions were identified as m/z: 935.5 [M – H]<sup>-</sup>, 726.5 [b – H<sub>2</sub>PO<sub>3</sub> – H<sub>2</sub>O]<sup>-</sup>, 588.6 [m/z 935.5 – AMP – H<sub>2</sub>O]<sup>-</sup>, 425.8 (fragment a), 408.0 [m/z 425.8 – H<sub>2</sub>O]<sup>-</sup> 356.9 [fragment c – m/z 408]<sup>-</sup>, 328.2 [m/z 408.0 – HPO<sub>3</sub>]<sup>-</sup>.

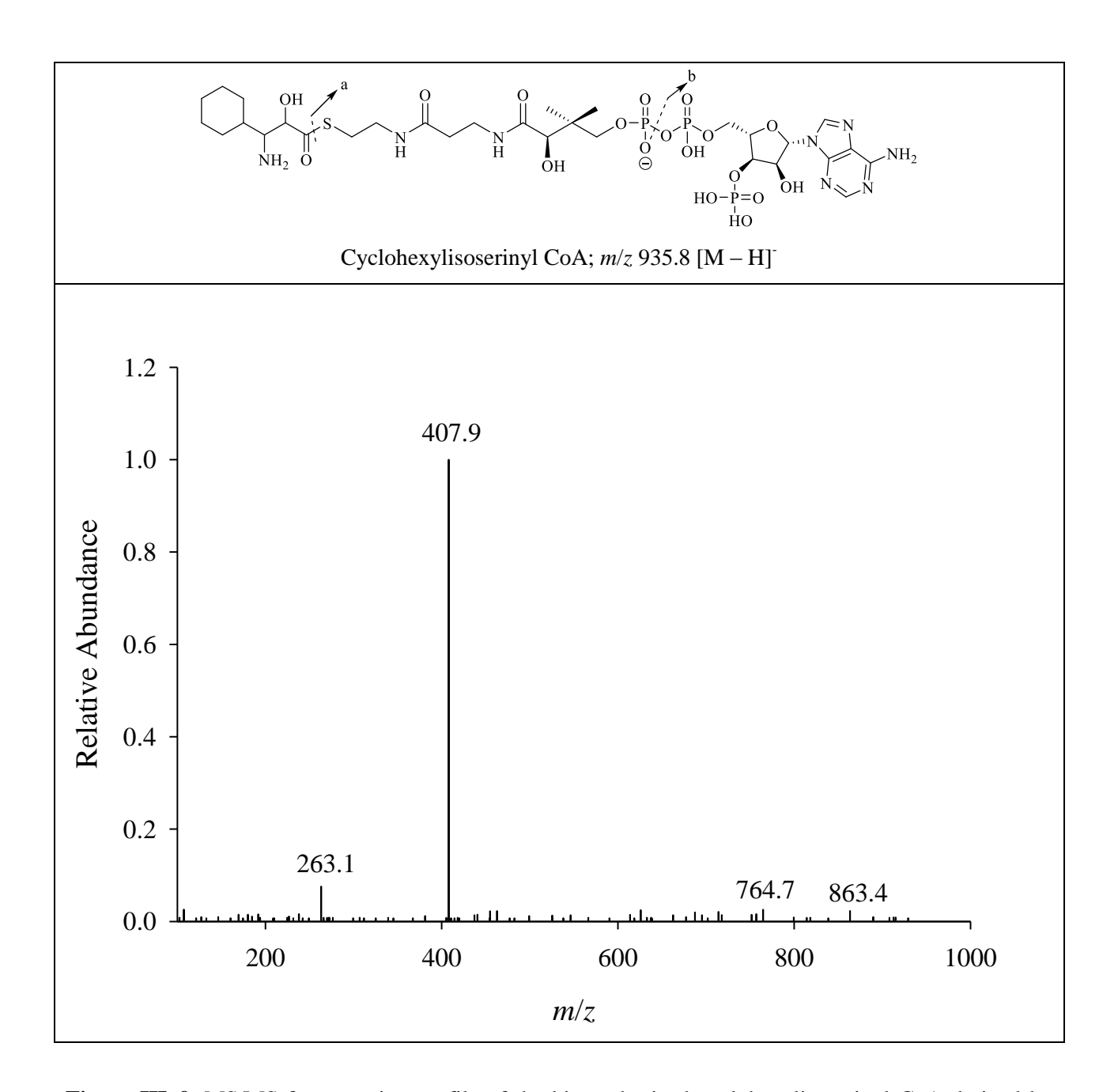


**Figure III–9.** MS/MS fragment ion profile of the biosynthesized cyclohexylisoserinyl CoA derived by Tyc(Phe–AT) catalysis is shown. The diagnostic fragment ions were identified as m/z: 863.4 [M – 4(H<sub>2</sub>O)], 764.7 (fragment a), 408.0 [fragment b – H<sub>2</sub>O].

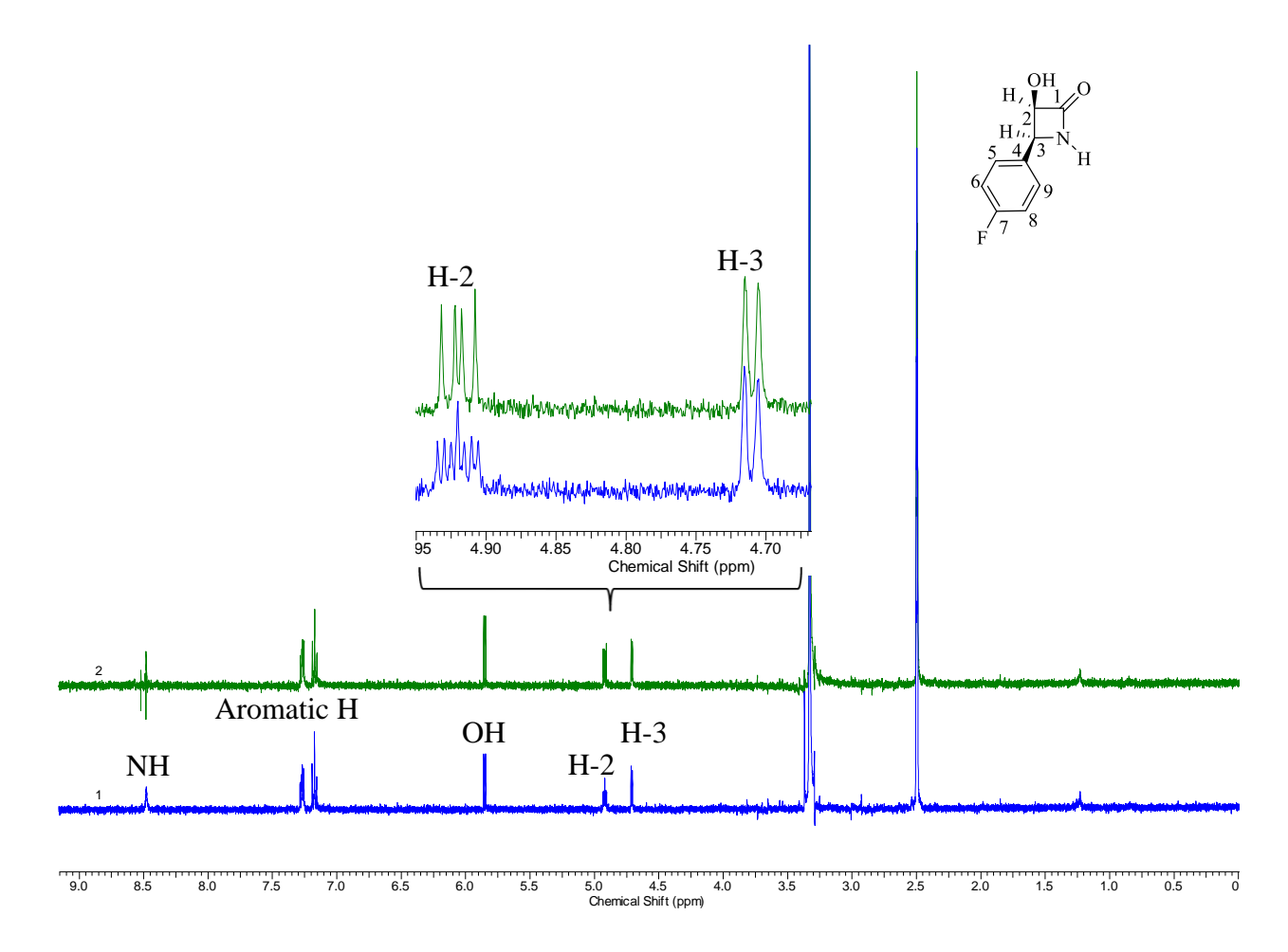


**Figure III–10.**  $^{1}$ H Homodecoupling NMR spectrum of 3-Hydroxy-4-(4-fluorophenyl)azetidin-2-one. Panel 1 shows the  $^{1}$ H-NMR before decoupling where H-2' gave a ddd (J = 7.34, 4.89, 2.45 Hz) as a result of long range coupling with NH as well as 3'-H and 2'-OH protons. Panel 2 shows loss of coupling for H-2' when NH was decoupled resulting to a dd (coupling with 3'-H and 2'-OH, J = 7.34, 4.89 Hz). The inset shows the change in splitting pattern of H-2' before (blue) and after (green)  $^{1}$ H Homodecoupling NMR.

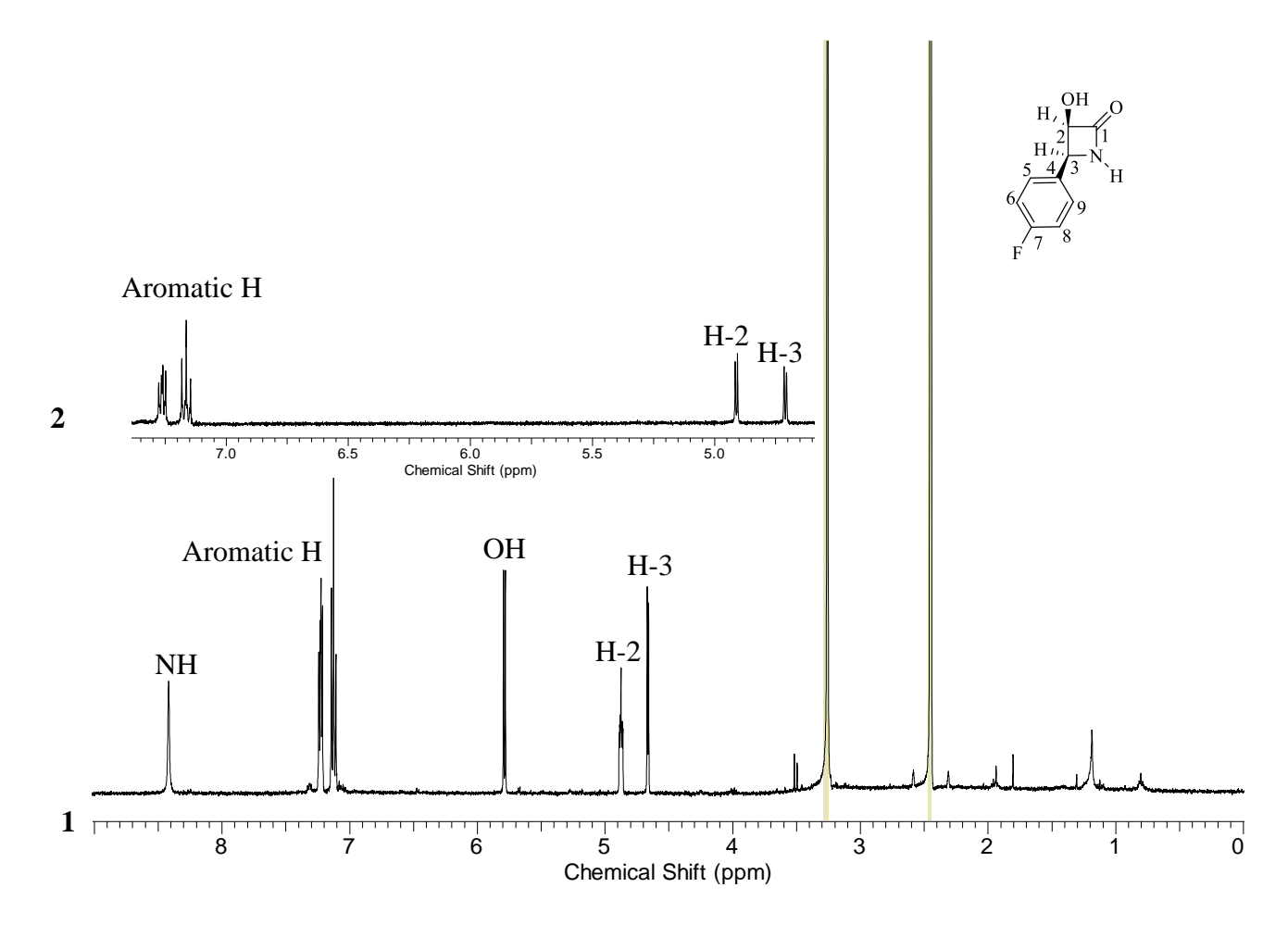
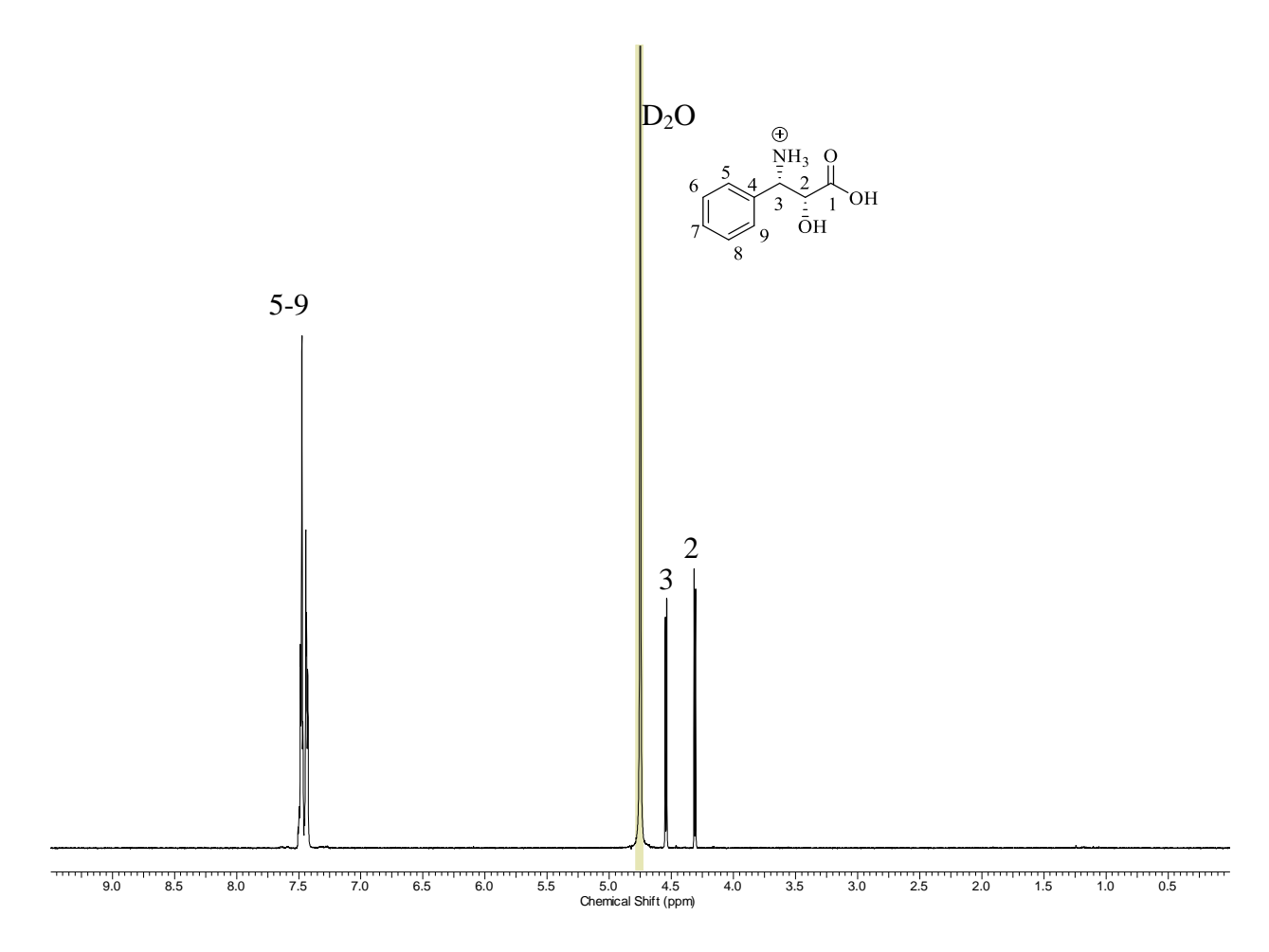
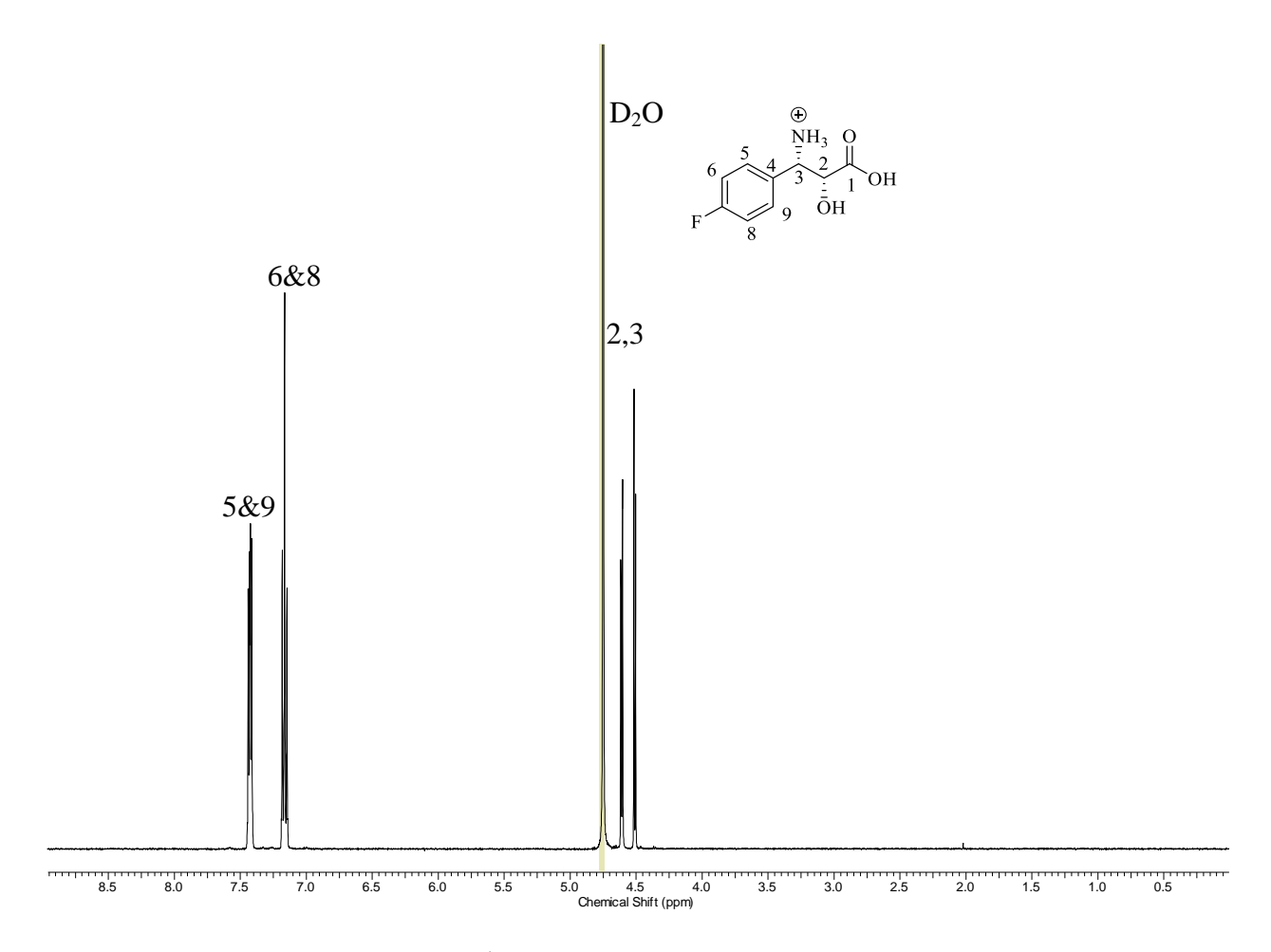


Figure III–11.  $\underline{\text{H}_2\text{O}/\text{D}_2\text{O}}$  exchange NMR spectrum of 3-Hydroxy-4-(4-fluorophenyl)azetidin-2-one. Panel 1 shows the H-NMR before  $D_2\text{O}$  exchange where OH and NH proton peaks are observed. Panel 2 shows loss of a doublet at 5.89 corresponding to 2'-OH, and a broad singlet at 8.46 ppm corresponding to NH proton. Also, there is loss of coupling to the H-2' which changed from a ddd to a doublet. This confirms coupling of the 2'-H with OH as well as NH.



**Figure III–12**. <sup>1</sup>H-NMR spectrum of phenylisoserine.



**Figure III–13**. <sup>1</sup>H-NMR spectrum of *p*-F–phenylisoserine.

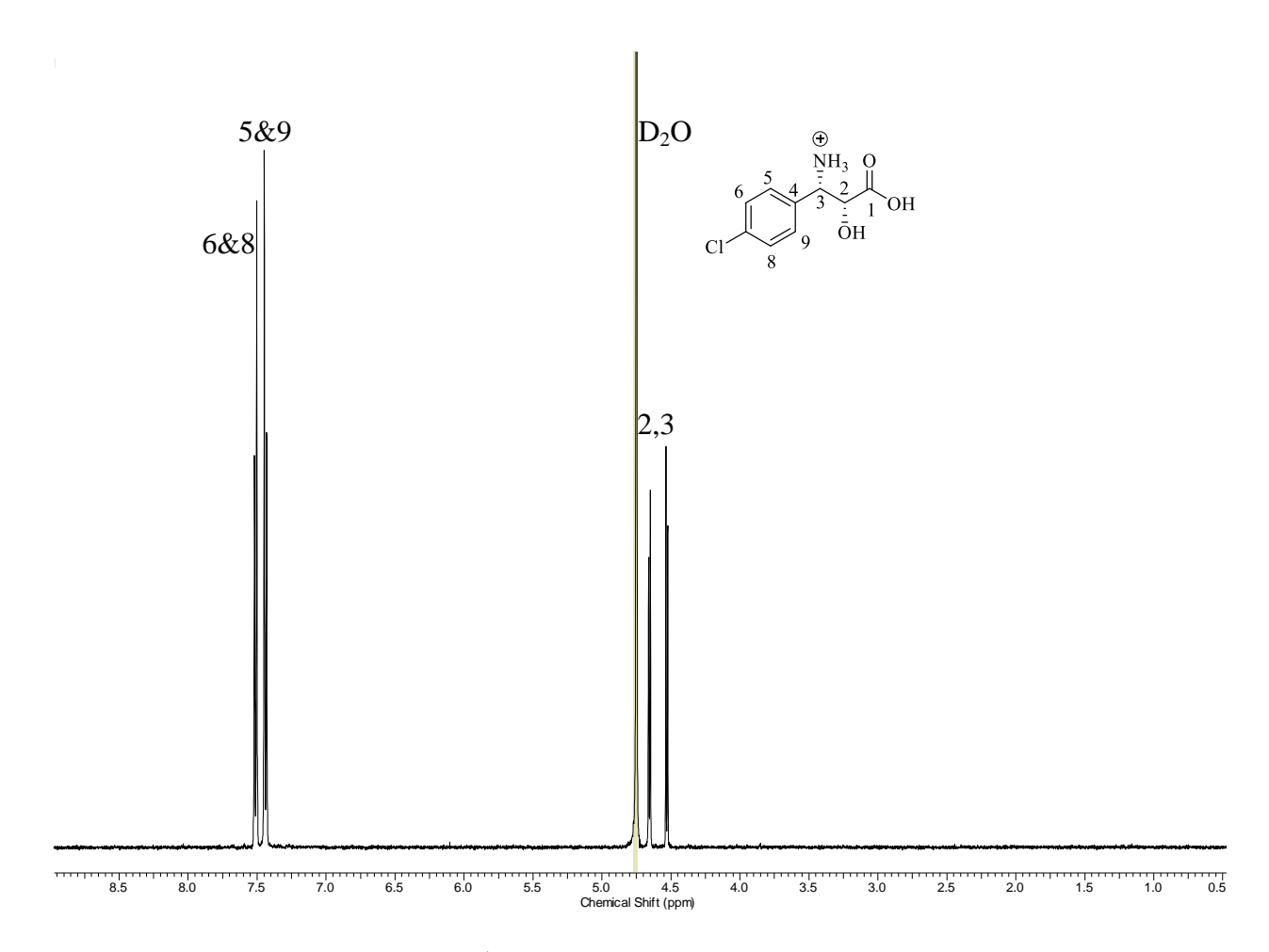


**Figure III–14**. <sup>1</sup>H-NMR spectrum of *p*-Cl–phenylisoserine.

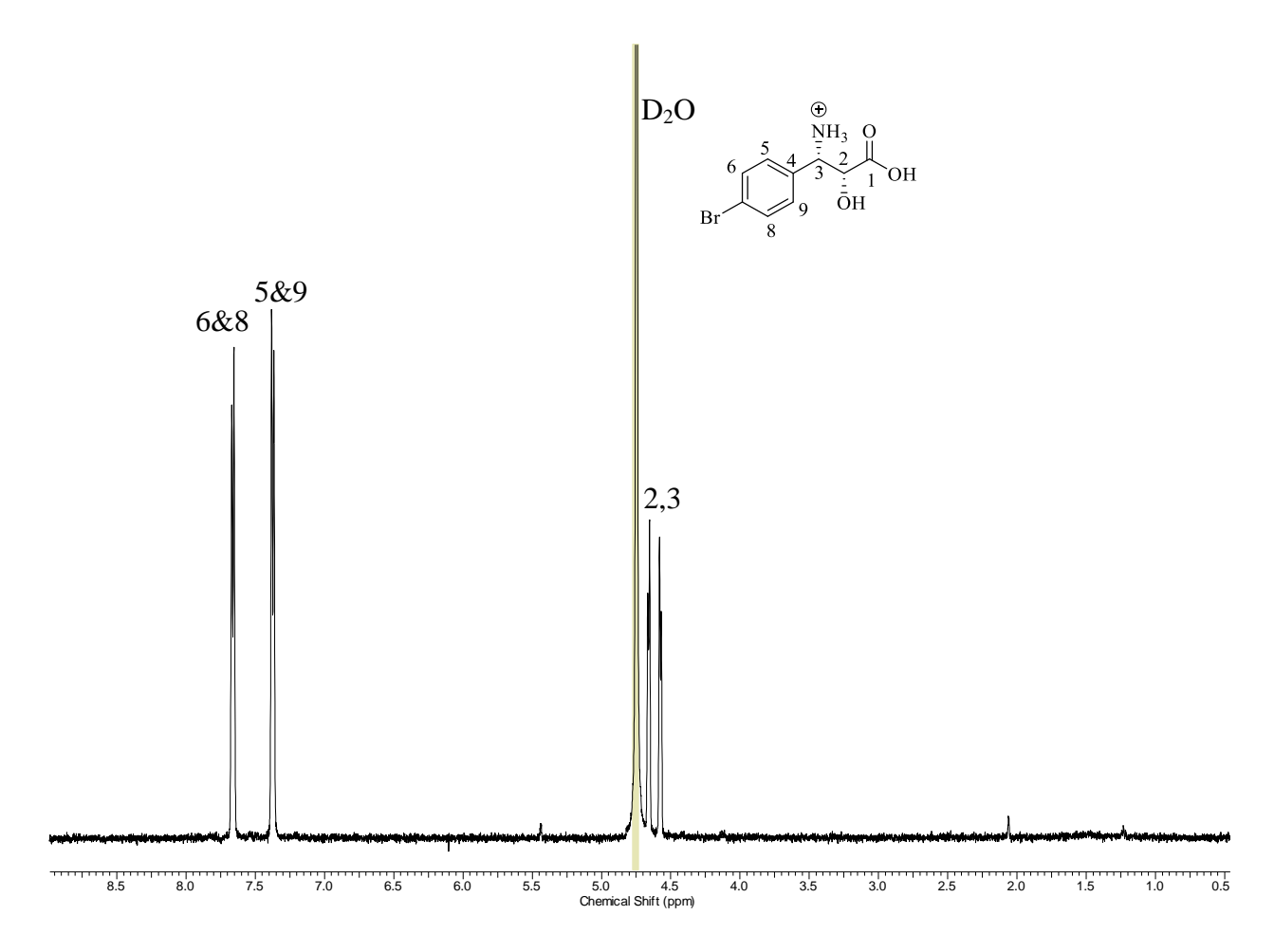


**Figure III–15**. <sup>1</sup>H-NMR spectrum of *p*-Br–phenylisoserine.

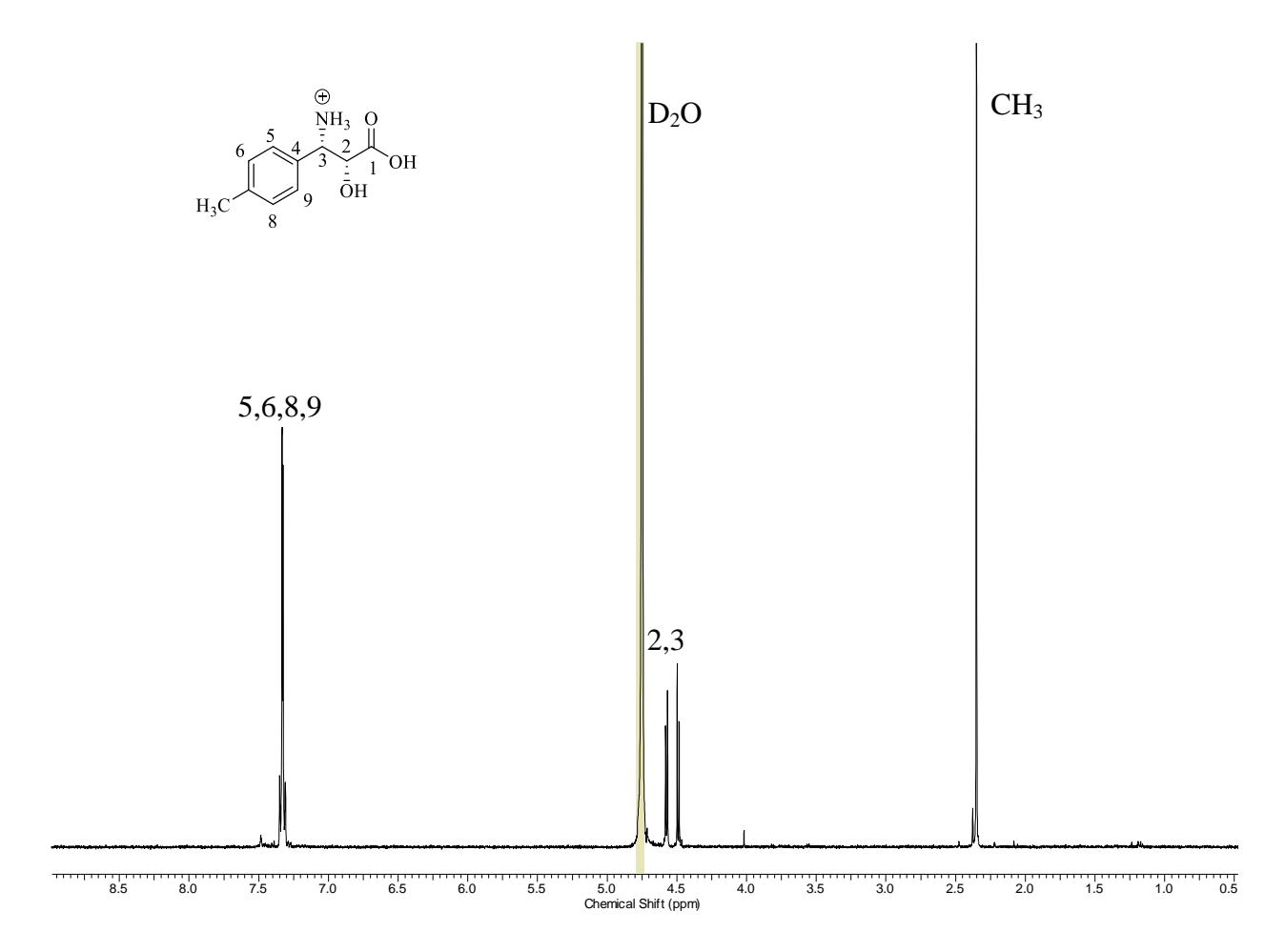


**Figure III–16**. <sup>1</sup>H-NMR spectrum of *p*-Me–phenylisoserine.

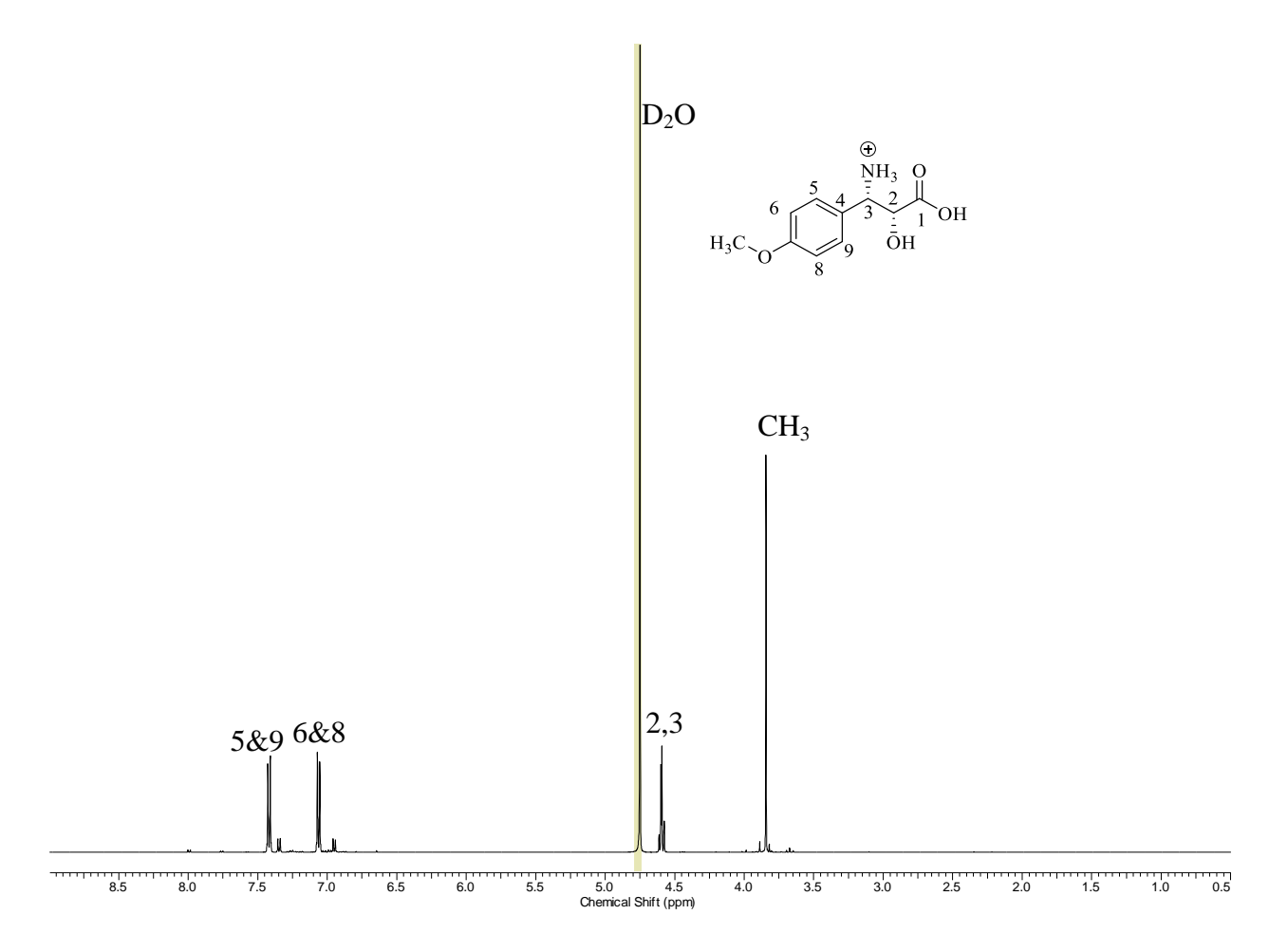


**Figure III–17**. <sup>1</sup>H-NMR spectrum of *p*-OMe–phenylisoserine.

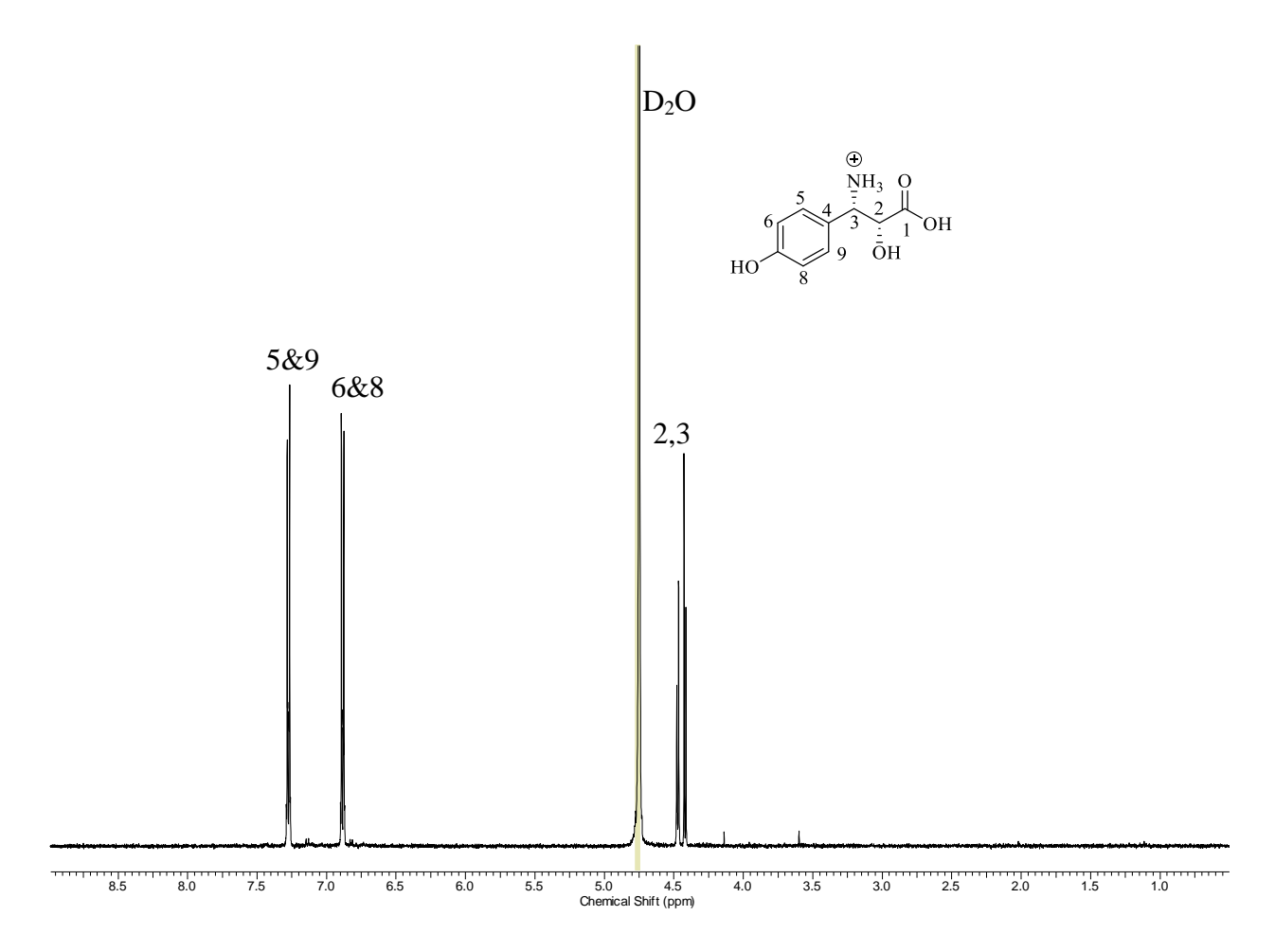


**Figure III–18**. <sup>1</sup>H-NMR spectrum of *p*-OH–phenylisoserine.

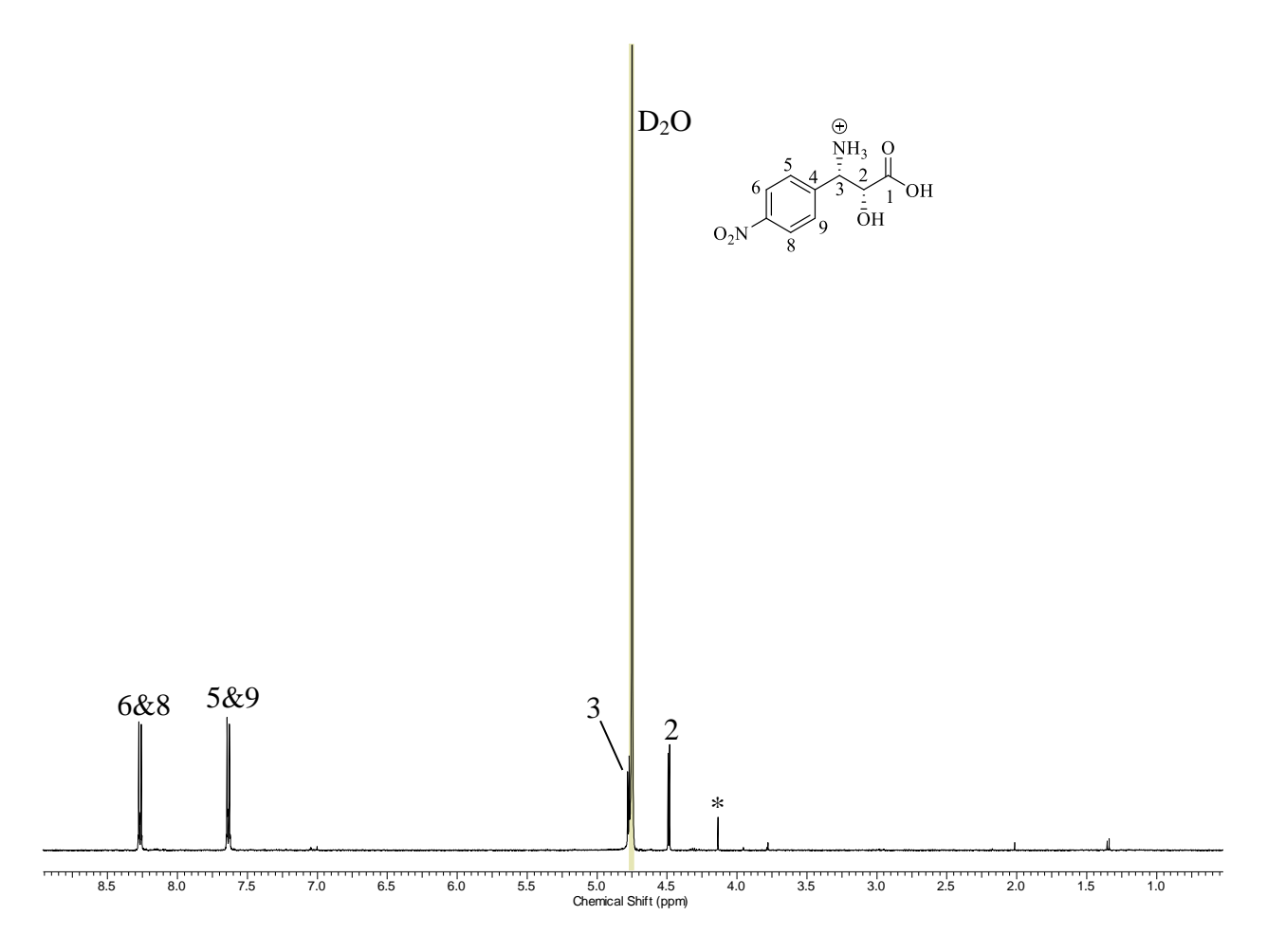


**Figure III–19**. <sup>1</sup>H-NMR spectrum of *p*-NO<sub>2</sub>—phenylisoserine. The asterisk (\*) denotes an impurity.

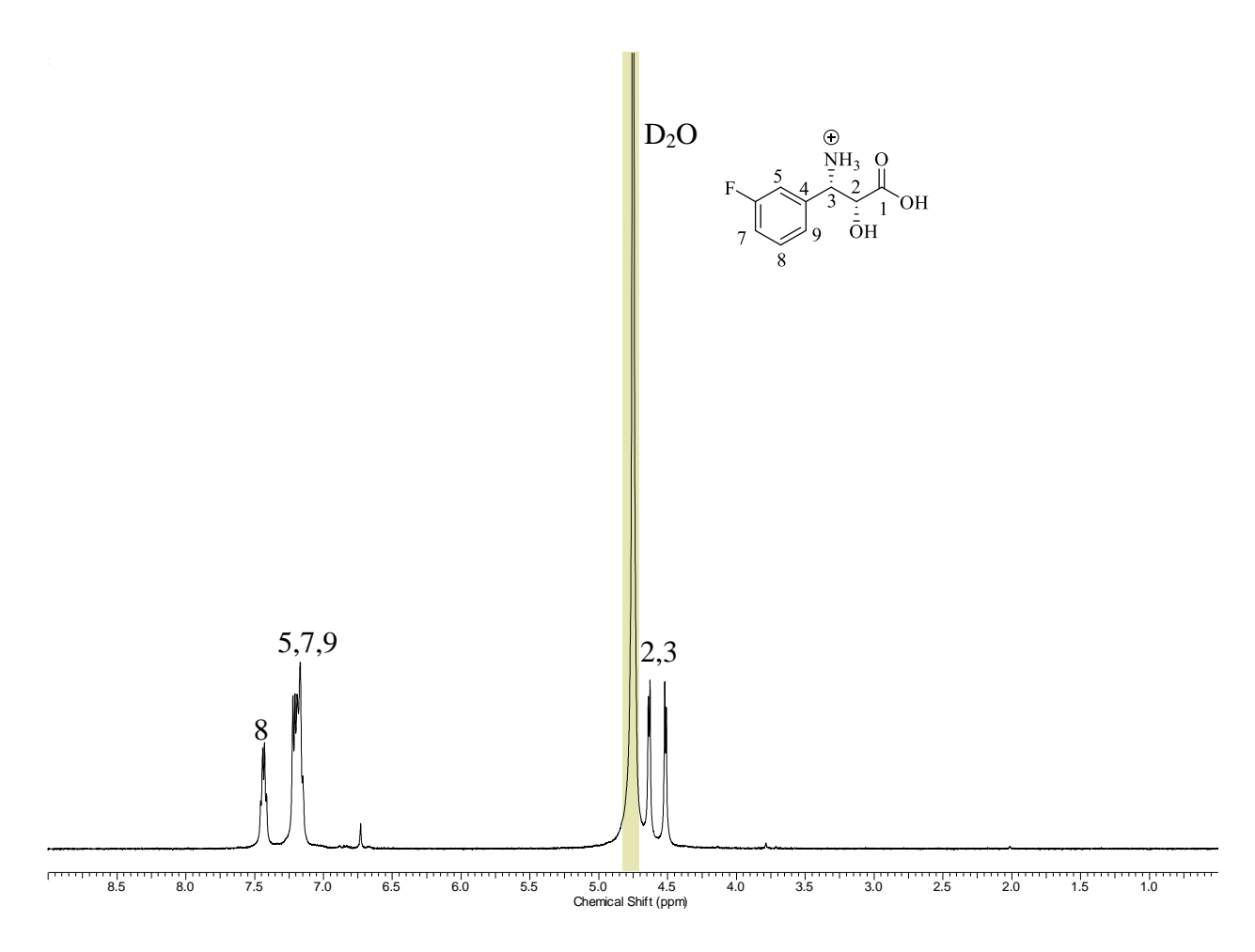


**Figure III–20**. <sup>1</sup>H-NMR spectrum of *m*-F–phenylisoserine.

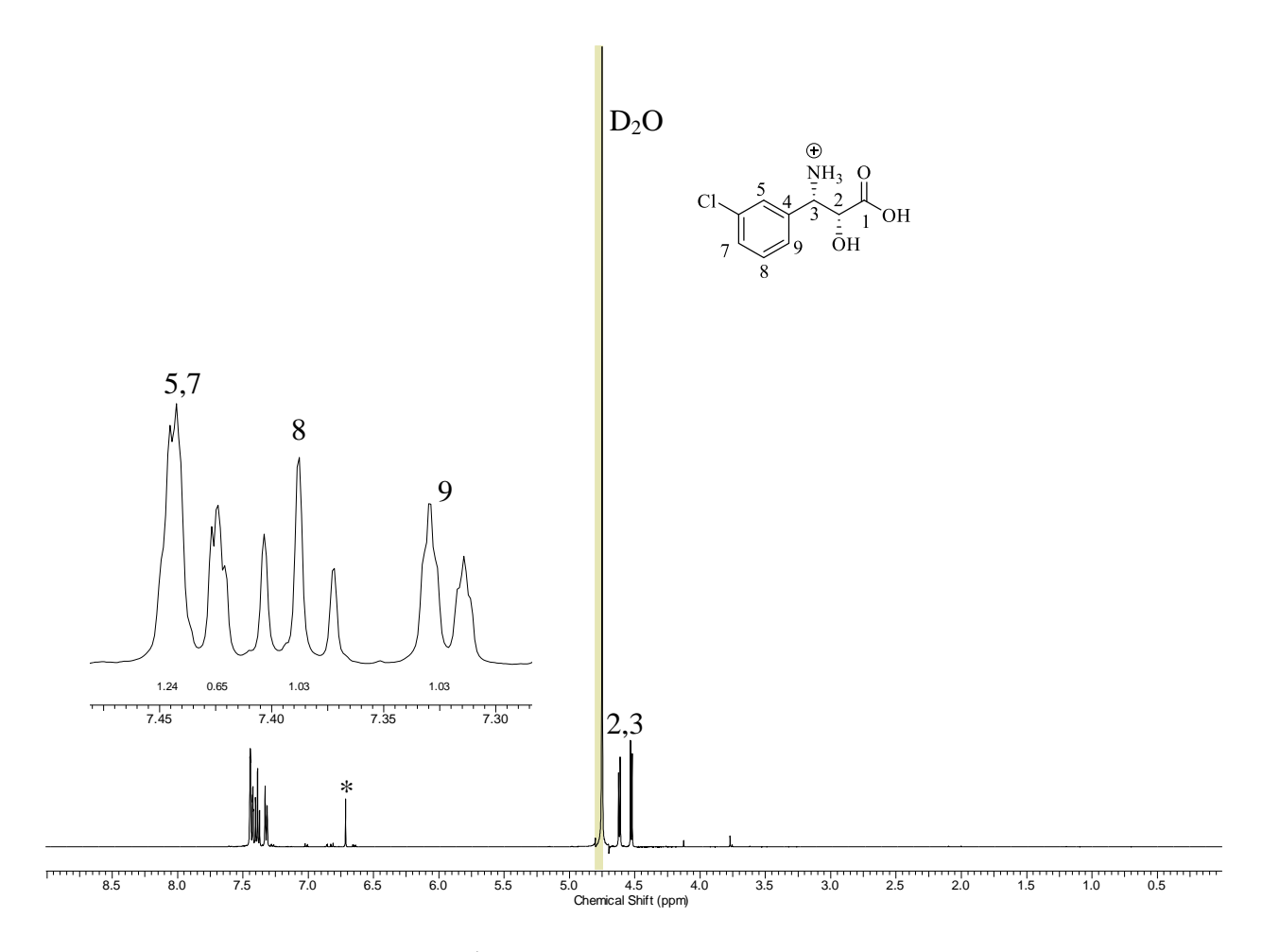


**Figure III–21**. <sup>1</sup>H-NMR spectrum of *m*-Cl–phenylisoserine.

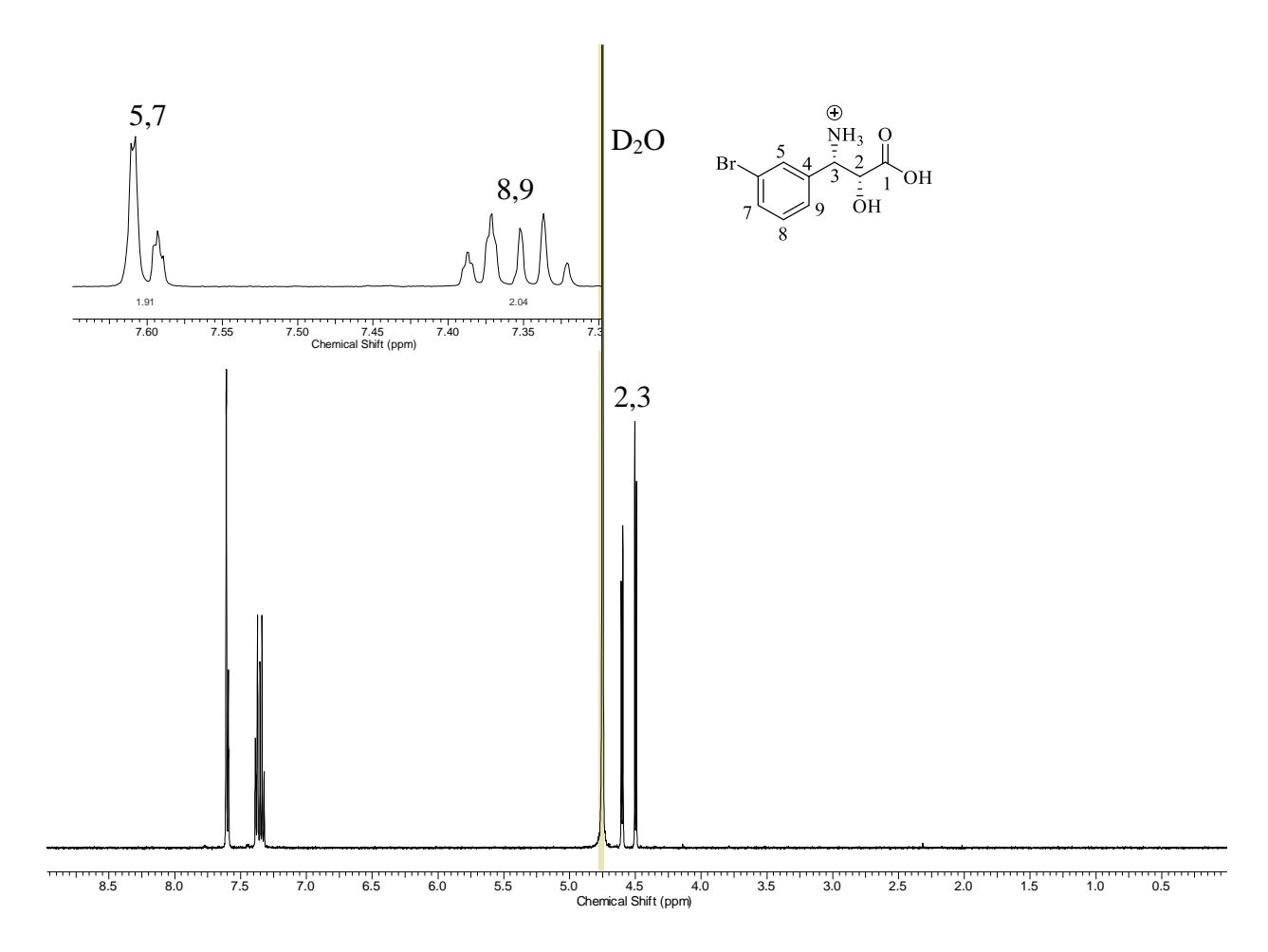


**Figure III–22**. <sup>1</sup>H-NMR spectrum of *m*-Br–phenylisoserine.

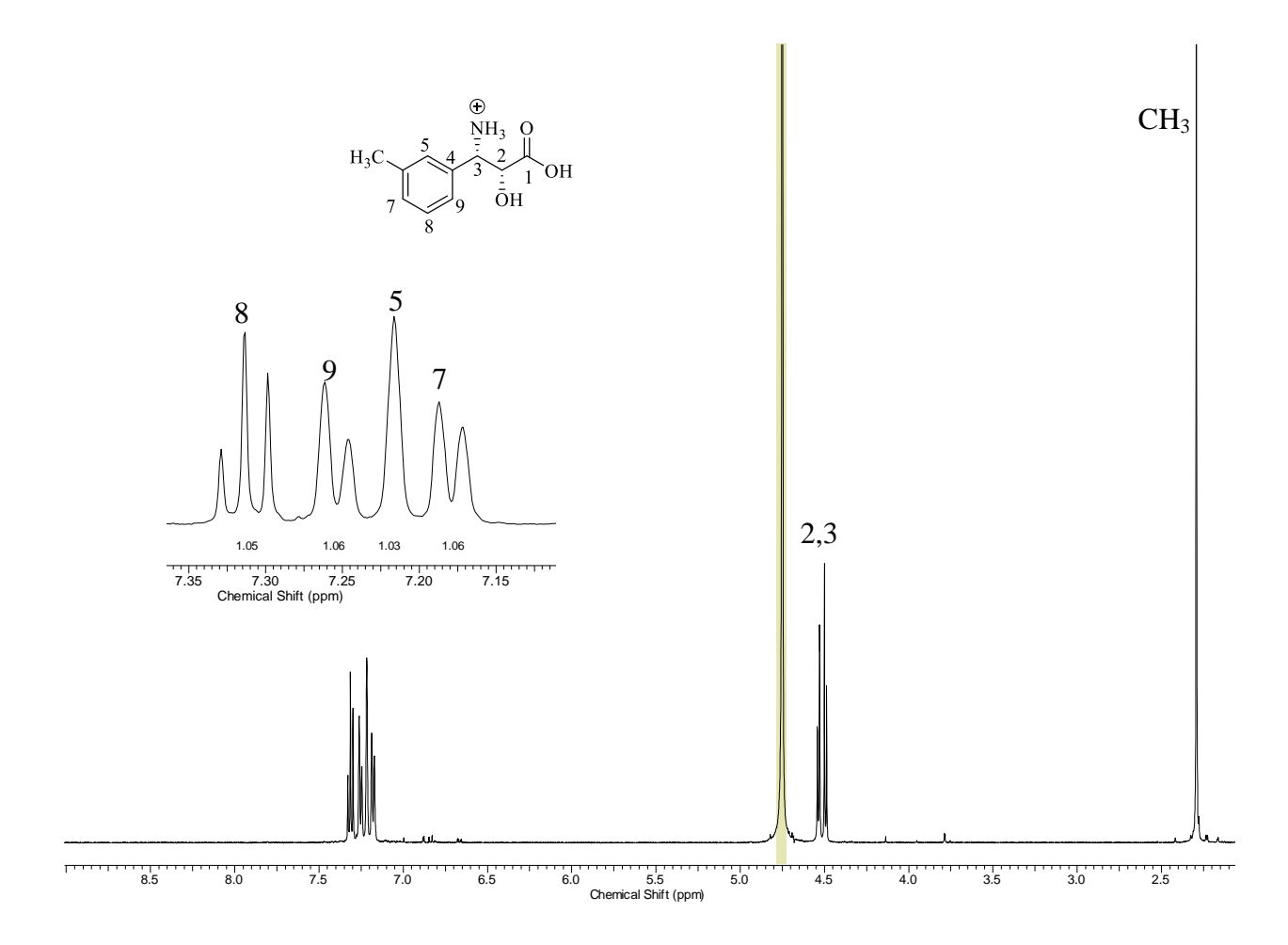


**Figure III–23**. <sup>1</sup>H-NMR spectrum of *m*-Me–phenylisoserine.

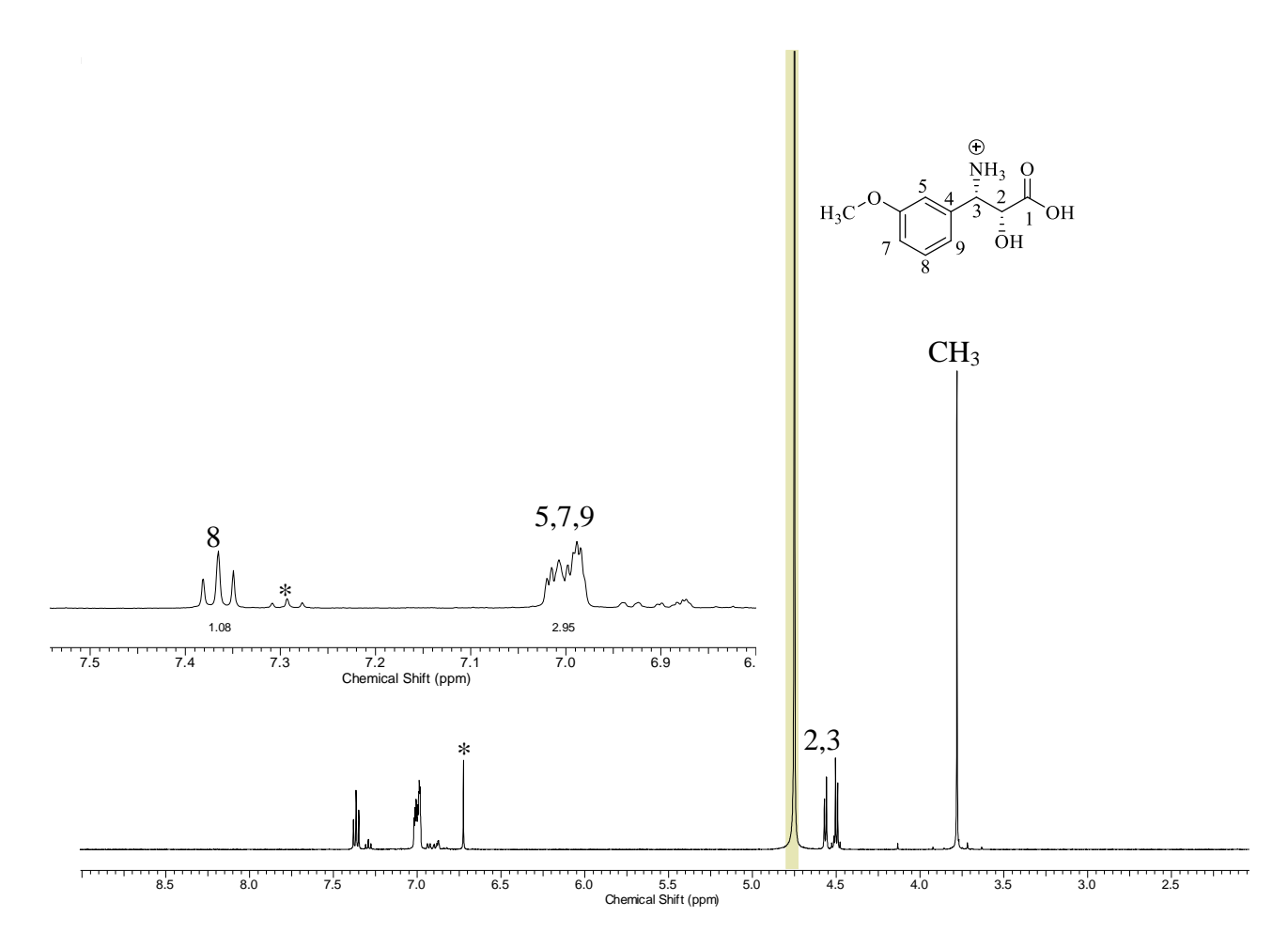


**Figure III–24**. <sup>1</sup>H-NMR spectrum of *m*-OMe–phenylisoserine.

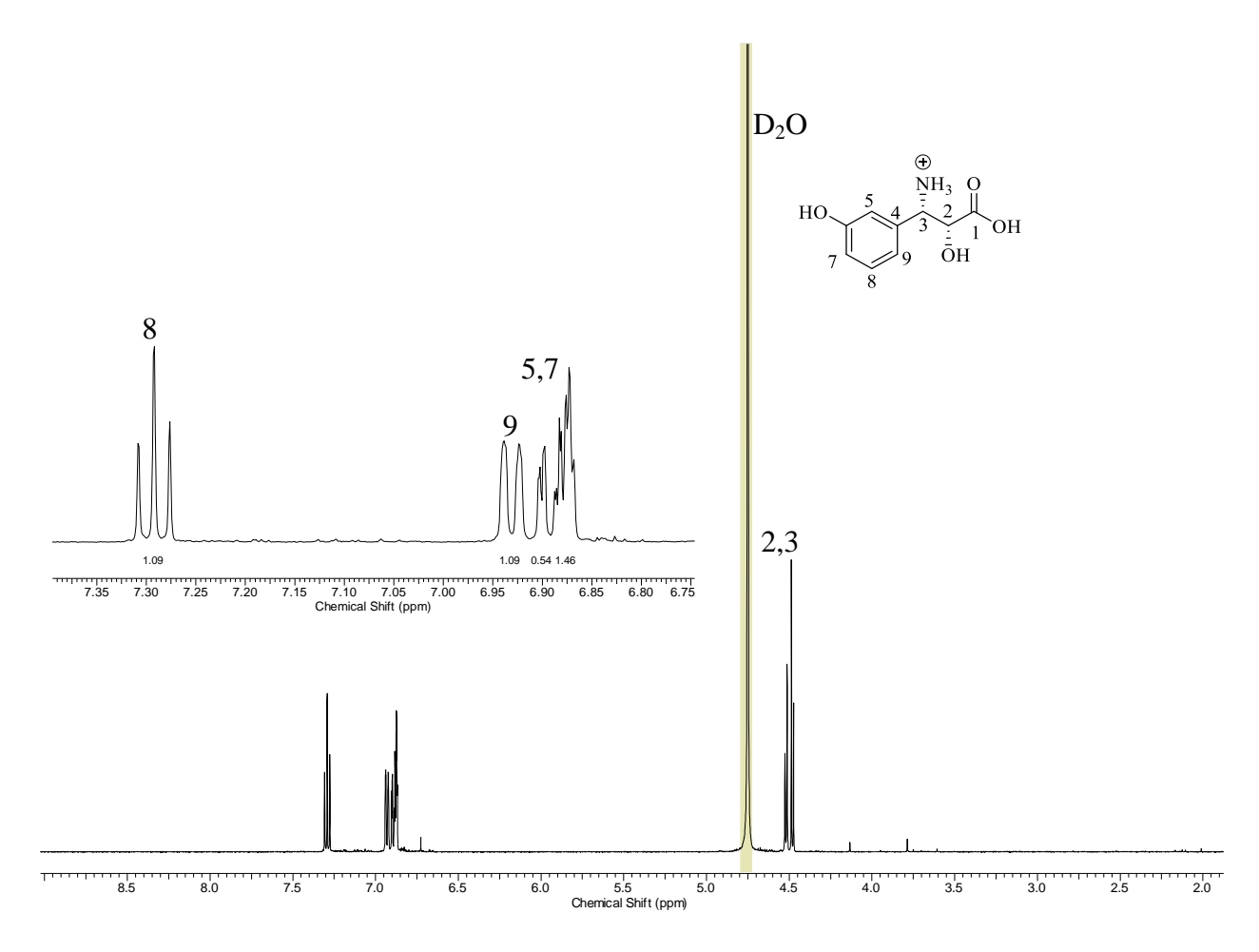


**Figure III–25**. <sup>1</sup>H-NMR spectrum of *m*-OH–phenylisoserine.

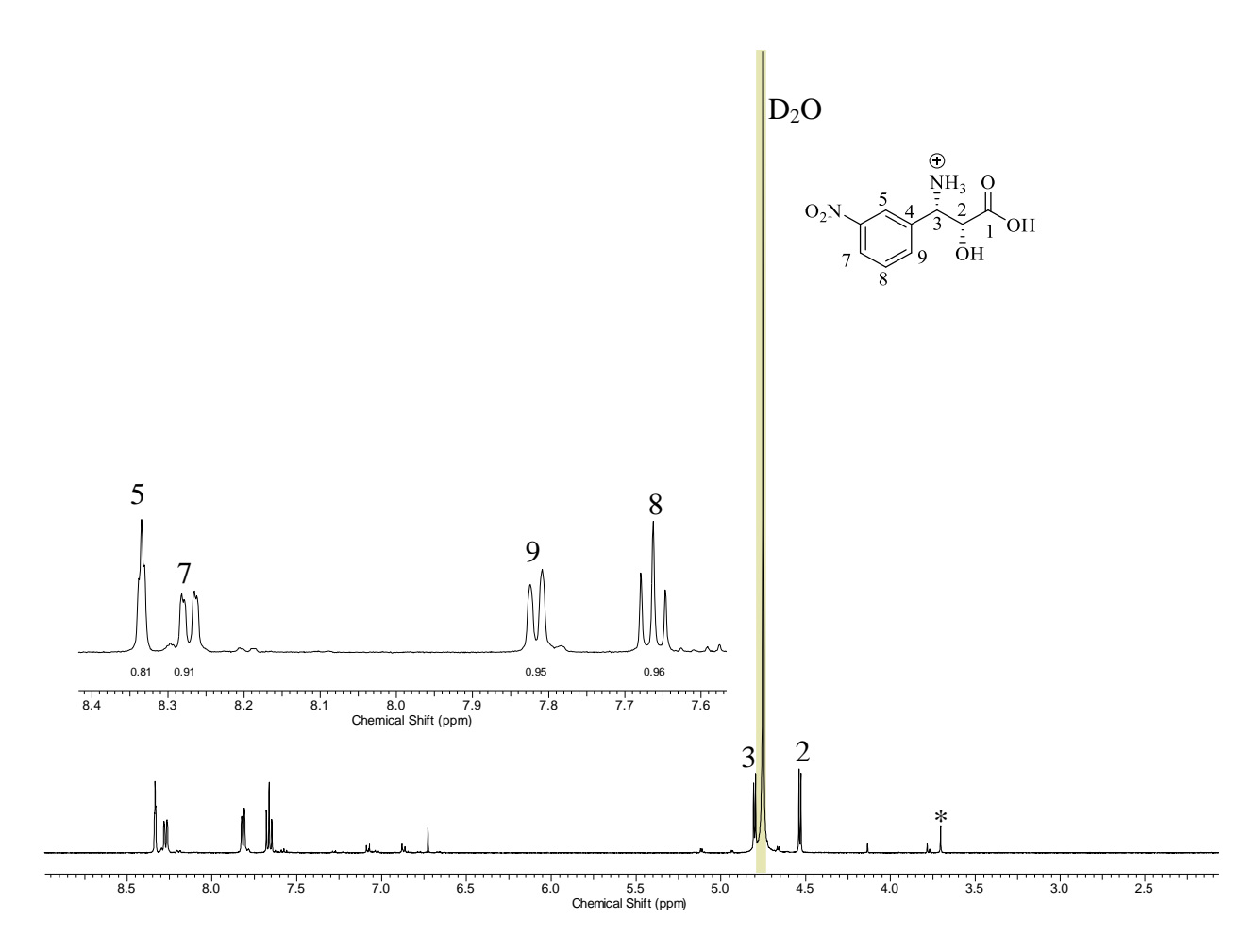


**Figure III–26**. <sup>1</sup>H-NMR spectrum of *m*-NO<sub>2</sub>–phenylisoserine.

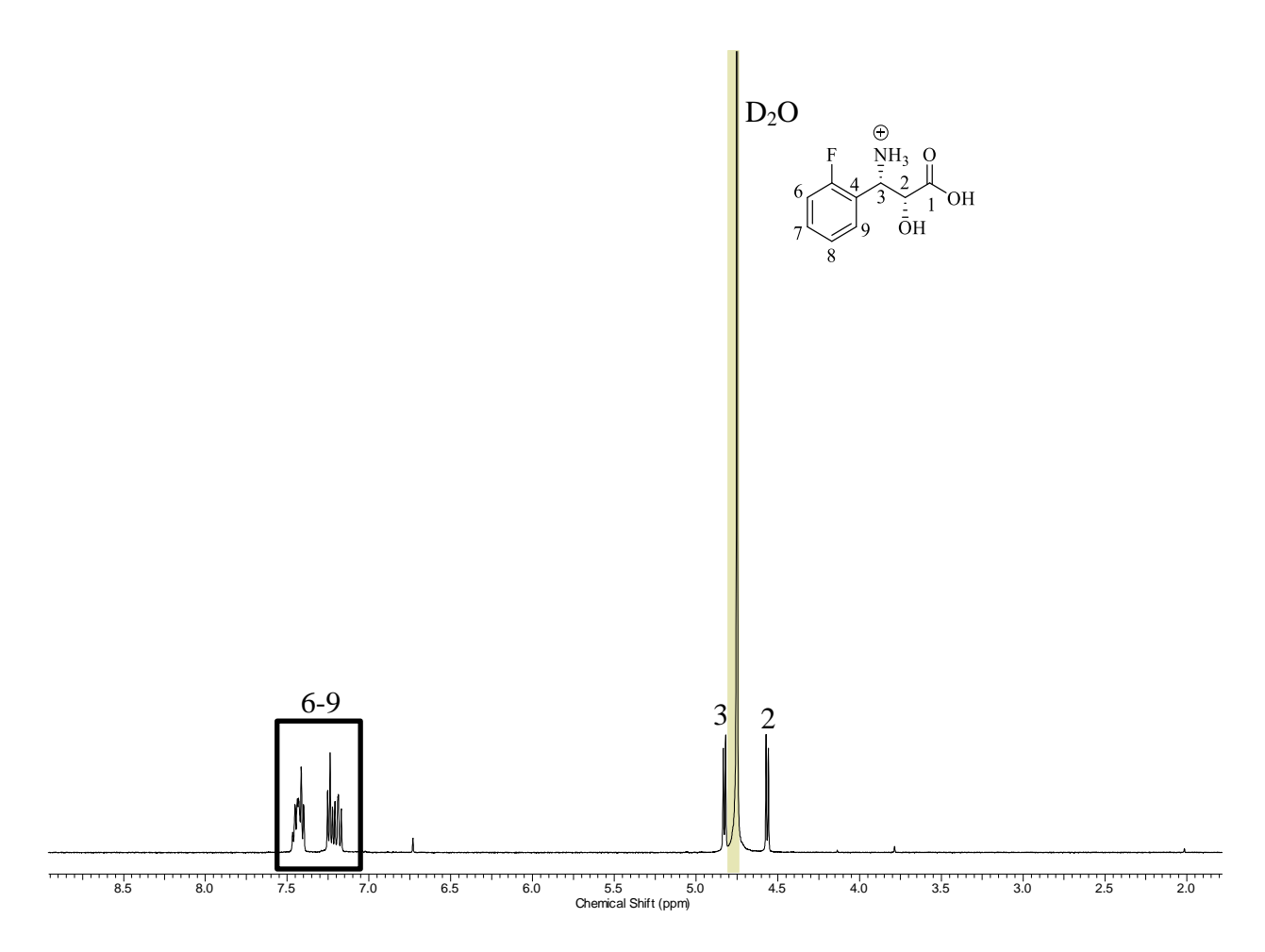


**Figure III–27**. <sup>1</sup>H-NMR spectrum of *ο*-F–phenylisoserine.

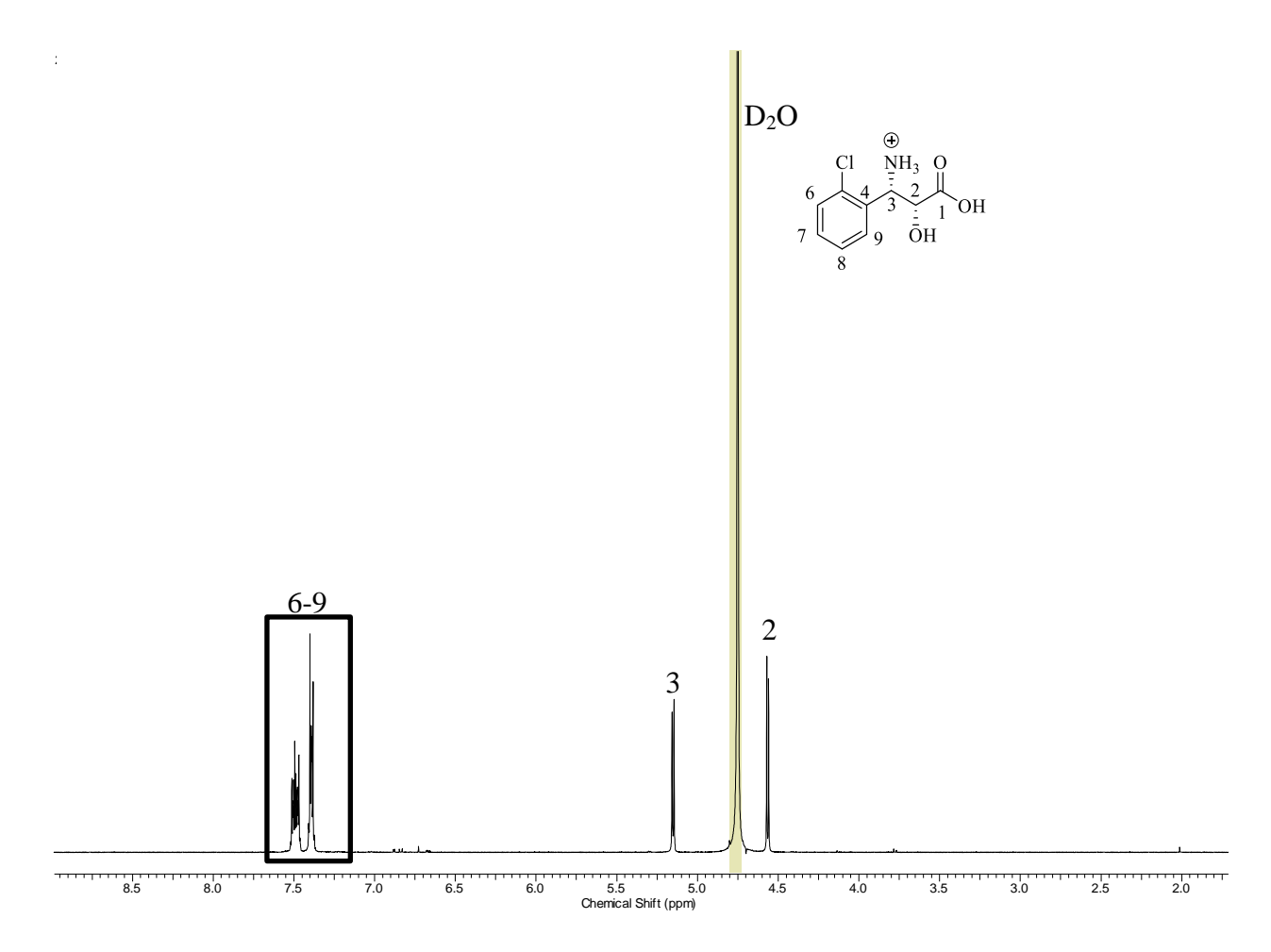


**Figure III–28**. <sup>1</sup>H-NMR spectrum of *o*-Cl–phenylisoserine.

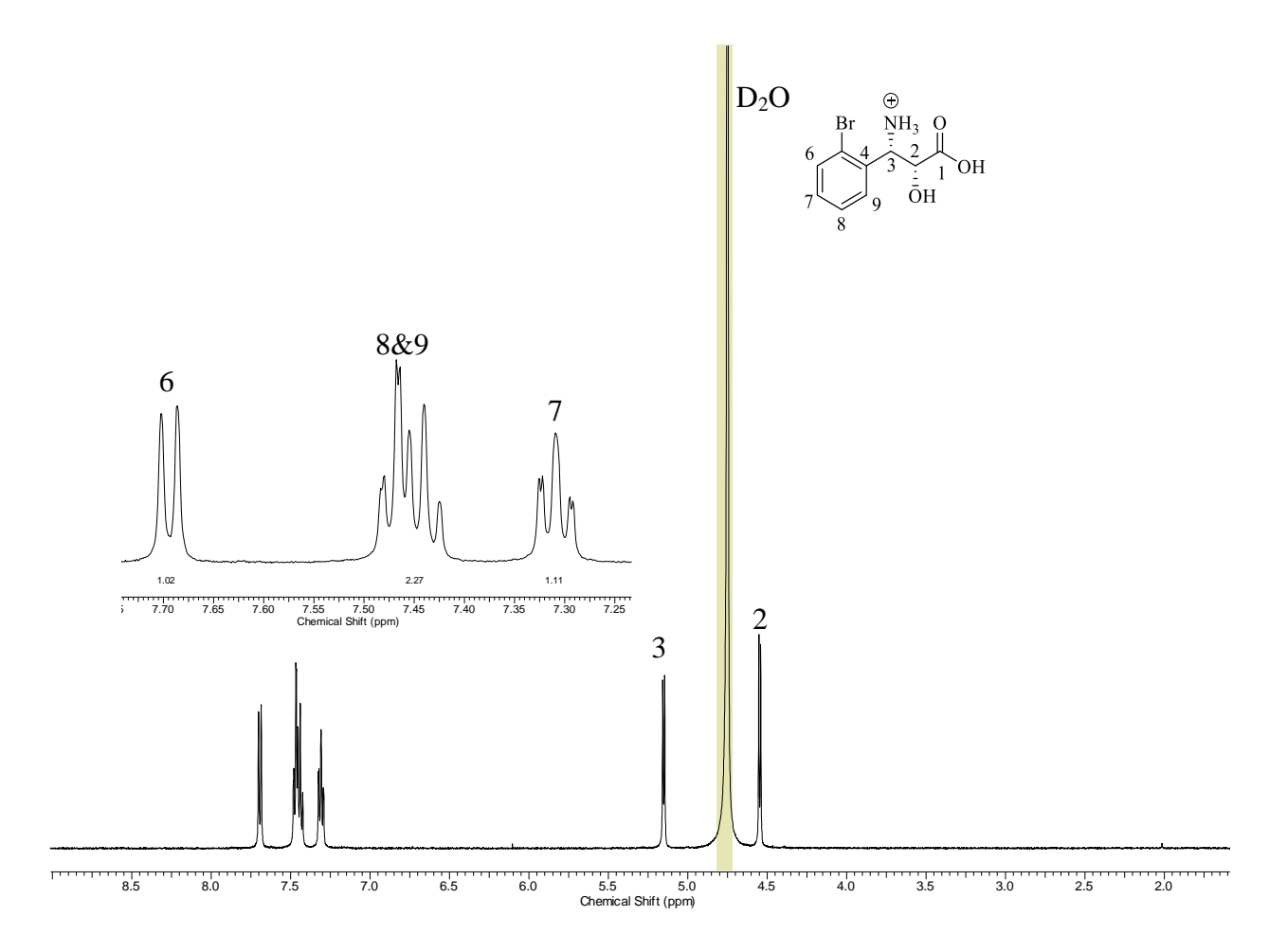


**Figure III–29**. <sup>1</sup>H-NMR spectrum of *o*-Br–phenylisoserine.

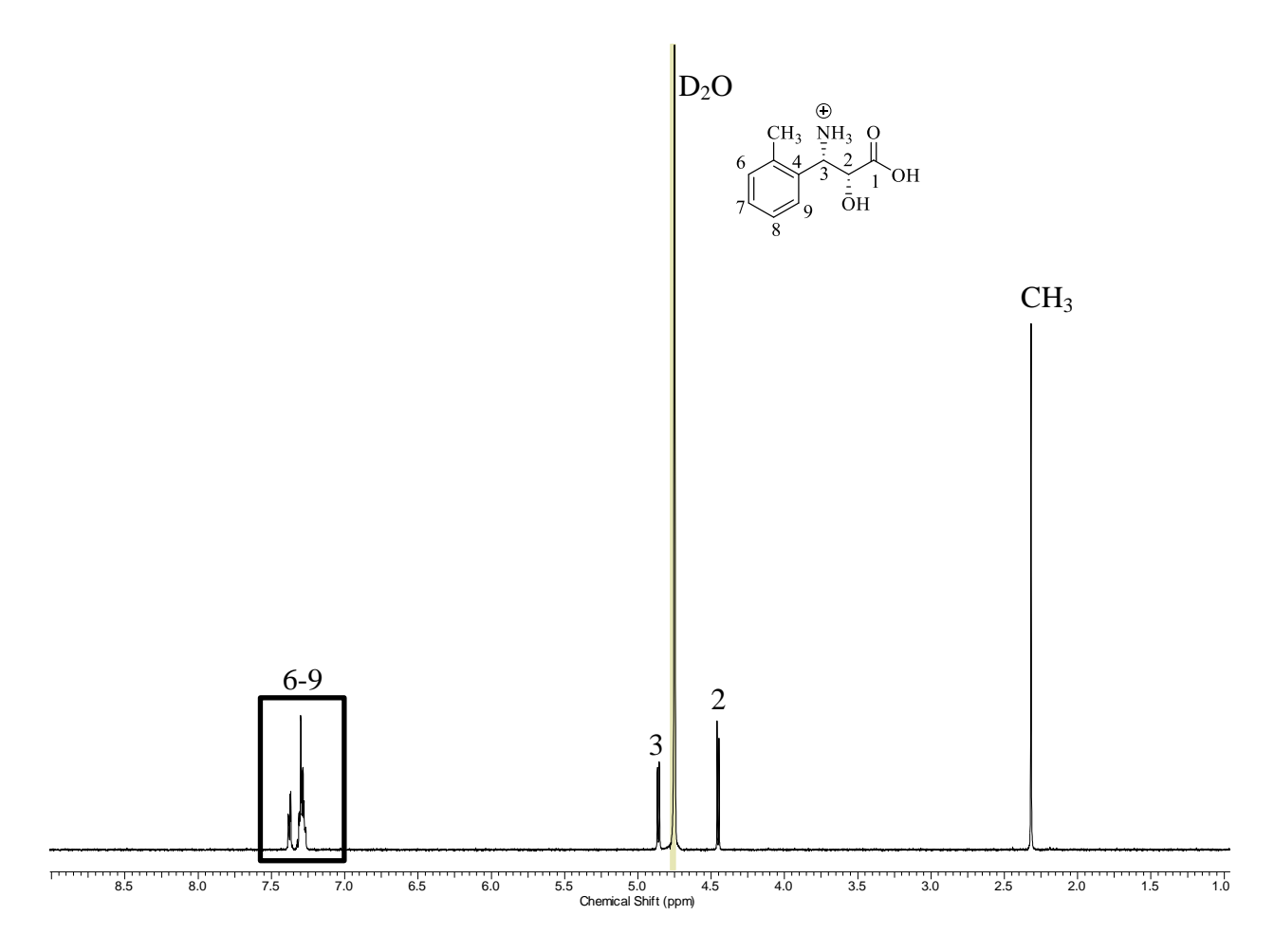


**Figure III–30**. <sup>1</sup>H-NMR spectrum of *o*-Me–phenylisoserine.

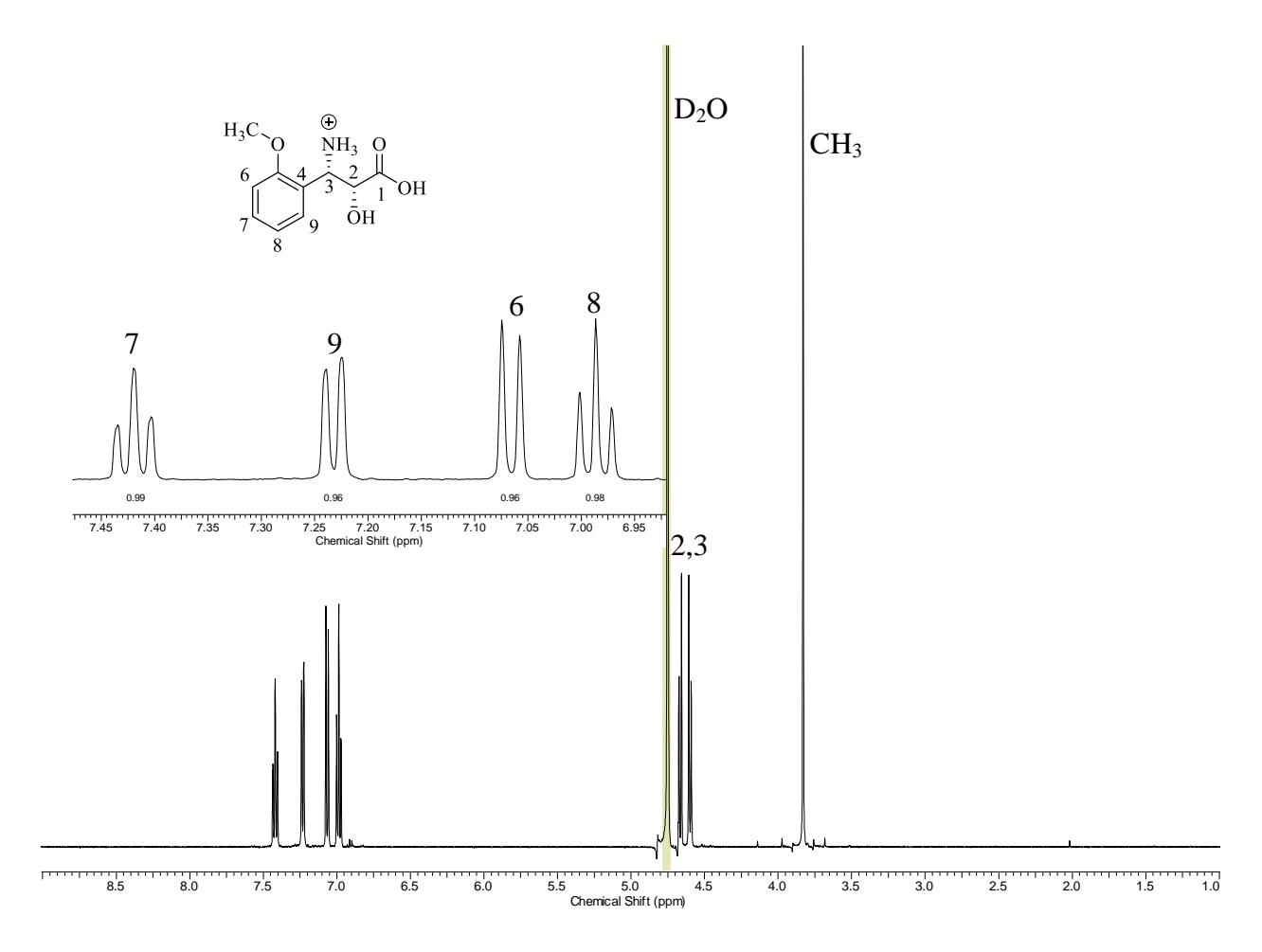


**Figure III–31**. <sup>1</sup>H-NMR spectrum of *o*-OMe–phenylisoserine.

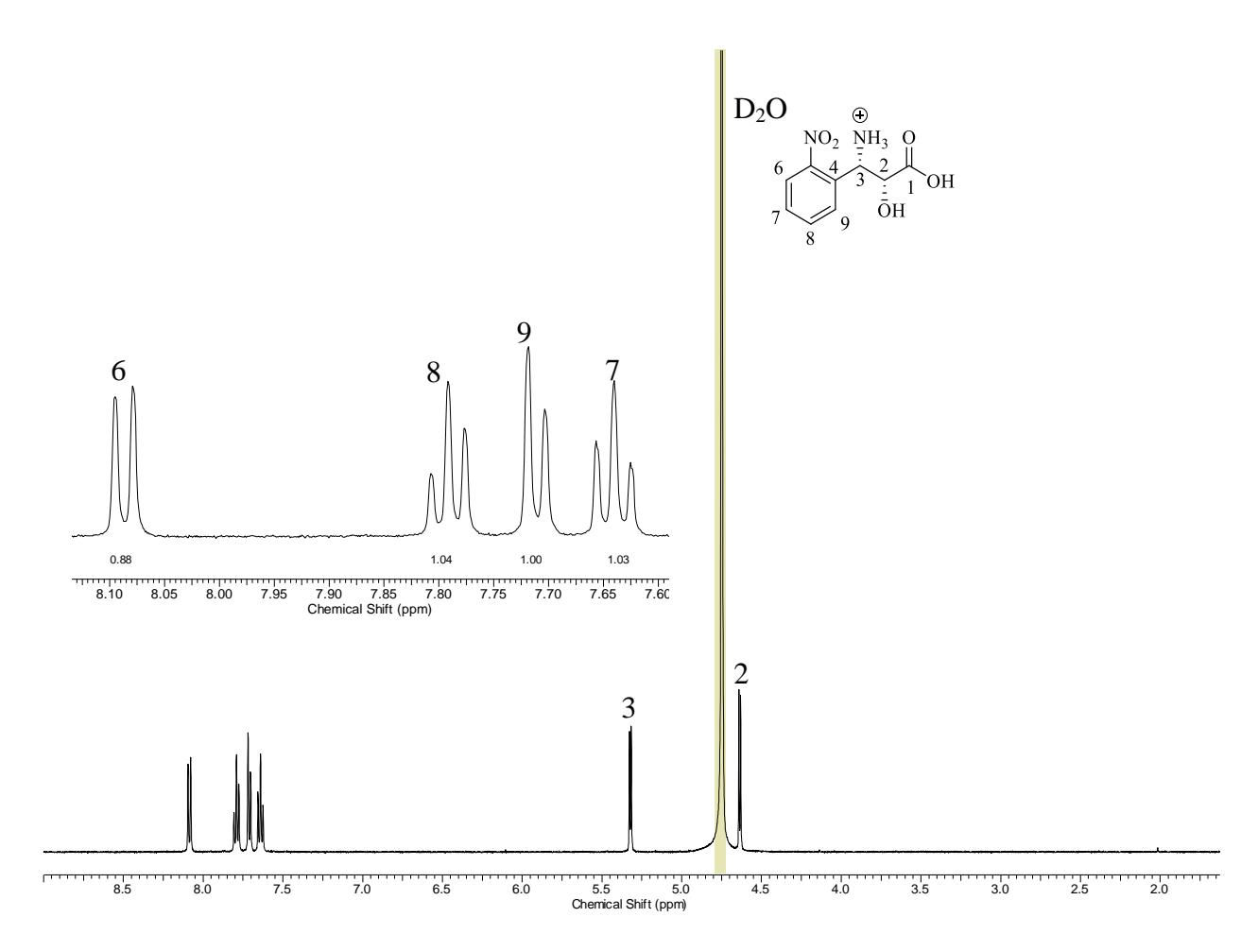


**Figure III–32**. <sup>1</sup>H-NMR spectrum of *o*-NO<sub>2</sub>—phenylisoserine.

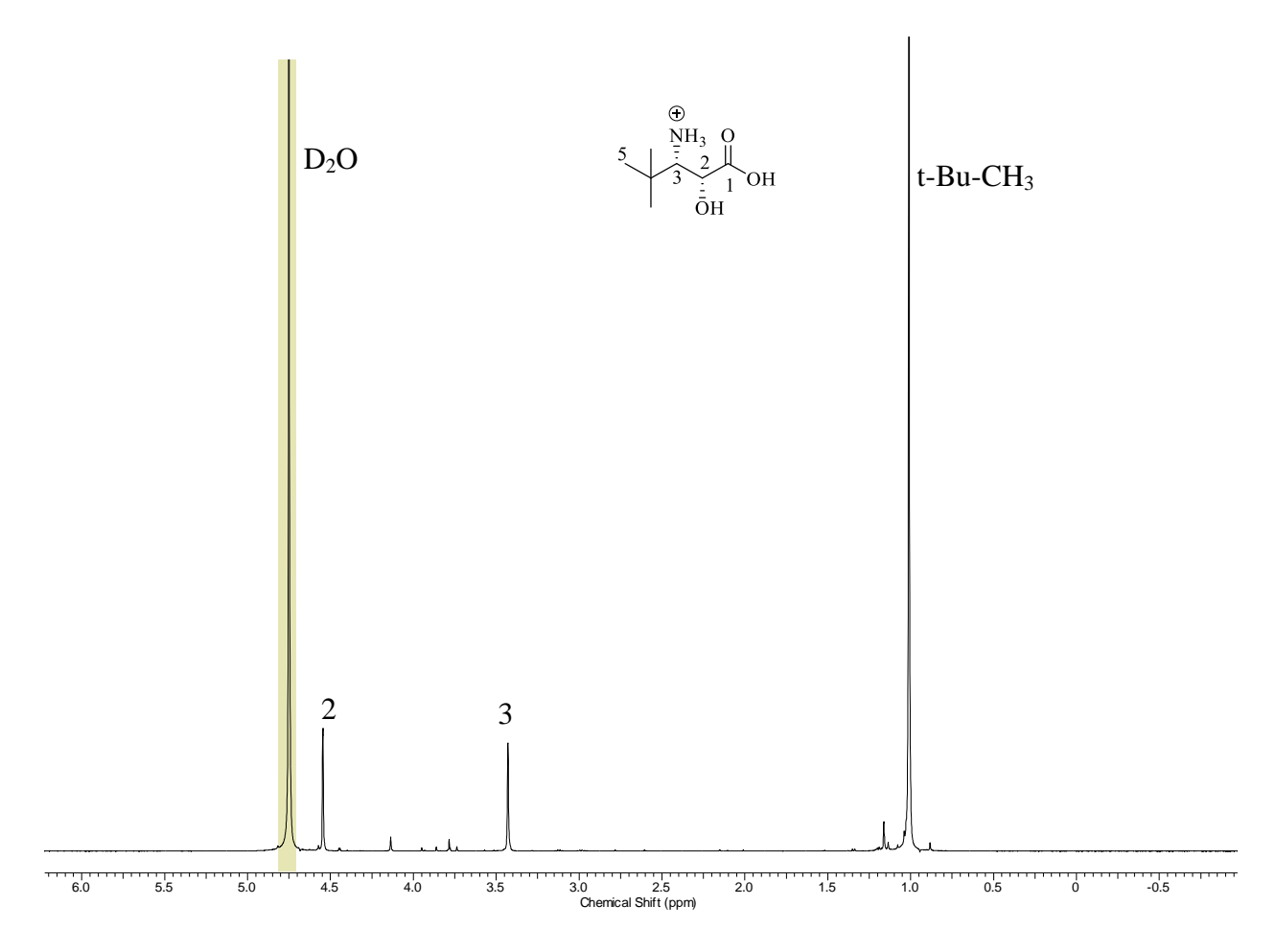


**Figure III–33**. <sup>1</sup>H-NMR spectrum of trimethylisoserine.

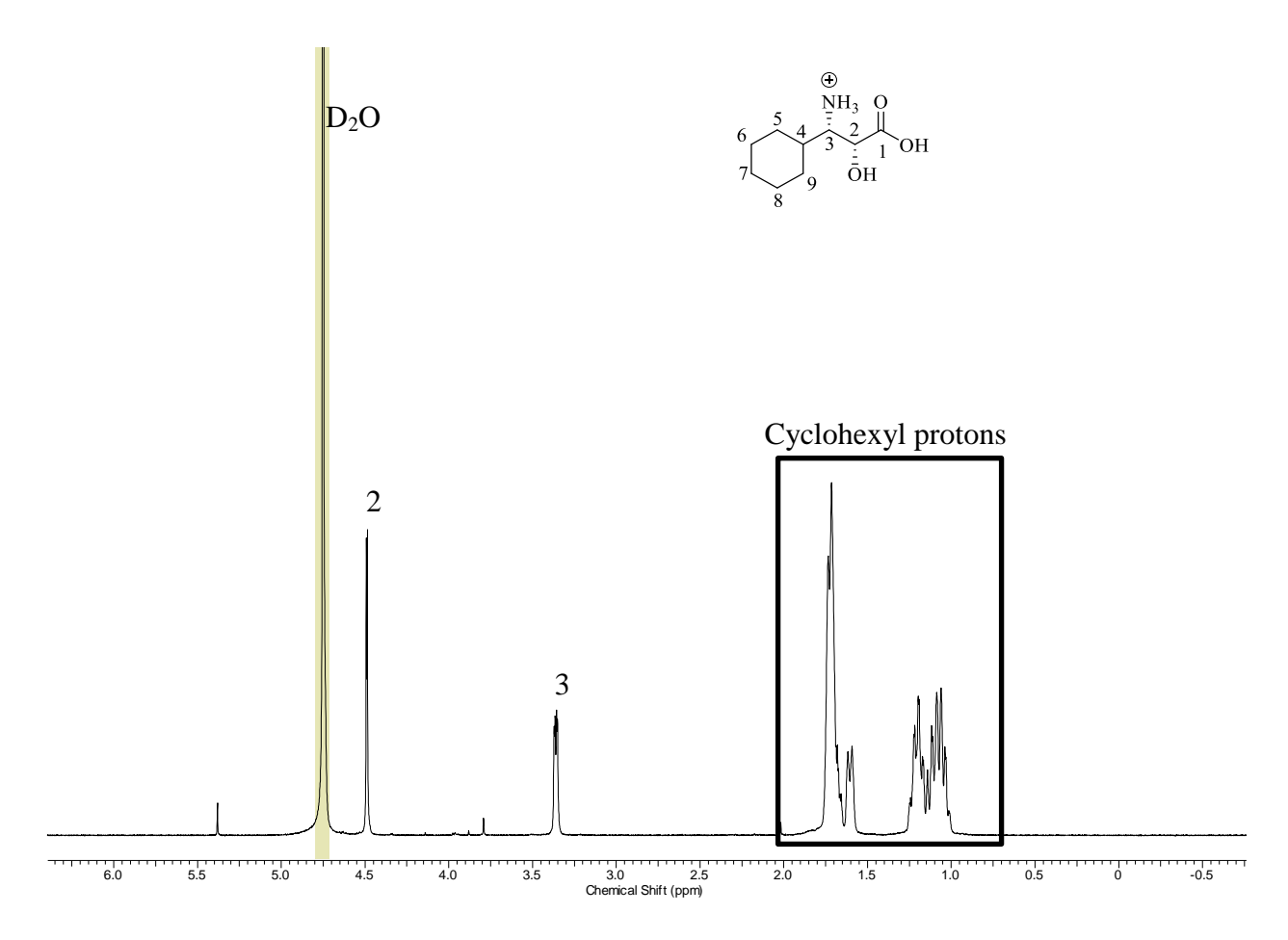


**Figure III–34**. <sup>1</sup>H-NMR spectrum of cyclohexylisoserine.

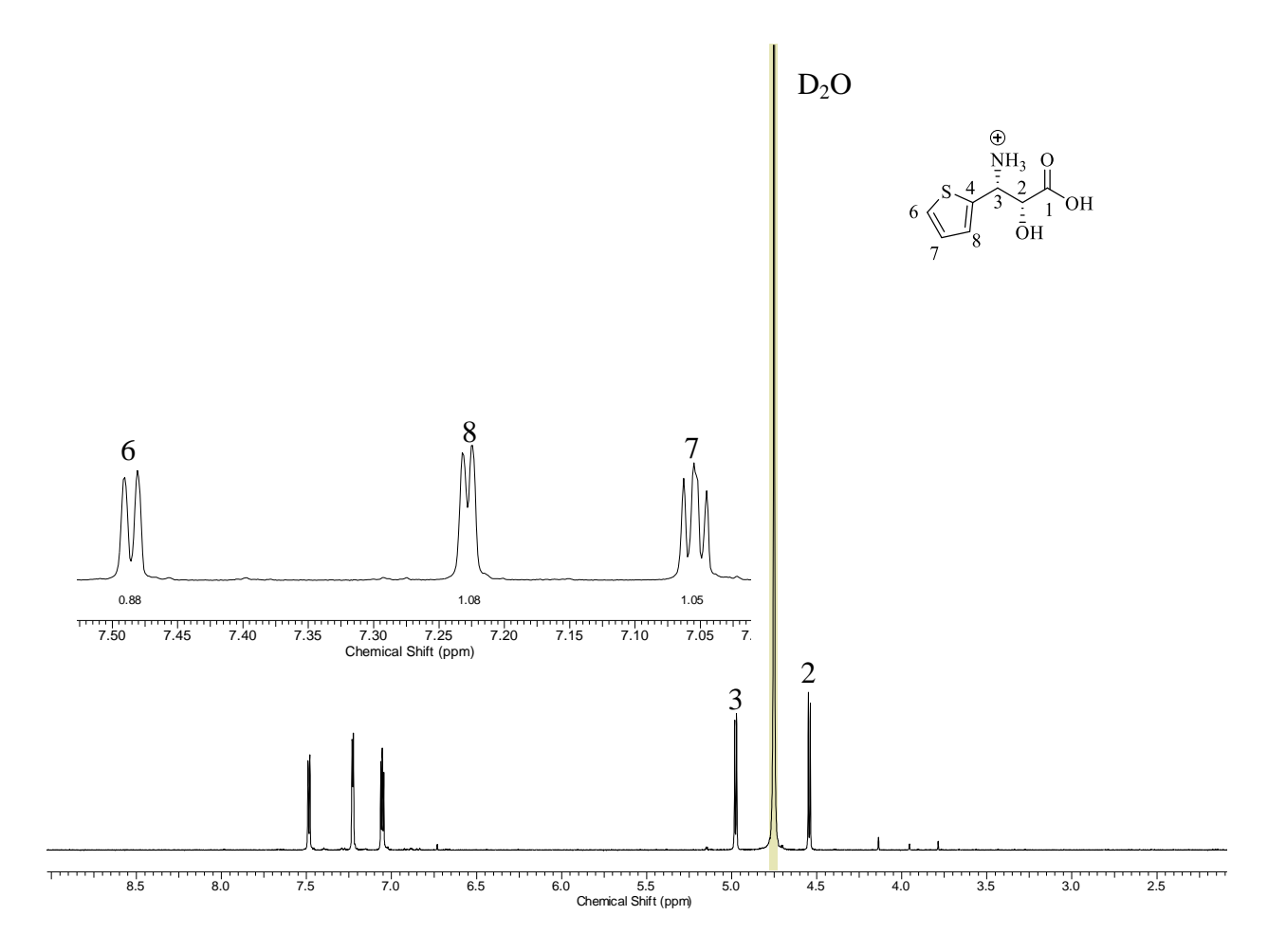


**Figure III–35**. <sup>1</sup>H-NMR spectrum of thiopheneisoserine.

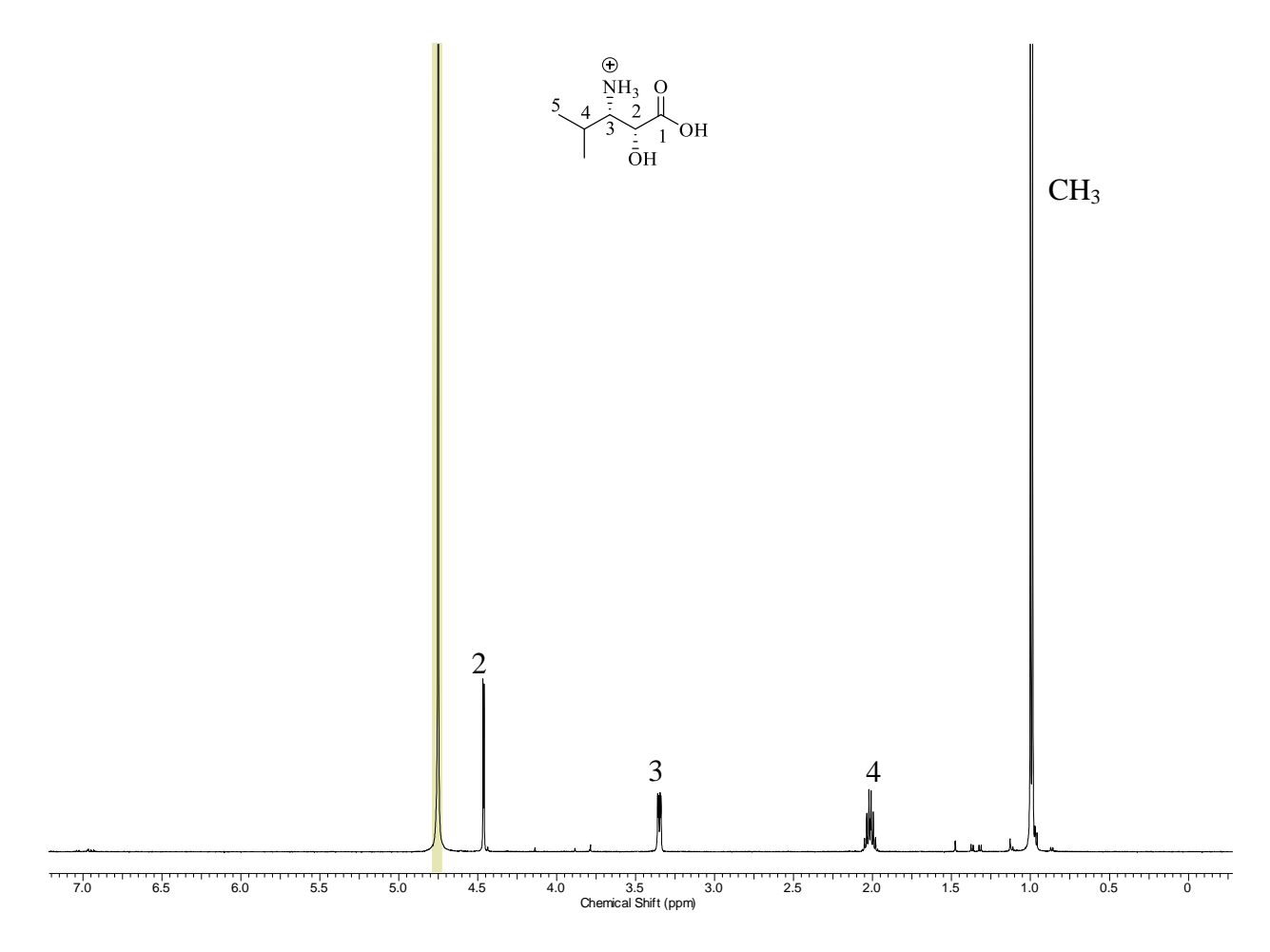


**Figure III–36**. <sup>1</sup>H-NMR spectrum of isopropylisoserine.

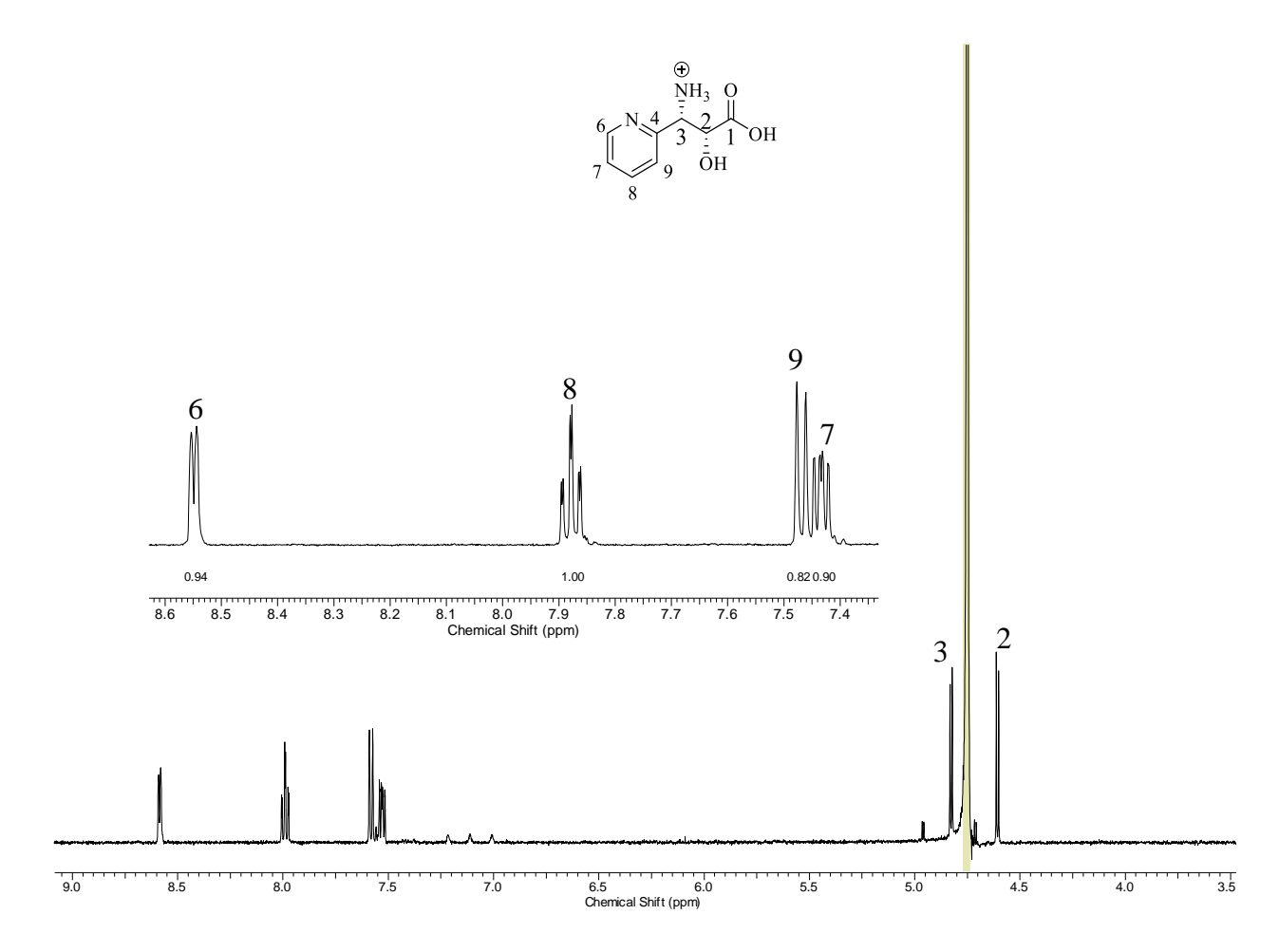


**Figure III–37**. <sup>1</sup>H-NMR spectrum of 2-pyridinylisoserine.

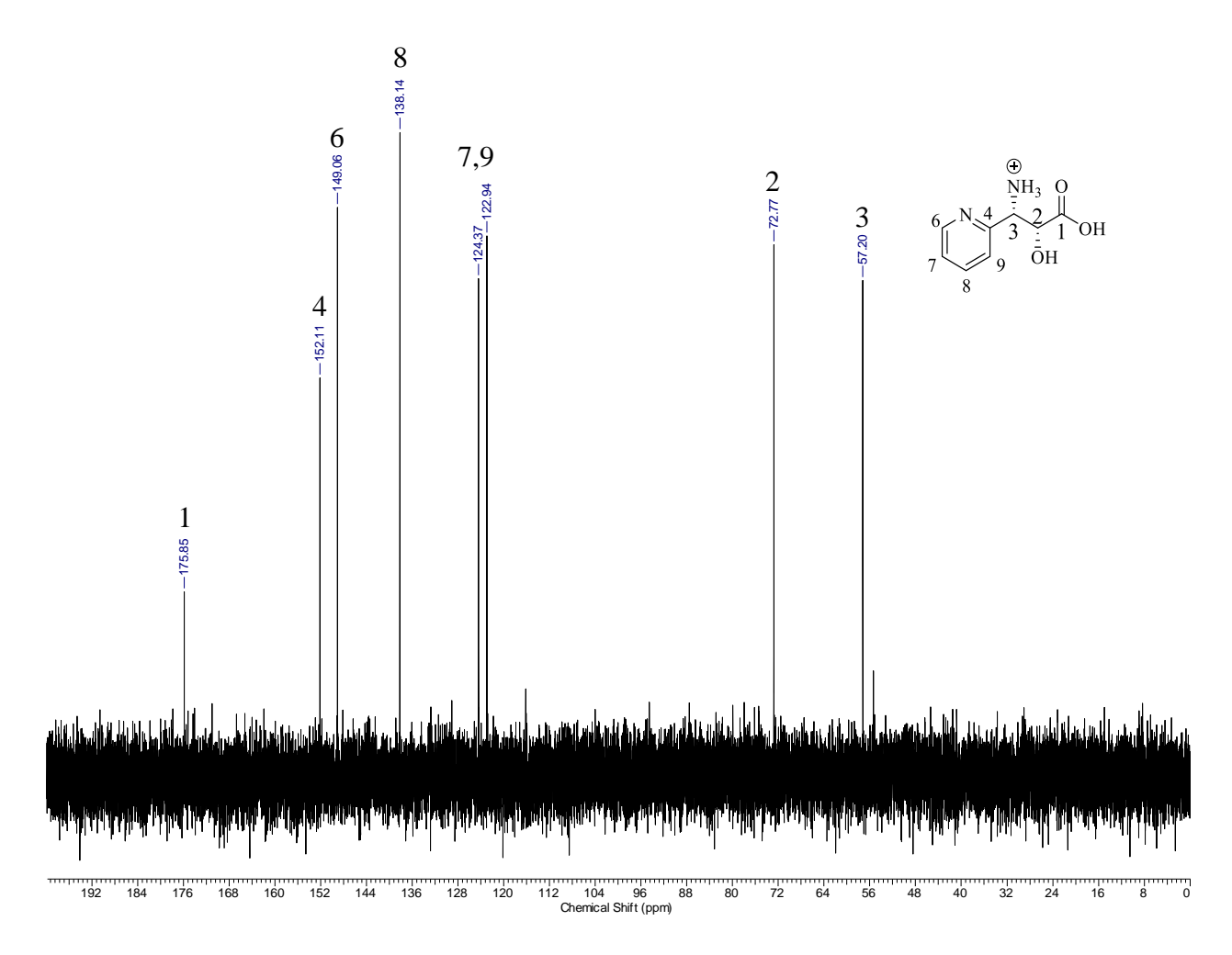


**Figure III–38**. <sup>13</sup>C-NMR spectrum of 2-pyridinylisoserine.

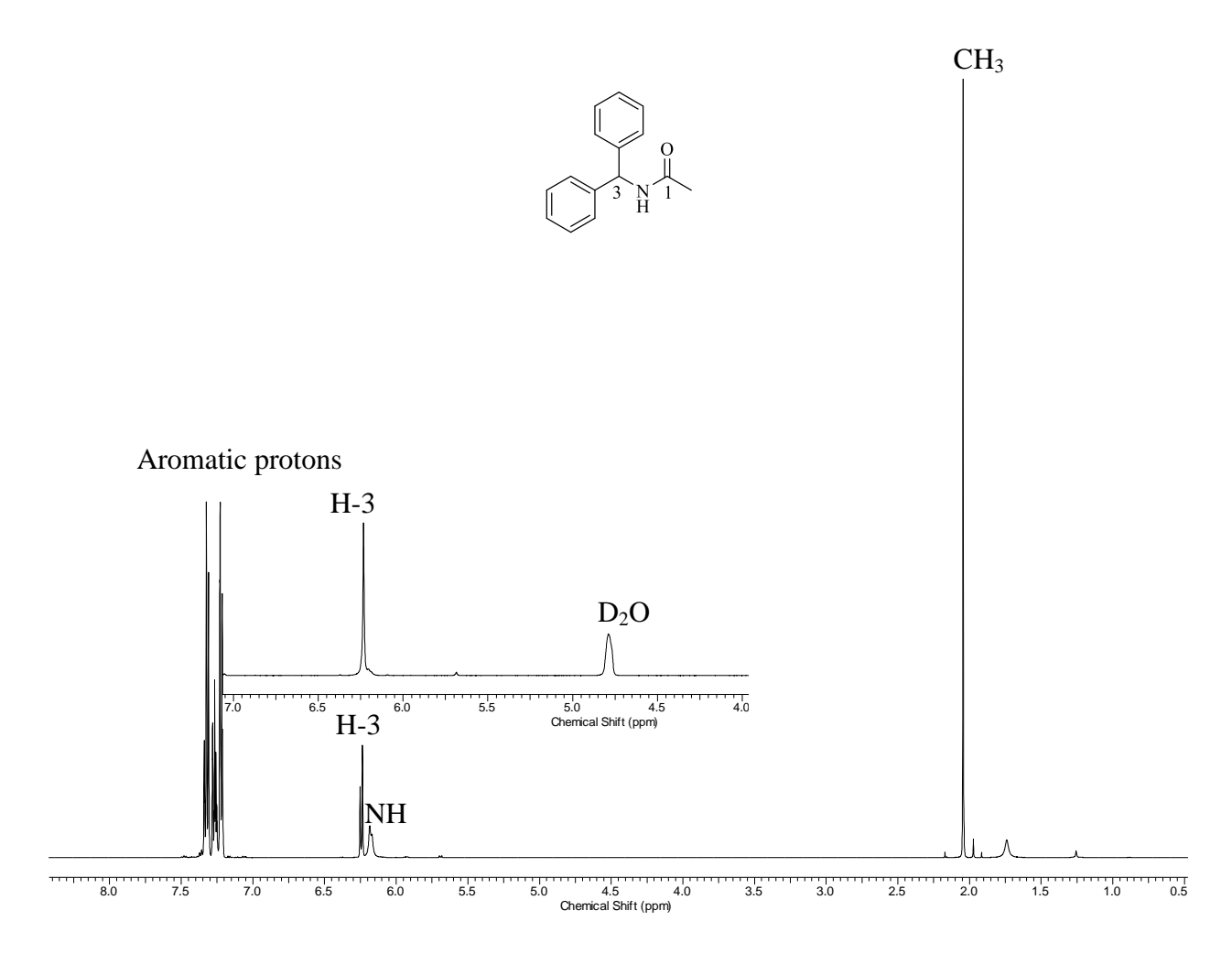


**Figure III–39**. <sup>1</sup>H-NMR spectrum of *N*-benzhydrylacetamide (bottom panel). H<sub>2</sub>O/D<sub>2</sub>O exchange NMR shows the disappearance of NH coupling to CH and the disappearance of NH peak (top panel).

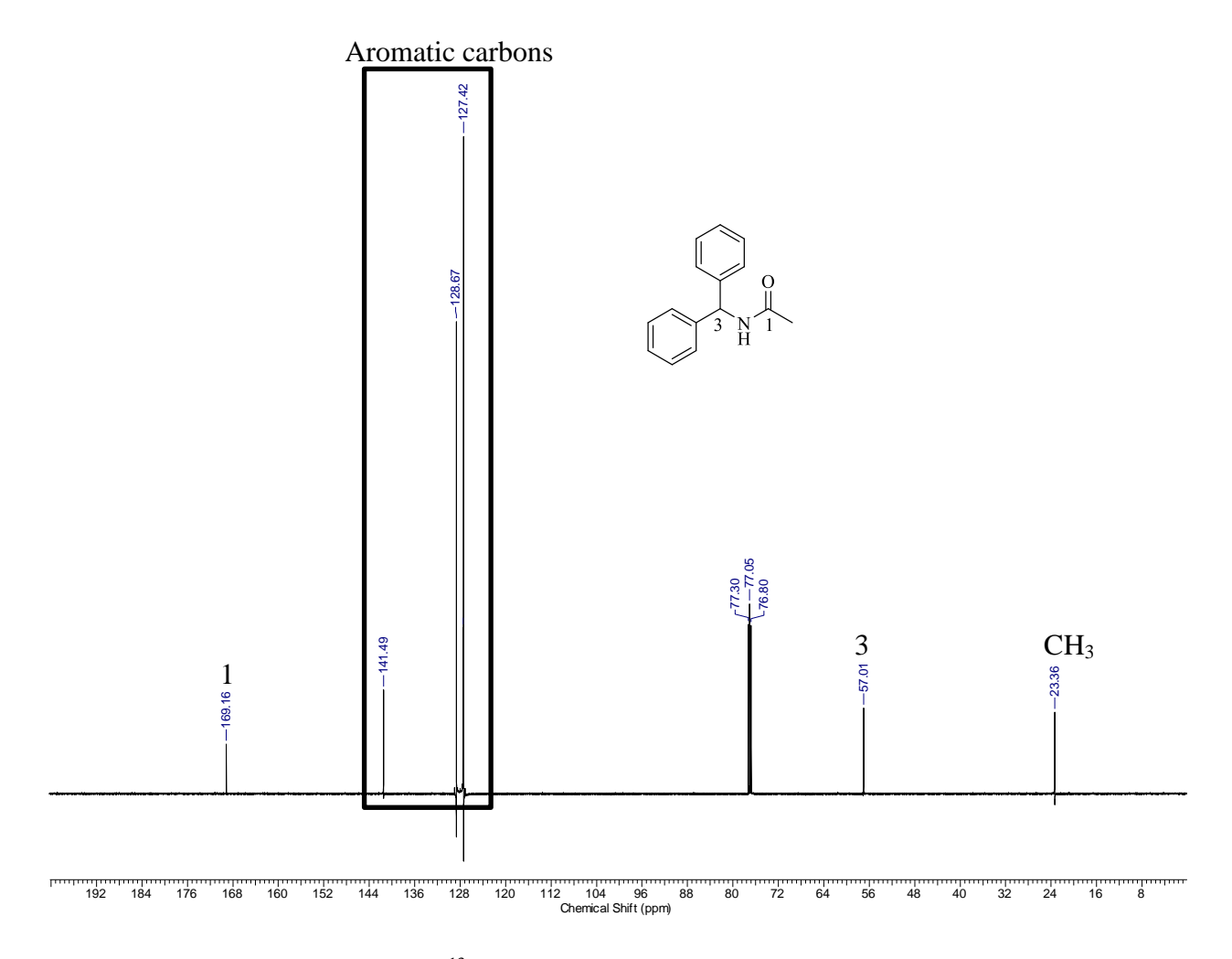


**Figure III–40**. <sup>13</sup>C-NMR spectrum of *N*-benzhydrylacetamide.

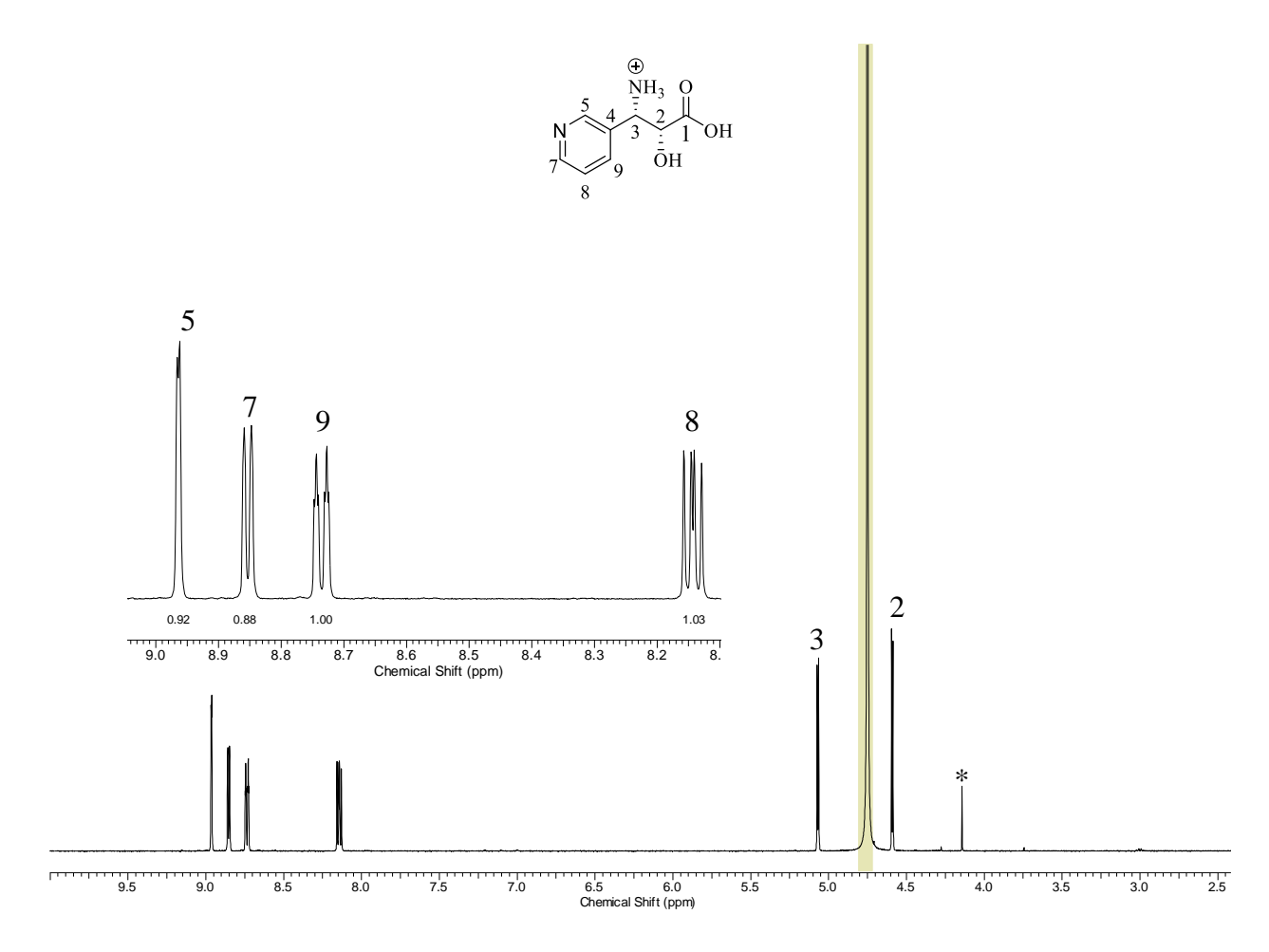


**Figure III–41**. <sup>1</sup>H-NMR spectrum of 3-pyridineisoserine.

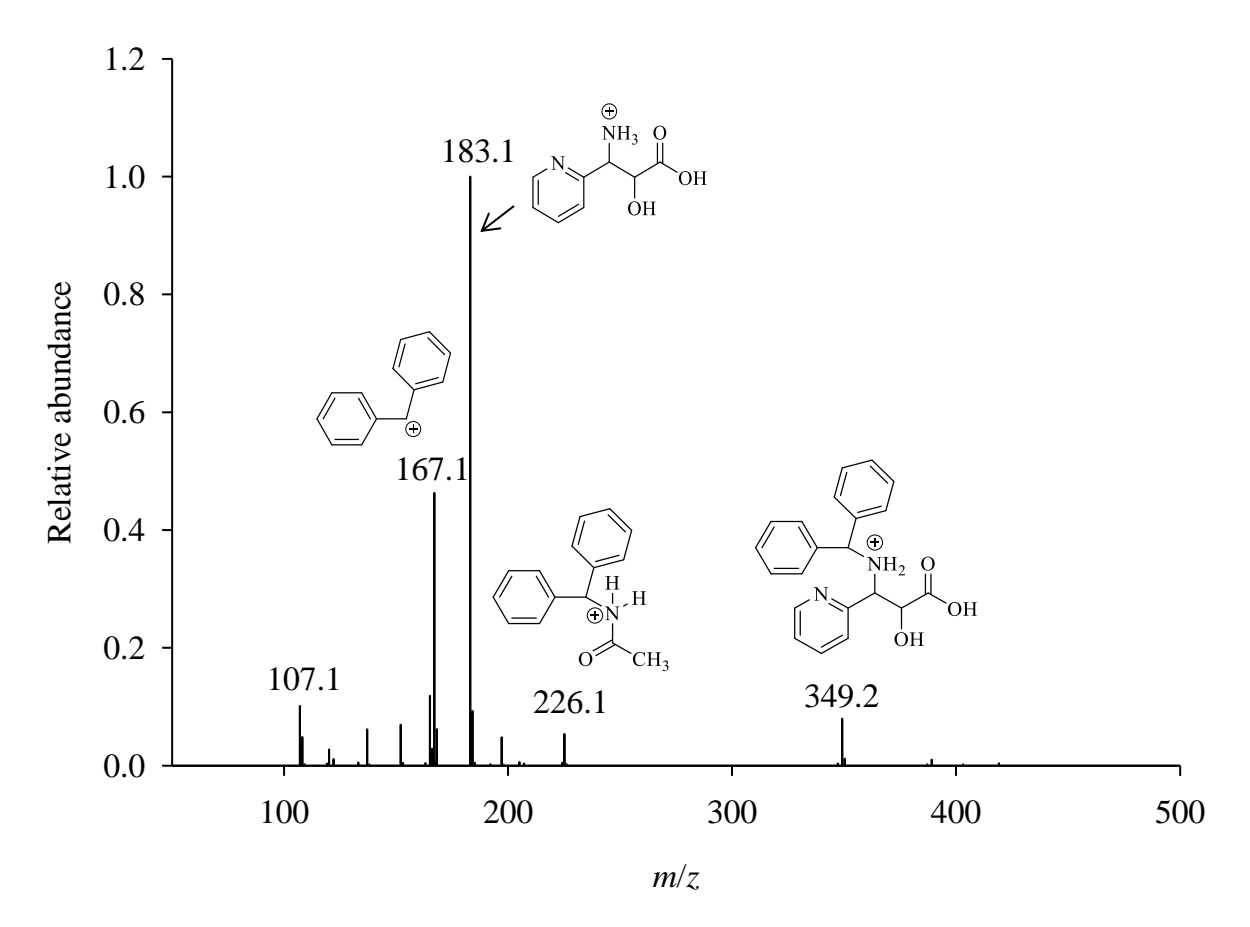


**Figure III–42**. <u>LC-ESI-MS of intermediates and products obtained from the hydrolysis and deprotection of *N*-benzhydryl-3-acetoxy-4-(2-pyridinyl)azetidin-2-one.</u>

# **REFERENCES**

### REFERENCES

- (1) Skeel, R. T. *Handbook of cancer chemotherapy*; Lippincott Williams & Wilkins: Philadelphia [etc.], 1999.
- (2) Jennewein, S.; Croteau, R. Appl. Microbiol. Biotechnol. 2001, 57, 13.
- (3) Ojima, I.; Chen, J.; Sun, L.; Borella, C. P.; Wang, T.; Miller, M. L.; Lin, S.; Geng, X.; Kuznetsova, L.; Qu, C. *J. Med. Chem.* **2008**, *51*, 3203.
- (4) Rowinsky, M., Eric K Annu. Rev. Med. 1997, 48, 353.
- (5) Ojima, I.; Duclos, O.; Kuduk, S. D.; Sun, C.-M.; Slater, J. C.; Lavelle, F.; Veith, J. M.; Bernacki, R. J. *Bioorg. Med. Chem. Lett.* **1994**, *4*, 2631.
- (6) Ojima, I.; Duclos, O.; Zucco, M.; Bissery, M.-C.; Combeau, C.; Vrignaud, P.; Riou, J. F.; Lavelle, F. *J. Med. Chem.* **1994**, *37*, 2602.
- (7) Ojima, I.; Fenoglio, I.; Park, Y. H.; Pera, P.; Bernacki, R. J. *Bioorg. Med. Chem. Lett.* **1994**, *4*, 1571.
- (8) Georg, G. I.; Cheruvallath, Z. S.; Himes, R. H.; Mejillano, M. R.; Burke, C. T. *J. Med. Chem.* **1992**, *35*, 4230.
- (9) Gunda I, G.; Zacharia S, C.; Himes, R. H.; Mejillano, M. R. *Bioorg. Med. Chem. Lett.* **1992**, 2, 1751.
- (10) Ojima, I.; Wang, T.; Miller, M. L.; Lin, S.; Borella, C. P.; Geng, X.; Pera, P.; Bernacki, R. J. *Bioorg. Med. Chem. Lett.* **1999**, *9*, 3423.
- (11) Kingston, D. In Anticancer Agents from Natural Products; CRC Press: 2005.
- (12) Exposito, O.; Bonfill, M.; Moyano, E.; Onrubia, M.; Mirjalili, M. H.; Cusido, R. M.; Palazon, J. *Anti-Cancer Agents in Med. Chem.- Anti-Cancer Agents* **2009**, *9*, 109.
- (13) Kingston, D. G.; Chaudhary, A. G.; Chordia, M. D.; Gharpure, M.; Gunatilaka, A. L.; Higgs, P. I.; Rimoldi, J. M.; Samala, L.; Jagtap, P. G.; Giannakakou, P. *J. Med. Chem.* **1998**, *41*, 3715.
- (14) Jiménez-Barbero, J.; Souto, A. A.; Abal, M.; Barasoain, I.; Evangelio, J. A.; Acuña, A. U.; Andreu, J. M.; Amat-Guerri, F. *Bioorg. Med. Chem.* **1998**, *6*, 1857.

- (15) Gueritte-Voegelein, F.; Guenard, D.; Lavelle, F.; Le Goff, M. T.; Mangatal, L.; Potier, P. *J. Med. Chem.* **1991**, *34*, 992.
- (16) Kant, J.; Huang, S.; Wong, H.; Fairchild, C.; Vyas, D.; Farina, V. *Bioorg. Med. Chem. Lett.* **1993**, *3*, 2471.
- (17) Qi, X.; Lee, S.-H.; Yoon, J.; Lee, Y.-S. *Tetrahedron* **2003**, *59*, 7409.
- (18) Sharma, S.; Lagisetti, C.; Poliks, B.; Coates, R. M.; Kingston, D. G. I.; Bane, S. *Biochemistry* **2013**, *52*, 2328.
- (19) Georg, G. I.; Cheruvallath, Z. S.; Harriman, G. C. B.; Hepperle, M.; Park, H.; Himes, R. H. *Bioorg. Med. Chem. Lett.* **1994**, *4*, 2331.
- (20) Georg, G. I.; Boge, T. C.; Cheruvallath, Z. S.; Harriman, G. C.; Hepperle, M.; Park, H.; Himes, R. H. *Bioorg. Med. Chem. Lett.* **1994**, *4*, 1825.
- (21) Boge, T. C.; Himes, R. H.; Vander Velde, D. G.; Georg, G. I. *J. Med. Chem.* **1994**, *37*, 3337.
- (22) Holton, R. A.; Nadizadeh, H.; Biediger, R. J.; EP Patent 0,534,708: 1995.
- (23) Flores, J. P.; Saif, M. W. J. Clin. Invest. 2013, 3, 333.
- (24) Saif, M.; Sarantopoulos, J.; Patnaik, A.; Tolcher, A.; Takimoto, C.; Beeram, M. *Cancer Chemother. Pharmacol.* **2011**, *68*, 1565.
- (25) Suffness, M. Taxol: science and applications; CRC press, 1995; Vol. 22.
- (26) Croteau, R.; Ketchum, R. B.; Long, R.; Kaspera, R.; Wildung, M. *Phytochem. Rev.* **2006**, *5*, 75.
- (27) Holton, R. A.; Biediger, R. J.; Boatman, P. D. *Taxol: science and applications* **1995**, 97.
- (28) Dunn, P. J.; Wells, A.; Williams, M. T. *Green Chemistry in the pharmaceutical industry*; John Wiley & Sons, 2010.
- (29) Tabata, H. Curr. Drug Targets **2006**, 7, 453.
- (30) Frense, D. Appl. Microbiol. Biotechnol. **2007**, 73, 1233.
- (31) Jennewein, S.; Wildung, M. R.; Chau, M.; Walker, K.; Croteau, R. *Proc. Natl. Acad. Sci. U. S. A.* **2004**, *101*, 9149.

- (32) Walker, K.; Fujisaki, S.; Long, R.; Croteau, R. *Proc. Natl. Acad. Sci. U. S. A.* **2002**, *99*, 12715.
- (33) Nevarez, D. M.; Mengistu, Y. A.; Nawarathne, I. N.; Walker, K. D. *J. Am. Chem. Soc.* **2009**, *131*, 5994.
- (34) Ondari, M. E.; Walker, K. D. J. Am. Chem. Soc. 2008, 130, 17187.
- (35) Nawarathne, I. N.; Walker, K. D. J. Nat. Prod. **2010**, 73, 151.
- (36) Schaffer, M. L.; Otten, L. G. J. Mol. Catal. B-Enzym. 2009, 59, 140.
- (37) Villiers, B. R. M.; Hollfelder, F. *Chembiochem* **2009**, *10*, 671.
- (38) Song, C. E.; Lee, S. W.; Roh, E. J.; Lee, S.-g.; Lee, W.-K. *Tetrahedron: Asymmetry* **1998**, *9*, 983.
- (39) Anderson, L.; Hunter, C. L. *Mol. Cell. Proteomics* **2006**, *5*, 573.
- (40) Georg, G. I.; Harriman, G. C. B.; Hepperle, M.; Himes, R. H. *Bioorg. Med. Chem. Lett.* **1994**, *4*, 1381.
- (41) Wuts, P. G. M.; Gu, R. L.; Northuis, J. M. Tetrahedron: Asymmetry **2000**, 11, 2117.
- (42) Choudary, B. M.; Chowdari, N. S.; Madhi, S.; Kantam, M. L. *J. Org. Chem.* **2003**, *68*, 1736.
- (43) Hamamoto, H.; Mamedov, V. A.; Kitamoto, M.; Hayashi, N.; Tsuboi, S. *Tetrahedron: Asymmetry* **2000**, *11*, 4485.
- (44) Palomo, C.; Aizpurua, J. M.; Ganboa, I.; Oiarbide, M. Eur. J. Org. Chem. 1999, 1999, 3223.
- (45) Lopez, R.; Sordo, T. L.; Sordo, J. A.; Gonzalez, J. J. Org. Chem. **1993**, 58, 7036.
- (46) Soloshonok, V. A.; Fokina, N. A.; Rybakova, A. V.; Shishkina, I. P.; Galushko, S. V.; Sorochinsky, A. E.; Kukhar, V. P.; Savchenko, M. V.; Švedas, V. K. *Tetrahedron: Asymmetry* **1995**, *6*, 1601.
- (47) Ghanem, A.; Aboul-Enein, H. Y. *Chirality* **2005**, *17*, 1.
- (48) Cunha, R. L. O. R.; Ferreira, E. A.; Oliveira, C. S.; Omori, Á. T. *Biotechnol. Adv.* **2015**.
- (49) Li, X.-G.; Kanerva, L. T. *Tetrahedron: Asymmetry* **2005**, *16*, 1709.

- (50) Forró, E.; Fülöp, F. Chem. Eur. J. 2007, 13, 6397.
- (51) Mohrig, J. R.; Shapiro, S. M. J. Chem. Educ. 1976, 53, 586.
- (52) Tasnádi, G.; Forró, E.; Fülöp, F. Tetrahedron: Asymmetry 2008, 19, 2072.
- (53) Forró, E.; Fülöp, F. *Tetrahedron: Asymmetry* **2010**, *21*, 637.
- (54) Hutchinson, C. R. *Proc. Natl. Acad. Sci. U. S. A.* **1999**, *96*, 3336.
- (55) Rix, U.; Fischer, C.; Remsing, L. L.; Rohr, J. Nat. Prod. Rep. 2002, 19, 542.
- (56) Firn, R. D.; Jones, C. G. Mol. Microbiol. **2000**, *37*, 989.
- (57) Firn, R. D.; Jones, C. G. Nat. Prod. Rep. **2003**, 20, 382.
- (58) Drauz, K.; Waldmann, H. *Enzyme catalysis in organic synthesis: a comprehensive handbook*; John Wiley & Sons, 1995.
- (59) Liese, A.; Seelbach, K.; Wandrey, C. *Industrial biotransformations*; John Wiley & Sons, 2006.
- (60) Schmid, A.; Dordick, J. S.; Hauer, B.; Kiener, A.; Wubbolts, M.; Witholt, B. *Nature* **2001**, *409*, 258.
- (61) Patel, R. N. Stereoselective biocatalysis; CRC Press, 2000.
- (62) Shen, Y.; Yoon, P.; Yu, T.-W.; Floss, H. G.; Hopwood, D.; Moore, B. S. *Proc. Natl. Acad. Sci. U. S. A.* **1999**, *96*, 3622.
- (63) Anilkumar, G. N.; Selyutin, O.; Rosenblum, S. B.; Zeng, Q.; Jiang, Y.; Chan, T.-Y.; Pu, H.; Wang, L.; Bennett, F.; Chen, K. X. *Bioorg. Med. Chem. Lett.* **2012**, 22, 713.
- (64) Knight, Z. A.; Gonzalez, B.; Feldman, M. E.; Zunder, E. R.; Goldenberg, D. D.; Williams, O.; Loewith, R.; Stokoe, D.; Balla, A.; Toth, B. *Cell* **2006**, *125*, 733.
- (65) Norman, M. H.; Liu, L.; Lee, M.; Xi, N.; Fellows, I.; D'Angelo, N. D.; Dominguez, C.; Rex, K.; Bellon, S. F.; Kim, T.-S. *J. Med. Chem.* **2012**, *55*, 1858.
- (66) Pireddu, R.; Forinash, K. D.; Sun, N. N.; Martin, M. P.; Sung, S.-S.; Alexander, B.; Zhu, J.-Y.; Guida, W. C.; Schönbrunn, E.; Sebti, S. M. *MedChemComm* **2012**, *3*, 699.

- (67) Wu, R.; Reger, A. S.; Lu, X.; Gulick, A. M.; Dunaway-Mariano, D. *Biochemistry* **2009**, *48*, 4115.
- (68) Anilkumar, G. N.; Lesburg, C. A.; Selyutin, O.; Rosenblum, S. B.; Zeng, Q.; Jiang, Y.; Chan, T.-Y.; Pu, H.; Vaccaro, H.; Wang, L. *Bioorg. Med. Chem. Lett.* **2011**, *21*, 5336.
- (69) Miyamoto, Y.; Banno, Y.; Yamashita, T.; Fujimoto, T.; Oi, S.; Moritoh, Y.; Asakawa, T.; Kataoka, O.; Yashiro, H.; Takeuchi, K. *J. Med. Chem.* **2011**, *54*, 831.
- (70) van Eis, M. J.; Evenou, J.-P.; Floersheim, P.; Gaul, C.; Cowan-Jacob, S. W.; Monovich, L.; Rummel, G.; Schuler, W.; Stark, W.; Strauss, A. *Bioorg. Med. Chem. Lett.* **2011**, *21*, 7367.
- (71) Schonbrunn, E.; Betzi, S.; Alam, R.; Martin, M. P.; Becker, A.; Han, H.; Francis, R.; Chakrasali, R.; Jakkaraj, S.; Kazi, A. *J. Med. Chem.* **2013**, *56*, 3768.
- (72) Ho, G. D.; Yang, S.-W.; Smotryski, J.; Bercovici, A.; Nechuta, T.; Smith, E. M.; McElroy, W.; Tan, Z.; Tulshian, D.; McKittrick, B. *Bioorg. Med. Chem. Lett.* **2012**, 22, 1019.
- (73) Jacobs, J.; Grum-Tokars, V.; Zhou, Y.; Turlington, M.; Saldanha, S. A.; Chase, P.; Eggler, A.; Dawson, E. S.; Baez-Santos, Y. M.; Tomar, S. *J. Med. Chem.* **2013**, *56*, 534.

# 5. PRELIMINARY SITE-DIRECTED MUTAGENESIS STUDIES AND FUTURE DIRECTION IN THE BIOSYNTHESIS OF AMINOACYL COA THIOESTERS

### 5.1. Introduction

## **5.1.1.** Application of Bioengineering to Enhance Enzymatic Catalysis

Bioengineering is undoubtedly a powerful technique in enzymology. Site-directed mutagenesis has been employed in various studies aimed at improving enzyme catalysis, substrate specificity, and selectivity.<sup>2,3</sup> For example, a single A312G mutation in phenylacetate tRNA synthetase increased the activity for (3R)- $\beta$ -phenylalanine by 4-fold. In a different study, an H322E mutation in the AspA adenylation domain of surfactin synthetase changed the selectivity from aspartate to asparagine.<sup>3</sup> Additionally, computational-guided mutations in the adenylation domain (Grs1(Phe-A)) of gramicidin synthetase 1 shifted its selectivity from phenylalanine to leucine after incorporating a double mutation T278L/A301G into the Grs1(Phe–A) domain.<sup>4</sup> This last study heavily relied on structure-function information rather than sequence-based analysis which enabled accurate and rapid predictions on substrate selectivity for Grs1(Phe-A) mutants.<sup>4</sup> The successes of the earlier mutational studies prompted us to explore the effects of pointmutations of Tyc(Phe-AT) for binding and catalyzing various value-added arylisoserine substrates. Some of our preliminary proposed mutations (Section 5.1.2) were guided by sequence homology; however, computational methods could potentially reduce the anecdotal trial-anderror approach towards obtaining beneficial mutations. Coupling computational based selection of protein mutations with structural and sequence homology studies is advantageous over traditional sequence alignment methods alone.<sup>4</sup>

### 5.1.2. Tyc(Phe–AT) Point Mutation Sites to Expand the Aryl Ring Binding Site

The A-domain of Tyc(Phe–AT) was modeled on the structure of the homologous Grs1(Phe–A) solved in complex with AMP and (2S)– $\alpha$ –phenylalanine at 1.9 Å resolution.<sup>5</sup> As mentioned earlier in Chapters 3 and 4, the residues that surround the phenyl ring are mainly hydrophobic (A224, W227, T266, A289, A310, I318 and C319) and favor binding of hydrophobic aryl substrates.<sup>6</sup> Although the binding site of Tyc(Phe–AT) adenylation domain is highly specific for the natural substrate (2S)– $\alpha$ –phenylalanine), an earlier study showed its substrate tolerance for other natural and unnatural amino acids<sup>6-8</sup> (see Chapter 4, Figure 4.7). However, the  $k_{cat}$  of Tyc(Phe–AT) is reduced for substrates containing substituents on the aryl ring compared to phenylalanine.<sup>6,7</sup> Also, when several arylisoserine were used as substrates, Tyc(Phe–AT) was biased against *para*-substituted analogs, showing reduced activity (see Chapter 4, Section 4.3.3). Thus, to increase Tyc(Phe–AT) substrate specificity for the ring-substituted arylisoserines and heteroarylisoserines, mutations of the residues lining the binding pocket are potentially necessary.

The Tyc(Phe–AT) model (**Figure 5.1**) revealed that the residue, W227 forms π–stacking interactions with the phenyl ring of the substrate and is oriented next to the *para*-carbon. Therefore, W227 plays a key role in substrate binding. We hypothesized that mutation of this residue could effect change in the substrate scope of Tyc(Phe–AT) for *para*-substituted isoserine analogs. The binding sites of 200 homologous adenylation enzymes were surveyed using the ConSurf Program, and tryptophan (W) occurs frequently (43%), at the position similar to Tyc(Phe–AT) W227 (**Figure 5.1**). When tryptophan was not present in the various homologs, there were instead natural replacements including hydrophilic residues (C, E, K, M, S, T), which occur in 19% of the 200 homologs surveyed and smaller hydrophobic residues (A, G, I, L)

occurring in 20% of the homologs. The mutations of Tyc(Phe–AT) herein were based on the occurrence of these residues.

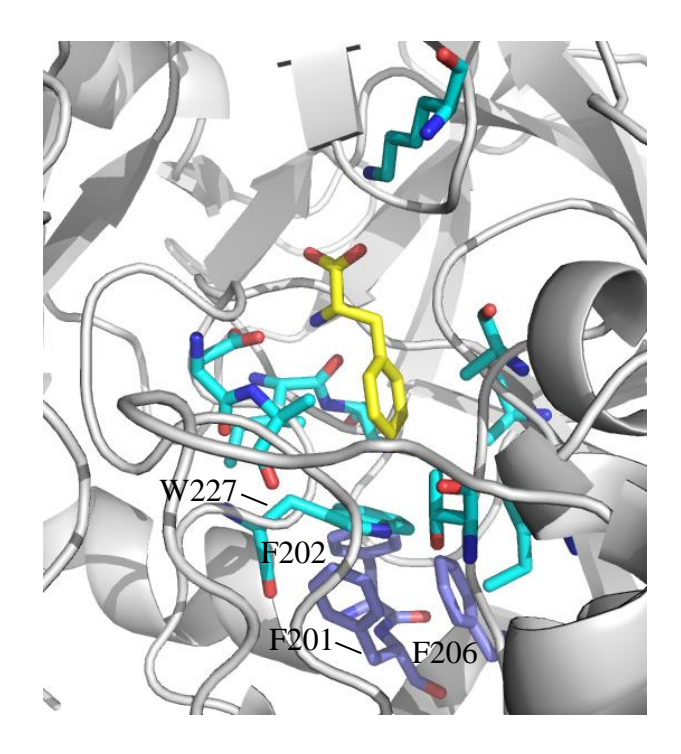


**Figure 5.1.** Tyc(Phe–AT) model (grey cartoon) in complex with phenylalanine (yellow sticks) showing the active site residues (cyan). The F201, F202, and F206 residues that border the binding pocket closest to the active site W227 are shown in blue sticks.

The survey of Tyc(Phe–AT) homologs showed that second shell residues border W227. In Tyc(Phe–AT), three second shell Phe residues (F201, F202, and F206) surround W227 and likely align W227 for favorable  $\pi$ –stacking with the substrate. Considering the function of these second-shell residues towards supporting the residue at 227 of Tyc(Phe–AT), the mutation of W227 was accompanied by tandem mutations of the second tier Phe triad to residues that normally accompany the replacement residues found in the Tyc(Phe–AT) homologs. The aim here was to maintain the architecture of the binding site. The tandem mutations of interest are proposed to replace W227 with smaller residues (**Table 5.1**). As a proof-of-concept, a few mutations were designed and tested for activity as described in the following sections.

**Table 5.1**. The proposed mutations of F201, F202, and F206 of Tyc(Phe–AT) in tandem with W227 replacement residues.

W227A <sup>a</sup>	W227S	W227G	W227Q	W227L
$FFF \rightarrow \underline{ARY}^b$	<u>AYF</u>	FFF→ANY	FFF→FTT	FFF→AMF
<u>A</u> WF	FFF→ <u>A</u> L <u>F</u>	AWF	FFF→HQT	FFF→AMP
FFF→SQC	FFF→ <u>AQF</u>	AWY	WHL	FFF→GAA
$FFF \rightarrow TL\underline{Y}$	FFF→DL <u>F</u>	AYY	WHY	FFF→GIA
W <u>RY</u>	FFF→ <u>AQ</u> S	FFF→CQF	WQI	FFF→GMI
	FFF→G <u>QF</u>	FFF→LSY	WQT	FFF→QTY
WASTE	FFF→NIL	SWF		FFF→SML
W227T	FFF→SQN	WYH		FFF→SMF
FFF→AMA			W227M	FFF→SMP
WAY			FFF→AQF	FFF→NTA
WCY	W227E	W227K	FFF→NNA	WHY
WFA	FFF→AAY	FFF→ALA	WRY	WNF
WFN	FFF→ALY	FFF→AFK		
WKY	FFF→DAF	FFF→GLG		
WSY	FFF→SAF	FFF→GLQ	W227C	
YCY	FFF→SAY	WYC	FFF→QAH	
YFV	FFF→TAY			
	WRY			

<sup>&</sup>lt;sup>a</sup>The residues in homologs that are positioned similarly to W227 in Tyc(Phe–AT) are indicated as W227B. <sup>b</sup>Three letter sequences indicate residues occurring in tandem with W227B in at least one of the 200 homologs that align with F201, F202, and F206 respectively in Tyc(Phe–AT); FFF→XYZ indicates proposed mutations of F201, F202, and F206 respectively.

#### 5.2. Experimental

#### 5.2.1. Substrates, Reagents, and General Instrumentation

CoA was purchased from Lee BioSolutions (St. Louis, MO), DNA oligos were obtained from IDT Corporation (San Jose, CA), and Phusion DNA polymerase was purchased from New England BioLabs (Ipswich, MA). All the other reagents were obtained from Sigma–Aldrich and were used without further purification, unless noted otherwise. Quattro–Premier ESI–MS coupled with Acquity® UPLC system was used for mass spectral analysis.

#### 5.2.2. Tandem Site–Directed Mutagenesis of *tyc(phe–at)* cDNA

## 5.2.2.1. Mutation of Tyc(Phe–AT) to Tyc(Phe–AT(W227A, FFF $\rightarrow$ ARY)) and Tyc(Phe–AT(W227A))

Tyc(Phe–AT) homologs that have Ala in the place of W227 are accompanied by several different residues that align with the Phe triad (F201, F202, and F206 in Tyc(Phe–AT)) in the second shell (**Table 5.1**). Hence, mutations F201A, F202R, and F206Y were proposed based on the frequency of occurrence among Tyc(Phe–AT) homologs (residues underlined under W227A column, **Table 5.1**). In the following procedure, the resultant mutant cDNA plasmids were sequence verified (MSU Research Technology Support Facility: Genomics, East Lansing, MI).

In Chapter 3, *tyc(phe–at)* cDNA encoding Tyc(Phe–AT) was obtained by truncating *tyc(phe–ate)* that encodes Tyc(Phe-ATE) (Chapter 3, Section 3.2.6). The *tyc(phe–at)* cDNA was used herein as the template to incorporate F201A mutation. The mutagenic oligonucleotide primers used to incorporate F201A into *tyc(phe–at)* were as follows (modified bases are underlined): 5'–F201A Forward primer – GCC AAT TTG CAA TCC GCT TTC CAA AAT TCG TTT GGC –3' and 5'–F201A Reverse primer – GCC AAA CGA ATT TTG GAA AGC GGA TTG CAA ATT GGC –3'. The resultant plasmid was designated Tyc(Phe–AT(F201A))–His and was used as a template to incorporate the W227A mutation. The mutagenic primers used to incorporate this mutation are as follows (modified bases are underlined): 5'–W227A Forward primer – TCG TTC GAC GCA TCC GTT GCG GAA ATG TTC ATG GCT TTG –3' and 5'–W227A Reverse primer – CAA AGC CAT GAA CAT TTC CGC AAC GGA TGC GTC GAA CGA –3'. The resultant plasmid was designated Tyc(Phe–AT(F201A:W227A))–His and was used as a template to incorporate the last two mutations (F202R and F206Y) in a single step. The mutagenic primers used to incorporate these mutations are as follows (modified bases are

underlined): 5'–F202R/F206Y Forward primer – AAT TTG CAA TCC <u>GCT CG</u>C CAA AAT TCG <u>TA</u>T GGC GTC ACC GAG –3' and 5'–F202R/F206Y Reverse primer – CTC GGT GAC GCC <u>ATA CGA ATT TTG GCG AGC GGA TTG CAA ATT –3'.</u> The resultant plasmid was designated Tyc(Phe–AT(W227A:F201A:F202R:F206Y))–His.

In a separate experiment, tyc(phe-at) cDNA that encodes Tyc(Phe-AT) was used as the template to incorporate a single W227A mutation by site-directed mutagenesis. The mutagenic primers used to incorporate this mutation are as follows (modified bases are underlined): 5'-W227A Forward primer – TCG TTC GAC GCA TCC GTT GCG GAA ATG TTC ATG GCT TTG –3' and 5'-W227A Reverse primer – CAA AGC CAT GAA CAT TTC CGC AAC GGA TGC GTC GAA CGA –3'. The plasmid was designated Tyc(Phe-AT(W227A))-His.

## 5.2.2.2. Mutation of Tyc(Phe–AT) to Tyc(Phe–AT(W227S, FFF $\rightarrow$ AQF)) and Tyc(Phe–AT(W227S))

Tyc(Phe–AT) homologs that have Ser positioned similarly to W227 generally have second shell replacements of F201A and F202Q, based on frequency of occurrence among the homologs. Mutation of F206 in Tyc(Phe–AT) was not necessary since the Phe was already present in homologs in which W227 was replaced by Ser (residues underlined under W227S column in **Table 5.1**). A similar procedure as described in Section 5.2.2 above was followed in the introduction of the tandem mutations. Briefly, the *tyc(phe–at(*F201A)) plasmid generated above (Section 5.2.2.1) was used as the template to incorporate W227S mutation. The mutagenic primers used to incorporate this mutation are as follows (modified bases are underlined): 5′–W227S Forward primer – TCG TTC GAC GCA TCC GTT TCG GAA ATG TTC ATG GCT TTG –3′ and 5′–W227S Reverse primer – CAA AGC CAT GAA CAT TTC CGA AAC GGA

TGC GTC GAA CGA –3'. The resultant plasmid was designated Tyc(Phe–AT(W227S:F201A))—His and was used as a template to incorporate the F202Q mutation. The mutagenic primers used to incorporate this mutation are as follows (modified bases are underlined): 5'– F202Q Forward primer – GCC AAT TTG CAA TCC GCT CAG CAA AAT TCG TTT GGC GTC –3' and 5'– F202Q Reverse primer – GAC GCC AAA CGA ATT TTG CTG AGC GGA TTG CAA ATT GGC –3'. The resultant plasmid was designated Tyc(Phe–AT(W227S:F201A:F202Q))—His.

In a separate experiment, tyc(phe-at) cDNA that encodes Tyc(Phe-AT) was used as the template to incorporate a single W227S mutation. The mutagenic primers used to incorporate this mutation are as follows (modified bases are underlined): 5'– W227S Forward primer – TCG TTC GAC GCA TCC GTT TCG GAA ATG TTC ATG GCT TTG –3' and 5'–W227S Reverse primer – CAA AGC CAT GAA CAT TTC CGA AAC GGA TGC GTC GAA CGA –3'. The resultant plasmid was designated Tyc(Phe-AT(W227S))–His.

## 5.2.3. Protein Expression and Activity Assays of Tyc(Phe–AT) Mutants with Phenylisoserine Analogs and CoA

The tyc(phe-at(W227A)) and tyc(phe-at(W227S)) plasmids encoding a C-terminal His-tag (designated Tyc(Phe-AT(W227A))-His and Tyc(Phe-AT(W227S))-His, respectively) described in Sections 5.2.2.1 and 5.2.2.2, were separately used to transform E. coli BL21 (DE3) cells. Cultures of E. coli (10-mL) transformed with pET28a vector were separately grown in LB medium supplemented with kanamycin (50  $\mu$ g·mL<sup>-1</sup>) at 37 °C for 12 h. The seed culture of each mutant was used separately to inoculate LB medium (1 L), and the bacteria grown at 37 °C to OD<sub>600</sub> ~0.6. Isopropyl  $\beta$ -D-1-thiogalactopyranoside (IPTG) was added (0.5 mM final concentration), and the culture was grown for 18 h at 16 °C. The cells were pelleted by

centrifugation (30 min, 4000g) at 4 °C, resuspended in Binding buffer (20 mM Tris–HCl (pH 7.8), 0.5 M NaCl, and 5 mM imidazole), lysed by sonication, and then centrifuged at 15,000g for 0.5 h. The supernatant was decanted and centrifuged at 135,000g for 1.5 h to remove cellular debris. To test for functional expression of either Tyc(Phe–AT(W227A)) or Tyc(Phe–AT(W227S)) mutants, a 1-mL aliquot of the crude soluble enzyme was assayed separately with (R)– $\beta$ –phenylalanine, (2R,3S)–phenyl-, 4-OH–phenyl-, or 4-OMe–phenylisoserine each at 2 mM in assays containing ATP (1 mM), CoA (1 mM), and MgCl<sub>2</sub> (3 mM) in 100 mM HEPES (pH 8.0). The assays were incubated at 31 °C for 2 h, and then quenched to pH 3.0 using 10% aqueous formic acid (~50  $\mu$ L). The assays were then lyophilized to dryness and dissolved in dH<sub>2</sub>O (200  $\mu$ L).

The biosynthetic aminoacyl CoA products were analyzed on a Quattro–Premier Electro–Spray Mass Spectrometer coupled to an Acquity<sup>®</sup> UPLC system fitted with a C18 Ascentis Express column ( $2.5 \times 50$  mm,  $2.7 \mu m$ ) at 30 °C. An aliquot ( $10 \mu L$ ) of each sample was loaded onto the column and the analytes eluted with a solvent gradient of acetonitrile (Solvent A) and 0.05% triethylamine in distilled water (Solvent B): held at 2.5% Solvent A for 3.17 min, increased to 100% Solvent A over 5 sec with a 2–min hold, and then returned to 2.5% Solvent A over 5 sec with a 50–sec hold at a flow rate of 0.4 mL/min. The effluent from the column was directed to the mass spectrometer set to negative ion mode with a scan range of m/z 100 – 1200 atomic mass units.

The *tyc(phe–at*(W227A:F201A:F202R:F206Y)) and *tyc(phe–at*(W227S:F201A:F202Q)) plasmids encoding C–terminal His–tags (designated Tyc(Phe–AT(W227A:F201A:F202R:F206Y))–His and Tyc(Phe–AT(W227S:F201A:F202Q))–His, respectively) were used separately to transform *E. coli* BL21 (DE3) cells. Cultures of *E. coli* 

(10-mL) transformed with pET28a vector were grown separately in LB medium supplemented with kanamycin (50 μg·mL<sup>-1</sup>) at 37 °C for 12 h. The seed culture of each mutant was separately used to inoculate LB medium (1 L) and grown at 37 °C to OD<sub>600</sub> ~0.6, at which time IPTG was added to a final concentration of 0.5 mM, and the culture grown for 18 h at 16 °C. The cells were harvested, lysed and pelleted down as described above. The crude lysate obtained from each soluble enzyme fraction was used to test the activity of Tyc(Phe-AT(W227A:F201A:F202R:F206Y)) or Tyc(Phe–AT(W227S:F201A:F202Q)) mutant. The crude soluble enzyme fraction was separately assayed with (R)- $\beta$ -phenylalanine, (2R,3S)-phenyl-, 4-OH-phenyl-, or 4-OMe-phenylisoserine each at 2 mM in assays containing ATP (1 mM), CoA (1 mM), and MgCl<sub>2</sub> (3 mM) in 100 mM HEPES (pH 8.0). The assays were incubated at 31 °C for 2 h, and then quenched to pH 3.0 using 10% aqueous formic acid (50 μL). The assays were lyophilized to dryness and dissolved in dH<sub>2</sub>O (200 µL). The reactions were analyzed using Quattro Premier LC-MS as described in this section.

#### 5.2.4. Protein Purification of Tyc(Phe–AT) Mutants

Crude soluble proteins isolated from bacteria expressing the Tyc(Phe–AT) mutants were separately loaded into nickel–nitrilotriacetic affinity column (Qiagen, Valencia, CA) and eluted according to the protocol described by the manufacturer. The column was eluted with increasing concentration of imidazole (20 – 300 mM) in Binding buffer (20 mM Tris–HCl buffer containing 0.5 M NaCl and 5 mM imidazole at pH 7.8). Fractions containing the His–tagged enzymes were identified by SDS–PAGE and Coomassie Blue staining. The enzyme solution (100 mL) for each purified enzyme was concentrated to 1 mL by size–selective centrifugation (Centriprep 30,000 MWCO unit; Millipore, Billerica, MA). The Binding buffer was exchanged with Assay buffer

(50 mM HEPES containing 100 mM NaCl and 1 mM EDTA at pH 8.0) over five dilution/concentration cycles. The enzyme purity was estimated using SDS–PAGE and Coomassie Blue staining. The extinction coefficient and molecular weight of the mutants ( $\varepsilon_{280} = 60,405 \text{ M}^{-1} \text{ cm}^{-1}$  and 69.57 kDa, respectively), were calculated, and the concentration of each protein was measured at  $A_{280}$  absorbance on a NanoDrop ND1000 Spectrophotometer (Thermo Scientific, Wilmington, DE): Tyc(Phe–AT(W227S)–His (15 mg/mL), Tyc(Phe–AT(W227A)–His (1.5 mg/mL), Tyc(Phe–AT(W227A:F201A:F202R:F206Y)–His (0.25 mg/mL), and Tyc(Phe–AT(W227S:F201A:F202Q)–His)) (0.5 mg/mL). The purified proteins were stored at  $-80 \, ^{\circ}$ C.

#### 5.2.5. Activity of Tyc(Phe–AT) Mutants with Isoserine Analogs

Separate assays with (R)– $\beta$ –phenylalanine, (R)– $\beta$ –phenylalanine, (2R,3S)–phenyl-, 4-OH–phenyl-, or 4-OMe–phenylisoserine (for synthesis, see Chapter 4, Section 4.2.1) at 2 mM concentration were carried out by incubating ATP (1 mM), CoA (1 mM), and MgCl<sub>2</sub> (3 mM) with each purified Tyc(Phe–AT) mutant (1 mg/mL) in 100 mM HEPES (pH 8.0). The reactions were incubated for 2 h at 31 °C, and transferred to 96 well plates, quenched with 10% formic acid (10  $\mu$ L) after which acetyl CoA was added as an internal standard (1  $\mu$ M) and the reactions analyzed by LC–MS as described earlier (Section 5.2.3).

Tyc(Phe-AT(W227S)) mutant showed activity in the conversion of (R)- $\beta$ -phenylalanine, (2R,3S)-phenyl-, 4-OH-phenyl-, and 4-OMe-phenylisoserine to their corresponding CoA thioesters. To test the substrate specificity of Tyc(Phe-AT(W227S)) mutant, isoserine analogs (Refer to Table 5.2) were used at 2 mM in separate assays containing the enzyme (1 mg/mL), ATP (1 mM), CoA (1 mM), and MgCl<sub>2</sub> (3 mM) in 100 mM HEPES (pH 8.0). The reactions were

incubated for 2 h at 31°C and transferred to 96 well plates, quenched with 10% formic acid (10  $\mu$ L) after which acetyl CoA was added as an internal standard (1  $\mu$ M). The reactions were analyzed by LC–MS as described earlier (Section 5.2.3).

#### 5.3. Results and Discussion

### **5.3.1.** Protein Expression and Purification of Tyc(Phe–AT) Mutants

Four Tyc(Phe–AT) mutants (MW 69.5 kDa) [Tyc(Phe–AT(W227A))–His, Tyc(Phe–AT(W227S))–His, Tyc(Phe–AT(W227A:F201A:F202R:F206Y))–His, and Tyc(Phe–AT(W227S:F201A:F202Q))–His] were heterologously expressed in *E. coli* BL21(DE3). To test for the expression of these mutants, protein in the crude lysates were analyzed by SDS–PAGE and Coomassie Blue staining (**Figure 5.2**). The crude enzymes were purified separately using Ni–affinity column and concentrated to ~0.25 – 15 mg/mL (**Figure 5.2**).

The yields of recovered purified enzyme was variable amongst the heterologously expressed Tyc(Phe–AT) mutants. Tyc(Phe–AT(W227S)) (15 mg/mL) expressed the best. Tyc(Phe–AT(W227A), Tyc(Phe–AT(W227A:F201A:F202R:F206Y)), and Tyc(Phe–AT(W227S:F201A:F202Q)) were obtained at low yields ranging from 0.25 – 1.5 mg/mL. This was not too surprising, since seemingly minor changes in the expressed protein may affect expression levels. <sup>10</sup>

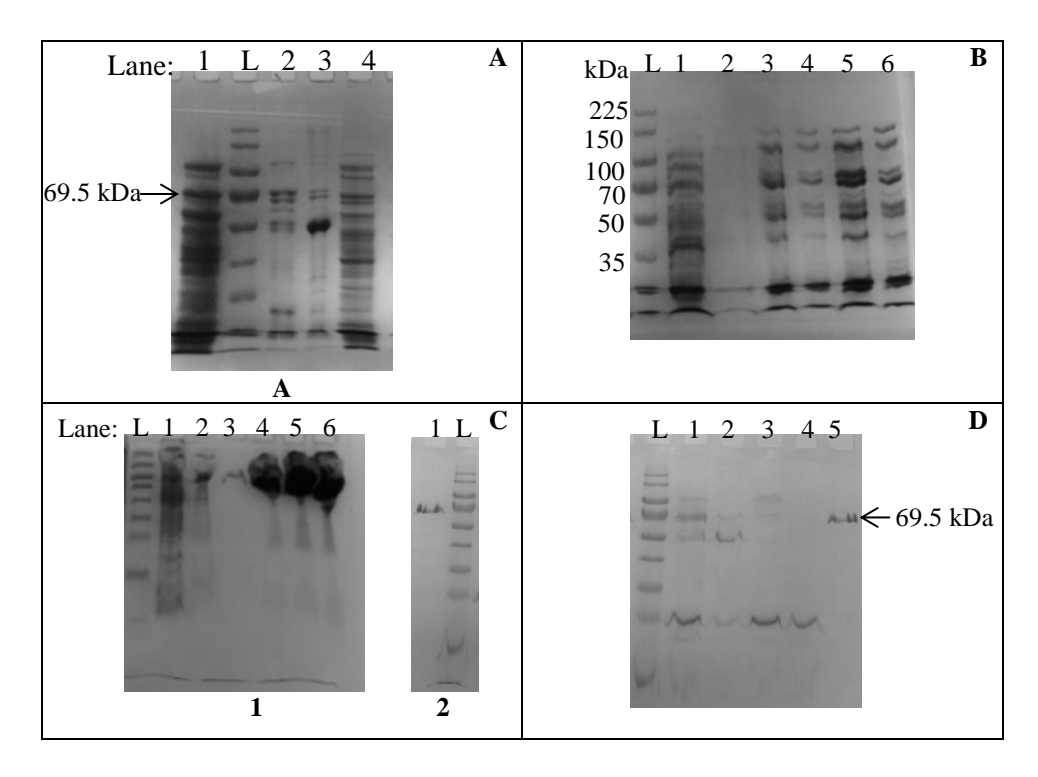


**Figure 5.2.** SDS-polyacrylamide gel electrophoresis (12% acrylamide) and Coomassie blue staining of recombinantly expressed Tyc(Phe–AT) mutants which were separately isolated from *E. coli* BL21(DE3). **A)** Tyc(Phe–AT(W227A))–His; Lane 1A: crude lysate. The profile of the soluble protein eluted from nickel–affinity resin chromatography with Binding buffer contained the following; Lane 2A: 300 mM imidazole (fraction 1); Lane 3A: Tyc(Phe–A) (positive marker, 70 μg); Lane 4A: flow through; L: Molecular weight standard. **B)** Tyc(Phe–AT(W227A:F201A:F202R:F206Y))–His; Lane 1B: crude lysate; Lane 2B: empty; Lane 3B: 100 mM imidazole (fraction 1, 5 μL (from 25 mL elution)); Lane 4B: 300 mM imidazole (fraction 2, 0.75 μg); Lane 5B: 100 mM imidazole (fraction 1, 10 μL); Lane 6B: 300 mM imidazole (fraction 2, 0.75 μg). **C)** Tyc(Phe–AT(S563A))–His; **C1)** Lane 1C: Flow through; Lane 2C: 10 mM imidazole (wash 1); Lane 3C: 20 mM imidazole (wash 2); Lane 4C: 300 mM imidazole (fraction 1, 75 μg); Lane 5C: 300 mM imidazole (fraction 1, 15 μg). **D)** Tyc(Phe–AT(W227S:F201A:F202Q))–His; Lane 1: 50 mM imidazole (fraction 1); Lane 2: 100 mM imidazole (fraction 2); Lane 3: 200 mM imidazole (fraction 3); Lane 4: 300 mM imidazole (fraction 4); Lane 5: Tyc(Phe–AT) (positive marker, 10 μg).

#### 5.3.2. Activity Assays of Tyc(Phe–AT) Mutants with Phenylisoserine Analogs

The activity of four Tyc(Phe–AT) mutants was determined in separate assays containing ATP, MgCl<sub>2</sub>, CoA, and (R)– $\beta$ –phenylalanine, (2R,3S)–phenyl–, 4-OH–phenyl–, or 4-OMe–phenylisoserine substrate. Analysis of the assay products by LC–ESI–MS showed aminophenylpropanoyl CoA products only in assays containing Tyc(Phe–AT(W227S)). No

aminophenylpropanoyl CoA products were detected in assays containing crude or purified Tyc(Phe–AT(W227A), Tyc(Phe–AT(W227A:F201A:F202R:F206Y), or Tyc(Phe–AT(W227S:F201A:F202Q) mutants.

### 5.3.2.1. Activity Evaluation of Tyc(Phe–AT(W227S)) in the Screen for Isoserine Analogs in Isoserinyl CoA Biosynthesis

The Tyc(Phe–AT(W227S)) activity screen with isoserine analogs (see Chapter 4, Section 4.2.2) was done in separate assays. Each assay contained an isoserine substrate (2 mM), ATP (1 mM), CoA (1 mM), and Tyc(Phe-AT(W227S)) (1 mg). The assays were analyzed using Quattro Premier LC-ESI-MS in negative ion mode. It was envisioned that the mutation of W227 to smaller residues (for example Ala and Ser) would reduce steric interactions and enable binding of phenylisoserine analogs with bulky substituents on the para-carbon (for example, p-methyl-, p-methoxy-, and p-nitrophenylisoserine). Further, changes in the electronic properties of the binding site around the para-position from hydrophobic to hydrophilic (W227S) would enhance the binding of hydrophilic substituents through H-bonding interaction. There was a drastic reduction or complete loss in the activity of Tyc(Phe–AT(W227S) for most variously substituted aryl isoserine analogs compared to that of Tyc(Phe-AT) (Table 5.2). Notably, 2-F-, 3-Me-, 3-F-, and 3-Cl-substituted phenylisoserines decreased the turnover of Tyc(Phe-AT(W227S)) by two-orders of magnitude compared to that of Tyc(Phe-AT). This suggests that W227 plays a major role in positioning the phenyl ring of the substrate in a catalytically competent conformation.

Tyc(Phe–AT) and Tyc(Phe–AT(W227S)) similarly turned over the *para*-substituted analogs, with the exception of 4-F–phenylisoserine (the  $v_{app}$  was ~100-fold lower). Surprisingly,

this mutant turned over 4-OMe-phenylisoserine and 2-pyridinylisoserine, which were not productive substrates of Tyc(Phe–AT).

> **Table 5.2**. The rates  $(v_{app})$  of Tyc(Phe–AT(W227S)) mutant in comparison to Tyc(Phe-AT) in the biosynthesis of isoserinyl CoA analogs

	Tyc(Phe–AT(W227S))	Tyc(Phe–AT)	
Substrate	$v_{\rm app} ({\rm nmol \cdot h}^{-1}) (\times 10^2)$	$v_{\rm app}  ({\rm nmol \cdot h}^{-1})$	
Phenylisoserine	4.4	$7.3 \pm 0.91$	
3-F–Phenylisoserine	2.8	$6.1 \pm 0.41$	
3-Cl–Phenylisoserine	1.7	$1.7 \pm 0.27$	
3-Br-Phenylisoserine	1.8	$1.4 \pm 0.15$	
3-Me–Phenylisoserine	0.6	$2.6 \pm 0.15$	
3-NO <sub>2</sub> –Phenylisoserine	*ND	$5.2 \pm 0.10$	
3-OMe-Phenylisoserine	1.5	$0.6 \pm 0.07$	
3-OH–Phenylisoserine	ND	$0.3 \pm 0.03$	
Thiophenylisoserine	ND	$0.9 \pm 0.09$	
4-F–Phenylisoserine	4.6	$4.0 \pm 1.0$	
4-Cl–Phenylisoserine	40	$0.45 \pm 0.12$	
4-Br-Phenylisoserine	7.3	$0.22 \pm 0.05$	
4-Me-Phenylisoserine	42	$1.1 \pm 0.019$	
4-OH–Phenylisoserine	ND	$0.04 \pm 0.01$	
4-NO <sub>2</sub> –Phenylisoserine	ND	$0.05 \pm 0.01$	
4-OMe-Phenylisoserine	4.4	ND	
2-F–Phenylisoserine	0.5	$0.98 \pm 0.12$	
2-Cl–Phenylisoserine	ND	$0.11 \pm 0.02$	
2-NO <sub>2</sub> –Phenylisoserine	ND	$0.18 \pm 0.02$	
Cyclohexylisoserine	0.2	$0.09 \pm 0.01$	
2-Pyridinylisoserine	0.4	ND	

<sup>\*</sup>ND indicates that the rates of either enzyme for these substrates could not be determined because their respective CoA thioester products were below detection limit of the LC-ESI-MS.

The recovered catalytic activity of the Tyc(Phe-AT(W227S)) mutant for 4-OMephenylisoserine to its CoA thioester suggest that the steric barrier present in Tyc(Phe-AT) was likely overcome by the W227S substitution, which supports our hypothesis. It is not immediately evident, however, why the Tyc(Phe-AT(W227S)) mutant was able to catalyze 2pyridinylisoserine to its CoA thioester. One can imagine that the pyridinyl nitrogen is able to H-bond to the backbone amide of an active site residue placing the substrate in the correct trajectory for catalysis (See Chapter 4, Section 4.3.3).

In summary, the Tyc(Phe-AT(W227S)) mutation showed new activity for 4-OMephenylisoserine and 2-pyridinylisoserine as discussed above. As part of future direction, mutation of the residues around the aryl binding pocket in Tyc(Phe–AT) would be necessary in improving the substrate specificity. The mutations outlined in **Table 5.1** target W227 and aim at improving the binding of para-substituted phenylisoserine substrates. As mentioned previously, computational-guided predictions may provide information about favorable mutations that would likely improve Tyc(Phe-AT) activity and substrate specificity with the isoserine analogs, and also reduce the work load involved in the biochemical characterization of the sequenceguided mutations. One approach towards designing plausible mutations is through docking the isoserine substrates into the structure models of Tyc(Phe-AT) mutants bearing different mutations around the phenyl ring. This approach was previously demonstrated with Grs1(Phe-A).4 In this study, the computationally predicted Grs1(Phe-A) mutants showed increase in the enzyme catalytic efficiency  $(k_{cat}/K_{\rm M})$  for non-natural substrates compared to the wild-type enzyme.<sup>4</sup> For example, Grs1(Phe-A(T278L/A301G)) mutant showed a 19-fold increase in the  $k_{\text{cat}}/K_{\text{M}}$  with leucine in comparison to the wild-type Grs1(Phe–A).<sup>4</sup>

# 5.4. Tyc(Phe–AT) and BAPT–Coupled Assays Towards the Biosynthesis of Precursors of Paclitaxel Analogs

The structure activity relationship studies of paclitaxel revealed the importance of C–13 side chain bearing the correct stereochemistry for biological activity. 11-13 The biosynthetic

incorporation of C–13 side chain is dependent on the catalytic activity of a 13–*O*–3–aminophenylpropanoyltransferase (BAPT) that transfers aminoacyl groups from aminoacyl CoA thioesters to baccatin III (Chapter 4, Section 4.1.3). From the studies described in Chapters 3 and 4, Tyc(Phe–AT) catalyzes the biosynthesis of various aminoacyl CoA thioesters. Thus, coupling the reactions catalyzed by Tyc(Phe–AT) and BAPT (**Figure 5.3**) has the potential to overcome the challenges associated with the semisynthesis of paclitaxel, namely multiple reaction steps and hazardous reagents (see Chapter 1, Sections 1.2 and 1.3). Also, a biosynthetic method is environmentally friendly and does not incur huge expenses required for solvent disposal.

$$\begin{array}{c} \overset{\bullet}{\text{NH}_3} \overset{\bullet}{\text{O}} \\ \overset{\bullet}{\text{OH}} & \overset{\bullet}{\text{O}} \\ \overset{\bullet}{\text{OH}} & \overset{\bullet}{\text{O}} \\ \overset{\bullet}{\text{OH}} & \overset{\bullet}{\text{O}} \\ \overset{\bullet}{\text{O}} & \overset{\bullet}{\text{O}} & \overset{\bullet}{\text{O}} \\ \overset{\bullet}{\text{O}} & \overset{\bullet}{\text{O}} & \overset{\bullet}{\text{O}} \\ \overset{\bullet}{\text{O}} & \overset{\bullet}{\text{O}} \\ \overset{\bullet}{\text{O}} & \overset{\bullet}{\text{O}} & \overset{\bullet}{\text{O}} & \overset{\bullet}{\text{O}} \\ \overset{\bullet}{\text{O}} & \overset{\bullet}{\text{O}} & \overset{\bullet}{\text{O}} & \overset{\bullet}{\text{O}} \\ \overset{\bullet}{\text{O}} & \overset{\bullet}{\text{$$

**Figure 5.3.** Proposed Tyc(Phe–AT) and BAPT-coupled assays aimed at novel biosynthesis of paclitaxel analogs.

### **REFERENCES**

#### **REFERENCES**

- (1) Brannigan, J. A.; Wilkinson, A. J. Nat. Rev. Mol. Cell Biol. 2002, 3, 964.
- (2) Koetsier, M. J.; Jekel, P. A.; Wijma, H. J.; Bovenberg, R. A. L.; Janssen, D. B. *FEBS Lett.* **2011**, *585*, 893.
- (3) Stevens, B. W.; Lilien, R. H.; Georgiev, I.; Donald, B. R.; Anderson, A. C. *Biochemistry* **2006**, *45*, 15495.
- (4) Chen, C.-Y.; Georgiev, I.; Anderson, A. C.; Donald, B. R. *Proc. Natl. Acad. Sci. U. S. A.* **2009**, *106*, 3764.
- (5) Conti, E.; Stachelhaus, T.; Marahiel, M. A.; Brick, P. *Embo J.* **1997**, *16*, 4174.
- (6) Villiers, B. R. M.; Hollfelder, F. *Chembiochem* **2009**, *10*, 671.
- (7) Schaffer, M. L.; Otten, L. G. J. Mol. Catal. B-Enzym. 2009, 59, 140.
- (8) Muchiri, R.; Walker, Kevin D. Chem. Biol. 2012, 19, 679.
- (9) Celniker, G.; Nimrod, G.; Ashkenazy, H.; Glaser, F.; Martz, E.; Mayrose, I.; Pupko, T.; Ben-Tal, N. *Isr. J. Chem.* **2013**, *53*, 199.
- (10) Palomares, L. A.; Estrada-Moncada, S.; Ramírez, O. T. 2004; Vol. 267, p 15.
- (11) Jiménez-Barbero, J.; Souto, A. A.; Abal, M.; Barasoain, I.; Evangelio, J. A.; Acuña, A. U.; Andreu, J. M.; Amat-Guerri, F. *Bioorg. Med. Chem.* **1998**, *6*, 1857.
- (12) Kingston, D. G.; Chaudhary, A. G.; Chordia, M. D.; Gharpure, M.; Gunatilaka, A. L.; Higgs, P. I.; Rimoldi, J. M.; Samala, L.; Jagtap, P. G.; Giannakakou, P. J. Med. Chem. 1998, 41, 3715.
- (13) Gueritte-Voegelein, F.; Guenard, D.; Lavelle, F.; Le Goff, M. T.; Mangatal, L.; Potier, P. J. Med. Chem. 1991, 34, 992.
- (14) Holton, R. A.; Biediger, R. J.; Boatman, P. D. *Taxol: science and applications* **1995**, 97.
- (15) Dunn, P. J.; Wells, A.; Williams, M. T. *Green Chemistry in the pharmaceutical industry*; John Wiley & Sons, 2010.